PROCEEDINGS OF THE 21ST INTERNATIONAL GHRSST SCIENCE TEAM ON-LINE MEETING

1ST - 4TH JUNE 2020

ISSN 2049–2529
Issue 1.1

Edited by the GHRSST Project Office

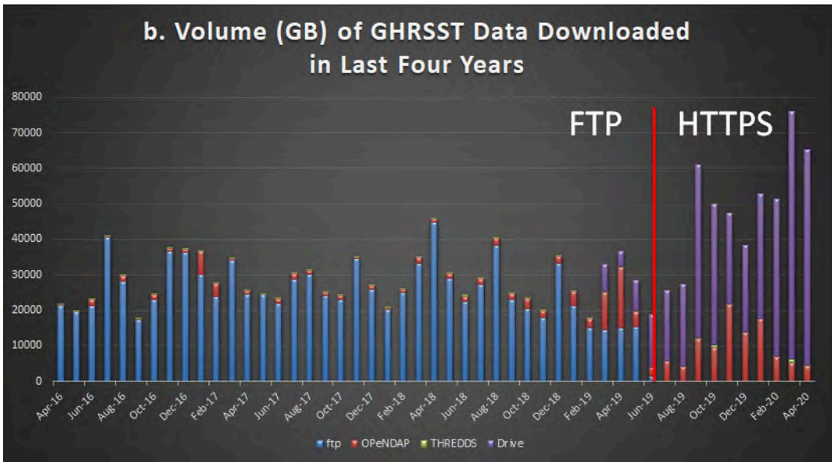

On-line meeting hosted by:

EUMETSAT

GHRSST International Project Office

Karen Veal, Project Co-ordinator
gpc@ghrsst.org

Silvia Bragaglia-Pike, Project Administrator
gpa@ghrsst.org

www.ghrsst.org

The GHRSST Project Office is funded by the European Union

Figure on front page: *Fig. 3 from 'GLOBAL DATA ASSEMBLY CENTER (GDAC) REPORT TO THE GHRSST SCIENCE TEAM' by E. Armstrong et al. '*

Table of Contents

WELCOME OF SCIENCE TEAM CHAIR TO THE MEETING PARTICIPANTS

Welcome to the 21st International Science Team meeting of the Group for High Resolution Sea-Surface Temperature (GHRSST XXI).

This year we are holding the meeting online due to the Covid-19 pandemic. We are very sorry not to be able to meet together in Boulder as originally planned, but hope that you and all our friends and colleagues around the world are keeping safe and well.

We welcome the opportunity for a new way of collaborating and interacting and I hope that the opportunity brings in new participation by scientists and colleagues who wouldn't usually be able to attend the meeting in person. We will have to learn new technologies, and advance our skills in online communications, but I hope this will develop further the possibilities of ways of working together in future years. We should also take the opportunity to increase our capabilities and productivity for intersessional work. I hope also that it gives more of an opportunity for early-career scientists to participate and to employ and teach us all their online social skills with more opportunities for leading particularly within their subjects of interest.

Last year we carefully questioned the need for how often we meet in person, considering the impacts of travel on the climate, concluding that yearly meetings are still crucial for advancing Sea Surface Temperature science and observations. The need for SST observations is as ever critical for weather and ocean forecasting and for the continuation of climate monitoring and data records. It is important that we continue with identified improvements and priorities. However, this year the pandemic has made this decision for us, reducing drastically all our travel carbon budgets. But we must continue to collaborate and progress with our work on SST and this is why we have made the decision to organise the meeting online instead of delaying it till later months. I hope you all enjoy the meeting and find it productive and fruitful.

The provision of high quality SST data from a broad satellite constellation has continued, with the particular good news in December 2019 that AMSR-3 was officially approved as a new project with a target launch date of 2023. AMSR-3 will be installed on the Global Observation SATellite for Greenhouse gases and water cycle.

Many improvements to SST products, data access and systems have continued over the last year including: the release of GCOM-C/SGLI SST in GDS2.0 in February 2020, the release of NASA MUR SST data in the cloud supporting future ways of analysing data, upgrades to iQuam and the ingestion of NOAA VIIRS SST into Australian SST products in November 2019. Activities of Fiducial Reference Measurements have continued including on TRUSTED HRSST drifting buoys, the ships4sst radiometers and the use of Saildrone measurements.

Last September the OceanObs19 conference took place in Hawaii where a number of GHRSST science team members participated including presenting a poster on our OceanObs19 white paper on Observational needs of Sea Surface Temperature. Our user driven priorities for SST observations over the next decade have been identified as: improving data quality in the Arctic, Improving coastal SST data quality, improving SST feature resolution. The paper can be found from https://www.frontiersin.org/articles/10.3389/fmars.2019.00420/full.

In addition, we contributed to the OceanObs19 satellite innovation breakout, combining efforts with the Sea Surface Salinity and other ocean communities. Further key priorities that arose are the importance of continuity, better accuracy, higher resolution including new technology providing resilience to RFI for SST; improved satellite stability / uncertainty and error estimation / validation including enhanced Fiducial Reference Measurements; and enhanced knowledge of SST variability and physics of measurements. The importance of international collaboration was highlighted for all domains.

Another publication released this year was the white paper of Current and future sea surface temperature missions: Towards 2050, by the CEOS Sea Surface Temperature Virtual Constellation (SST-VC). The white paper will be available from ceos.org soon.

At this year's meeting we will have pre-recorded oral and poster presentations focused on Validation and Calibration, Applications, Retrieval Algorithms, Services and Products, and Analyses and Reanalyses. We will also progress on the several on-going Task Team topics. In particular, we will hear about the latest status from the Regional / Global Task Sharing team and how to proceed with the implementation aspects.

I am looking forward to an interesting and stimulating week and I hope you enjoy the meeting and find it productive and useful.

Have a great week!

Anne O'Carroll

(Chair of the GHRSST Science Team)

SECTION 1: PROGRAMME

Below are the links to individual presentations (also available on the GHRSST website under the 'Resources' of the G-XXI meeting page (https://www.ghrsst.org/agenda/ghrsst-xxi/).

MONDAY 1ST JUNE 2020	Presenter
Science 1: Retrieval Algorithms Chair: Marouan Bouali Co-chairs: Pradeep Thapliyal, Jonathan Mittaz	
ORAL PRESENTATIONS - EXTENDED ABSTRACTS	
S1-1 - Infrared Radiative Simulated SSTskin Through Aerosol-Burdened Atmosphere	Bingkun Luo
S1-3 - Modis Sea-Surface Temperatures: Characteristics of the R2019.0 Reprocessing of the Terra and Aqua Missions	Peter Minnett
S1-4 - Retrieval of SST from Copernicus Imaging Microwave Radiometer (CIMR) observations	Jacob Hoyer
POSTER PRESENTATIONS	
S1-P1 - Operational Sea Surface Temperature Retrieval using GK2A of KMA	JaeGwan Kim
S1-P2 - SST retrieval developments for the ESA Climate Change Initiative	Owen Embury
S1-P3 - Error estimation of Pathfinder Version 5.3 SST Level 3C using extended triple collocation approach	Korak Saha
S1-P4 - SGLI SST Ver. 2.0	Yukio Kurihara
S1-P5 - Overview of AMSR-3 on the Global Observing Satellite for Greenhouse Gases and Water Cycle (GOSAT-GW)	Misako Kachi
S1-P6 - A Priori Bias Effects in the Optimal Estimation of Sea Surface Temperature Retrievals from Satellite IR Radiometers	Goshka Szczodrak
S1-P7 - SST Observations during the SLSTR Tandem Phase	Jonathan Mittaz
S1-P8 - Feasibility Analysis Of Sea Ice Concentration Data Reconstruction Over Arctic Based On Chinese Satellite-Borne Microwave Radiometer	Qimao Wang/Lijian Shi

AGENCY REPORTS	
AR-1 - GHRSST system Components: GDAC	Ed Armstrong
AR-2 - GHRSST system Components: EU GDAC	Jean-François Piollé
AR-3 - GHRSST system Components: LTSRF	John Huai-Min Zhang
AR-4 - GHRSST system Components: SQUAM and iQUAM	Alexander Ignatov
AR-5 - Report from CMA	Sujuan Wang
AR-6 - Report from ESA	Craig Donlon
AR-7 - Report from MISST	Chelle Gentemann
AR-8 - Report from NSOAS	Qimao Wang/Lijian Shi
AR-9 - RDAC Update: ABoM	Helen Beggs
AR-10 - RDAC Update: CMC	Dorina Surcel-Colan

AR-11 - RDAC Update: CMEMS	Bruno Buongiorno Nardelli
AR-12 - RDAC Update: EUMETSAT	Anne O'Carroll
AR-13 - RDAC Update: JAXA	Misako Kachi
AR-14 - RDAC Update: JMA	Toshiyuki Sakurai
AR-15 - RDAC Update: Met Office	Chongyuan Mao
AR-16 - RDAC Update: NASA	Ed Armstrong
AR-17 - RDAC Update: NAVO	Bruce McKenzie
AR-18 - RDAC Update: NOAA NCEI	Huai-Ming Zhang
AR-19 - RDAC Update: NOAA NESDIS STAR 1	Alexei Ignatov
AR-20 - RDAC Update: NOAA/NESDIS/STAR SST2	Eileen Maturi
AR-21 - RDAC Update: NOAA NCEI	Huai-Ming Zhang
AR-22 - RDAC Update: OSI-SAF	Stéphane Saux Picart
AR-23 - GHRSST Connection with CEOS: SST-VC	Ed Armstrong

TUESDAY 2ND JUNE 2020	Presenter
Science 2: Calibration and Validation Chair: Simon Good Co-chairs: Kyung-Ae Park, Gary Wick	
ORAL PRESENTATIONS - EXTENDED ABSTRACTS	
S2-1 - Comparison of satellite derived sea surface temperature and sea surface salinity gradients: Comparisons with the Saildrone Baja and Gulf Stream deployments	Jorge Vazquez
S2-2 - Evaluation of HRSST drifters using Copernicus SLSTR	Gary Corlett
S2-3 - Sentinel-3 SLSTR SST Validation using a Fiducial Reference Measurements (FRM) Service	Werenfrid Wimmer
S2-4 - On the applicability of Copernicus Sentinel-3A and Sentinel-3B Sea and Land Surface Temperature Radiometers as reference sensors	Gary Corlett
S2-5 - 2019 Arctic Saildrone Field Campaign: Measurements of Sea Surface Salinity and Temperature for Validation of Satellite Retrievals	Chelle Gentemann
POSTER PRESENTATIONS	
S2-P1 - Forty-five years of oceanographic and meteorological observations at a coastal station in the NW Mediterranean: a ground truth for satellite observations	Jorge Vazquez
S2-P2 - Comparison of SGLI and M-AERI skin SST	Yukio Kurihara
S2-P3 - EUMETSAT SLSTR Sea Surface Temperature Multi-mission Matchup Database	Igor Tomazic
S2-P4 - Inter-comparison of Daily Sea Surface Temperature Data and *in situ* Temperatures at Korean Coastal Regions	Kyung-ae Park
S2-P5 - High Resolution Sea surface Temperature Retrieval Using Landsat 8 Oli/Tirs Data at coastal region	Kyung-ae Park
S2-P6 - Initial assessment for the calibration of HY-1C COCTS infrared channels	Mingkun Liu

TUESDAY 2ND JUNE 2020 (CONT'D)	Presenter
Science 3: Analyses and Reanalyses Chair: Helen Beggs Co-chairs: Andy Harris, Stéphane Saux Picart	
ORAL PRESENTATIONS - EXTENDED ABSTRACTS	
S3-1 - The intercomparison of Sea Surface Temperature Products in the framework of the Copernicus Climate Change Service	Chunxue Yang
S3-2 - Daily ICOADS3.0.2 and its impact on DOISSThttp://adf5c324e923ecfe4e0a-6a79b2e2bae065313f2de67bbbf078a3.r67.cf1.rackcdn.com/GHRSST%20XXI%20-%20Virtual%20sponsored%20by%20EUMETSAT/S3-2-Liu_C_Daily_ICOADS3.0.2_OISST-GHRSST_XXI_compressed.pdf	Chunying Liu
S3-3 - A geometrical approach for Level 3 (super) collated and Level 4 SST analysis	Marouan Bouali
S3-4 - Ingesting VIIRS SST into the Bureau of Meteorology's Operational SST Analyses	Helen Beggs
POSTER PRESENTATIONS	
S3-P1 - Improvements of the Daily Optimum Sea Surface Temperature (DOISST) Version 2.1	Boyin Huang
S3-P2 - OSTIA: past and future developments	Simon Good
S3-P3 - The recent update of SST analysis in NCEP GFS and a few related fundamental issues	Xu Li
S3-P4 - Towards 2nd reanalysis of NOAA AVHRR GAC Data (RAN2): Evaluation	Victor Pryamitsyn
S3-P5 - Towards 2nd reanalysis of NOAA AVHRR GAC Data (RAN2): Methodology	Boris Petrenko
S3-P6 - Optimum Interpolation Analysis For Sea Surface Temperature Using The Oriented Elliptic Correlation Scales	Zhihong Liao

WEDNESDAY 3RD JUNE 2020	Presenter
Science 4: Services and Products Chair: Misako Kachi Co-chairs: Edward Armstrong, Owen Embury	
ORAL PRESENTATIONS - EXTENDED ABSTRACTS	
S4-1 - A new era of science	Chelle Gentemann
S4-2 - Connecting Users and Applications with PO.DAAC hosted GHRSST data	Edward Armstrong
S4-3 - A Lagrangian Global Dataset of Sea Surface Temperature	Shane Elipot
S4-4 - Ingesting SLSTR SST into IMOS Multi-sensor SST composites	Pallavi Govekar
POSTER PRESENTATIONS	
S4-P1 - Towards Global L3S Products at NOAA	Olafur Jonasson
S4-P2 - CMEMS SST-TAC: achievements during the second year (2019) and evolutions plans in 2020	Andrea Pisano
S4-P3 - Advancing data discovery and services in support of the GHRSST community	Wen-Hao Li
S4-P4 - EUMETSAT Copernicus Marine Training and User Support	Hayley Evers-King
S4-P5 - A Comparison between Iquam and "external" *in situ* SST Quality Controls	Haifeng Zhang
S4-P6 - The Oceanview (Ov): Towards a Web-Application for Integrated Visualization of Satellite, In Situ, and Model Data & Ocean Events – The Concept and The Plan	Prasanjit Dash
S4-P7 - Status of VIIRS SST Products at NOAA	Olafur Jonasson
S4-P8 - Status of Metop SST Products at NOAA	Victor Pryamitsyn
S4-P9 - Data reduction service for the v2.1 sea surface temperature analysis from the ESA Climate Change Initiative	Chris Merchant
S4-P10 - NAVOCEANO SST Processing	Danielle Carpenter

THURSDAY 4TH JUNE 2020	Presenter
Science 5: Applications Chair: Jorge Vazquez Co-chairs: Sujuan J Wang, Salvatore Marullo	
ORAL PRESENTATIONS - EXTENDED ABSTRACTS	
S5-1 - Comparison of multiple SST products using the Marine Heatwave Tracker	Robert Schlegel
S5-2 - Integrating regionally optimised sea surface temperature and ocean colour earth observation products to detect and monitor harmful algal blooms in support of small scale fishers and the abalone aquaculture industry in the Southern Benguela Upwelling System	Christo Whittle
S5-3 - Multi-Decadal Examination of Thermal Habitat Suitability for the Endangered Delta Smelt in the San Francisco Estuary using Landsat 5, 7, and 8	Gregory Halverson
S5-4 - On the use of sea surface temperature (SST) for improving the altimeter derived surface currents: a sensitivity study to SST products	Daniele Ciani
POSTER PRESENTATIONS	
S5-P1 - NOAA's Ocean Heat Content Suite for the Indian Ocean	Eileen Maturi
S5-P2 - Address Tropical Climate Variability with Neural Network Models	Francesca Leonelli
S5-P3 - The Mediterranean, almost 40 years of continued warming	Francisco Pastor

Task Teams Session 1 Chair: Charlie Barron Co-chairs: Misako Kachi, Craig Donlon	
TTS1-1 - Cloud masking	Chris Merchant
TTS1-2 - Regional and Global Task Sharing Task Team	Jean-François Piollé
TTS1-3 - Single Sensor Error Statistics and L4	Andy Harris
TTS1-4 - Pixel to pixel variation,	Peter Cornillon
TTS1-5 - Coral heat stress - user needs,	William Skirving
TTS2-1 - Shipborne radiometry	Werenfrid Wimmer
TTS2-2 - GHRSST Match-up Dataset	Igor Tomazic
TTS2-3 - GHRSST Climatology and L4 Inter-comparison	Helen Beggs and Chunxue Yang
TTS2-4 - High-Latitude SST	Chelle Gentemann
TTS2-5 - Climate Data Assessment Framework	Jonathan Mittaz

SECTION 2: SESSION REPORTS AND PRESENTATION ABSTRACTS

SCIENCE SESSION 1: RETRIEVAL ALGORITHMS

S1 - SESSION REPORT

Marouan Bouali[1], Pradeep Thapliyal[2] and Jonathan Mittaz[3]

(1) Institute of Oceanography of the University of São Paulo (IOUSP), marouan.bouali@usp.br
(2) Space Applications Centre, (ISRO), pkthapliyal@gmail.com
(3) University of Reading, UK, j.mittaz@reading.ac.uk

ABSTRACT

The session 1 on "Retrieval Algorithms" had three pre-recorded oral presentations and 8 posters, associated with recent advances in the retrieval/uncertainty estimation of SST (SIC) from satellite observations. Following is a brief summary of the session presentations.

1. ORAL PRESENTATIONS

1.1. Infrared Radiative Simulated SSTskin Through Aerosol Burdened Atmosphere - *Bingkun Luo*

- Used data from MERRA-2 and Terra MODIS BTs as input in RTTOV to simulate SST_{skin} under clear-sky and aerosol affected conditions
- SST_{skin} from M-AERI used to estimate SST_{skin} errors
- Used output of RTTOV simulations to evaluate the impact of aerosol vertical distribution on SST_{skin} errors
- Highlighted the importance of accounting for aerosol type/vertical distribution in the calibration of SST retrieval algorithms and the potential use of CALIPSO data.

1.2. Modis Sea-Surface Temperatures: Characteristics of the R2019.0 Reprocessing of the Terra and Aqua Missions - *Peter Minnett*

- Presented major changes of the latest reprocessing of MODIS SST from OBPG and GSFC
- New MODIS SST uses CMC instead of Reynolds as first guess SST
- Replaced BDT with ADT in cloud masking for increased coverage at L2 and L3
- Included a correction for aerosol using DSDI
- SST coefficients optimized for High-Latitudes/Arctic (>60N)
- Improved discrimination of cloud and sea ice

1.3. Retrieval of SST from Copernicus Imaging Microwave Radiometer (CIMR) observations - *Jacob Hoyer*

- Presented preliminary results of OE and statistical regression (RE) retrieval for upcoming CIMR mission using different combinations of channels
- Discussed characteristics of the tested Matchup Dataset (MMD6C)
- Comparison between OE and RE done on spatial distribution, seasonal variation and regional differences
- For both OE and RE, inclusion of additional channels improves retrieval performance
- Performance of CIMR similar to AMSR-E for OE and RE retrieval algorithms

2. POSTER PRESENTATIONS

2.1. Operational Sea Surface Temperature Retrieval using GK2A of KMA - *JaeGwan Kim*

- Presented SST products developed at the NMSC/KMA derived from the geostationary sensor GK-2A
- Operational SST retrieval for GK-2A is based on a Multi-Band algorithm with MCSST, NLSST and Hybrid used for contingency
- Validation with drifter buoys and OSTIA indicate biases <0.05 K and RMSE<0.51 K
- KMA also produces regional L4 SST from GK2A, N18/19 AVHRR, GPM GMI and *in situ* data.
- Future plans include production of global L4 SST

2.2. SST retrieval developments for the ESA Climate Change Initiative - *Owen Embury*

- Presented ongoing developments of the ESA Climate Change Initiative with respect to Climate Data Record version 3
- Sentinel SLSTR-A/B now used as reference sensors
- AVHRR GAC and FRAC tuned to *in situ*, ATSR or SLSTR depending on coverage period
- OE used in CDR v2 is replaced with a bias-aware OE in CDR v3 to account for measurement biases
- CDR v3 will use HIRS to improve retrieval in the presence of stratospheric aerosols
- RTTOV 12.3 will be used to reduce biases due to dust aerosol

2.3. Error estimation of Pathfinder Version 5.3 SST Level 3C using extended triple collocation approach - Korak Saha

- Discussed the benefits of using Tripe Collocation (TC) to estimate errors in SST
- Provided brief technical background on TC and Extended TC (ETC)
- Applied the ETC method using Pathfinder 5.3 L3C, AATSR ARC and *in situ* SST.
- Analysed data independence, RSMSE/correlation for several types of *in situ* data (Ships, Drifters, Argo and Tropical/Coastal moored buoys)
- RMSEs for PF53 and correlation using ETC indicate consistency with the ARC dataset.

2.4. SGLI SST Ver. 2.0 - Yukio Kurihara

- Introduced a new cloud masking strategy for near land seas and inland waters for JAXA's SGLI SST v2 which includes a specific "coast test"
- Provided information on SST retrieval algorithm used for SGLI SST (similar in v1 and v2)
- Provided information on changes on Quality Levels from v1 to v2
- Presented validation results of SGLI SST v2 for Daytime and Nighttime

2.5. Overview of AMSR-3 on the Global Observing Satellite for Greenhouse Gases and Water Cycle (GOSAT-GW) - *Misako Kachi*

- Provided overview of GOSAT-GW satellite specification
- Presented main goals of the AMSR3 mission
- Provided a description of AMSR3 sensor characteristics and available channels
- Provided a list of standard and research products anticipated for AMSR3 and highlighted differences with AMSR2 products

2.6. A Priori Bias Effects in the Optimal Estimation of Sea Surface Temperature Retrievals from Satellite IR Radiometers - *Goshka Szczodrak*

- Provided technical background on Optimal Estimation (OE)
- Applied OE with MODIS (Collection 6, channels 11 and 12 μm) in the North Atlantic Ocean and the Mediterranean Sea for the 2015-2016 period, using several Quality flags for matchups
- Forward model is based on RTTOV v12.1
- OE outperforms NLSST but only for nighttime SST retrieval
- Future work will focus on testing bias-aware OE

2.7. SST Observations during the SLSTR Tandem Phase - *Jonathan Mittaz*

- Compared SLSTR SST from S3A and S3B during tandem phase
- Analysed differences for several retrieval algorithms and quality flags
- Evaluated SST uncertainties using ESA CCI theoretical uncertainty
- Analysed biases and standard deviation as a function of cloud probability for several retrieval algorithms
- Highlighted the importance of the tandem phase data to identify and mitigate issues with SLSTR SST

2.8. Feasibility Analysis Of Sea Ice Concentration Data Reconstruction Over Arctic Based On Chinese Satellite-Borne Microwave Radiometer - *Qimao Wang/Lijian Shi*

- Described inter-sensor calibration of BTs derived from FY-3C/MWIR and F17/SSMIS
- Described the retrieval methodology of Sea Ice Concentration from BTs
- Illustrated consistency between SIC derived from FY-3C/MWIR and NSIDC

S1 - ORAL PRESENTATIONS - EXTENDED ABSTRACTS

S1-1: INFRARED RADIATIVE SIMULATED SSTSKIN THROUGH AEROSOL-BURDENED ATMOSPHERE

Bingkun Luo[(1)], Peter J Minnett[(1)], Nicholas R. Nalli[(2)]

(1) Rosenstiel School of Marine and Atmospheric Science, University of Miami,
Email: LBK@rsmas.miami.edu
(2) IMSG, Inc. at NOAA/NESDIS/STAR

1. INTRODUCTION

Infrared satellite observations of sea surface temperature (SST) have become essential for many applications in meteorology, climatology, and oceanography. Tropospheric aerosol concentrations increase infrared signal attenuation and affect the accuracy of infrared satellite SST retrievals. Dust present at different altitudes has varying effects on the skin SST (SST_{skin}) retrieval errors. To further investigate the physical mechanism of aerosol effects on satellite derived SST_{skin}, the aerosol radiative effect on the brightness temperature are being studied. Measurements of the vertical atmospheric temperature and relative humidity profiles using Vaisala RS92 radiosondes were obtained throughout the Aerosols and Ocean Science Expeditions. Radiosonde atmospheric profiles along with Modern-Era Retrospective analysis for Research and Applications, Version 2 (MERRA-2) three-dimensional dust aerosol has been used as input for radiative transfer model simulation; trying to find the vertical distributions of aerosol on simulated SST_{skin}. With the increasing of aerosol height, the SST_{skin} retrieval has larger negative bias, as the radiation effect depends on the temperature contrast between the dust layer and the sea surface. The goal of this study is to understand better the characteristics of vertical aerosol effects on satellite retrieved infrared SST_{skin}, and to derive empirical formulae for improved accuracies in aerosol-contaminated regions.

2. ABSTRACT

Sea surface temperature (SST) is an Essential Climate Variable (ECV). The radiative impact of mineral dust is one of the major contributors to inaccuracies in the satellite-retrieved sea surface skin temperature (SSTskin). Different aerosol dust vertical distributions have varying effects on the satellite-derived SSTskin (Luo et al. 2019). To further investigate the physical mechanisms of aerosol effects on TERRA MODerate-resolution Imaging Spectroradiometers (MODIS) derived SST_{skin}, the aerosol radiative effects were studied with a fast-radiative transfer model. Measurements of the SST_{skin} using highly accurate infrared radiometers on ships as well as of vertical atmospheric temperature and water vapour values using Vaisala RS92 radiosondes were obtained throughout the AERosols and Ocean Science Expeditions (AEROSE; Nalli et al. (2011)). The AEROSE data have been withheld from data assimilation schemes. The NASA Modern-Era Retrospective analysis for Research and Applications, Version 2 (MERRA-2; Gelaro et al. (2017)) three-dimensional aerosol dust concentrations have been used as input to radiative transfer model simulation. Based on the model simulations, we found that the TERRA MODIS retrieved SSTskin inaccuracies are related to 1) dust concentration in the atmosphere, 2) the dust layer altitude, which is related to 3) the aerosol dust layer temperature.

3. FIGURES

Inaccuracies in the TERRA MODIS retrieved SST_{skin} can be investigated by using atmospheric radiative transfer modelling. Brightness temperature simulations for TERRA MODIS infrared channels 20 (λ=3.8 μm), 29 (λ=8.9 μm), 31 (λ=11 μm) and 32 (λ=12 μm) have been performed with the RTTOV model, and the brightness temperatures are used to derive SST_{skin} according to NLSST.

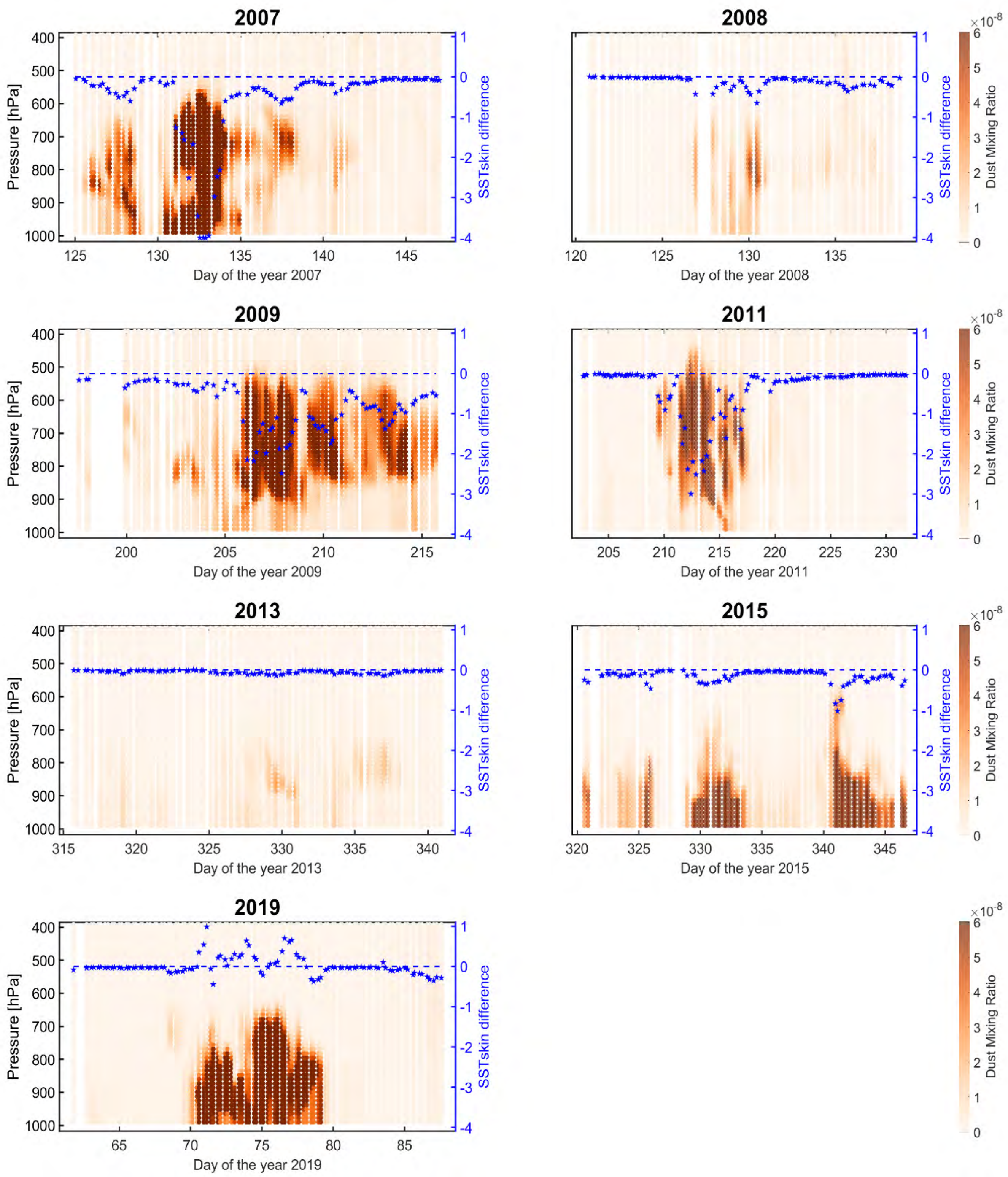

Figure 1: SST_{skin} differences from RTTOV simulations along the cruise tracks. The blue stars indicate the simulated SST_{skin} error caused by the aerosol according to the y-axis scale at right.

Figure 1 shows the RTTOV simulated results along each AEROSE cruise in this region; the blue stars are the simulated SST_{skin} error associated with the right y-axis (also blue). The left y-axis indicates the RTTOV pressure layer. The results from AEROSE 2007 to 2011 show that the negative SST_{skin} difference can be marked when the ship entered significant, large-scale Saharan dust outflow regions. Moreover, the uncertainties are related to the dust layer thickness and altitude.

Table 1. Dust layer altitude range and corresponding RTTOV pressure layers.

Altitude	Pressure
0 km - 1 km	922.46 hPa, 957.44 hPa, 985.88 hPa, 1005.43 hPa
1 km – 2 km	795.09 hPa, 839.95 hPa, 882.8 hPa
2 km – 3 km	702.73 hPa, 749.12 hPa
3 km – 4 km	610.60 hPa, 656.43 hPa

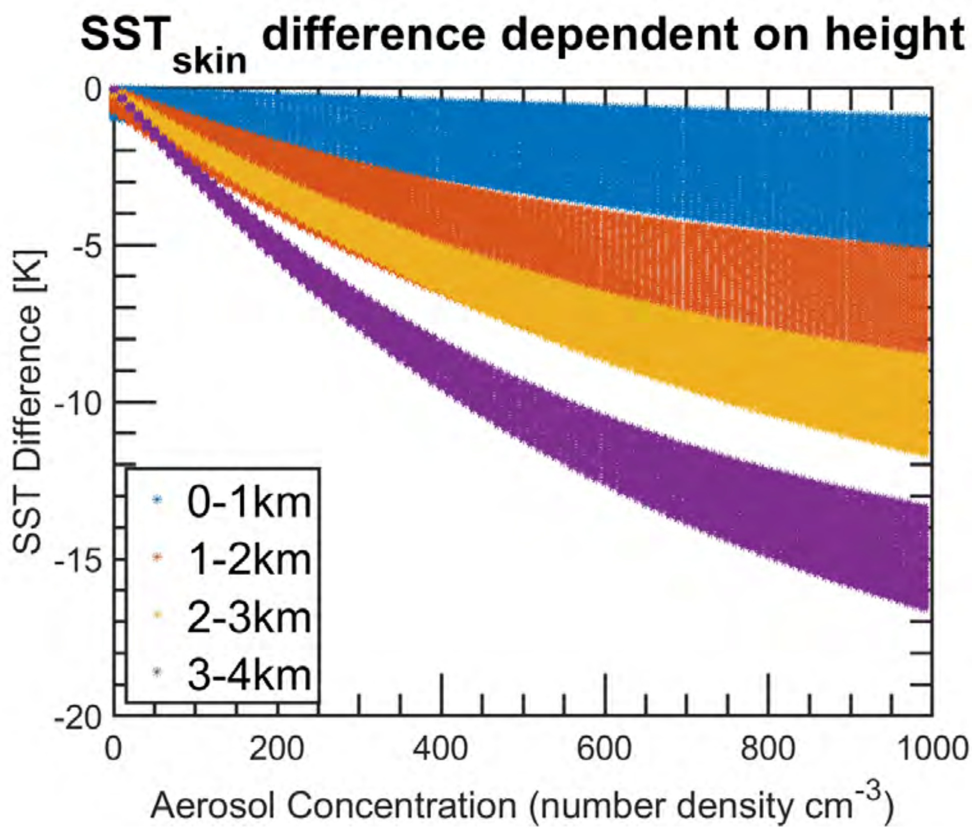

Figure 2. RTTOV simulation results showing the impact on the SST_{skin} retrieval of the altitude of the aerosol layer. Different colours indicate different altitudes of the dust layer. As the aerosol height is increased, the SST difference becomes more negative, except for very small concentrations.

Although the RTTOV simulations demonstrate a clear trend of an increasing error with denser and higher dust layers, the SST_{skin} retrieval sensitivity to varying vertical distributions can be better determined by simulations with a fixed atmospheric profile. Determining the sensitivity is the subject of this section. The RTTOV model was run with fixed atmospheric conditions taken from the McClatchey Standard Tropical Profile (McClatchey 1972), together with various dust concentrations and vertical distributions. Dust is inserted at four different altitudes in this study, corresponding to the defined RTTOV pressure levels shown in Table 2.

The SST_{skin} error between aerosol-contaminated and clear-sky situations is shown in Figure 2, with different colours indicating different altitudes. All of the simulations show a cooling effect due to dust; as expected, the cooling varies over a range of aerosol concentrations and dust heights. As shown in Figure 2, dust present at lower altitudes introduces a smaller SST_{skin} error.

4. CONCLUSION

The TERRA satellite provides a long-term, consistent and high-quality set of data records of the Earth system. SST_{skin}, as one of the mature products retrieved from MODIS onboard TERRA, has been developed and improved continually for many research and operational applications such as climate change studies and weather prediction. High-accuracy shipboard derived SST_{skin}, using M-AERI (Minnett et al. 2001), have been used to assess the aerosol dust effects. The variability in the thickness, altitudes and temperatures of dust layers can introduce additional uncertainties into comparisons between satellite- and M-AERI-derived SST_{skin}. As the aerosol altitude increases, the SST_{skin} difference becomes more negative, because higher dust layers have larger temperature contrasts to the sea surface. Saharan dust layers present in the lower troposphere are usually accompanied with high air temperatures, so the consequences on the MODIS-derived SST_{skin} are positive.

This study focuses on MODIS onboard TERRA but the MODIS onboard AQUA has consistent design and performance in terms of their spectral channels, calibration stability and other characterizations (Xiong et al. 2009). We expect similar results would be obtained for Aqua MODIS SST_{skin} retrievals. Future work is planned to include a scheme to reduce the infrared satellite SST_{skin} errors by accounting for the vertical dust distribution.

5. REFERENCES

Gelaro, R., McCarty, W., Suárez, M.J., Todling, R., Molod, A., Takacs, L., Randles, C.A., Darmenov, A., Bosilovich, M.G., Reichle, R., Wargan, K., Coy, L., Cullather, R., Draper, C., Akella, S., Buchard, V., Conaty, A., Silva, A.M.d., Gu, W., Kim, G.-K., Koster, R., Lucchesi, R., Merkova, D., Nielsen, J.E., Partyka, G., Pawson, S., Putman, W., Rienecker, M., Schubert, S.D., Sienkiewicz, M., & Zhao, B. (2017). The Modern-Era Retrospective Analysis for Research and Applications, Version 2 (MERRA-2). Journal of Climate, 30, 5419-5454

Luo, B., Minnett, P.J., Gentemann, C., & Szczodrak, G. (2019). Improving satellite retrieved night-time infrared sea surface temperatures in aerosol contaminated regions. Remote Sensing of Environment, 223, 8-20

Minnett, P.J., Knuteson, R.O., Best, F.A., Osborne, B.J., Hanafin, J.A., & Brown, O.B. (2001). The Marine-Atmospheric Emitted Radiance Interferometer (M-AERI), a high-accuracy, sea-going infrared spectroradiometer. Journal of Atmospheric and Oceanic Technology, 18, 994-1013

Nalli, N.R., Joseph, E., Morris, V.R., Barnet, C.D., Wolf, W.W., Wolfe, D., Minnett, P.J., Szczodrak, M., Izaguirre, M.A., Lumpkin, R., Xie, H., Smirnov, A., King, T.S., & Wei, J. (2011). Multiyear Observations of the Tropical Atlantic Atmosphere: Multidisciplinary Applications of the NOAA Aerosols and Ocean Science Expeditions. Bulletin of the American Meteorological Society, 92, 765-789

Xiong, X., Wenny, B.N., & Barnes, W.D. (2009). Overview of NASA Earth Observing Systems Terra and Aqua moderate resolution imaging spectroradiometer instrument calibration algorithms and on-orbit performance. Journal of Applied Remote Sensing, 3, 032501

S1-3: MODIS SEA-SURFACE TEMPERATURES: CHARACTERISTICS OF THE R2019.0 REPROCESSING OF THE TERRA AND AQUA MISSIONS

Peter J Minnett[(1)], Kay Kilpatrick[(1)], Goshka Szczodrak[(1)], Miguel Izaguirre[(1)], Bingkun Luo[(1)], Chong Jia[(1)], Chris Proctor[(2)], Sean W. Bailey[(2)], Edward Armstrong[(3)], Jorge Vazquez-Cuervo[(3)], and Wen-Hao Li[(3)]

(1) Rosenstiel School of Marine and Atmospheric Science, University of Miami, Miami, FL, USA,
Emails: pminnett@rsmas.miami.edu, kkilpatrick@rsmas.miami.edu, goshka@rsmas.miami.edu
mizagruirre@rsmas.miami.edu, lbk@rsmas.miami.edu, chong.jia@rsmas.miami.edu
(2) NASA Goddard space Flight Center, Greenbelt, MD, USA
Emails: christopher.w.proctor@nasa.gov, sean.w.bailey@nasa.gov
(3) NASA Jet Propulsion Laboratory, Pasadena, CA, USA.
Emails: edward.m.armstrong@jpl.nasa.gov,
jorge.vazquez@jpl.nasa.gov, wen-hao.li@jpl.nasa.gov

1. INTRODUCTION

The Moderate Resolution Imaging Spectroradiometer (MODIS) is a 36-band imaging radiometer on the NASA Earth Observing System satellites *Terra*, launched in December 1999, and *Aqua*, launched in May 2002. Included in the innovations in the design of MODIS are (i) multiple detectors - ten - for each spectral band so that ten lines of pixels are measured simultaneously across the swath, (ii) a dual-sided scan mirror, and (iii) several advances to ensure the calibration, both radiometric and spectral, of the measurements. For calibration of the IR measurements, a grooved plate blackbody target with twelve embedded thermometers was developed, and the measurements of this along with those of cold space provided a two-point radiance calibration (Minnett and Smith, 2014). The swath width of MODIS is 2330 km meaning a single day's coverage is not entire with interswath gaps at low latitudes, but the gaps from one day are filled in on the next. The spatial resolution of the IR bands is 1 km at nadir. Further details of the ocean remote sensing of MODIS are given by Esaias et al. (1998). MODIS is much more complex than other radiometers used for deriving SST, but uses the same atmospheric transmission "windows." The two bands in the 10–12 μm wavelength interval have bandwidths of ~0.5 μm, which are about half of those of the AVHRR and ATSR-SLSTR series. MODIS also has three narrow bands in the 3.7–4.1 μm window, which, although limited by solar effects during the day, generally produce more accurate retrievals of SST during the night (Kilpatrick et al., 2015). Several of the other MODIS bands contribute to improving the SSTs by better identification of residual cloud and aerosol contamination (Kilpatrick et al., 2015; Kilpatrick et al., 2019).

At the end of 2019, the Ocean Biology Processing Group at NASA Goddard space Flight Center (GSFC) completed the reprocessing of SST_{skin} retrievals from the measurements of MODIS on *Terra* and *Aqua*. The L2P data files have been generated at NASA Jet Propulsion Laboratory and are available at the Physical Oceanography Distributed Active Archive Center (PO.DAAC).

The focus here is the 11-12 μm "split-window" atmospheric correction algorithm based on the Non-Linear SST (NLSST; Walton et al., 1998), with coefficients optimized for months and latitude bands, derived from matchups with drifting buoys (Kilpatrick et al., 2015). The Match-Up Data Bases (MUDBs) for MODIS on *Terra* and *Aqua* are very large sets of comparisons between MODIS brightness temperatures and collocated within 10km and coincident within 30 minutes measurements of drifting and moored buoys taken from the NOAA *in situ* SST quality monitor (iQuam v 2.1; Xu and Ignatov, 2014), and the ship-board radiometers M-AERIs (Marine-Atmospheric Emitted Radiance Interferometer; Minnett et al., 2001) and ISARs (Infrared SST Autonomous Radiometer; Donlon et al., 2008). Subsets of the MUDBs are used to develop the cloud-screening and atmospheric correction algorithms to derive SST_{skin} from the MODIS measurements, and a withheld subset is used to assess the accuracy of the SST_{skin} retrievals. The ship radiometer data are withheld from the algorithm development and so are also available for accuracy assessment.

2. R2019 ALGORITHM IMPROVEMENTS

The previous version of the MODIS SST_{skin} retrievals is referred to as R2014 (or Collection 6 in the older designation scheme). The major changes in R2019, discussed below, address a number of issues to improve the performance of the SST_{skin} retrieval algorithms, both in improved accuracy and coverage.

2.1. Replacing the NOAA OI "Reynolds" SSTs, with the CMC as the reference field.

It has been a concern over some time that the quality and coverage of the so-called "Reynolds" SSTs derived by Optimum Interpolation of AVHRR data has become degraded (Liu et al., 2019), and so these have been replaced as the reference SST fields in the MODIS retrieval scheme by those of the Canadian Meteorological Centre (CMC; Brasnett and Surcel-Colan, 2016).

2.2. New cloud screening – Alternating Decision Tree.

Building on our experience with the AVHRR Pathfinder SST program (Kilpatrick et al., 2001), cloud screening in the R2014 and earlier schemes was based on a linear Binary Decision Tree (BDTree) comprising a sequence of tests to identify signatures of clouds being present based on spatial and spectral tests. A pixel, or groups of pixels, must pass all tests to be classified as cloud-free. The BDTree has been found to be too conservative and misclassified clear-pixels as cloudy, and in common with all cloud masking schemes, misclassifying cloudy pixels as clear. Misclassification of a cloud-contaminated pixel as clear obviously introduces errors in SST_{skin} retrievals: unidentified cloud within a pixel nearly always results in a negative bias in SST (Ackerman et al., 1998). In contrast, an overly conservative cloud mask can introduce significant sampling errors, as many truly cloud-free pixels are excluded from spatially-binned SST fields, leading to incomplete SST coverage. More importantly, the excessive censoring of lower (yet cloud-free) SST values leads to a failure in capturing the true geophysical variability of SST (Liu and Minnett, 2016; Liu et al., 2017; Kilpatrick et al., 2019). False masking of valid yet anomalously cold sea surface pixels is a pervasive problem for cloud detection algorithms (Merchant et al., 2005).

The R2019 processing uses an Alternating Decision Tree (ADTree) in which similar spatial and spectral tests are applied, but the results from all tests are retained, and a weighted average of outcomes determines the likelihood of being cloud-free (Freund and Mason, 1999; Pfahringer et al., 2001; Kilpatrick et al., 2019). The algorithm and the weights that are applied to the results of each test were determined by an AI analysis of a subset of the MUDBs.

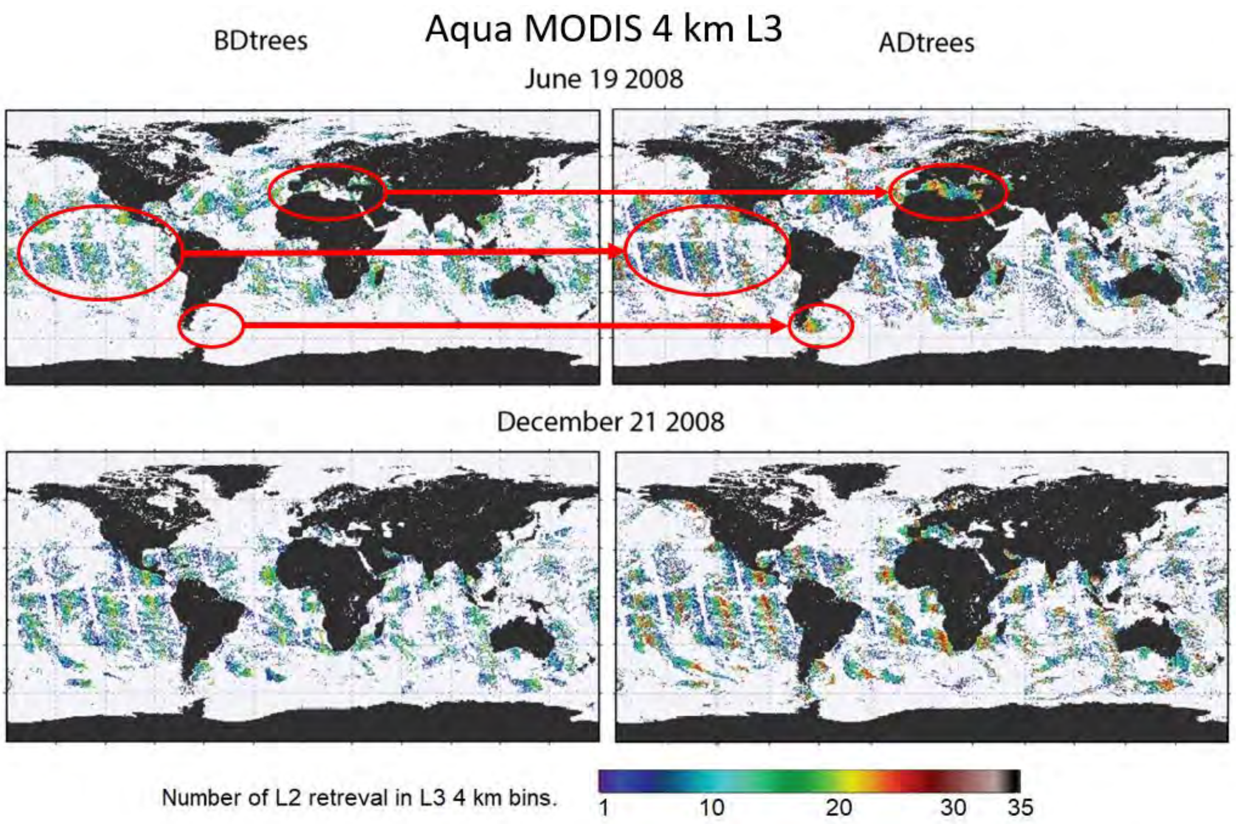

Figure 1. The increase in MODIS SST_{skin} retrieval coverage resulting from the use of ADTree (right) compared to BDTree (left) cloud screening algorithms for two representative days. Examples of areas where the benefit are highlighted in red. After Kilpatrick et al. (2019).

Figure 1 illustrates the increase in the coverage that results from the introduction of the ADTree cloud screening in the derivation of *Aqua* MODIS SST_{skin} fields on two representative days. Although the improvement is widespread, areas that benefit significantly include at high latitudes and the Mediterranean Sea. Further details of the ADTree cloud screening algorithms are given by Kilpatrick et al. (2019).

2.3. Aerosol Correction.

The presence of dense aerosol layers in the atmosphere has long been recognized as a source of error in satellite retrievals of SST using satellite infrared radiometry (Kilpatrick et al., 2001; Vazquez-Cuervo et al., 2004; Díaz et al., 2001). An area that is especially prone to such aerosol effects is the equatorial and tropical north Atlantic Ocean where frequent outflows of Saharan dust aerosol occur (Adams et al., 2012). The effects of the Saharan dust on the derivation of SST_{skin} from MODIS measurements is further complicated by the fact that the dust layers are frequently embedded in very dry layers in the atmosphere (Szczodrak et al., 2014). An analysis of a subset of the MUDBs and infrared radiative transfer simulations using RTTOV (Hocking et al., 2018) resulted in the definition of an index indicating when an additional aerosol correction term should be applies to the standard MODIS SST_{skin} retrieval algorithm. The index and aerosol correction term have been derived using measurements at wavelengths of 3.8, 8.9, 11.0 and 12.0 µm; because of the use of mid-IR measurements, the correction can only be used at night (Luo et al., 2019).

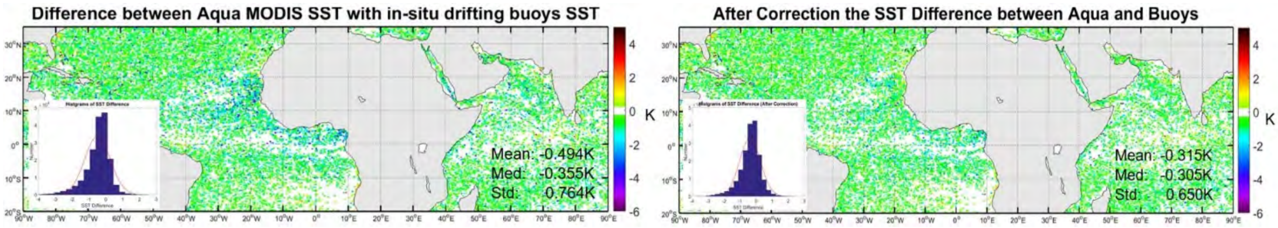

Figure 2. Distributions of the differences in the Aqua MODIS SST_{skin} and subsurface temperatures from drifting buoys (which are adjusted by -0.17 K to account for a mean skin effect) before the application of the aerosol correct (left) and after (right), Insets show the histograms of the differences. From Luo et al. (2019).

The occurrence of larger negative retrievals errors are shown in Figure 2 (left) in blue, and indicate the area influenced by Saharan dust outbreaks off West Africa. The improvements resulting from the application of the dust correction are apparent in Figure 2 (right). Although the correction was derived using data taken in the region of Saharan dust outflows, the correction is applicable elsewhere as is seen in the Arabian Sea, where the aerosols have different origins. Further details are given by Luo et al. (2019).

2.4. High-Latitude coefficients.

Given that the NLSST atmospheric correction algorithm is based on compensating the radiative effects of atmospheric water vapour which has a wavelength dependence in the atmospheric transmission “window” in the thermal infrared, inaccuracies in the Arctic SST_{skin} retrievals from satellite infrared radiometers are generally greater than elsewhere because the Arctic atmosphere is often drier and colder. The relationship between the atmospheric effect and radiance measurements at different wavelengths is not robust (Jia, 2019) Thus, improvement to Arctic SST_{skin} retrieval accuracy is imperative as these are required to support research into Arctic Amplification of the changing climate (Serreze and Barry, 2011; Pithan and Mauritsen, 2014).

In the R2014 retrieval scheme, high northern latitude retrievals were derived from matchups > 40°N (Kilpatrick et al., 2015), so are not optimized for retrievals in Arctic conditions. An analysis of records in the MUDBs taken north of 60°N, which are primarily in the Norwegian, Iceland and Greenland Seas, in the years 2013-2017 shows a strong seasonal pattern (Figure 3). Deriving coefficients north of 60°N from the MUDBs greatly reduces the season variations. The median differences are reduced from -0.475 K for R2014 coefficients to – 0.185 K for R2019 coefficients. However, robust standard deviations are not improved: 0.481 K becomes 0.486 K. For the R2019 processing algorithm, coefficients for the latitude bands 40-60°N and > 60°N were derived from the entire missions.

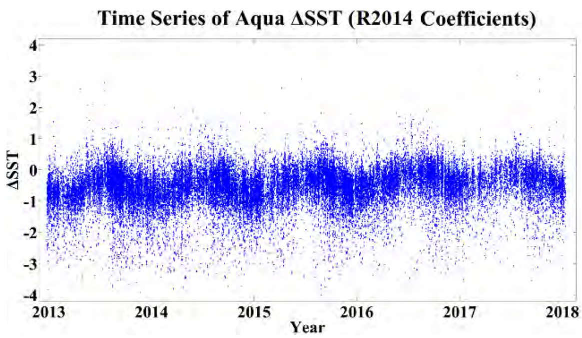

Figure 3. Time series of the differences between Aqua MODIS SST_{skin} and subsurface temperatures from drifting buoys (which are adjusted by -0.17 K to account for a mean skin effect) in the area north of 60°N. The coefficients in the atmospheric correction algorithm were derived from matchups north of 40°N.

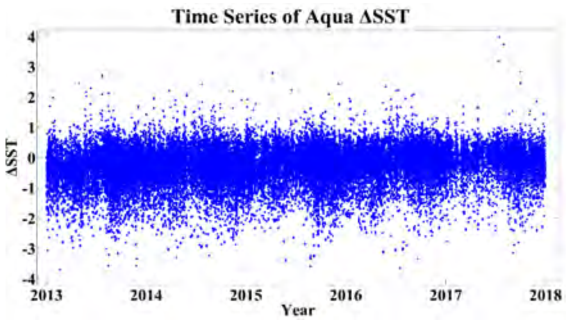

Figure 4. As Figure 3 but with R2019 coefficients derived from matchups north of 60º N.

2.5. Improvement to cloud-ice discrimination.

A daytime flag for ice was introduced in the R2019 processing scheme, using reflectances at wavelengths of 1.6 µm and 671 nm to reduce the misclassification of ice as open water during transitional ice conditions. The reflectance thresholds were determined from spectral histograms of images visually classified as snow or ice from Sentinel-2 MSI (MultiSpectral Instrument) calibrated reflectance (Hollstein et al., 2016).

The thresholds for the ice are:

$$(\rho(671\text{ nm}) > 0.3)\ \&\ (0.1 > \rho(1.6\ \mu\text{m}) \geq 0.006)$$

3. OUTLOOK

Both MODISs are in good physical and radiometric condition after > 20 years on orbit for *Terra* and > 18 years for *Aqua*. Prospects are good for these satellites and the MODISs they carry to continue for several years into the future. Funding for the missions and science teams is through the NASA Senior Review process, which has a three-year cycle. Currently we are in the second year. A proposal for continuing SST_{skin} studies for another three years have been submitted.

4. SUMMARY & CONCLUSION

Despite their very long lifetimes on orbit, both MODIS's are very stable and accurate instruments in the IR. The R2019 algorithm developments show improved coverage and accuracy; further details are available at https://oceancolor.gsfc.nasa.gov/atbd/sst/.

The R2019 SST_{skin} fields are available at the OBPG (L2 and L3) and PO.DAAC (L2p and L3). The regeneration of the R2019 MODIS MUDBs is a casualty of the restricted operations at NASA Goddard due to the COVID-19 pandemic and will be resumed as soon as possible.

Future developments include new approach to SSES derivation and specification (Kumar et al., 2020), and further research will focus on:

- Improvements to aerosol correction, including daytime corrections.
- High-latitude improvements, including new algorithm formulation with explicit emissivity dependence and exploiting Saildrone data in the Arctic (Gentemann et al., 2020).

5. REFERENCES

Adams, A.M., Prospero, J.M., & Zhang, C. (2012). CALIPSO-Derived Three-Dimensional Structure of Aerosol over the Atlantic Basin and Adjacent Continents. *Journal of Climate 25*, 6862-6879. 10.1175/JCLI-D-11-00672.1

Brasnett, B., & Surcel-Colan, D. (2016). Assimilating Retrievals of Sea Surface Temperature from VIIRS and AMSR2. *Journal of Atmospheric and Oceanic Technology 33*, 361-375. 10.1175/jtech-d-15-0093.1

Díaz, J.P., Arbelo, M., Expósito, F.J., Podestá, G., Prospero, J.M., & Evans., R. (2001). Relationship between errors in AVHRR-derived sea surface temperature and the TOMS Aerosol Index. *Geophysical Research Letters 28*, 1989–1992.

Donlon, C., Robinson, I.S., Reynolds, M., Wimmer, W., Fisher, G., Edwards, R., & Nightingale, T.J. (2008). An Infrared Sea Surface Temperature Autonomous Radiometer (ISAR) for Deployment aboard Volunteer Observing Ships (VOS). *Journal of Atmospheric and Oceanic Technology 25*, 93-113.

Esaias, W.E., Abbott, M.R., Barton, I., Brown, O.B., Campbell, J.W., Carder, K.L., Clark, D.K., Evans, R.H., Hoge, F.E., Gordon, H.R., Balch, W.M., Letelier, R., & Minnett., P.J. (1998). An Overview of MODIS Capabilities for Ocean Science Observations. *IEEE Transactions on Geoscience and Remote Sensing 36*, 1250-1265. doi: 10.1109/36.701076

Freund, Y., & Mason, L. (1999). The alternating decision tree learning algorithm. In Proceedings of Proceeding of the Sixteenth International Conference on Machine Learning, Bled, Slovenia, I. Bratko, & S. Dzeroski (Eds.), (124-133 pp). doi:

Gentemann, C.L., Minnett, P.J., Steele, M., Vazquez, J., Tang, W., Hoyer, J., Skarpalezos, S., Zhang, C., Zhang, D., & Jenkins, R. (2020). 2019 Arctic Saildrone Field Campaign: Measurements of Sea Surface Salinity and Temperature for Validation of Satellite Retrievals. In Proceedings of 21sr Science Team Meeting of the Group for High Resolution Sea-Surface Temperature, (xx pp). doi: tbd.

Hocking, J., Rayer, P., Rundle, D., Saunders, R., Matricardi, M., Geer, A., Brunel, P., & Vidot, J. (2018). RTTOV v12 Users Guide, *EUMETSAT Satellite Application Facility on Numerical Weather Prediction (NWP SAF)*, (142 pp.): EUMETSAT. Available at https://www.nwpsaf.eu/site/ download/documentation/rtm/docs_rttov12/NWPSAF-MO-DS-029_Prod_Spec_RTTOV12.pdf.

Hollstein, A., Segl, K., Guanter, L., Brell, M., & Enesco, M. (2016). Ready-to-Use Methods for the Detection of Clouds, Cirrus, Snow, Shadow, Water and Clear Sky Pixels in Sentinel-2 MSI Images. *Remote Sensing 8*, 666.

Jia, C. (2019). Satellite Infrared Retrievals of Sea Surface Temperature at High Latitudes. MS Thesis, Meteorology and Physical Oceanography. University of Miami. Miami. FL, USA. pp. 79. Available at https://scholarlyrepository.miami.edu/oa_theses/788/.

Kilpatrick, K.A., Podestá, G., Walsh, S., Williams, E., Halliwell, V., Szczodrak, M., Brown, O.B., Minnett, P.J., & Evans, R. (2015). A decade of sea surface temperature from MODIS. *Remote Sensing of Environment 165*, 27-41. http://dx.doi.org/10.1016/j.rse.2015.04.023

Kilpatrick, K.A., Podestá, G., Williams, E., Walsh, S., & Minnett, P.J. (2019). Alternating Decision Trees for Cloud Masking in MODIS and VIIRS NASA Sea Surface Temperature Products. *Journal of Atmospheric and Oceanic Technology 36*, 387-407. DOI: 10.1175/jtech-d-18-0103.1

Kilpatrick, K.A., Podestá, G.P., & Evans, R.H. (2001). Overview of the NOAA/NASA Pathfinder algorithm for Sea Surface Temperature and associated Matchup Database. *Journal of Geophysical Research 106*, 9179-9198.

Kumar, C., G. P. Podestá, K. A. Kilpatrick, & Minnett., P.J. (2020). A Machine Learning Approach to Estimating the Error in Satellite Sea Surface Temperature Retrievals. *Remote Sensing of Environment. In revision.*

Liu, C., Freeman, E., Kent, E.C., Huang, B., Zhang, H.M., Berry, D.I., Worley, S.J., Ouellet, M., Gaboury, I., Li, Z., & Banzon, V.F. (2019). ICOADS Drifting Buoy Data Recovery from BUFR and Its Impact on the OISST and ERSST. Presented at American Meteorological Society 99th annual Meeting, Phoenix, AZ, USA. (https://ams.confex.com/ams/2019Annual/webprogram/Paper352621.html), Liu, Y., Chin, T.M., & Minnett, P.J. (2017). Sampling errors in satellite-derived infrared sea-surface temperatures. Part II: Sensitivity and parameterization. *Remote Sensing of Environment 198*, 297-309. http://dx.doi.org/10.1016/j.rse.2017.06.011

Liu, Y., & Minnett, P.J. (2016). Sampling errors in satellite-derived infrared sea-surface temperatures. Part I: Global and regional MODIS fields. *Remote Sensing of Environment 177*, 48-64. http://dx.doi.org/10.1016/j.rse.2016.02.026

Luo, B., Minnett, P.J., Gentemann, C., & Szczodrak, G. (2019). Improving satellite retrieved night-time infrared sea surface temperatures in aerosol contaminated regions. *Remote Sensing of Environment 223*, 8-20. https://doi.org/10.1016/j.rse.2019.01.009

Merchant, C.J., Harris, A.R., Maturi, E., & MacCallum, S. (2005). Probabilistic physically based cloud screening of satellite infrared imagery for operational sea surface temperature retrieval. *Quarterly Journal of the Royal Meteorological Society 131*, 2735–2755. doi: 10.1256/qj.05.15

Minnett, P.J., Knuteson, R.O., Best, F.A., Osborne, B.J., Hanafin, J.A., & Brown, O.B. (2001). The Marine-Atmospheric Emitted Radiance Interferometer (M-AERI), a high-accuracy, sea-going infrared spectroradiometer. *Journal of Atmospheric and Oceanic Technology 18*, 994-1013.

Minnett, P.J., & Smith, D.L. (2014). Postlaunch Calibration and Stability: Thermal Infrared Satellite Radiometers. In G. Zibordi, C.J. Donlon, & A.C. Parr (Eds.), *Experimental Methods in the Physical Sciences, Vol 47, Optical Radiometry for Ocean Climate Measurements* (pp. 201-243): Academic Press. 1079-4042. http://dx.doi.org/10.1016/B978-0-12-417011-7.00008-8.

Pfahringer, B., Holmes, G., & Kirkby, R. (2001). Optimizing the Induction of Alternating Decision Trees. In Proceedings of Fifth Pacific-Asia Conference on Advances in Knowledge Discovery and Data Mining., Hong Kong, China, (477-487 pp). doi:

Pithan, F., & Mauritsen, T. (2014). Arctic amplification dominated by temperature feedbacks in contemporary climate models. *Nature Geosci 7*, 181-184. 10.1038/ngeo2071

Serreze, M.C., & Barry, R.G. (2011). Processes and impacts of Arctic amplification: A research synthesis. *Global and Planetary Change 77*, 85-96. http://dx.doi.org/10.1016/j.gloplacha.2011.03.004

Szczodrak, M., Minnett, P.J., & Evans, R.H. (2014). The effects of anomalous atmospheres on the accuracy of infrared sea-surface temperature retrievals: Dry air layer intrusions over the tropical ocean. *Remote Sensing of Environment 140*, 450-465. http://dx.doi.org/10.1016/j.rse.2013.09.010

Vazquez-Cuervo, J., Armstrong, E., & Harris, A. (2004). The effect of Aerosols and Clouds on the Retrieval of Infrared Sea Surface Temperatures. *Journal of Climate 17*, 3921-3933.

Walton, C.C., Pichel, W.G., Sapper, J.F., & May, D.A. (1998). The development and operational application of nonlinear algorithms for the measurement of sea surface temperatures with the NOAA polar-orbiting environmental satellites. *Journal of Geophysical Research 103*, 27,999-928,012.

Xu, F., & Ignatov, A. (2014). In situ SST Quality Monitor (iQuam). *Journal of Atmospheric and Oceanic Technology 31*, 164-180. 10.1175/JTECH-D-13-00121.1

S1-4: RETRIEVAL OF SST FROM COPERNICUS IMAGING MICROWAVE RADIOMETER (CIMR) OBSERVATIONS

Jacob Hoeyer

Danish Meteorological Institute, Email: jlh@dmi.dk

SHORT ABSTRACT

The Copernicus Imaging Microwave Radiometer (CIMR) being investigated by ESA for the Copernicus Expansion program of the European Union is a polar mission, designed to observe all-weather, high-resolution, high-accuracy, sub-daily observations of sea surface temperature and sea ice. It is the intention to include several of the radiometer channels which are also on AMSR2 and it is therefore important to assess the impact of using different channel selections.

This presentation will assess and discuss the optimal channel selection for SST retrievals using two different SST retrieval algorithm types, a physical and a statistical retrieval algorithm for AMSR observations. The first is an Optimal Estimation (OE) algorithm (Nielsen-Englyst et al, 2018), which inverts a forward model to retrieve SST. The second retrieval algorithm has been used to generate the ESA CCI PMW CDR and is made up of a two-stage regression model where stage one retrieves wind speed and stage two applies localized algorithms to retrieve SST using the retrieved wind speeds from stage one and information from NWP (Alerskans et al., 2020).

The different combinations of AMSR channels have been tested to assess the impact of using fewer channels in different combinations compared to using all channels. The SST retrieved by the two algorithm types are compared to independent in-situ SSTs from drifting buoys and Argo floats to assess the most optimal channel selection and the strengths and weaknesses for each of the two algorithms. Overall, the performance increases as expected when more channels are included in the retrieval. Both retrieval algorithms agree that the three-channel configuration 6, 10, 18 GHz (V and H polarization) is better than the 6, 10, 23 GHz configuration (V and H polarization). Furthermore, this analysis shows that generally, a Copernicus Imaging Microwave Radiometer (CIMR) like channel configuration (excluding the 23 GHz channels) provides an equally good performance compared to the AMSR-E channel configuration for most regions using both retrieval algorithms.

S1 - POSTER PRESENTATIONS - SHORT ABSTRACTS

S1-P1: OPERATIONAL SEA SURFACE TEMPERATURE RETRIEVAL USING GK2A OF KMA

JaeGwan Kim, JunTae Choi, SeongHun Cheong

National Meteorological Satellite Center of KMA
Email: kimjgwan@korea.kr

SHORT ABSTRACT

The GEO-KOMPSAT-2A (GK2A), the 2nd geostationary meteorological satellite of the South Korea, was launched on 4th December 2018. National Meteorological Satellite Center (NMSC) of the Korea Meteorological Administration (KMA) developed Sea Surface Temperature (SST) retrieval algorithm with Himawari-8 and tuned with GK2A data during the In-Orbit Test (IOT) period. The SST algorithm is based on Multi-band SST (MSST) with 4 infrared channels. The SST was verified with *in situ* data and the bias and RMSE are less than 0.1 degree and 0.5 degree in Celsius, respectively. For the contingency plan, other algorithms are also prepared, which are Hybrid-SST, Non-Linear SST, and Multi-Channel SST. As the SST observed by imager sensor works only on cloud free area, the GK2A SST is composited with 1day, 5days, and 10days to fill the void area on the ocean. In addition, SST data from several satellites are blended to produce a multi-sensor SST every day. These composite and blended SST data are verified with OSTIA data. The SST products has been serviced operationally in KMA since March of 2020. Finally, the era of GK2A satellite has begun to produce sea surface temperature on the sea over Asia and Oceania.

In this study, we will introduce the algorithms of the GK2A SST and validation results of the GK2A SST.

S1-P2: SST RETRIEVAL DEVELOPMENTS FOR THE ESA CLIMATE CHANGE INITIATIVE

Owen Embury

Department of Meteorology, University of Reading
Email: o.embury@reading.ac.uk

SHORT ABSTRACT

Understanding the state of the climate requires long-term, stable observational records of essential climate variables (ECVs) such as sea surface temperature (SST). ESA's Climate Change Initiative (CCI) was set up to exploit the potential of satellite data to produce climate data records (CDRs). The initiative now includes over 20 projects for different ECVs, including SST, which released the second major version of the SST CCI CDR last year and is now beginning the third phase of the project which will focus on two main areas of development: including further developments towards bringing passive microwave (PMW) data into the main CDR, and improving the early infrared data used in the 1980s.

The early IR record will be addressed in two ways. Firstly, through the use of an improved "bias-aware" optimal estimation (OE) framework where bias correction and error covariance parameters are estimated using a form of Kalman filtering. Secondly through the use of the High-resolution Infra Red Sounder (HIRS) data to correct for the effects of El Chichon and Saharan dust aerosol in the retrievals.

S1-P3: ERROR ESTIMATION OF PATHFINDER VERSION 5.3 SST LEVEL 3C USING EXTENDED TRIPLE COLLOCATION APPROACH

Korak Saha[(1)], Prasanjit Dash[(3,4)], Xuepeng Zhao[(2)], Huai-Min Zhang[(5)]

(1) CISESS-Maryland, University of Maryland, College Park, MD 20740, USA; NCEI, NOAA/NESDIS, Silver Spring, MD 20910, USA, Email: korak.saha@noaa.gov
(2) National Centers for Environmental Information (NCEI), NOAA/NESDIS, Silver Spring, MD 20910, USA;
(3) Cooperative Institute for Research in Atmosphere (CIRA), Colorado State University, Fort Collins, CO 80523, USA;
(4) Center for Satellite Applications and Research (STAR), NOAA/NESDIS, College Park, MD 20740, USA; National Centers for Environmental Information (NCEI),
(5) NOAA/NESDIS, Asheville, NC 28801, USA

SHORT ABSTRACT

Generally, for validation purposes, satellite-derived SST products are compared against the *in situ* SSTs which have inaccuracies due to spatial/temporal inhomogeneity between *in situ* and satellite measurements. A standard deviation in their difference fields usually have contributions from both satellites as well as the *in situ* measurements. A real validation of any geophysical variable must require the knowledge of the “true” value of this variable. Therefore, a one-to-one comparison of satellite-based SST with *in situ* data does not truly provide us the real error in the satellite SST and there will be ambiguity due to errors in the *in situ* measurements and their collocation differences. A Triple collocation (TC) or three-way error analysis using three mutually independent error-prone measurements, is used to estimate root-mean square error (RMSE) associated with each of the measurements with a high level of accuracy without treating any one system a perfectly-observed “truth”. In this study, we are estimating the absolute random errors associated with Pathfinder Version 5.3 Level-3C (PF53) SST Climate Data Record. Along with the *in situ* SST data, the third source of the dataset used for this analysis is the AATSR reprocessing of climate (ARC) dataset for the corresponding period. All three SST observations are collocated, and statistics of the difference between each pair are estimated. Instead of using a traditional TC analysis we have implemented the Extended Triple Collocation (ETC) approach to estimate the correlation coefficient of each measurement system w.r.t. the unknown target variable along with their RMSEs. The RMSE ranged from 0.31 to 0.37 K for PF53 and 0.18 to 0.33 K for the ARC data. These values are reasonable, as evident from the very high unbiased SNR values (~0.98).

S1-P4: SGLI SST VER. 2.0

Yukio Kurihara[(1)], Kazunori Ogata, Hiroshi Murakami, Misako Kachi

(1) JAXA/EORC, Tsukuba-shi, Ibaraki, Japan,
Email: kurihara.yukio@jaxa.jp , ykuri.kiyo@gmail.com

SHORT ABSTRACT

It has been more than 2 years since the launch of the GCOM-C satellite which carries an optical sensor SGLI. SGLI SSTs from January 2018 to the latest, which have been retrieved from the split-window data of SGLI, are available at the JAXA Global Portal System (G-Portal)[*1]. Furthermore, JAXA started to provide SGLI SSTs in the GDS 2.0 in March 2020. The real-time SGLI SST product is available at the GHRSST server of JAXA/EORC[*2]. As the next step, JAXA is planning to update the SGLI SST product from version 1 to version 2.0 in 2020. In the next version, cloud masking will be improved, especially for coastal seas and inland waters. The quality flag will also be modified with the improvements in cloud masking. We compared SGLI SST 2.0 with buoy data. The comparison result shows good agreements between them. Bias and SD were almost stable from January 2018 to the end of 2019, and any remarkable seasonal cycle was not found. Meanwhile, cloud contamination is still conspicuous at nighttime, which is an issue with SGLI SST.

*1) https://www.gportal.jaxa.jp/gp/top.html

*2) https://suzaku.eorc.jaxa.jp/GHRSST/

S1-P5: OVERVIEW OF AMSR-3 ON THE GLOBAL OBSERVING SATELLITE FOR GREENHOUSE GASES AND WATER CYCLE (GOSAT-GW)

Misako Kachi[(2)], Naoto Ebuchi[(1,2)], Takashi Maeda[(2)], Nodoka Ono[(2)], Hideyuki Fujii[(2)], Kazuya Inaoka[(2)], Marehito Kasahara[(2)], Yasushi Kojima[(2)]

(1) Hokkaido University,
(2)Japan Aerospace Exploration Agency (JAXA)
Email: Kachi.misako@jaxa.jp

SHORT ABSTRACT

JAXA's Advanced Microwave Scanning Radiometer 2 (AMSR2) on the Global Change Observation Mission – Water (GCOM-W) has been operating in orbit since May 2012, succeeding AMSR-E observation since 2002. AMSR2 has 16 channels from 6.9 to 89 GHz, which enable to estimate various water-related parameters including SST, and the biggest antenna, which enables higher spatial resolution, among the passive microwave imagers in the world. Both GCOM-W and AMSR2 are in healthy condition to continue its operation in future.

JAXA has started development of AMSR2 follow-on mission, AMSR3 on the Global Observing SATellite for Greenhouse gases and Water cycle (GOSAT-GW), since December 2019, to succeed long-term observations of water cycle variations by AMSR-E and AMSR2. The GOSAT-GW satellite carries AMSR3 and the Greenhouse gases Observing SATellite-2 (GOSAT-2) successor mission led by Ministry of the Environment of Japan (MOE) and National Institute for Environmental Studies (NIES). AMSR3 will have 21 channels from 6.9 to 183.3±7 GHz with 2.0 m antenna. High-frequency channels of 165.5 GHz, 183±3 GHz, and 183±7 GHz V-polarization are newly available for snowfall retrievals and water vapour analysis in numerical weather prediction in meteorological agencies. Additional 10 GHz V and H polarization channels with wider band width and improved NEDT are also available to develop higher resolution sea surface temperature especially for fisheries around 30 km offshore from the coast. The GOSAT-GW satellite is currently targeting the launch in Japanese Fiscal Year of 2023.

S1-P6: A PRIORI BIAS EFFECTS IN THE OPTIMAL ESTIMATION OF SEA SURFACE TEMPERATURE RETRIEVALS FROM SATELLITE IR RADIOMETERS

Goshka Szczodrak, Peter Minnett

Rosenstiel School of Marine and Atmospheric Science, University of Miami, Miami, FL, USA
Email: goshka@rsmas.miami.edu

SHORT ABSTRACT

The Optimal Estimation (OE) approach gained popularity in the satellite sea surface temperature (SST) retrieval community with the promise of improving over the traditional non-linear SST retrieval algorithms especially their problem with regional biases.

The NLSST algorithms rely on coefficients that are obtained by least-squares regression to *in situ* data (buoy or drifter measurements) and therefore produce good estimates of SST in conditions that are represented by these coefficients. When the sea or atmospheric conditions depart from the average state the NLSST estimates can be quite erroneous. One way of reducing the NLSST errors is to derive multiple sets of coefficients specific to different seasons and geographical regions. In the OE approach a prior knowledge of the state of the ocean and the atmosphere at the time and place of each measurement is used to derive the SST so the OESST estimates should in principle be bias free.

However, the OE process can depend rather strongly on the *a priori* information. If, for example, the *a priori* SST field used is biased the OE will produce biased OESST estimates. Since typically a good *a priori* is needed to produce good OESST, the question arises how much the OESST estimates are an improvement of the *a priori* itself and are they really an improvement over the NLSST. We try to answer this question with an example of OESST retrievals for the MODIS instrument and the data in the MODIS match-up database.

S1-P7: SST OBSERVATIONS DURING THE SLSTR TANDEM PHASE

Jonathan Mittaz[(1)], Sam Hunt, Dace Smith

[(1)]*University of Reading, Reading, UK, Email: j.mittaz@reading.ac.uk*

SHORT ABSTRACT

We will present the initial analysis of the derived sea surface temperature (SST) products from the Sentinel-3A and Sentinel-3B Tandem phase data concentrating on observations taken at closest approach (a 30 second time difference). We will show that for the highest quality pixels from S3A and S3B agree to with 0.13K (1 sigma) even when S3B uses S3A retrieval coefficients showing that the two instrument are very similar in overall performance. Looking in more depth we will then show that there are clear small biases between the SSTs derived by the different SST algorithms (N2, N3, D2, D3) and the associated uncertainties show algorithm variations with some algorithms seemingly overestimating the uncertainties whereas other retrieval algorithms underestimate them.

Moving on to the other quality level data (GHRSST quality levels 3 and 4) a similar story can be seen to the case with excellent quality data. We will also show that a small but significant number of pixels change quality between the S3A and S3B observations which shows that the assigned quality level of a pixel is itself subject to some level of uncertainty. The effect of changing quality level also has an impact on the distribution of SST differences relative to uncertainty giving rise to the prospect of estimating any extra uncertainty which may be required for lower quality level SST data such as due to small levels of cloud contamination.

The Tandem phase for SLSTR on Sentinel-3A and Sentinel-3B has shown the power of having near contemporaneous observations which allow a study of aspects of SST retrieval not easily studied using *in situ* networks including studies not only between retrieval algorithms and associated uncertainties can be made but also of the presence and consequences of an uncertainty on SST quality levels which can also be studied for the first time.

S1-P8: FEASIBILITY ANALYSIS OF SEA ICE CONCENTRATION DATA RECONSTRUCTION OVER ARCTIC BASED ON CHINESE SATELLITE-BORNE MICROWAVE RADIOMETER

Qimao Wang, Lijian Shi

National Satellite Ocean Application Service, China,
Email: qmwang@mail.nsoas.org.cn

SHORT ABSTRACT

Sea ice concentration data of about 40 years with space-borne microwave radiometer has become the main data for global climate change research and polar prediction. The observation frequency setting of Chinese HY-2 and FY-3 Series satellites microwave radiometer is similar to that of DMSP/SSMIS, which has the potential to become the main data source of polar sea ice observation. Based on the brightness temperature data of HY-2B, FY-3C and FY-3D, this paper evaluates the feasibility of using them to retrieve the high-resolution sea ice concentration over the polar region. Firstly, Amazon forest and Greenland are selected as high-temperature and low-temperature targets respectively to evaluate the brightness temperature data uniformity and stability of different channels of the above satellites. Then, based on the brightness temperature data of F18/SSMIS in 2019, the corresponding band data of the above three satellites are inter-sensor calibrated to evaluate the stability and seasonal variation of the calibration coefficient throughout the year. Finally, based on different satellite brightness temperature data after inter-sensor calibration, different data reconstruction methods are used to build high-resolution brightness temperature data, and the feasibility of using it to retrieve sea ice concentration is evaluated by comparing with high-resolution image data.

S1 – AGENCY REPORT SUMMARY

Anne O'Carroll[1], Eileen Maturi[2], Yukio Kurihara[3]

(1) EUMETSAT, Darmstadt, Germany, Email: anne.ocarroll@eumetsat.int
(2) NOAA, Washington DC, USA, Email: eileen.maturi@noaa.gov
(3) JAXA, Japan, Email: ykuri.kiyo@gmail.com

1. INTRODUCTION

Day-1 of the 21st international GHRSST science team meeting included a session on agency reporting, together with contributions from 22 organisations. The agency summary slides include two-page summaries from each contributor. The individual agency summary slides are available on the GHRSST website under resources for Monday 1st June 2020 (https://www.ghrsst.org/agenda/ghrsst-xxi/).

This report contains a summary of the questions and discussions arising during the forum session.

2. SUMMARY OF AGENCY DISCUSSION POINTS

2.1. Report from CMA: Sujuan Wang

There was a comment on the good quality of SSTs from FY3D. It was noted that OSTIA is SST_{fnd} and a question on whether it works well as initial SST. Interest shown in the validation results.

At present, the first guess SST of operational FY3D/MERSI is OISST_DailyClim_1982-2011.nc. Comparisons of FY3D/MERSI 5-min granule SST (with optimal quality flag) with L4 CMC of April 2020, gives a daytime bias of -0.15 K with STD 0.78 K, and a nighttime bias of -0.29 K with STD 0.61 K. The first guess SST of FY3/VIRR reprocessing is OSTIA, including regional biases for many VIRR granules. Validation of daily FY3C/VIRR L3C SST from 2015 to 2016 against L4 CMC, gives the nighttime bias of 0.01 K with STD 0.67 K. One of the most important issues for FengYun SST retrieval is to choose the best first guess SST for the NLSST Algorithm. For the FY3C/VIRR nighttime reprocessing SST, there is a seasonal cycle at present (the recalibration of FY3C/VIRR history satellite data is in progress), and the daily STD at summer is sometimes slightly bigger than 1K.

The discussion concluded that these represented good results and that there is no large difference with the choice of initial SST.

There was a final question on a validation paper of FY3D MERSI SST and VIRR RV1. This has been written for FY3C/VIRR and is available from the Journal of Applied Meteorological Science.

2.2. RDAC update from OSI-SAF: Stephane Saux Picart

There was a request from the Bureau of Meteorology for information on when the OSI SAF Metop-C AVHRR L2P are available in parallel to Metop-B, as input for the BoM operational IMOS multi-sensor L3S product, and a request for the validation results. A validation report on Metop-C has been prepared by the OSI SAF and will be made available once a EUMETSAT review process is complete. The results are comparable to Metop-B, but with a slightly higher standard deviation during the day-time, which may be a cloud-masking issue.

There was clarification that the OSI SAF GEO products are mono-sensor L3 products. These include an hourly product which selects the best pixels within the hour, but with no averaging or interpolation.

There was a question on the schedule for release of Metop-C. For Metop-C this will happen after September 2020, and will be via the usual routes.

There is also an outstanding issue with regard to the DOI policy for OSI SAF datasets in the PO.DAAC and this is being followed up.

2.3. RDAC update from UK Met Office: Chonguan Mao

The discussion clarified recent updates to OSTIA: SLSTR-B was included operationally in OSTIA on 4th December 2019, and both SLSTR-A and SLSTR-B are planned to be used as the reference at the next system upgrade (together with N20 VIIRS); NOAA-19 AVHRR was removed and NOAA-20 VIIRS L3U SSTs introduced from 4th December 2019 (however NOAA-20 VIIRS is used in the reference but NOAA-19 AVHRR wasn't). The same change went into FOAM at the same time, but they do not use any satellite SSTs in their reference); both NPP and N20 are used for VIIRS.

There was a discussion on the observed cool bias in VIIRS SST, and conclusion that this should be investigated further together with NOAA, EUMETSAT and the Met Office.

2.4. Report from MISST: Chelle Gentemann

For those interested in using Saildrone data they can be found here: https://podaac.jpl.nasa.gov/announcements/NASA_Saildrone_Arctic_Campaign_Dataset_Released.

Ed Armstrong is interested in collaborating on the clarification of data for cloud computing, as part of the PO.DAAC and the SST-VC.

2.5. RDAC update from NAVO: Bruce McKenzie

Further information was requested on NAVOCEANO Metop-C AVHRR L2P, and these are provided in a poster from this year's meeting. Further information was requested between day/night and these were provided in the Moodle forum as an attachment. Excellent results were confirmed.

2.6. RDAC Update from JAXA: Misako Kachi

There were questions on the performance of AMSR-2 (and GCOM-W). No clear degradation's are seen. Some warm biases are observed in AMSR2 SST Version 3 in some regions, and there are plans to update SST to version 4 in 2020.

More information on SGLI (Second Generation Global Imager) was requested, particularly for 250 m resolution. The observation swath of SGLI is 1400 km for SWIR and TIR channels (~1100 km for VNR & Polarization channels), so SST coverage is ~1400 km for both 250 m (coastal area) and 1km resolution. It is in GDS2.0 format too.

Here is a link to validation results of SGLI SST with example images prepared by Yukio: https://suzaku.eorc.jaxa.jp/GHRSST/docs/JAXA_JOINT_PI_2019.pdf.

Appreciation was expressed for all JAXA programs and missions.

2.7. Report from ESA: Craig Donlon

Further information on the launch dates of CIMR and LSTM were requested.

All of the High Priority Copernicus Missions (HPCM) will start contract negotiations in the coming months and each will have its own timeline. For CIMR we may expect a first launch no earlier than 2028. For the Land Surface Temperature Monitoring (LSTM) it will be a similar timescale but perhaps a launch before CIMR (Copernicus Imaging Microwave Radiometer) since this is less technically complex compared to CIMR. We cannot yet say which consortia have "won" the contracts for Phase B2/C/D/E1 at this time.

This link (https://www.youtube.com/watch?v=TPTROy69q4k&feature=youtu.be) is a nice animation prepared by the HPS (High Performance Solutions) consortium that has been developing a European technical capability (initially with European Commission Funding) to build large deployable mesh reflector systems. There are also several on-going studies at ESA. HPS use a double pantograph deployable ring structure which is shown in the video that is quite a nice design: it is very lightweight, has good stiffness and can be packed into a relatively small volume which is important to fit the stowed reflector and boom into the launcher fairing. This is a complex business since the deployed reflector is trying to approximate a solid parabola shape. But in fact the surface shape is made up of triangulated facets that, depending on the frequency, lead to grating lobes within the antenna gain pattern. These must be accounted for in the L1b processing which will be a challenge. The video shows some of the activities of HPS including hinges to form the long boom supporting the reflector and how to deploy the reflector in a 1 G environment. Toward the end a mission that looks similar to CIMR is shown with an 8 m rotating reflector.

2.8. SQUAM and iQuam: Alexander Ignatov

There was appreciation for SQUAM and iQuam with many teams finding it useful for their validation activities. The inclusion of further datasets would be beneficial when possible.

2.9. GHRSST LTSRF: John Huai-Min Zhang

There was discussion on the latest status of products of NCEI and the LTSRF and how to request changes. The contact is Yongsheng.Zhang@noaa.gov. NCEI continues its integration from the old three Data Centers regime into an integrated one NCEI. NCEI-MD/Silver Spring is being merged into NCEI-NC/Asheville under the NESDIS MSN migration. CLASS is one tool for NCEI archive option; others include the NCEI Common Ingest system, and potentially other systems being migrated from other NCEI sites to NCEI-NC. Things are still being discussed through NCEI organization. If these datasets fall into the GHRSST system, NCEI would archive them according to GHRSST set up. NCEI Silver Spring LTSRF mechanism might be moved into NCEI common ingest with data being archive at NCEI, not CLASS. NCEI is still waiting for PO.DAAC to send G17 and HO8 to NCEI, so there is no update on these datasets this time. The G17 and H08 data should be ingested from PO.DAAC to NCEI handled by the NCEI Silver Spring LTSRF mechanism.

Ken Casey gave information that new NESDIS Common Cloud Framework (NCCF), where over the next several years they are working to migrate all their data (whether it is in NCEI, or CLASS, or STAR, or anywhere else in NESDIS for that matter) into the cloud. That will mean some changes but the details are still to be determined. Since GHRSST LTSRF has always provided a wide range of ways to get to the data (ftp, http, Hyrax, Live Access Server, TDS) they hope to add to those kind of services the ability for users to interact with the data directly in the cloud. It should open up new possibilities for everyone.

There was a question on user metadata on the LTSRF. NCEI doesn't log where the NCEI users are going after exploring GHRSST dataset landing pages. Not all of the requests are to download files per se. Many of the requests are using the HTTP HEAD method, rather than the HTTP GET method. HEAD will only download headers, not the entire file. Also, many of the requests are retrieving directory listings rather than files. These are counted as file downloads by the web statistics software, but they have much lower volume than retrieving the same number of complete data files. We do see the downloading volume doesn't rise so high compared to the number of hits.

2.10. GDAC: Ed Armstrong

NOAA commented that two geostationary ACSPO SSTs - G17 and H08 have been added to the GDAC. Together with G16, the three 3rd gen geo ABI/AHI sensors now cover ~60% of the ocean. NOAA also plan to produce SST from MTG FCI planned for launch in late 2021. This will add another 20%, leaving only Indian Ocean missing from the 3rd gen geo sensors coverage. NOAA plan on aggregating individual geo L3C products into a "global" L3S-GEO product.

2.11. RDAC Update from NASA: Ed Armstrong

There was a question whether MUR L4 includes VIIRS SST. This is not planned as yet as MUR has recently undergone a major platform and software migration. However, new data sources will be looked at next as it is realised VIIRS SST would provide a good improvement.

2.12. RDAC update from CMC: Dorina Surcel Colan

There was a question on whether Sentinel-3 SLSTR will be included. CMC are investigating downloading these data and will contact EUMETSAT with questions if needed.

2.13. RDAC update from NOAA/NESDIS/STAR1: Alexander Ignatov

There was a question on GEO coverage including over the Indian Ocean. Products will not be derived for the Indian Ocean until a new generation sensor is available. There will be 24 L3S-GEO files per day and consideration is being given into extending the 4 L3S-LEO files into 24 hourly files per day of super collated L3S.

2.14. RDAC update from CMEMS: Bruno Buongiorno Nardelli

It was clarified that major improvements come from using dual view as a reference in the Mediterranean / Black Sea sensor bias adjustment procedure, and the inclusion of nadir view SSTs require bias adjustment and give a slightly better final coverage.

There was a question on the details of the global CMEMS L3S product: more details can be found from https://resources.marine.copernicus.eu/documents/PUM/CMEMS-OSI-PUM-010-003-010.pdf. The ingestion of SLSTR and VIIRS in the L3S will be released later this year in an upcoming CMEMS update. It will also include additional geostationary data from Himawari, MSG data over the Indian Ocean and GOES-16.

2.15. RDAC update from NOAA/NESDIS/STAR 2: Eileen Maturi

Information was requested on the new blended 1km L4 products that are planned. These involve six high-resolution regions initially for Coral Reef Watch and are:

(Gulf of Mexico/Caribbean)

(Guam and the Commonwealth of the Northern Marianas Islands)

(American Samoa)

(Hawaii, including the Northwestern Hawaiian Islands)

(Australia's Great Barrier Reef)

(The Coral Triangle.)

In the future, it is planned to produce 1km lake water temperatures starting with N. America and expanding globally.

The OSTIA Analysis is the reference for the GEO-Polar Blended SST Analysis, so that is why it is so closely linked in SQUAM. In the future, there are plans to use Sentinel-3 SLSTR-SST for improving the bias corrections of individual data types used in the Geo-Polar SST analysis and not use OSTIA as the reference.

The reference is Maturi et al., 2017, NOAA's new high-resolution Sea Surface Temperature blended analysis.

2.16. RDAC update from JMA: Toshiyuki Sakurai

There is a plan to expand HIMSST analysis into 0.1 x 0.1 degree global area and introduce geostationary satellites SST data of HIMAWARI, GOES-16, -17 and Meteosat. However, development has been postponed since last summer, because several tasks must be completed by this early-fall (new operational ocean forecast and assimilation system and so on). Focus has been on introducing new satellites data into MGDSST for now.

A new QC method of HIMAWARI night-time SSTs was introduced into operation in November 2018. The new QC is the comparison between day- and night-SSTs and this eliminates the unnatural warm SST values of HIMAWARI-8.

2.17. RDAC update from EUMETSAT: Anne O'Carroll

There was a question on the SLSTR retrieval algorithm and FRM radiometer data. The SLSTR retrieval is a regression against Radiative Transfer modelling. More information on the algorithm can be found from the link to the ATBD via slstr.eumetsat.int. IASI SST is a surface skin SST from the sounding retrieval profiles using an all-sky statistical retrieval process. The FRM radiometers for the lake experiment are the ISAR by Werenfrid

Wimmer (more information in his presentations) and the KIT radiometer. The experiment is currently planned for July (now changed to September, Covid-19 permitting).

2.18. RDAC update from ABoM: Helen Beggs

Nicole Morgan has now reprocessed all of the RV Investigator ISAR data from April 2019 to March 2020. Janice Sisson is manually QC'ing the data, comparing the ISAR skin SST with SBE38 SST_{depth} and meteorological data from the same vessel. She has finished QC'ing the IN2019_V06 (19 Oct - 17 Dec 2019) and IN2019_V03 data and this looks very good quality. Nicole has uploaded these two cruises to the Ifremer Ships4SST FTP area. If you prefer, you can also access the L2R data directly from http://opendap.bom.gov.au:8080/thredds/catalog/imos_isar_archive/Investigator_data/Reprocessed_v3.8/catalog.html. Janice will merge the ISAR data with the ship meteorological data in IMOS format files shortly, and these merged ISAR_QC files will be available from the AODN. Time-series plots can also be provided.

2.19. Report from NSOAS: Qimao Wang and Lijian Shi

There was a question on whether the SST product is provided in GDS format. The data format in HDF or NC and the accuracy is 0.8K.

3. CONCLUSION

The full agency slide deck and discussion forums can be found through the GHRSST online Moodle site: https://training.eumetsat.int/course/view.php?id=367.

GLOBAL DATA ASSEMBLY CENTER (GDAC) REPORT TO THE GHRSST SCIENCE TEAM

Edward Armstrong[(1)], Jorge Vazquez[(1)], Wen-Hao Li[(2)], Chris Finch[(1)]

(1) Jet Propulsion Laboratory, California Institute of Technology, Pasadena, CA, 91109 USA
(2) Raytheon Corp., Pasadena, CA 91101
Email: edward.m.armstrong@jpl.nasa.gov

ABSTRACT

In 2019-2020 the Global Data Assembly Center (GDAC) at NASA's Physical Oceanography Distributed Active Archive Center (PO.DAAC) provided ingest, archive, distribution and user services for GHRSST operational data streams with improved and evolved tools, services, and tutorials, and interfaced with the user community to address technical inquiries. Several new GHRSST datasets including reprocessed MODIS Aqua/Terra L2P with improved cloud screening were made available. The PO.DAAC participated in the evolving GHRSST data management re-architecture and development activities. GHRSST Science Team member Edward Armstrong assumed the role of co-leader of the CEOS SST Virtual Constellation. The following sections summarize and document the specific achievements of the GDAC to the GHRSST community.

1. INTRODUCTION

The primary contributions to GHRSST for this period are in three categories: Data Management and User Services, Tools and Services, and R/G TS evolution. For data management, the GDAC ingested twelve new or updated GHRSST datasets from multiple data providers (See Appendix A). The GDAC continued to support operational data streams for L2P/L3/L4 data from 14 unique RDACs and maintain linkages to the NASA Common Metadata Repository (CMR; https://search.earthdata.nasa.gov/search) and LTSRF archive. For user community engagement the PO.DAAC responded to GHRSST user queries through its help desk and user forum, and improved data recipes with data and tutorials (also promulgated on the PO.DAAC user forum) and established a GitHub site for open source software. The PO.DAAC collaborated with the Farallon Institute to make the MUR dataset available in a cloud optimized Zarr format on the Amazon Web Service Cloud.

PO.DAAC Drive has been fully implemented and is now a nominal part of the PO.DAAC user services suite for data access.

Members of the PO.DAAC also collaborated on the development to re-architect the Regional Global Task Sharing (R/G TS) framework to decentralize the GHRSST data ingest and distribution nodes including designing a data producer user survey.

The PO.DAAC has also received certification as a data centre with a CoreTrustSeal by the World Data System.

2. DISTRIBUTION METRICS

The following figures show distribution metrics and relative popularity of GHRSST datasets. On a typical monthly basis GHRSST datasets are consistently among the most popular products in the entire PO.DAAC catalogue. Users, data volumes and number of files are all steady or have slightly increased. Users are continuing their uptake to leverage services such as OPeNDAP, THREDDS and LAS.

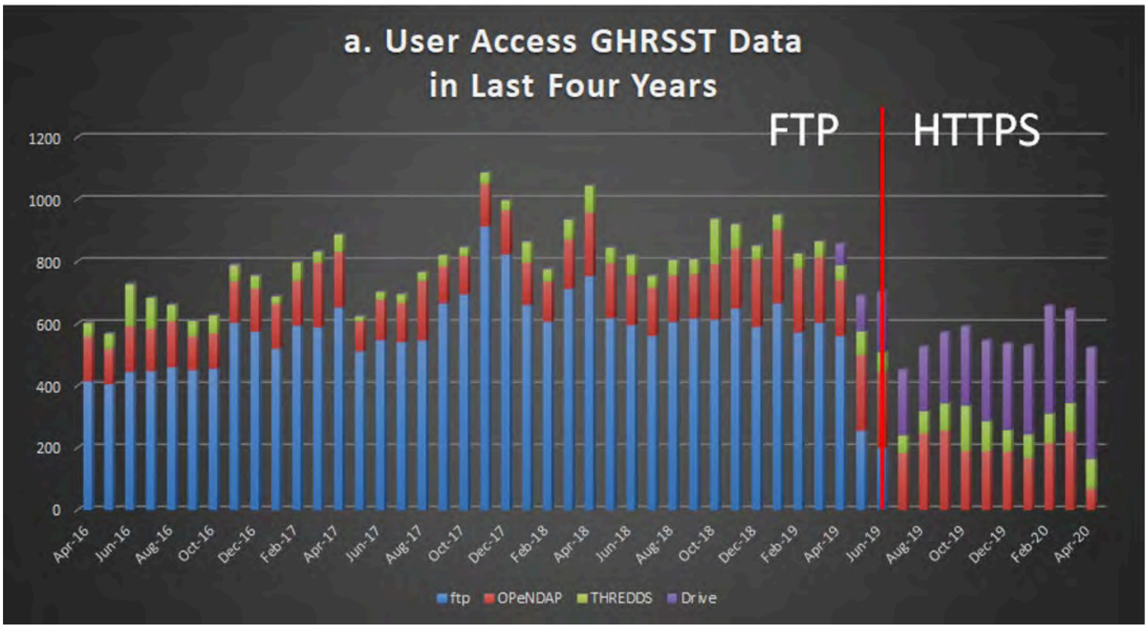

Figure 1. Monthly unique users by FTP/Drive, OPeNDAP, or THREDDS over last four years. Red vertical around June 2019 bar indicates FTP termination date.

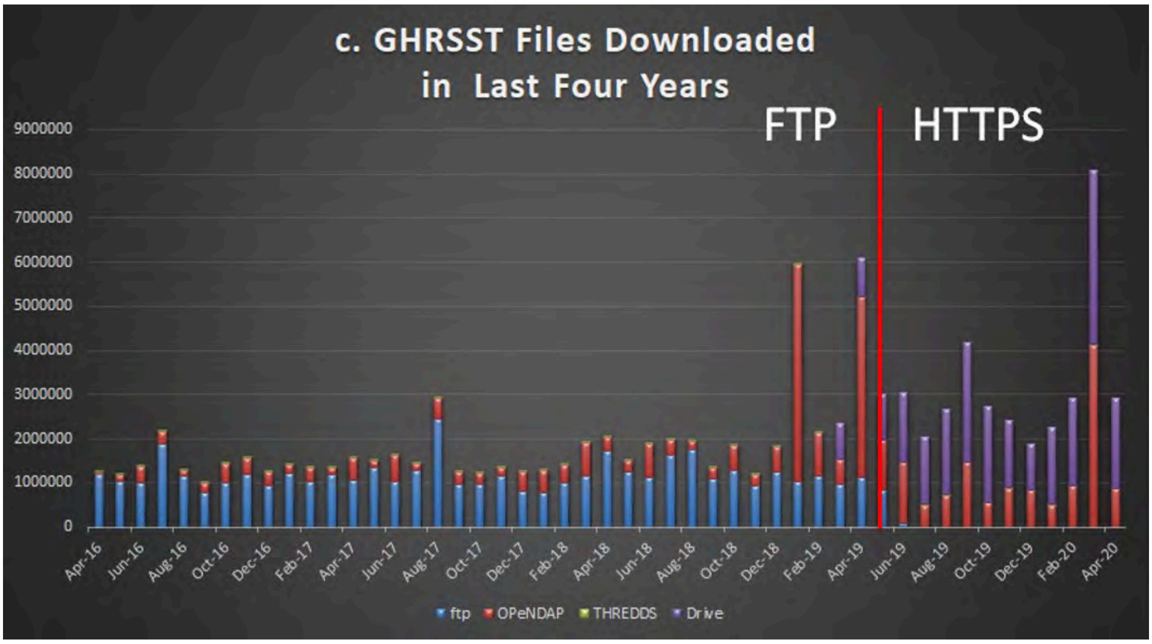

Figure 2. Number of monthly files distributed. OPeNDAP requests are increasing.

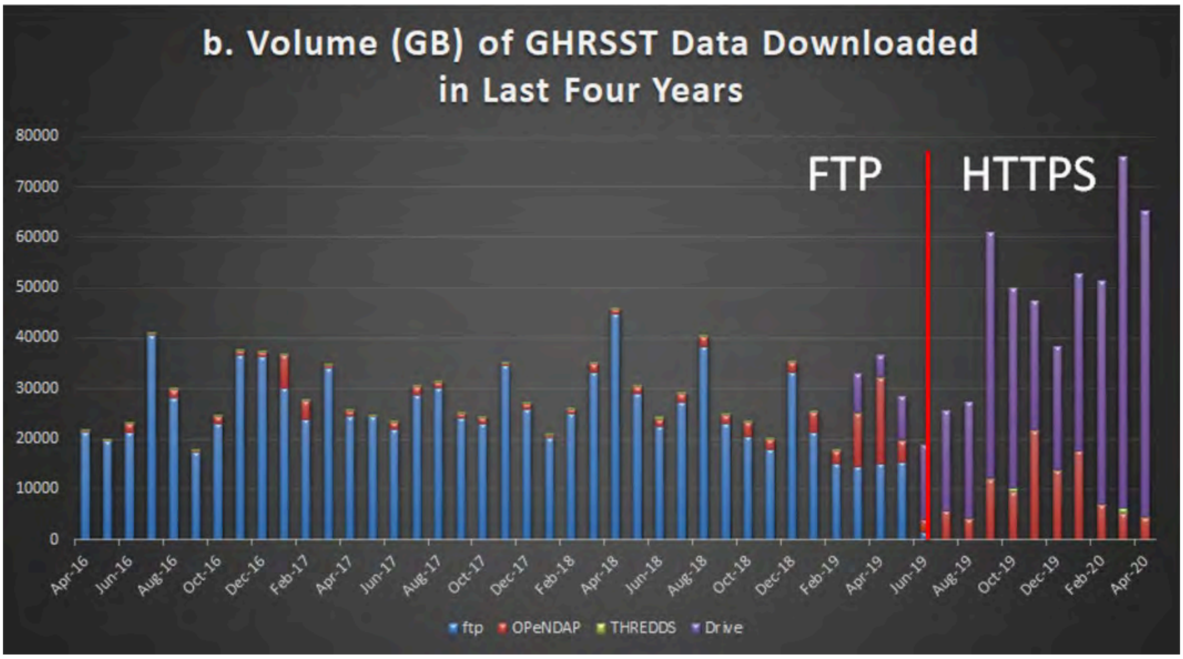

Figure 3. Volume of monthly files (GBs) distributed.

3. TOOLS AND SERVICES

The following summarizes the improvements, ongoing activities and availability of various tools and services for GHRSST data.

- PO.DAAC Earthdata Drive fully implemented
- State Of The Ocean (SOTO) version 4.5 released
    - Includes MODIS v2019.0 L3 (more usable pixels)
    - MUR25 SST and SST anomalies
- Progress on SOTO v5 (with data analytics) continues
- HiTIDE L2 subsetting
    - More GHRSST layers added
- ERDDAP data server under evaluation
- New mission/measurement themed PO.DAAC web site released
    - Uses the NASA Earthdata Search API for dataset and future granule discovery
    - All GHRSST metadata in the NASA Common Metadata Repository (CMR)
- Collaborated on AWS Open Data Registry MUR Zarr dataset
- Continued to develop more data recipes and Jupyter notebooks for GHRSST data

4. NEW *IN SITU* DATASETS

PO.DAAC released Saildrone data from the Arctic cruises supported by the NOPP-MISST project. See https://podaac.jpl.nasa.gov/datasetlist?search=%22SAILDRONE_ARCTIC%22

Acknowledgements

These activities were carried out at the Jet Propulsion Laboratory, California Institute of Technology, under a contract with the National Aeronautics and Space Administration (80NM0018F0848). Dedicated funding for PO.DAAC activities is through a grant from NASA's ESDIS Project.

Appendix A. New or updated GHRSST datasets ingested in the last 12 months (June 2019 – May 2020)

- RAMSSA_09km-ABOM-L4-AUS-v01
- GAMSSA_28km-ABOM-L4-GLOB-v01
- MUR-JPL-L4-GLOB-v4.1 (added sst_anomaly)
- MUR25-JPL-L4-GLOB-v04.2
- VIIRS_NPP-JPL-L2P-v2016.2
- MODIS_A-JPL-L2P-v2019.0
- MODIS_T-JPL-L2P-v2019.0
- AVHRR_OI-NCEI-L4-GLOB-v2.1
- ABI_G17-STAR-L2P-v2.71
- AHI_H08-STAR-L2P-v2.70
- ABI_G17-STAR-L3C-v2.71
- AHI_H08-STAR-L3C-v2.70

SCIENCE SESSION 2: CALIBRATION AND VALIDATION

S2 - SESSION REPORT

Simon Good[(1)], Kyang-Ae Park[(2)], Gary Wick[(3)]

(1) Met Office, UK, Email: simon.good@metoffice.gov.uk
(2) Seoul National University, Korea, Email: kapark@snu.ac.kr
(3) NOAA/OAR/PSL, USA, Email: gary.a.wick@noaa.gov

1. INTRODUCTION

The topic of Science Session 2 was Calibration and Validation and it took place on Tuesday 2nd June 2020. The session included five oral presentations and six posters. The oral presentations covered a range of topics; they discussed the use of high quality drifting buoys to evaluate satellite data, saildrone data and their use in validating gradients, and the suitability of data from the Sea and Land Surface Temperature Radiometer (SLSTR) sensors for use as reference sensors. The posters were even more diverse and included calibration of a satellite sensor, intercomparison of different satellite data, an SLSTR matchup dataset, a long *in situ* record in the Mediterranean Sea and studies in coastal regions on comparison between satellite and *in situ* data and satellite retrieval of SST. In the sections below, the topics covered by each oral and poster presentation and the discussion that resulted from these are briefly summarised.

2. ORAL PRESENTATIONS

2.1. Validation of SST and SSS gradients using the Saildrone Baja and Gulf Stream deployments - J. Vazquez-Cuervo, Marouan Bouali, Jose Gomez-Valdes (S2-1)

2.1.1. Summary

In this presentation Jorge presented a comparison between sea surface temperature (SST) and sea surface salinity (SSS) gradients derived from two Saildrone deployments and existing satellite-derived products. For SST, the comparison was against multiple level 4 data sets while for SSS the comparison was against the Remote Sensing Systems SMAP version 4.0 and JPL CAP Version 4.2 products. To complete the comparisons, the Saildrone data were averaged within the respective satellite grid points, and gradients were then derived from the collocated time series. The results showed that while the individual SST products were generally very well correlated against the actual Saildrone SST measurements, the derived gradients agreed much less well.

2.1.2. Discussion

The presentation generated a large amount of online discussion. One question by P. Dash asked for clarification on how the gradient was computed between successive points in a time series. The answer, provided by M. Bouali, was that the gradient was still computed with respect to the distance difference between the points. H. Beggs asked if the method could be applied to other high frequency *in situ* SST data such as research ships to which the answer was yes, though the Saildrone can be guided to specific targeted locations. Helen followed up with a further question asking if there were anything particularly unique about the Saildrone data as there is also a large amount of research vessel data that have not been ingested into L4 datasets. J. Vazquez answered that continuous SST ship data were also another potential source and agreed that this could be a topic of further discussion during Task Team session 2. L. Guan noted that different gradient operators incorporating more than two successive points could also be used to reduce the impacts of noise. J. Vazquez replied that they had actually compared different methodologies without a significant change in statistics. The selected method gave more matchups. D. Gilbert asked if results might have been different if the analysis could have been done with Aquarius SST data (as opposed to SMAP) to which Jorge replied that he would have expected the Aquarius gradients to be much reduced due to the lower resolution sampling.

A small side discussion was initiated by G. Corlett who asked whether, since a L4 product is derived from observations from a previous day, should *in situ* data from a day be validated against the following day's L4. H. Beggs noted that she typically uses a verification method comparing observations minus analysis (O-A) against observations minus background (O-B) and has obtained very different O-B results using buoy data that were not truly independent. She questioned this approach, citing results from her presentation. G. Corlett replied that he hadn't viewed her specific slides but would do so. G. Corlett also initially asked if they had looked at L2 data as well and J. Vazquez replied that this would be next step and they anticipated improved results. M. Bouali noted that they had done some preliminary experiments against MODIS L2 data and saw some improved correlations, but that the values were still relatively low (did not exceed 0.5).

C. Merchant commented that the results were poorer than we would like but not really poorer than we would expect, noting that there were potentially many reasons that errors in L4 gradients could arise. These could include reduced retrieval sensitivity at L2 and L3, gaps in in the L2 and L3 products and subsequent smoothing by the L4 analysis. He suggested starting with L2 and L3 products and asked if they planned to do so. Chris also commented that he wouldn't have expected a negative bias in the analysis in the gradients and wondered if they had looked if there was any difference in the gradient bias as a function of the gradient. E. Armstrong followed up asking if they had looked at the time of the most recent IR observation to see if gradients based primarily on microwave data only could be given less weight. J. Vazquez replied agreeing that there could be many reasons for differences and that all of this would be a major issue for future work. H. Beggs commented that this was to be a subject to be pursued in Task Team Session 2 as a new feature comparison of SST analyses. I. Tomazic echoed the desire to pursue this further with L2 data and asked if such a comparison could be performed using existing matchup databases or if there were additional requirements. Jorge expressed an interest to explore further.

2.2. Evaluation of HRSST drifters using Copernicus SLSTR - Gary Corlett, Anne O'Carroll, Igor Tomazic (S2-2)

2.2.1. Summary

High quality *in situ* data are required for satellite SST validation. Most drifting buoys are now designed to meet the 'HRSST-2' standard for data quality. This presentation discussed the use of SLSTR data to evaluate drifter data. New drifting buoys from the 'TRUSTED' project were used in the study. These have a conventional SST sensor and a second sensor that provides high frequency sampling. Work is ongoing, but initial results suggest an improvement of drifting buoy quality over time. An eventual aim is to be able to use drifting buoy data and supplementary metadata to 'self quality control' the data.

2.2.2. Discussion

In the discussion, Gary provided additional clarification on the definition of the HRSST standards (this is also discussed in the introductory slide of his presentation): desired features of the data include frequency of reporting (hourly), depth measurement, accurate geolocation (within 0.5km), accurate SST (total uncertainty of 0.05 K or better and reported at 0.01 K precision), netCDF format following climate and forecasting (CF) standards and accurate time stamps (within 5 minutes). The HRSST-1 standard provided the location and time accuracy, while HRSST-2 added the SST accuracy. The NOAA Global Drifter Program (GDP) deploy the majority of drifters and they estimate that two thirds meet the HRSST-2 standard. TRUSTED drifters are able to also provide the depth and timestamp requirements. They also have a strain gauge to detect when the drogue is lost, which can mark a degradation in quality. However, TRUSTED data do not currently represent a separate 'HRSST-3' standard, which still needs to be agreed. A list of which buoys meet the HRSST standards is required by some, and this is something that Gary is working on.

In addition, a clarification was provided that the high frequency sampling occurs over the 5 minute period when the conventional SST sensor would be measuring. It was also noted that comparisons between satellite and *in situ* data will be affected by the *in situ* data being point measurements and the satellite data representing an area. However, satellite cloud contamination is the likely cause of some of the largest discrepancies that Gary showed.

2.3. Sentinel-3 SLSTR SST validation using a Fiducial Reference Measurements (FRM) service – W. Wimmer, T. Nightingale, J. Høyer, R. Wilson, H. Kelliher, C. Donlon (S2-3)

2.3.1. Summary

This presentation presented the validation results of Sentinel-3 SLSTR SST using ships4sst FRM data in the global ocean for the period from April 2016 to 2018. Comparisons made for each matchup grade (1, 2a, 2b, 3, 4 with different temporal and spatial intervals) showed good agreement globally, mean differences (-0.01 to 0.12) and robust standard deviations (RSD) (0.2~0.3). Overall, nighttime data showed better results than daytime data with small scatters in the histogram of the differences (SAT-RAD). Also, uncertainty of the matchup data was estimated by using quality level (QI) methods. The lower RSD at night indicates that SLSTR performs at least as well as AATSR.

2.3.2. Discussion

Positive comments were raised that the study would be greatly helpful for JAXA's development of SGLI SST algorithm. Several questions were raised on the QL scheme not working well for SLSTR, especially in the daytime. Also, it was suggested that detailed information and explanations on the new version of the data set and the latest modifications need to be provided.

2.4. On the applicability of Copernicus Sentinel-3A and Sentinel-3B Sea and Land Surface Temperature Radiometers as reference sensors – Gary Corlett, Anne O'Carroll, Igor Tomazic (S2-4)

2.4.1. Summary

The predecessor to SLSTR – the Advanced Along-Track Scanning Radiometer (AATSR) – was used as a reference sensor to underpin daily level 4 analyses. This presentation examined whether the SLSTR could be similarly used.

Both SLSTR and AATSR have/had dual view capability so four SST retrievals can be made, using 2 or 3 channels and 1 or 2 views. SLSTR provides skin SST, and this remains the case after removal of SSES bias. SLSTR data are being routinely compared to drifter and Argo matchups. Dual-view (2 or 3 channel) SSTs were found to be suitable to be used as reference data, but only quality level 5 data must be used.

The methods can also be used to evaluate other datasets: a cool skin effect can be seen in sub-skin infra-red data and level 4 analyses do not seem to reflect foundation SST but seem more representative of a daily average.

2.4.2. Discussion

The analysis that highlighted the cool skin effect in sub-skin SST data was said to be useful and interest was shown in investigating this further. It was clarified that the plots with matchup time difference on the x-axis are showing the diurnal variability around the satellite overpass time. In comparisons between SLSTR and radiometers, some variations for the 2-channel daytime retrievals around 10 ms^{-1} wind speed and 90˚ solar zenith angle were queried. Gary replied that it might be an issue with the retrieval in high water vapour areas, but this needs further investigation.

2.5. 2019 Arctic Saildrone Field Campaign: measurements of sea surface salinity and temperature for validation of satellite retrievals - Chelle L Gentemann, Peter J Minnett, Michael Steele, Jorge Vazquez, Wenquing Tang, Jacob Hoyer, Sotirios Skarpalezos, Chidong Zhang, Dongxiao Zhang, Richard Jenkins (S2-5)

2.5.1. Summary

Chelle presented an overview of the 2019 Arctic Saildrone campaign highlighting the unique data collected and associated issues. The data were noted to already have revealed interesting air-sea temperature differences, diurnal warming, and issues with existing L4 analyses. Previous questions about potential inconsistencies between multiple sensors onboard the platforms appear to be largely associated with periods of notable stratification. Data are available through the NASA PO.DAAC and more data from additional cruises will be coming in the future.

2.5.2. Discussion

Subsequent discussion acknowledged the potential value of the data and pursued additional detail. G. Corlett asked if there were any flag to indicate when the Saildrone is ice bound and if she had any thought to the source of the two larger STD events. Chelle responded that she is working on an ice flag and just needs to get it published on the PO.DAAC site. The flag will denote ice, diurnal warming, and fresh water events. She believed the two large STD events were during ice. I. Tomazic asked if there were a single or multiple datasets for the different instruments and inquired about the delay in accessing the data. Chelle replied that she is working to get many different cruises into the L1R format which would include one SST value from the CTD at 0.5 m depth. For more recent cruises the SST is put into GTS. For timeliness of data not on GTS, it is up to the cruise PI and when they release the data. It typically can be a few months. C. Merchant asked if any of the large stratification events were near the ice edge and to what extent the Saildrone itself disrupts the stratification. Chelle noted again the coming data flag to help identify where the events were and commented that, regarding disruptions, the keel is narrow and instrument sampling is in front of it, but there have not been detailed studies on the interaction. The Saildrone appears to still move in low wind speeds. G. Wick asked if she had any indications on the stability of the radiometric data to which she replied that there weren't any obvious drifts, but more exploration is needed. E. Armstrong asked if an accelerometer could indicate motion in stratified conditions. Chelle replied that there is one onboard and the change in depth of the sensors can be computed from data onboard, but the easiest way to flag the data is the standard deviation of the temperature measurements. T. Nightingale also asked if there were correlation between the high variability during stratification and recorded bobbing or rocking. S. Elipot asked if diurnal warming could be detected by looking solely at the 1.7 m depth SST record and Chelle replied yes. Finally H. Zhang expressed interest in ingesting the Saildrone data into iQuam.

3. POSTERS

3.1. Forty-five years of oceanographic and meteorological observations at a coastal station in the NW Mediterranean: a ground truth for satellite observations - Jordi Salat, Josep Pascual, Mar Flexas, Toshio Michael Chin, Jorge Vazquez-Cuervo (S2-P1)

3.1.1. Summary

This poster presented a unique record of marine and atmospheric parameters, including temperature observations from the surface to 80-m depth, extending from September 1973 at a coastal station 4 km offshore the Costa Brava in the NW Mediterranean. The dataset was shown to reveal notable trends in atmospheric temperatures and SST anomalies. Different trends were observed for different seasons, and the data also suggested changes in stratification.

3.1.2. Discussion

Comments to the poster acknowledged the value of the time series and expressed the desire that it should be continued. G. Wick asked for clarification on the depth of the shallowest measurement. J. Vazquez replied that there are multiple sensors, but the shallowest is at a depth of approximately one meter. S. Good asked if the dataset were publicly available and, if so, where to get it. J. Vazquez responded that the dataset was published in a paper in Ocean Dynamics by Salat. This paper also includes full details on all the sensors. E. Armstrong expressed further interest in exploring as to whether there were any differences in the trends between daytime and nighttime.

3.2. Comparison of SGLI and M-AERI skin SST – Yukio Kurihara (S2-P2)

3.2.1. Summary

SGLI SSTs are skin SSTs retrieved from the split-window data of GCOM-C/SGLI based on the quasi-physical method developed for the Himawari'8 SST product of JAXA. The SGLI SSTs were compared with the M-AERI skin SST data and showed almost no bias (0.19K) and small RSD (SD) of 0.28 K (0.35 K). This study suggested a further study to investigate the tendency that relatively high biases are possibly generated by atmospheric water vapour.

3.2.2. Discussion

Several questions and discussions were made as to the causes of higher RMS in nighttime than daytime, noticeable differences in the trends of SST RMS values especially from one of the matchup databases (the Ronald Brown). Some factors, such as cloud contamination, land contamination, or TPWV, could be potential sources of the errors, but further improvements can be accomplished to understand the differences between daytime and nighttime.

3.3. EUMETSAT SLSTR sea surface temperature multi mission matchup database - I. Tomažić, A. O'Carroll, G. Corlett, J.F. Piolle (S2-P3)

3.3.1. Summary

Their poster touched on many aspects of the matchup database, including details on the sources of data, format, status, and access. Matchups are built around the SLSTR but also include other satellite products. In situ data are taken from multiple buoy and ship-borne radiometer sources, including the new TRUSTED data, and include a time history. Additional data includes ancillary meteorological data covering the surrounding region in both space and time. Access to the database is available to all Sentinel-3 Validation Team (S3VT) members.

3.3.2. Discussion

G. Wick asked as to whether there was some regular process for quality control of the input data and if they could confirm that the source of the meteorological data was from ECMWF. Igor replied that the quality control is dependent on the source of the dataset. He also confirmed that the meteorological data does come from ECMWF. Forecast fields are used for near real-time data while analysis results are used for reprocessed data. G. Wick also asked if there were regular deadlines to apply for becoming a S3VT member or if there was an ongoing application opportunity. Igor answered that the call is open and ongoing and encouraged applications. The application can be as brief as a half page proposal. When approved, one would be given access to the database. C. Liu from NOAA/NCEI was curious as to whether the TRUSTED drifters appeared in the ICOADS data and asked if the WMO ID list of the TRUSTED drifters could be shared. Igor shared a complete list of TRUSTED WMO IDs, noting that that not all of them are live. C Liu responded that some of those IDs do appear in ICOADS but it is unclear as to whether ICOADS includes all the observations, and the data resolution in ICOADS could be reduced.

3.4. Inter-comparisons of daily sea surface temperature data and *in situ* temperatures at Korean coastal regions - Kyung-Ae Park, Hye-Jin Woo, Hee-Young Kim (S2-P4)

3.4.1. Summary

This study presents the validation and inter-comparisons of SST products (OSTIA, CMC, OISST, REMSS, MURSST, MGDSST) using temperatures from the coastal buoys. Most SST analyses tended to show good agreement in the open ocean, the differences had a tendency to be amplified at the coastal regions and frontal regions. Relatively high errors over 1K are associated with absence of both infrared and microwave SSTs, which is related to the diverse coastal environment of sea fog and clouds due to surface cold waters induced by strong tidal currents and wind-induced coastal upwelling. Also, this study presents wavelet coherence between the SST products and *in situ* temperatures to investigate the spectral similarity in the frequency domain. Other potential factors of coastal SST errors are discussed.

3.4.2. Discussion

Positive comments were raised about the importance of understanding how global SST products represent the coastal zones. Special concerns are focused on the geophysical interpretation of the wavelet coherence plots of the SST differences between GHRSST daily products and *in situ* coastal temperatures and their short temporal scales at the coastal area. Also, it is suggested that significant spatial and temporal variations of SSTs at the coastal regions could be considered in the merging strategy of daily SST products.

3.5. High-Resolution sea surface temperature retrieval from Landsat 8 OLI/TIRS data at coastal region - Kyung-Ae Park, Jae-Cheol Jang (S2-P5)

3.5.1. Summary

This study suggests SST formulation and coefficients to derive Landsat-8 SST at Korean coastal regions using over 4-year buoy data. Smallest errors (0.59 K) were found for the NLSST equation that considers the satellite zenith angle (SZA) and uses the first-guess SST, compared with the MCSST equations. The SST errors showed characteristic dependences on the atmospheric water vapour, the SZA, and the wind speed. In spite of the narrow swath width of the Landsat-8, the effect of the SZA on the errors was estimated to be significant and should be considered for all the formations.

3.5.2. Discussion

Some issues were raised about the inclusion of a satellite zenith angle term in the Landsat-8 SST formulation, how to improve the quality of Landsat-8 SST by considering columnar water vapour quantitatively in the SST formulation for coastal regions with highly variable atmospheric moisture levels. A suggestion was made about providing high-resolution SST gradients in coarser-resolution SST images. Another recommendation was given to improve the accuracy of Landsat-8 SST by considering the calibration problems related to diverse noises in the retrievals.

3.6. Initial assessment of the calibration from HY-1C COCTS infrared channels - Mingkun Liu, Lei Guan (S2-P6)

3.6.1. Summary

This poster described an assessment of the calibration of the Chinese Ocean Color and Temperature Scanner (COCTS) sensor onboard the HY-1C satellite. The assessment was done using comparisons with the IASI sensor on the Metop satellites. The mean brightness temperature (BT) differences (standard deviation) between COCTS and IASI were 2.61 K (0.59 K) in the 11 μm channel and 3.06 K (0.61 K) in the 12 μm channel. A dependence between the IASI BTs and the BT differences was found, suggesting a need for revising the COCTS calibration in future studies, but there was no significant dependence on water vapour.

3.6.2. Discussion

In the discussion, this website about space-based intercalibration was highlighted: http://gsics.atmos.umd.edu/wiki/Home. It was clarified that the plan for the future is to use IASI as a reference to correct the COCTS radiances and to try to shift the COCTS spectral response functions to remove biases, and to discuss the results with the satellite calibration team.

S2 - ORAL PRESENTATIONS - EXTENDED ABSTRACTS

S2-1: COMPARISON OF SATELLITE DERIVED SEA SURFACE TEMPERATURE AND SEA SURFACE SALINITY GRADIENTS: COMPARISONS WITH THE SAILDRONE BAJA AND GULF STREAM DEPLOYMENTS

Jorge Vazquez-Cuervo[(1)], Jose Gomez-Valdes[(2)], Marouan Bouali[(3)]

(1) Jet Propulsion Laboratory/California Institute of Technology, Pasadena, California, jorge.vazquez@jpl.nasa.gov
(2) Jose Gomez Valdes, CICESE Institute, Ensenada, Mexico Email: Jose Gomez Valdes jgomez@cicese.mx
(2) Marouan Bouali, University of Sao Paolo, Sao Paolo, Brazil, marouanbouali@gmail.com

1. INTRODUCTION

The paper aims to follow-up on previous work comparing sea surface temperature (SST) and sea surface salinity (SSS) with data from the Saildrone deployment off the California and Baja Coasts. High Resolution (MUR) SST, the Operational Sea Surface Temperature and Sea Ice Analysis (OSTIA) SST, the Canadian Meteorological Center SST were used. In this study we took the next step by comparing the gradients.

For SSS, the authors analysed the Jet Propulsion Laboratory Captive Active Passive (CAP) SSS and the Remote Sensing Systems (RSS) 40 km and 70 km derived SSS products from the Soil Moisture Active Passive (SMAP) satellite.

In this study, we extend the previous results by comparing satellite-based SST and SSS gradients with Saildrone measurements. The importance of also validating gradients with *in situ* measurements has been confirmed for both a data quality and scientific perspective [4,5]. References [6,7] have shown the coupling between the wind stress curl and SST gradients. Reference [6] found that the wind stress divergence was linearly related to the downwind SST gradients in the Eastern Tropical Pacific. The results clearly showed the air-sea coupling to be associated with the formation of thermal surface fronts. Reference [7] examined the coupling in the Cape Frio coastal upwelling region off south eastern Brazil. They determined that wind stress curl was more strongly correlated with SST gradients than SST. Thus, SST gradients were critical for the relationship between wind stress curl and the formation of localized upwelling events. A significant conclusion of the work was how wind stress curl could be modified through feedback mechanisms associated with coastal upwelling. In [8] one also found strong summertime coupling between wind stress and the formation of SST fronts in the California Current associated with coastal upwelling. The summertime coupling is associated with the seasonal intensification of the coastal upwelling system. The coupling was determined to exist for both wind stress divergence and wind stress curl. The results point to the importance of SST gradients in air–sea coupling. As such, precise and accurate measurements of gradients become critical for numerical modelling, inclusive of numerical weather prediction thus does not account for atmospheric processes specific to coastal upwelling regions.

Overall, warm SST biases, along with the air-sea coupling and an associated relationship to SST gradients, make the case that the validation of both SST and SSS, along with their respective gradients, is critical for coastal upwelling regions. In this work, we focus on two oceanic regions usually associated with spatial-temporal variability, i.e., a coastal upwelling region and a Western Boundary Current region. The unique ability of Saildrone to sample at high spatio-temporal resolutions over an extended period (i.e., several months) allows for the validation of both SST, SSS, and their corresponding gradients using data from two separate campaigns conducted in the California/Baja region and in the North Atlantic Gulf Stream.

2. METHODOLOGY

The co-location and gradient methodology can be explained as follows. Within a given satellite pixel all the Saildrone values were averaged. Gradients were then calculated based on the differences between successive time steps. This methodology was followed for all the remote sensing data sets, inclusive for both the SST and SSS data sets. The methodology used was an issue brought up in the discussion section of the abstract. This procedure gave robust results. When compared with using spatial, instead of temporal gradients, statistics were similar.

3. RESULTS

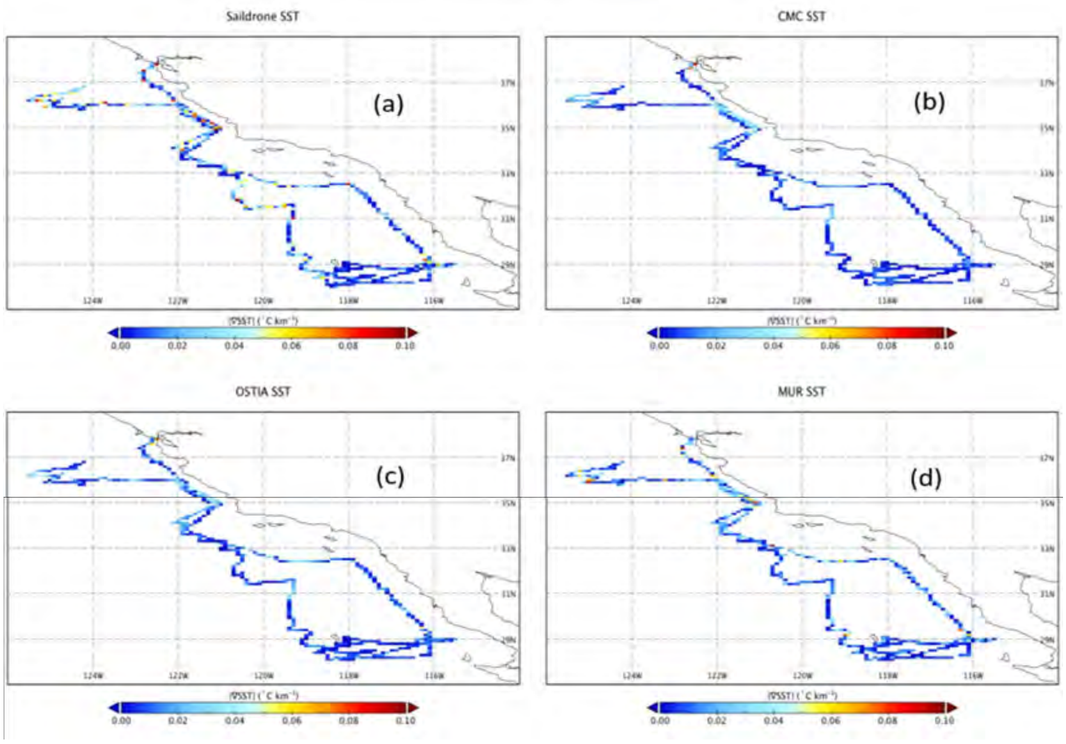

Figure 1: SST gradients

Data Set	Parameter	Bias	RMSD	Correlation
CMC	SST	0.074	0.417	0.975
	|∇SST|	0.009	0.022	0.315
K10	SST	0.137	0.475	0.969
	|∇SST|	0.007	0.022	0.293
REMSS	SST	0.075	0.401	0.977
	|∇SST|	0.007	0.023	0.243
OSTIA	SST	0.022	0.365	0.980
	|∇SST|	0.008	0.022	0.306
DMI	SST	0.040	0.489	0.966
	|∇SST|	0.008	0.023	0.255
MUR	SST	0.285	0.500	0.975
	|∇SST|	0.003	0.021	0.395
JPLSMAP	SSS	0.141	0.414	0.429
	|∇SSS|	0.002	0.005	0.128
RSSV4	SSS	0.170	0.336	0.464
	|∇SSS|	0.002	0.004	0.072

Table1: Comparison statistics. Units are Degrees Celsius, Degrees Celsius/km, PSU and PSU/km

4. CONCLUSION

Few studies have attempted to evaluate the ability of satellite-based products to capture the location and intensity of ocean fronts [16]. In this work, we have described a methodology that exploits the high sampling frequency of Saildrone in order to validate sea surface temperature and salinity gradients. Using data from two Saildrone campaigns conducted over regions known for intense frontal activity, we show that Level 4 satellite-based estimates of SST and SSS are overall statistically consistent with Saildrone measurements but fail to capture both locations and magnitude of surface fronts. We anticipate applying the methodology to other coastal regions, specifically as additional Saildrone deployments become available.

5. REFERENCES

1. Using Saildrones to Validate Satellite-Derived Sea Surface Salinity and Sea Surface Temperature along the California/Baja Coast. *Remote Sens.* **2019**, *11*, 1964. [CrossRef]
2. Meissner, T.; Wentz, F.J.; Le Vine, D.M. The Salinity Retrieval Algorithms for the NASA Aquarius Version 5 and SMAP Version 3 Releases. *Remote Sens.* **2018**, *10*, 1121. [CrossRef]

3. Gentemann, C.L.; Scott, J.P.; Mazzini, P.L.; Pianca, C.; Akella, S.; Minnett, P.J.; Cornillon, P.; Fox-Kemper, B.; Cetinic´, I.; Chin, T.M.; et al. Saildrone: Adaptively sampling the marine environment. *Bull. Am. Meteorol. Soc.* **2020**. [CrossRef]
4. Yang, H.; Gao, Q.; Ji, H.; He, P.; Zhu, T. Sea surface temperature data from coastal observation stations: Quality control and semidiurnal characteristics. *Acta Oceanol. Sin.* **2019**, *38*, 31–39. [CrossRef]
5. Hou, A.; Bahr, A.; Schmidt, S.; Strebl, C.; Albuquerque, A.L.; Chiessi, C.M.; Friedrich, O. Forcing of western tropical South Atlantic sea surface temperature across three glacial-interglacial cycles. *Glob. Planet. Chang.* **2020**, *188*, 103150. [CrossRef]
6. Chelton, D.B.; Schlax, M.G.; Freilich, M.H.; Milliff, R.F. Satellite Measurements Reveal Persistent Small-Scale Features in Ocean Winds. *Science* **2004**, *303*, 978–983. [CrossRef] [PubMed]
7. Castelao, R.M.; Barth, J.A. Upwelling around Cabo Frio, Brazil: The importance of wind stress curl. *Geophys. Res. Lett.* **2006**, *33*, 33. [CrossRef
8. Chelton, D.B.; Schlax, M.G.; Samelson, R.M. Summertime Coupling between Sea Surface Temperature and Wind Stress in the California Current System. *J. Phys. Oceanogr.* **2007**, *37*, 495–517. [CrossRef]
9. Vazquez-Cuervo, J.; Gomez-Valdes, J.; Bouali, M. Comparison of Satellite-Derived Sea Surface Temperature and Sea Surface Salinity Gradients Using the Saildrone California/Baja and North Atlantic Gulf Stream Deployments. *Remote Sens.* **2020**, *12*, 1839.

S2-2: EVALUATION OF HRSST DRIFTERS USING COPERNICUS SLSTR

Gary Corlett(1), Anne O'Carroll(2), Igor Tomazic(3)

(1) EUMETSAT, Eumetsat-Allee 1, 64295 Darmstadt, Germany, Email: gary.corlett@eumetsat.int
(2) EUMETSAT, Eumetsat-Allee 1, 64295 Darmstadt, Germany, Email: anne.ocarroll@eumetsat.int
(3) EUMETSAT, Eumetsat-Allee 1, 64295 Darmstadt, Germany, Email: igor.tomazic@eumetsat.int

1. INTRODUCTION

Reference data are essential for satellite sea surface temperature (SST) validation. One key dataset are drifter buoys, which are mainly provided through the NOAA Global Drifter Program (GDP) and coordinated internationally by the JCOMM Data Buoy Cooperation Panel (DBCP). The uncertainty of a drifter SST measurement was thought to be around 0.1 K. However, studies showed the uncertainty of the dataset as a whole to be closer to 0.2 K (O'Carroll et al., 2008). This led to the formation of a joint GHRSST/DBCP Pilot Project in around 2013 to further investigate the drifter uncertainty with the aim of deploying future drifters meeting a set of agreed requirements:

- Position accuracy and reporting to 0.01degrees
- Report of geographical location to ±0.5 km or better
- Hourly measurements
- Report of time of SST measurements to ±5 minutes
- Total standard uncertainty in measured SST to be < 0.05K
- Report design depth in calm water to ±5cm

Initial deployments had improved position and reporting precision, and were referred to as HRSST-1 drifters, with subsequent deployments also having improved calibration (and therefore a reduced uncertainty) and were referred to as HRSST-2 drifters. Most new drifters deployed today by the GDP data are HRSST-2.

2. DATA SOURCES

2.1. Copernicus SLSTR

Satellite SST data are from the Sea and Land Surface Temperature Radiometer (SLSTR). SLSTR is a dual view self-calibrating multi spectral radiometer onboard the Copernicus Sentinel-3 series of satellite. Two SLSTRs are currently in orbit, SLSTR-A and SLSTR-B. In addition to a dual view of the Earth to provide an enhanced atmospheric correction, the SLSTRs have exceptional radiometric performance and stability for their three infrared (IR) channels. SST is estimated from either 2- (in daytime) or 3- (at nighttime) IR spectral channels. The combination of two channels and two views means four different SST retrievals are possible, and are referred to as N2, N3, D2 and D3. The dual-view 3-channel retrieval (D3) is considered the most accurate and is used here.

2.2. TRUSTED

In support of this activity, a new project funded by Copernicus was initiated, which aimed to deploy up to 150 new HRSST drifters as Fiducial Reference Measurements (FRMs). A key development of the new TRUSTED drifters is that each one has two different SST sensors, which allows better characterisation of both the sensors and the drifter overall. One sensor performs as per conventional drifters where a sample is taken once every five minutes but is only reported every hour. In addition, each drifter has a high frequency SST sensor, which samples at 1 Hz. This is important as it allows us to better understand the uncertainty introduced by sampling every five minutes around every hour. The data are available via the Global Telecommunication System (GTS), but for the low-frequency measurements only. Additional metadata plus the high frequency data are provided with the SLSTR match-up database (MDB).

For further details of the TRUSTED project please see:

http://www.eumetsat.int/website/home/Data/ScienceActivities/ScienceStudies/TowardsfiducialReferencemeasUrementsofSeaSurfaceTemperaturebyEuropeanDriftersTRUSTED/index.html

3. METHODOLOGY

The aims of this work are first, to analyse SLSTR drifter matchups and identify issues affecting the validation results, especially those that influence any conclusions drawn from them. Second, we want to use the TRUSTED data to initiate a 'self-QC' process where the drifter data is quality controlled using only the data itself and its own metadata, i.e. no external data are used. Third, we will then apply any QC methods developed for the TRUSTED data to all HRSST drifters. Finally, we will be able to make an assessment of the overall accuracy of the HRSST drifters and to see if all issues identified as being due to drifters can be successfully removed by the self-QC process.

Here we use the SLSTR-A MDB, which as of the time of writing contained 6106 unique drifters, where the drifter quality level is either 4 or 5 (acceptable for use). Initially we will look for large satellite/drifter differences and at the variability of the drifter SSTs themselves.

4. RESULTS

A time series of all match-ups between SLSTR D3 A and drifters from the start of the mission to date is shown in Figure 1. Each match-up shown as black dot and all match-ups where the SST difference is > 5 K are shown by a red asterisk. The time series itself contains 107125 match-ups and out of these only 43 are greater than 5 K. The occurrence rate and magnitude of the large differences appears to decrease over time.

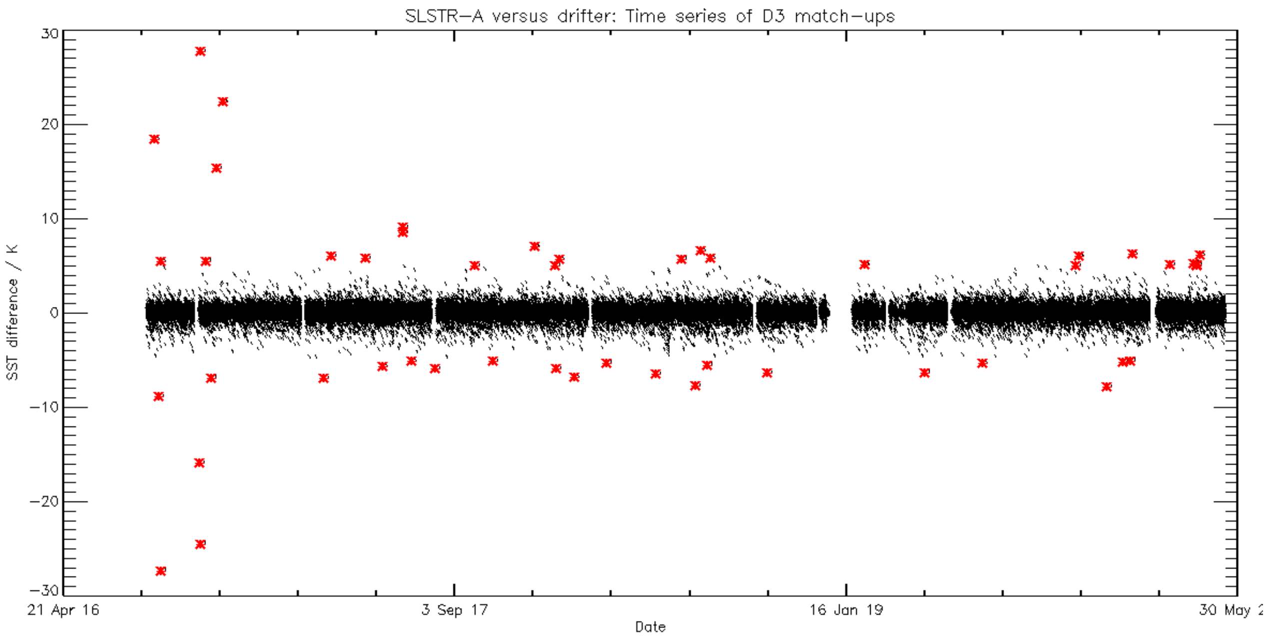

Figure 1: Time series of all match-ups between SLSTR D3 A and drifters from the start of the mission to date. Each match-up shown as black dot and all match-ups where the SST difference is > 5 K are shown by a red asterisk

Three examples of large satellite/*in situ* differences are shown in Figure 2. These have been selected to show issues identified with the *in situ* data stream. In top plot we have the *in situ* time series plotted in red and the green asterisk indicates an SLSTR SST that has passed the satellite QC process and in blue SLSTR SSTs that failed the satellite QC process. The example on the left and in the middle shows the *in situ* time series has degraded towards its end of life and this has not been picked up by the drifter QC process. Also, in the example in the middle and on the right, there are spikes in the time series that have not been picked up by the QC.

Although we have good agreement in general between the satellite and the drifter there are also cases where the satellite QC process in not optimal, and this is the importance of good quality reference data.

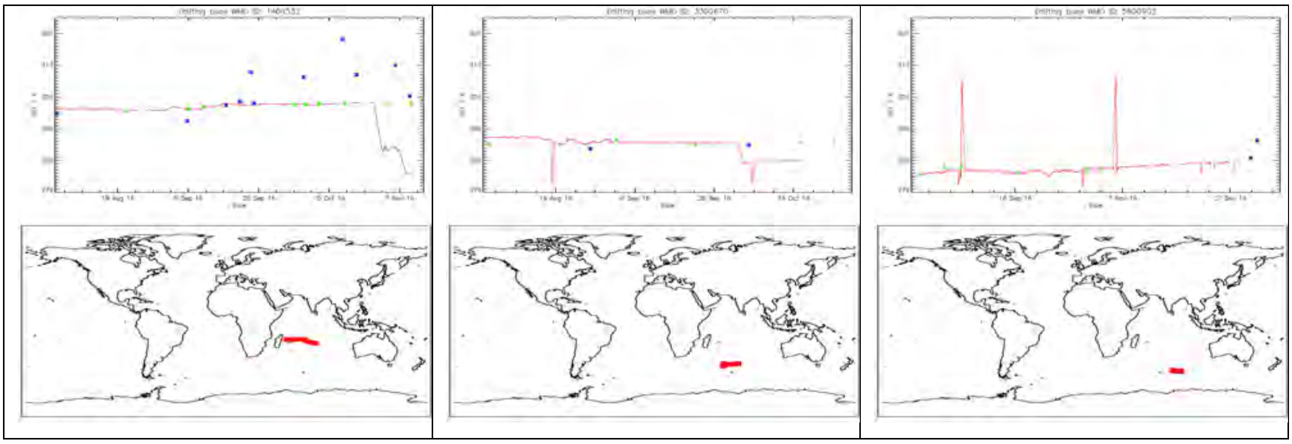

Figure 2: Upper plots: Time series of in situ SST at match-up location in red; blue asterisk indicates match-up rejected by satellite QC; green asterisk is good match-up (QL=5). Lower plots: Map of satellite / drifter match-up locations

This is further emphasised in Figure 3 where we look at three cases where we have significant variability in the drifter time series due to the larger range of regions and temperatures sampled. In all three cases there are no apparent issues seen in the drifter and in all three examples the large satellite/drifter differences are due to issues with the satellite data, most likely due to undetected cloud.

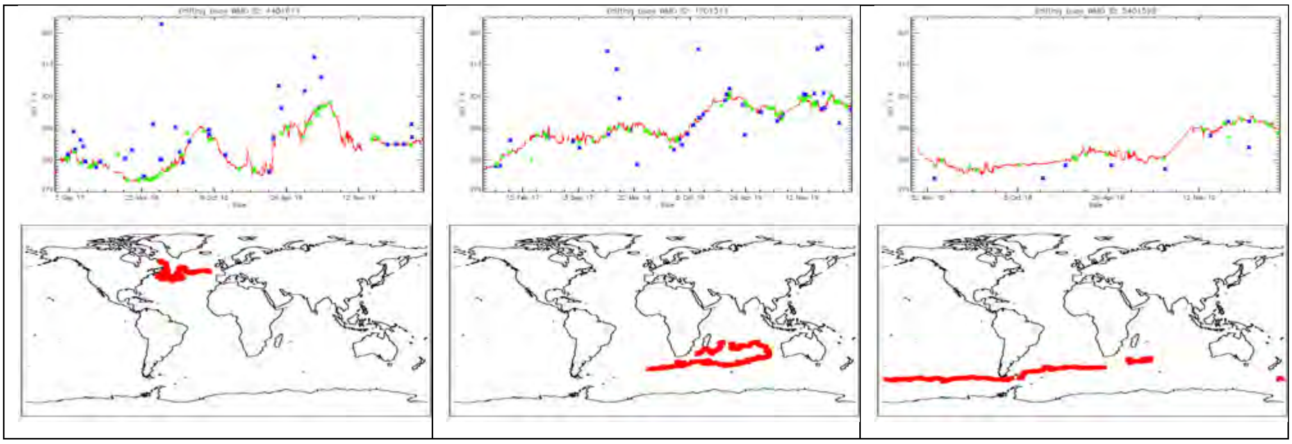

Figure 3: Upper plots: Time series of in situ SST at match-up location in red; blue asterisk indicates match-up rejected by satellite QC; green asterisk is good match-up (QL=5). Lower plots: Map of satellite / drifter match-up locations

5. CONCLUSION

Reference data from drifting buoys are essential for satellite SST validation. However, several issues limit the usefulness of the current drifter network, which will be further investigated as this work continues. The satellite and *in situ* communities are coordinating their efforts to better understand these limitations through the GHRSST/DBCP Pilot Project. Most drifters deployed are now HRSST-2 standard. A new Copernicus funded

FRM project, TRUSTED, is providing important new data to develop self-QC methods for all drifters. Early results of the project suggest the overall quality of the drifter network has improved in recent years.

A TRUSTED/HRSST workshop will be held next year at Meteo France in Paris on 2nd – 4th March 2021. The aim of the workshop is to review the HRSST projects and to show that HRSST is an improvement for satellite SST validation. All of the TRUSTED high-frequency data and metadata are available from the SLSTR MDB. The workshop is open to anyone with an interest in satellite SST validation and drifter data quality. A video link will be available for those unable to attend in person.

6. REFERENCES

O'Carroll, A. G., Eyre, J. R., and Saunders, R. W., (2008) Three-Way Error Analysis between AATSR, AMSR-E, and In Situ Sea Surface Temperature Observations, J. Atmos. Ocean. Tech., 25, 1197–1207, https://doi.org/10.1175/2007JTECHO542.1.

S2-3: SENTINEL-3 SLSTR SST VALIDATION USING A FIDUCIAL REFERENCE MEASUREMENTS (FRM) SERVICE

W. Wimmer[(1)], T. Nightingale[(2)], J. Høyer[(3)], H. Kelliher[(4)], R. Wilson[(4)], J-F. Piolle[(5)]

(1) University of Southampton, European Way, Southampton, SO14 3ZH, UK, Email: w,wimmer@soton.ac.uk
(2) RAL Space, Ditcot, UK,
(3) DMI, Copenhagen, Denmark
(4) SpaceConneXion, Harpenden, UK
(5) Ifremer, Brest, France

1. INTRODUCTION

ESA is building on almost 18 years of continuous Fiducial Reference Measurements (FRM) from UK-funded shipborne radiometers by establishing a service to provide historic and ongoing FRM measurements to the wider SST community through an International SST FRM Radiometer Network (ships4sst). The ships4sst is open for partners around the world, currently comprising of partners from the UK (University of Southampton, Rutherford Appleton Laboratory, Space ConneXions), Denmark (Danish Meteorological Institute) and France (Ifremer) and not only collects Shipborne radiometer data but also uses the data to validate SLSTR and other satellite SST products with the Felyx MDB tool.

2. THE SHIPS4SST NETWORK

The fiducial reference measurement (FRM) data used to validate SLSTR products comes from the ships4sst (www.ships4sst.org) project. The shisp4sst project provides a platform for shipborne infrared radiometers measuring SST_{skin} data, with protocols, a common data format and an archive for data download. Figure 1 shows the data currently held in the ships4sst archive.

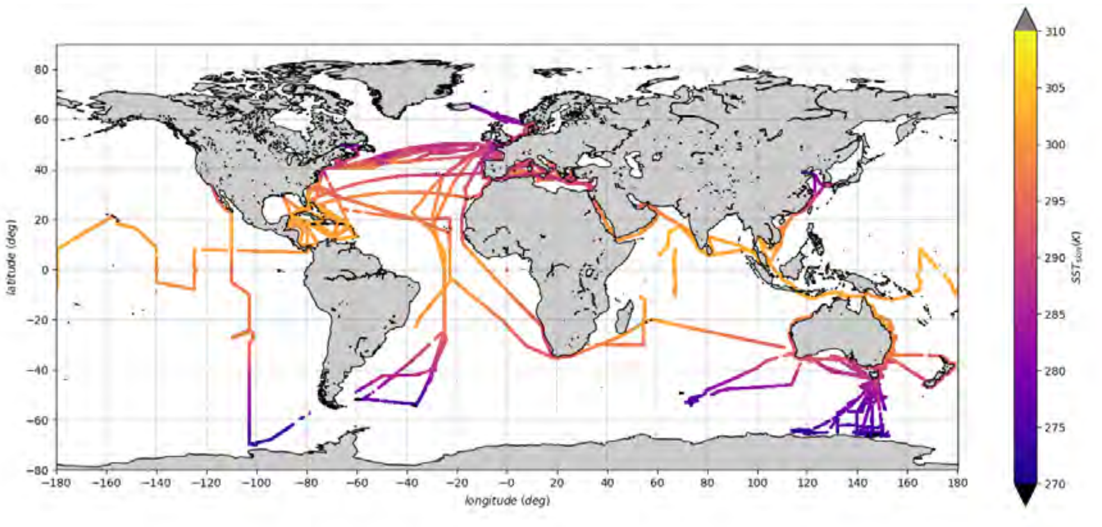

Figure 5: SST_{skin} data in the ships4sst archive.

3. VALIDATION RESULTS

For the validation of the SLSTR products we used five match-up windows, which are show in Table 1 (from Wimmer et.al 2012). The SLSTR data used for the validation is the reprocessed WST data from 2016 to 2018, for GHRSST quality level 5. Figure 2 shows the location of those match-ups colour coded by the SLSTR – radiometer data difference.

Table 1: Match-up window temporal and spatial size used for the SLSTR validation

Grade	Time	Spatial
1	± 0.5 h	± 1 km
2a	± 0.5 h	± 20 km
2b	± 2.0 h	± 1 km
3	± 2.0 h	± 20 km
4	± 6.0 h	± 25 km

The results have been stratified into day and night time match-ups and the histograms are shown in Figure 2, with the daytime data on the left plot and nighttime data on the right plot. The match-up statistics for the validation are presented in Table 2, again separated into day and night time results. The match-up statistics are computed by using robust statistics with a Huber T weighting function applied.

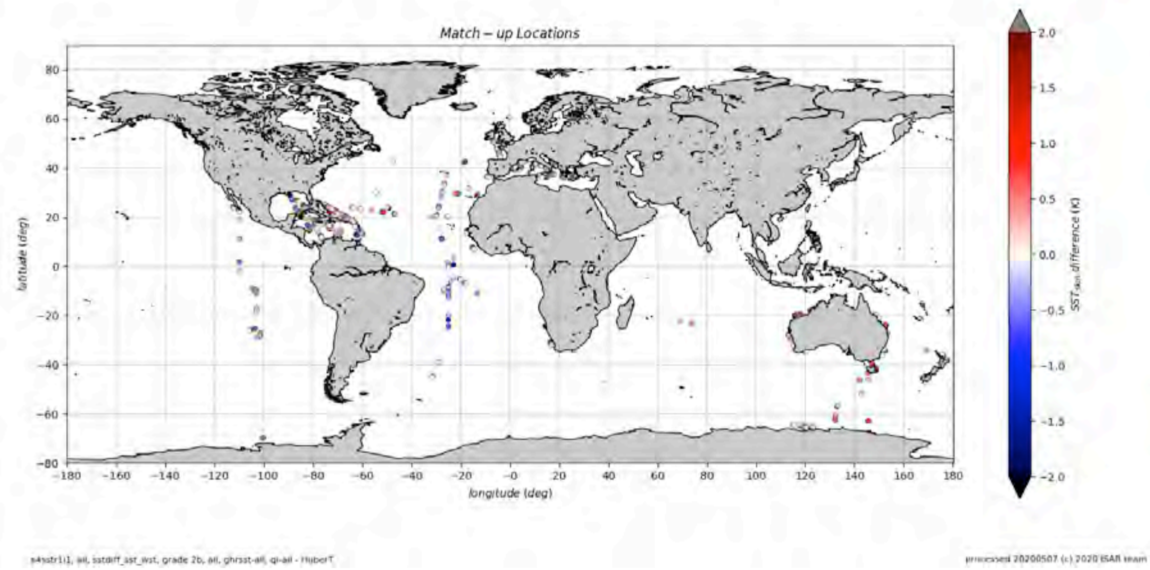

Figure 6: SLSTR Match-up locations for ships4sst data, 2016 to 2018.

The histograms and the match-up statistic show a small daytime mean difference between SLSTR and the ships4sst data with a near zero man difference at night. The robust standard deviation (RSD) increases with the match-up grade as expected, with the exception of grade 2a which shows a higher RSD than grade 2b. The reason for this is that a deviation in space between the SLSTR and ships4sst data has a larger impact on the match-up difference than a deviation in time as grade 2a allows for a matched pair difference of up to 20km and 0.5 H, where grade 2b allows for matched pair difference of up to 1km and 2h.

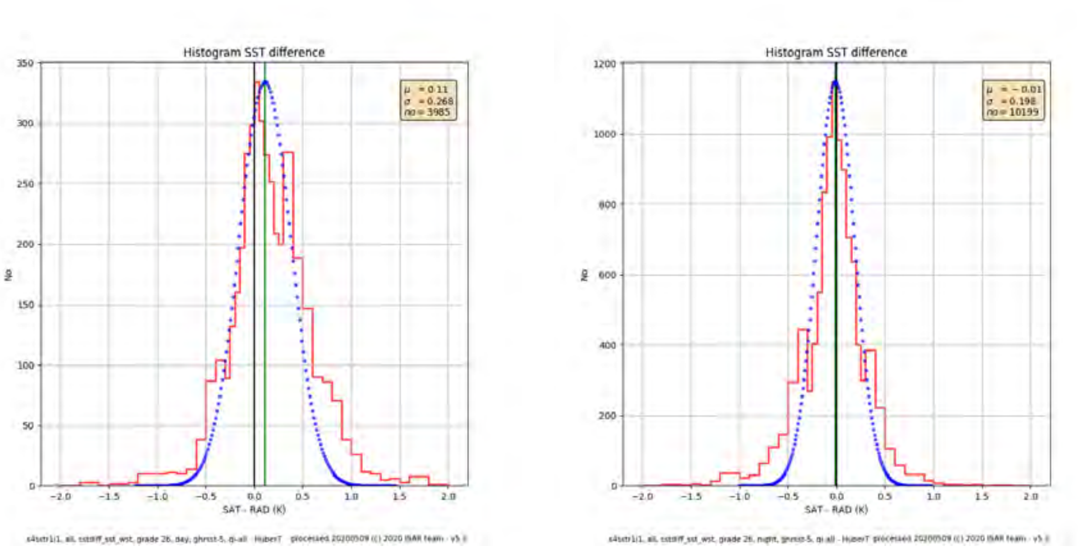

Figure 7: Histograms for the SLSTR Validation results, 2016 to 2018. The left plot shows the histograms for daytime matches and the right hand plot for nighttime matches for the WST product, GHRSST quality level 5 and match-up grade 2b.

Table 2: SLSTR Match-up statistics for 2016 to 2018 WST data, GHRSST quality level 5.

WST						
Day						
Grade	**MDiff**	**RSD**	**No**	**Overpass**	**Min Temp**	**Max Temp**
1	0.12	0.28	1521	193	271.95	304.30
2a	0.11	0.40	4888	367	270.48	307.29
2b	**0.12**	**0.32**	**6067**	**318**	**271.80**	**306.95**
3	0.12	0.43	18663	458	270.20	307.34
4	0.09	0.50	54823	643	270.20	307.48

WST						
Night						
Grade	**MDiff**	**RSD**	**No**	**Overpass**	**Min Temp**	**Max Temp**
1	-0.01	0.20	2997	349	272.38	304.28
2a	0.00	0.27	7660	600	271.80	304.68
2b	**-0.01**	**0.21**	**11447**	**501**	**272.38**	**305.55**
3	0.00	0.28	29475	703	271.30	305.55
4	0.00	0.31	77383	832	271.30	305.55

4. MATCH-UP INDICATORS

The results shown in section three indicate that the choice of match-up window does influence the validation results and therefore the estimated mean difference and RSD. Because the bias and standard deviation are used in the GHRSST project for SSES and SST analysis bias correction, the influence of the match-up window can have wide-ranging influence on the different products. To reduce such issues Wimmer (2012b) estimated the uncertainty associated with the match-up process and developed a technique to minimise such uncertainty, also known as the quality indicator (QI) method. This method uses a number of indicators and associated thresholds to estimate the uncertainties of the match-up process, e.g. spatial mismatch uncertainty, temporal mismatch uncertainty, spatial averaging to temporal averaging uncertainty. This was developed for AATSR validation and has now been implement for the SLSTR validation processing. And while the thresholds developed on an AATSR training data set do work, the results for SLSTR are not as convincing as they were for AATSR.

The reasons for the harder to interpret results for SLTR could be:

- That the QI method was originally derived for the English Channel and Bay of Biscay region and is now applied globally for SLSTR. Therefore the originally derived thresholds might need adjustments.
- The method was developed for ISAR (Donlon, et.al. 2008) data and is now applied to all shipborne infrared radiometer data in the ships4sst database. This might be a key issue as the radiometer SST_{skin} variability around the match-up seems to be higher than it was in the ISAR only case.

5. CONCLUSION

The SLSTR validation results shows excellent result for the WST data, which are comparable to AATSR (Wimmer et.al, 2012a), however this study used global data and Wimmer, et.al. 2012a used local data in the English Channel and Bay of Biscay.

The QI method showed promise when used on SLSTR, however further work is needed to understand the differences compared to AATSR when applied to SLSTR.

The validation results and the QI method are dependent on a high quality FRM data set, as demonstrated by the ships4sst data.

6. REFERENCES

C. Donlon, I. S. Robinson, M. Reynolds, W. Wimmer, G. Fisher, R. Edwards and T.J. Nightingale, 2008 An Infrared Sea Surface Temperature Autonomous Radiometer (ISAR) for Deployment aboard Volunteer Observing Ships (VOS), Journal of Atmospheric and Oceanic Technology, Vol. 25(1), pp 93-113

W. Wimmer, I. S. Robinson, and C. J. Donlon. Long- term validation of AATSR SST data products using shipborne radiometry in the Bay of Biscay and English Channel. In: Remote Sensing of Environment 116 (2012a), pp. 17–31.

W. Wimmer, (2012b) Variability and uncertainty in measuring sea surface temperature. University of Southampton, Ocean and Earth Science, Doctoral Thesis, 244pp.

S2-4: ON THE APPLICABILITY OF COPERNICUS SENTINEL-3A AND SENTINEL-3B SEA AND LAND SURFACE TEMPERATURE RADIOMETERS AS REFERENCE SENSORS

Gary Corlett[(1)], Anne O'Carroll[(2)], Igor Tomazic[(3)]

(1) EUMETSAT, Eumetsat-Allee 1, 64295 Darmstadt, Germany, Email: gary.corlett@eumetsat.int
(2) EUMETSAT, Eumetsat-Allee 1, 64295 Darmstadt, Germany, Email: anne.ocarroll@eumetsat.int
(3) EUMETSAT, Eumetsat-Allee 1, 64295 Darmstadt, Germany, Email: igor.tomazic@eumetsat.int

1. INTRODUCTION

Sea surface temperature (SST) is a fundamental physical variable for understanding the ocean/atmosphere interface. Operational services rely on daily SST analyses which provide a spatially interpolated best guess from all available *in situ* and satellite data. Part of the analysis procedure is to use the *in situ* data to bias correct the satellite data. Work pioneered by Meteo France using data from the Advanced Along Track Scanning Radiometer (AATSR) demonstrated the capability of a using dual-view IR radiometer as a reference sensor to support the *in situ* data (Le Borgne et al., 2012). In this paper we assess if the Sea and Land Surface Temperature Radiometer (SLSTR) can provide such data. We will do this by (1) assessing the quality of SLSTR, (2) comparing SLSTR to other satellite sensors and (3) looking at the quality of current SST analyses.

2. COPERNICUS SENTINEL-3 SEA SURFACE TEMPERATURE

An SLSTR is a dual view self-calibrating multi-spectral radiometer onboard the Copernicus Sentinel-3 series of satellite. There are currently two in orbit, SLSTR-A and SLSTR-B. In addition to a dual view (at nadir and 55°) of the Earth to provide an enhanced atmospheric correction, the SLSTRs have exceptional radiometric performance and stability for their infrared (IR) channels. SST is estimated from either 2- (in daytime) or 3- (at nighttime) IR spectral channels (at nighttime). The combination of two channels and two views means four different SST retrievals are possible, named N2, N3, D2 and D3. As SLSTR is an IR radiometer it provides a measure of SST_{skin} as defined by GHRSST, which are provided in two different products. The SL_2_WCT product provided all available SSTs, whereas the SL_2_WST product provided the best SST per pixel in GHRSST L2P format.

3. RESULTS

To assess the performance of SLSTR we routinely compare it to *in situ* measurements. Figure 1 shows match-ups between SLSTR-A and drifters and to Argo floats. For the Argo floats we use a single temperature extracted from the profile between 3 m and 5 m depth. Results are shown in each plot for the median difference and robust standard deviation (RSD). Daytime results for the 2-channel retrieval are shown in red, nighttime results in green and blue for 3- and 2- channels retrievals, respectively. Solid lines indicate dual-view retrievals and dashed lines indicate nadir-only retrievals. Plots are shown for three match-ups dependences, wind speed, solar zenith angle and time difference between satellite and *in situ* measurements. These three dependences are chosen as we expect to see differences between SLSTR SST_{skin} and *in situ* SST_{depth} due to real geophysical effects.

For example, if we look at the drifter results as a function of wind speed, we can see at nighttime a dependence towards low wind speeds, which is the cool-skin effect. We do not see this in daytime as there is now an additional contribution from diurnal warming. The dependence on SZA shows little variability at nighttime, whereas for daytime we see a clear dependence that increases towards lower SZA. This effectively is moving from the Poles towards the Equator and the increase is due to higher diurnal warming at low latitudes. A zero time difference means the satellite and *in situ* measurements were taken at the same time (which for SLSTR is 10:00 or 22:00), whereas a time difference of either +2 or -2 means the measurements were taken two hours apart. We see a clear dependence in both day and night, with a slightly larger gradient in the day, and what we are seeing is the ocean warming up in the daytime and cooling down at night. All three dependence plots are behaving as expected.

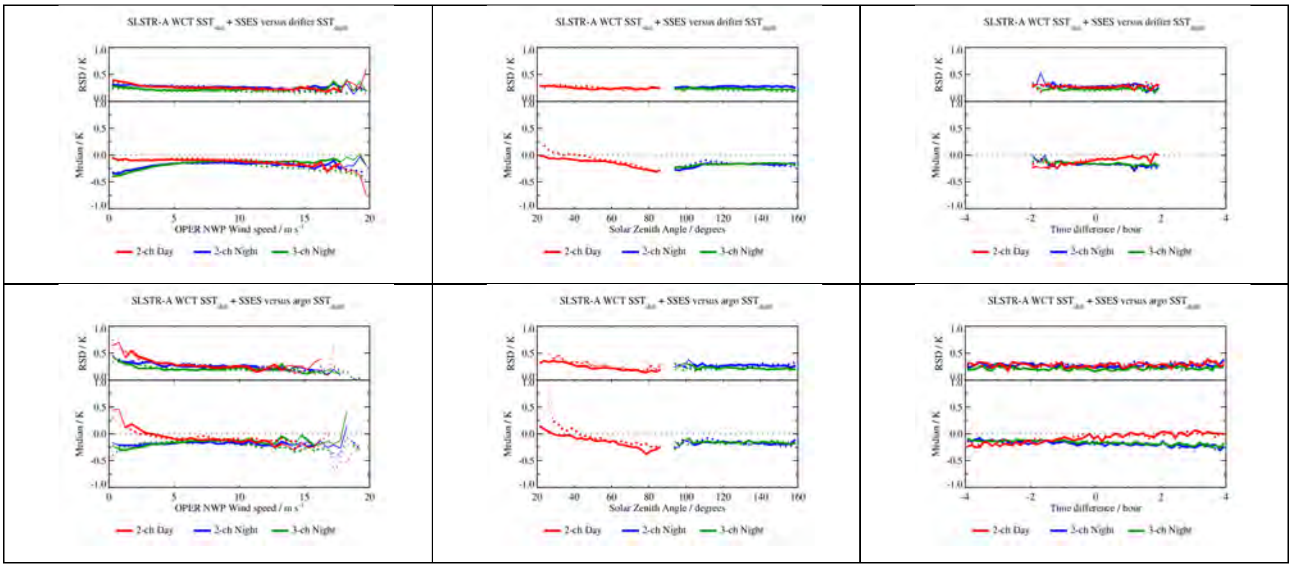

Figure 1: Dependence of the median difference and robust standard deviation of the differences between SLSTR-A and drifters (upper row) and Argo (lower row) as a function of (left) wind speed, (middle) solar zenith angle and (right) time difference between the satellite and in situ measurements. Daytime results for the 2-channel retrieval are shown in red, nighttime results in green and blue for 3- and 2- channels retrievals, respectively. Solid lines indicate dual-view retrievals and dashed lines indicate nadir-only retrievals.

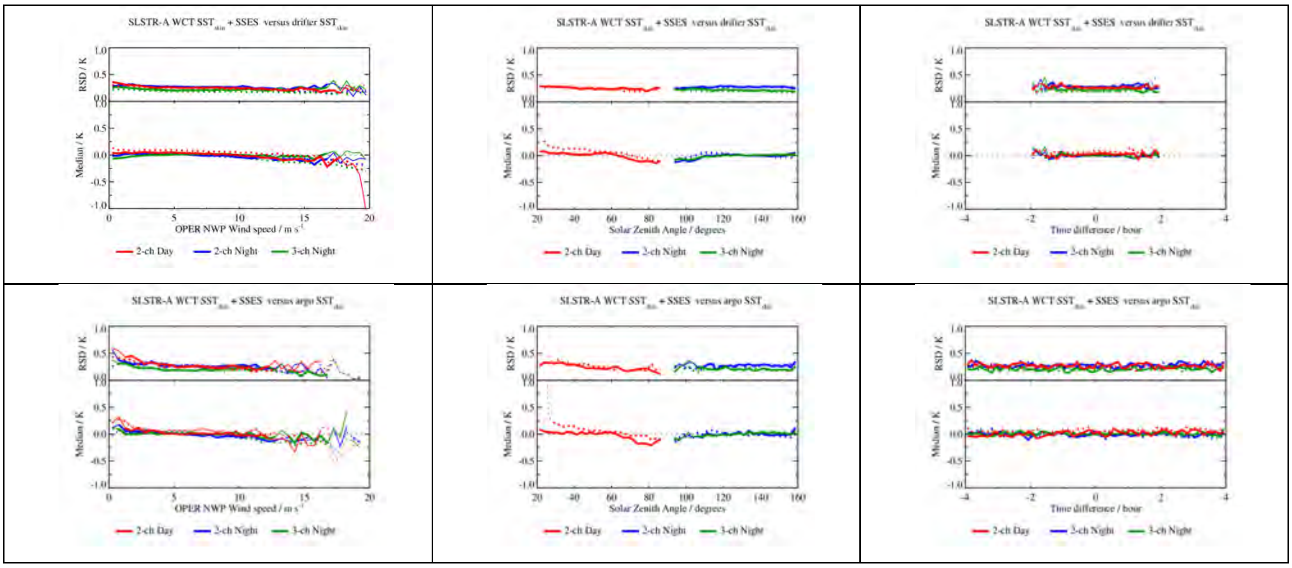

Figure 2: As per Figure 1 but with the addition of FKC adjustments as described in the text.

Similar results are seen for the Argo matchups in Figure 1. But as the Argo measurements are deeper than the drifter measurements, we see larger diurnal differences between the satellite SST_{skin} and *in situ* SST_{depth} at the overpass time of SLSTR. Also, at nighttime we do not see a clean cool-skin effect in the Argo results and we attribute this to residual warming in the upper ocean at around 22:00 compared to the Argo depth. The SZA dependence is similar as for drifters however a larger diurnal signal is seen as expected. The time difference plot shows a similar warming and cooling cycle as for drifters. However, the cross-over between the day and nighttime results is shifted further from zero due to the lower depth of the Argo measurements and the time it takes for the heat to transfer from the surface.

To correctly compare drifters and Argo with SLSTR we have to take into account these geophysical differences and to do this we use a combined skin-effect diurnal-variability model. The models used are the Fairall et al. (1996) cool-skin effect and the Kantha and Clayson (1994) diurnal-variability model (referred to collectively as the FKC model). For the plots shown here the FKC model is driven by ECMWF ERA-interim fluxes (Dee et al., 2011). The FKC model is used to make two adjustments: (1) to adjust the *in situ* SST_{depth} to *in situ* SST_{skin} at the *in situ* measurements time and (2) to adjust the *in situ* SST_{skin} to the same time as the satellite SST_{skin}.

Results from applying the models to the data are shown in Figure 2. The wind speed dependence shows the model accounts for most of the differences seen in the previous figure, although some residual issues remain at very low wind speeds. A similar result is seen for the dependence on SZA where most of the diurnal signal (and cool-skin effect) is removed. Indeed, we now see what appears to be a high latitude bias in the SLSTR data, which is much clearer now the geophysical effects have been removed. The time difference plots are now more or less flat for both day and night.

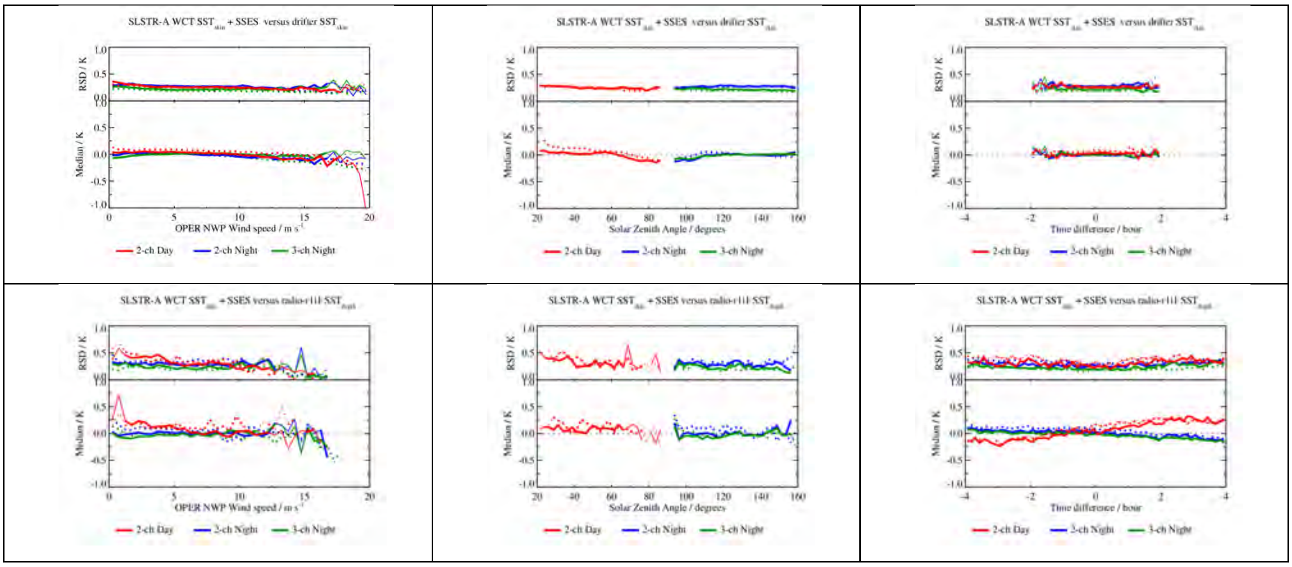

Figure 3: As per Figure 2 but comparing drifters (upper) and ship-borne radiometers.

We also have some independent SST_{skin} measurements from shipborne radiometers (Donlon et al., 2014) that we can use to check how well the FKC adjustments are performing. Ideally, we would only use SST_{skin} measurements, but these are only available from a small number of radiometers operating around the globe (http://www.shipborne-radiometer.org). Results in Figure 3 compare the drifter match-ups with FKC adjustments applied (top row) with the set of radiometer match-ups. The radiometer results show no evidence of a cool skin effect at night as expected. However, a small dependence is seen in daytime results towards lower wind speeds. No dependence is observed as a function of SZA. The time difference results do show a dependence as if you do not compare measurements taken at the same time there will be real geophysical differences even when comparing SST_{skin}. Indeed, it is the time difference between measurements that contributes to the observed daytime dependence on wind speed. The good agreement between the adjusted drifter matchups and the radiometer matchups provide good confidence in quality of all the measurements as well as the FKC adjustments.

Our second objective was to compare SLSTR to other satellite sensors. Figure 4 compares SLSTR to two other polar-orbiting IR sensors, AVHRR (Saux Picart, 2018) and VIIRS (Petrenko et al., 2014)). No additional adjustments have been made to account for differences in depth and time for the AVHRR and VIIRS matchups.

This is because after the application of the SSES_bias field both AVHRR and VIIRS provide an estimate of $SST_{subskin}$, which is more or less the same depth as the drifters. Surprisingly, there is evidence of a cool skin effect in both the AVHRR and VIIRS results. The dependence on time difference for VIIRS does not show the same symmetry as for SLSTR and AVHRR, which is due to the later overpass time being closer to the peak of the diurnal cycle.

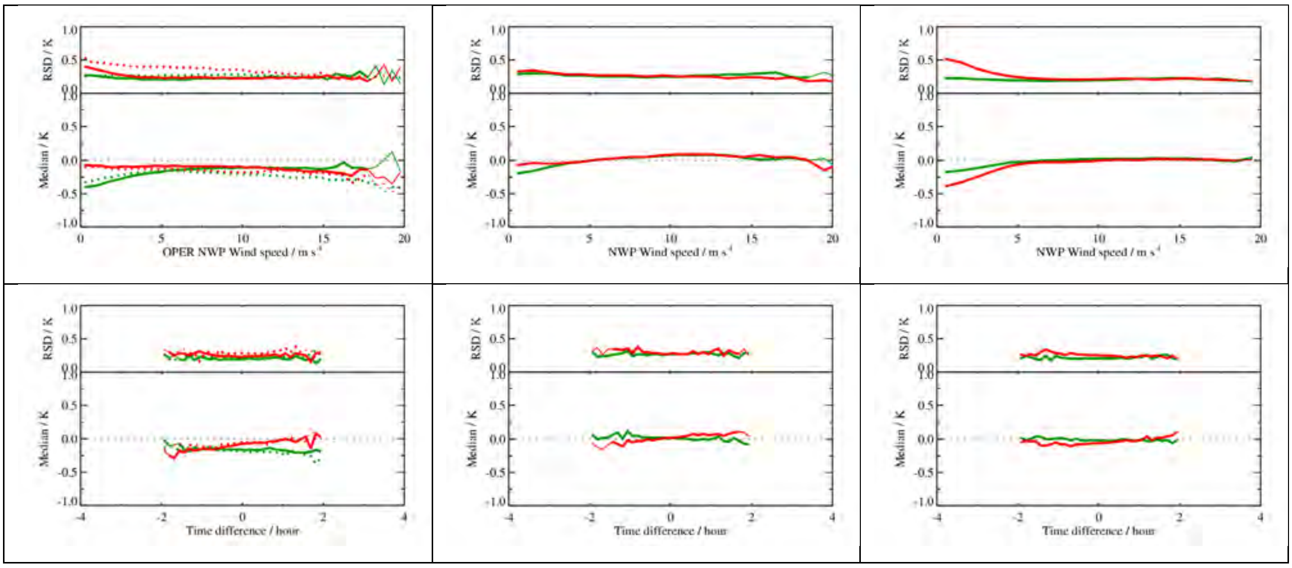

Figure 4: Dependence of the median difference between (left) SLSTR, (middle) AVHRR and (right) VIIRS and drifting buoys as a function of wind speed (upper) and time difference (lower). Plots are shown for day time in red and nighttime in green.

Finally, in Figure 5 we look at the quality of two Level 4 SST analyses compared to SLSTR. We now compare SLSTR to OSTIA (Donlon et al., 2011) and CMC (Brasnett, 2008) where the daily SST analyses are ingested into the SLSTR MDB, which allows us to generate an equivalent set of plots to those for SLSTR. For the wind speed dependence, we see what appears to be a cools kin effect in both the OSTIA and CMC results. Also, we note a clear day/night dependence in both the OSTIA and CMC plots as a function of time difference. Here, as for SLSTR, a zero time difference is either 10:00 or 22:00. The crossing point is around zero for both OSTIA and CMC.

4. CONCLUSION

SLSTR is providing data of a quality to be used as a reference sensor for the GHRSST community. Issues observed with Bayesian cloud mask, especially in coastal areas, are being addressed. SLSTR provides a measure of SST_{skin}, which is confirmed through independent validation using data from multiple depths. Sub-skin SSTs derived from IR sensors can have a residual cool-skin effect if no explicit wind speed dependence is included, which could be minimised using SSES. Daily SST analyses provide an SST closer to a daily mean than a foundation temperature. A residual cool-skin effect may also be present.

We remind users that the SL_2_WST (GHRSST L2P) format product contains both dual-view (D2, D3) and nadir-only (N2, N3) retrievals. We recommend using only dual-view retrievals for reference sensor and only QL=5 data; never use D2 or D3 QL=4 data. Users must apply the SSES bias adjustments. SLSTR-B is harmonised to SLSTR-A through SSES. Further details can be found in the Product Notices available from EUMETSAT Sea Surface Temperature Services webpage:

https://www.eumetsat.int/website/home/Satellites/CurrentSatellites/Sentinel3/SeaSurfaceTemperatureServices/index.html

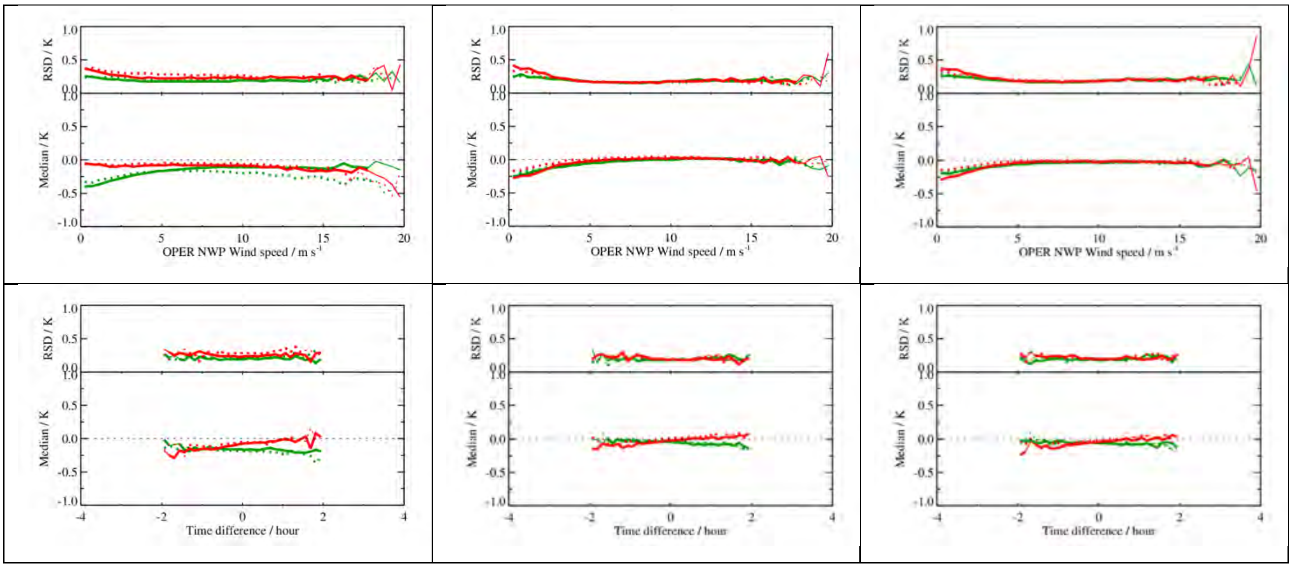

Figure 5: Dependence of the median difference between (left) SLSTR, (middle) OSTIA and (right) CMC and drifting buoys as a function of wind speed (upper) and time difference (lower). Plots are shown for daytime in red and nighttime in green.

5. REFERENCES

Brasnett B., 2008. The impact of satellite retrievals in a global sea-surface-temperature analysis. Q.J.R. Meteorol. Soc., 134.

Dee, D.P., Uppala, S.M., Simmons, A.J., Berrisford, P., Poli, P., Kobayashi, S., Andrae, U., Balmaseda, M.A., Balsamo, G., Bauer, P., Bechtold, P., Beljaars, A.C.M., van de Berg, L., Bidlot, J., Bormann, N., Delsol, C., Dragani, R., Fuentes, M., Geer, A.J., Haimberger, L., Healy, S.B., Hersbach, H., Hólm, E.V., Isaksen, L., Kållberg, P., Köhler, M., Matricardi, M., McNally, A.P., Monge-Sanz, B.M., Morcrette, J.J., Park, B.K., Peubey, C., de Rosnay, P., Tavolato, C., Thépaut, J.N., Vitart, F., 2011. The ERA- interim reanalysis: configuration and performance of the data assimilation system. Q. J. R. Meteorol. Soc. 137, 553–597.

Donlon, C. J., M. Martin, J. D. Stark, J. Roberts-Jones, E. Fiedler and W. Wimmer, 2011. The Operational Sea Surface Temperature and Sea Ice analysis (OSTIA). Remote Sensing of the Environment, 116, 140–158.

Donlon, C.J., Minnett, P.J., Jessup, A., Barton, I., Emery, W., Hook, S., Wimmer, W., Nightingale, T.J., Zappa, C., 2014. Ship-borne thermal infrared radiometer systems. In: Zibordi, G., Donlon, C.J., Parr, A.C. (Eds.), Experimental Methods in the Physical Sciences. Optical Radiometry for Ocean Climate Measurements 47. Academic Press, pp. 305–404.

Fairall, C. W., E. F. Bradley, J. S. Godfrey, G. A. Wick, J. B. Edson, and G. S. Young, 1996: Cool-skin and warm-layer effects on sea surface temperature. J. Geophys. Res., 101, 1295–1308.

Kantha, L. H., and C.A. Clayson, 1994: An improved mixed layer model for geophysical applications. J. Geophys. Res., 99, C12. 25234–25266.

Le Borgne, P., Marsouin, A., Orain, F., Roquet, H., 2012. Operational sea surface temperature bias adjustment using AATSR data. Remote Sens. Environ. 116, 93–106.

Petrenko, B., A. Ignatov, Y. Kihai, J. Stroup, and P. Dash, 2014, Evaluation and selection of SST regression algorithms for JPSS VIIRS, J. Geophys. Res. Atmos., 119.

Saux Picart, S., 2018. Algorithms Theoretical Basis Document for the Low Earth Orbiter Sea Surface Temperature Processing,

S2-5: 2019 ARCTIC SAILDRONE FIELD CAMPAIGN: MEASUREMENTS OF SEA SURFACE SALINITY AND TEMPERATURE FOR VALIDATION OF SATELLITE RETRIEVALS

Chelle Gentemann

Farallon Institute, California, USA, Email: cgentemann@faralloninstitute.org

SHORT ABSTRACT

In 2019 two NASA funded Saildrones, uninhabited surface vehicles (USVs), completed a 150-day field campaign in the Arctic Ocean, collecting in situ measurements in the Chukchi and Beaufort Seas, focused on sampling the marginal ice zone and regions with strong Sea Surface Temperature (SST) and Sea Surface Salinity (SSS) gradients. Our ability to access and observe the Arctic region has changed dramatically in recent years, owing to extreme seasonal sea ice melt-back and other climate-related impacts. In fact, this is now one of the most exciting areas of the world to study SST and SSS, in order to understand a variety of phenomena including heat exchange in the coupled air-sea system. However, satellite products in this region are presently very poorly validated, and are generally tuned to lower latitude in situ observations. These new in situ measurements, in concert with the advantages that come from multiple passes of polar-orbiting satellites at high latitudes, provide an opportunity to improve uncertainty estimates of SST and SSS in these challenging environments and improve our understanding of co-variability in SST and SSS in Arctic frontal regions.

S2 - POSTER PRESENTATIONS - SHORT ABSTRACTS

S2-P1: FORTY-FIVE YEARS OF OCEANOGRAPHIC AND METEOROLOGICAL OBSERVATIONS AT A COASTAL STATION IN THE NW MEDITERRANEAN: A GROUND TRUTH FOR SATELLITE OBSERVATIONS

Jorge Vazquez[(3)], Jordi Salar[(1)], Josep Pascual[(1)], Mar Flexas[(2)], Toshio. M. Chin[(3)]

(1) Instituto de Ciencias del Mar,
(2) California Institute of Technology,
(3) Jet Propulsion Laboratory, California Institute of Technology
Email: jorge.vazquez@jpl.nasa.gov

SHORT ABSTRACT

Marine and atmospheric parameters, including temperature observations from surface to 80 m (at 6 depths) are measured since September 1973 on a higher-than-weekly frequency, at a coastal station 4 km offshore L'Estartit (Costa Brava; NW Mediterranean). This constitutes the longest available uninterrupted oceanographic time series in the Mediterranean Sea. The present contribution focuses on observed climatic trends in temperature (°C/year) of air (AT; 0.05), sea surface (SST; 0.03), sea at 80 m depth (S80T; 0.02) and sea level (SL; 3.1 mm/year) as well as comparison with trends estimated from coincident high-resolution satellite data. The trending evolution is not uniform across seasons, being significantly higher in spring for both AT and SST, while in autumn for S80T. Other climatological results are a stratification increase (0.02 °C/year in summer temperature difference between 20 m (S20T) and S80T), trends in summer conditions at sea (when S20T > 18 °C), estimated as 0.5 and 0.9 days/year for the starting day and period respectively, and a decreasing trend of nearly 2 days/year in the period of conditions favourable for marine evaporation (when AT < SST). This last trend may be related to the observed decrease of coastal precipitation in spring. The long-term consistency in the *in situ* SST measurements presents an opportunity to validate the multi-decadal trends. The good agreement for 2013-2018 (RMS 0.5-0.6, bias -0.1 to -0.2; trends of 0.09 °C/year *in situ* vs. 0.06 to 0.08 °C/year from satellite) allows considering this observational site as ground truth for satellite observations and a monitoring site for climate change.

S2-P2: COMPARISON OF SGLI AND M-AERI SKIN SST NS

Yukio Kurihara

JAXA/EORC, kurihara.yukio@jaxa.jp, ykuri.kiyo@gmail.com

SHORT ABSTRACT

SGLI SST is an IR skin SST retrieved from the split-window data of SGLI, an optical sensor onboard the GCOM-C satellite. It is more than 2 years since the launch of GCOM-C, and we have SGLI SST from January 2018 to the latest. We usually validate SGLI SST by using buoy data. The latest validation result shows bias (median) and SD (RSD) of -0.12 K (-1.2 K) and 4.0 K (0.29 K) for daytime and -0.24 (-0.19 K) and 0.62 K (0.29 K) for nighttime. Although it is slightly contaminated by clouds, SGLI SST shows good agreements with buoy data. In this study, we compared SGLI SST with M-AERI skin temperature data. The comparison result will be introduced at GHRSST XXI.

S2-P3: EUMETSAT SLSTR SEA SURFACE TEMPERATURE MULTI-MISSION MATCHUP DATABASE

Igor Tomazic[(1)], Anne O'Carroll[(1)], Gary Corlett[(1)], Jean-François Piollé[(2)]

(1) EUMETSAT, Eumetsat-Allee 1, 64295 Darmstadt, Germany
(2) IFREMER, 38 Rue du Port Blanc, 35800 Dinard, France
Email : igor.tomazic@eumetsat.int

SHORT ABSTRACT

Sea surface temperature (SST) is an essential variable for operational forecasting and global climate monitoring and is one of the main products provided by the Copernicus Sentinel-3 Sea and Land Surface Temperature Radiometer (SLSTR) instruments. As such, there is a stringent requirement on SLSTR SST product performance: Its absolute accuracy should be better than 0.3 K and its temporal stability better than 0.1 K/decade.

One of the main SST Cal/Val activities to confirm these requirements is comparison with *in situ* reference measurements. To perform this activity we generate an SST matchup database (MDB) using the felyx application, from which we then analyse differences between SLSTR SST and *in situ* SST measurements. Currently we are using several *in situ* measurement types: drifters, Argo, moorings and ship-borne radiometers and recently we added *in situ* measurements from HRSST drifters built and deployed through the EUMETSAT/Copernicus TRUSTED project. The full SLSTR SST MDB contains variables from SL1 and SL2 products (both SL_2_WCT and SL_2_WST), as well as the main variables from the *in situ* datasets. The SLSTR MDB dataset for SLSTR-A is based on reprocessed data from the beginning of the mission until 04/2018, and operational NRT data onwards; the MDB for SLSTR-B is based on operational NRT data from 03/2019 onwards. As part of our internal validation activities, we also produce SST MDBs for AVHRR-B SST, IASI-B SST and VIIRS-NPP SST (L2 variables only), against all *in situ* types mentioned earlier.

This presentation will summarise our SLSTR SST MDB processing activities, including the most recent reprocessing of the radiometer dataset provided by the International SST (FRM) Radiometer Network (ISFRN), and the new HRSST TRUSTED drifters. The presentation will give an overview of the MDB content and format as well as details for access. Finally, we will summarise known issues and expected future improvements.

S2-P4: INTER-COMPARISON OF DAILY SEA SURFACE TEMPERATURE DATA AND IN SITU TEMPERATURES AT KOREAN COASTAL REGIONS

Hye-Jin Woo[(1)], Kyung-Ae Park[(2)], Hee-Young Kim[(3)]

(1) Dep. of Science Education, Seoul National University, Seoul, Korea, Email: hyejinwoo@snu.ac.kr
(2) Dep. of Earth Science Education, Seoul National University, Seoul, Korea, Email: kapark@snu.ac.kr
(3) Dep. of Science Education, Seoul National University, Seoul, Korea, Email: heeyoungkim@snu.ac.kr

SHORT ABSTRACT

This study presents results from the validation of six global blended sea surface temperature (SST) analyses using the *in situ* temperature measured from the coastal wave buoy and inter-comparison of them in the seas around the Korean Peninsula from 2014 to 2018: OSTIA (Operational SST and Sea Ice Analysis) CMC (Canadian Meteorological Centre) analysis, OISST (Optimum Interpolation SST), REMSS (Remote Sensing System) analysis, MURSST (Multi-scale Ultra-high Resolution SST), and MGDSST (Merged Satellite and In situ Data Global Daily SST). Overall, the root mean square error of each analysis for the *in situ* measurements was relatively high at a range from 1.27 °C (OSTIA) to 1.74 °C (REMSS). All analyses had warm biases over 0.29 °C, which were distinctive in the southwestern coastal region of the Korean peninsula with remarkable SST cooling due to strong tidal currents in summer. In the comparison of temporal variability, most analyses revealed low coherency (<0.5) in the period shorter than 10 days. The SST analyses have been compared against each other by investigating the spatial distributions of RMSE and bias errors. While most SST analyses tended to show good agreement in the open ocean, the differences had tendency to be amplified at the coastal regions and frontal regions. We discuss potential factors that cause the errors of SST analyses at the coastal regions by presenting the effects induced by grid sizes, distance from the coast, energy spectra, wavelet coherence, and thermal fronts in the marginal seas of the Northwest Pacific.

S2-P5: HIGH RESOLUTION SEA SURFACE TEMPERATURE RETRIEVAL USING LANDSAT 8 OLI/TIRS DATA AT COASTAL REGION

Hye-Jin Woo[(1)], Kyung-Ae Park[(2)], Hee-Young Kim[(3)]

(1) Dep. of Science Education, Seoul National University, Seoul, Korea, Email: hyejinwoo@snu.ac.kr
(2) Dep. of Earth Science Education, Seoul National University, Seoul, Korea, Email: kapark@snu.ac.kr
(3) Dep. of Science Education, Seoul National University, Seoul, Korea, Email: heeyoungkim@snu.ac.kr

SHORT ABSTRACT

High-resolution sea surface temperature (SST) images are essential to study the highly variable small-scale oceanic phenomena in the coastal region. Most of the previous SST algorithms are focused on the low or medium resolution SST from the near polar orbiting or geostationary satellites. The Landsat 8 Operational Land Imager and Thermal Infrared Sensor (OLI/TIRS) makes it possible to obtain high-resolution SST images of the coastal regions. This study performed a matchup procedure between 276 Landsat-8 images and in situ temperature measurements of buoys off the coast of the Korean Peninsula from April 2013 to August 2017. Using the matchup database, we investigated SST errors for each formulation of the Multi-Channel SST (MCSST) and the Non-Linear SST (NLSST) by considering the satellite zenith angle (SZA) and the first-guess SST. The retrieved SST equations showed RMS errors from 0.59 °C to 0.72 °C. Smallest errors were found for the NLSST equation that considers the SZA and uses the first-guess SST, compared with the MCSST equations. The SST errors showed characteristic dependences on the atmospheric water vapour, the SZA, and the wind speed. In spite of the narrow swath width of the Landsat-8, the effect of the SZA on the errors was estimated to be significant and considerable for all the formations. Although the coefficients were calculated in the coastal regions around the Korean Peninsula, these coefficients are expected to be feasible for SST retrieval applied to any other parts of the global ocean. This study also addressed the need for high-resolution, coastal SST, by emphasizing the usefulness of the high-resolution Landsat 8 OLI/TIRS data for monitoring the small-scale oceanic phenomena in the coastal regions.

S2-P6: INITIAL ASSESSMENT FOR THE CALIBRATION OF HY-1C COCTS INFRARED CHANNELS

Mingkun Liu, Lei Guan

Ocean University of China, Email: liumingkun@ouc.edu.cn

SHORT ABSTRACT

The Haiyang-1C (HY-1C) satellite was launched in September 2018, it is the successor satellite after HY-1A and HY-1B. The Chinese Ocean Color and Temperature Scanner (COCTS) onboard the HY-1C satellite has the capability of detecting the ocean colour parameters, as well as the sea surface temperature (SST). The initial assessment for the calibration accuracy of HY-1C COCTS infrared channels centred near 11 μm and 12 μm is undertaken through the inter-calibration of COCTS with the Infrared Atmospheric Sounding Interferometer (IASI) onboard Metop-B satellite. The IASI spectral radiances are convolved with the HY-1C COCTS spectral response functions to generate the IASI radiances. The matchups of HY-1C COCTS radiance with IASI are generated with a temporal window of 30 minutes, a spatial window of 0.12° and an atmospheric path tolerance of 3% for data in December 2018. The initial comparison result shows that COCTS 11 μm and 12 μm radiances are larger than IASI. The 11 μm and 12 μm BT differences show slight dependences on IASI BTs as well as total column water vapour. More analysis of COCTS infrared calibration accuracy will be investigated using long-time data, and the inter-calibration coefficients will be obtained based on the relationship of COCTS BTs with IASI in the future study.

SCIENCE SESSION 3: ANALYSES AND REANALYSES

S3 - SESSION REPORT

Helen Beggs[(1)], Andy Harris[(2)], Stéphane Saux Picart[(3)]

(1) Bureau of Meteorology, Melbourne, Vic, Australia, Email: helen.beggs@bom.gov.au
(2) NOAA/NESDIS/STAR, College Park, MD, USA, Email: andy.harris@noaa.gov
(3) Meteo-France, France, Email: stephane.sauxpicart@meteo.fr

1. INTRODUCTION

The Analyses and Reanalyses Science Session 3 was held on 2nd June 2020 with four presentations and six posters. These covered topics around inter-comparison of long-term SST analyses, new methods for assessing gradients in level 3 and level 4 SST products, updates to operational SST analyses, reprocessing of level 2 AVHRR SST datasets and new methods for generating level 4 SST analyses. We summarise here each presentation/poster and discussions.

2. SUMMARY OF ORAL PRESENTATIONS AND FORUM DISCUSSIONS

2.1. The Inter-comparison of Sea Surface Temperature Products in the framework of the Copernicus Climate Change Service (Chunxue Yang)

2.1.1. Summary

Chunxue presented the work of her Copernicus Climate Change Service (C3S) Independent Assessment of Essential Climate Variables (C3S_511) project team for SST at ISMAR and ENEA in Roma and Napoli (Italy), with the aim to inform data providers in order that they may improve their products and provide guidance for users. The project contributes to the activities of the GHRSST Climatology and Analysis Inter-comparison Task Team (IC-TT), with the aim to submit a final report and paper for publication in October 2020. The initial study reported here compared seven long-term SST analyses (ESA CCI SST v2.0, ERA5, HadISST1, Reynolds NCEP OIv2, MUR25, MGDSST and BoM Monthly OI SST) at a common 1 degree and monthly resolution against the ensemble mean. The most significant initial finding was that all seven datasets reproduce very similar spatial patterns of global SST trends. In addition, global mean warming trends as estimated from all the datasets are consistent (within the 95% confidence interval) with the global ocean warming trend as reported in the last IPCC report, estimated at 0.011 °C/year from 1980 to 2005.

2.1.2. Discussion

The work was discussed further in the Breakout IC Task Team Session on 4th June. Discussion in Session 3 centred around the Principle Component Analysis (PCA) of the SST, the data maturity matrix, mapping the project's metrics against the GHRSST Climate Data Assessment Framework (CDAF) document and expanding the assessment to include comparisons of SST gradients.

Igor Tomazic: A question related to data maturity matrix. Do you use it for all parameters and do you have some more information about the criteria you are using for grading?

Chunxue Yang: The data maturity matrix we will evaluate for the variables included in our service contract, spanning from ocean, land, atmosphere and glaciers domains. We developed our own guidance document to score the data maturity matrix and this will be published very soon in C3S CDS (probably July 2020).

Helen Beggs: Has your SST inter-comparison team in Italy checked your metrics against the GHRSST Climate Data Assessment Framework (CDAF) document at https://www.ghrsst.org/wp-content/uploads/2018/01/CDR-TAG_CDAF-v1.0.5.pdf ? It would be interesting to produce a table mapping which of the Independent Assessment of Essential Climate Variables (C3S_511) metrics/criteria are common to the CDAF metrics/criteria for an SST CDR.

Regarding your Recommendations to Users slide: Since you compared all L4 products at monthly 1° x 1° resolution, this precludes a comparison of feature resolution. In Jorge's Science Session 2 presentation he compares the ability of 6 high-resolution daily global SST analyses to accurately measure SST gradients.

- CY: We have written in our plan to do the SST gradients inter-comparison. It is also a point we need to discuss further.
- Chongyuan Mao: Have you investigated more about the other PCA modes? The second mode seems to be somewhat similar in most of the chosen products, but the third mode looks like they fall into two groups. Do you have a feeling if these modes have physical meaning and if so, what variability they might represent? Also, did you do PCA in other regions? I applied similar analysis to HadISST for the subpolar Atlantic back during my PhD, I'd be interested in comparing the results and see if there is anything in common.
- CY: For the PCA, in the SST inter-comparison, we only applied it to the tropical Pacific regions, and only commented on the first mode. We did not explore further in this report. One of our PhD students is working on Linear and Non-Linear PCA for the tropical Pacific and Indian Ocean, which is presented as a poster in Science Session 4. We will investigate further in terms of her work. Have you published a paper on your work in subpolar Atlantic? It will be very interesting for us to have a look.
- CM: My PhD thesis is accessible from https://ethos.bl.uk/OrderDetails.do?uin=uk.bl.ethos.618768. The work focused on long term variability of different seasons, hopefully it is somehow relevant.

2.2. Daily ICOADS3.0.2 and its impact on DOISST (Chunying Liu)

2.2.1. Summary

Chunying presented on recent updates to NOAA/NESDIS/NCEI's International Comprehensive Ocean-Atmosphere Data Set (ICOADS) to Revision 3.0.2 that now includes an operational daily *in situ* data set specifically to supply NCEI's new Daily Optimally Interpolated SST version 2.1 (DOISSTv2.1) analysis. The updates include merging the TAC (ASCII) and BUFR (binary) format drifting buoy, mooring, ice buoy, platform/rig, LightShip and ship SST data sets into ICOADS R3.0.2. The addition of the BUFR format data significantly increased the amount and spatial coverage of drifting buoy, mooring and ship SST data ingested into ICOADS and DOISST systems. ICOADS R3.0.2 greatly improves OISST analyses, reducing known cold biases on global and regional scales. Future work will include studying SST differences between the different *in situ* platforms on regional and temporal scales.

2.2.2. Discussion

Discussions revolved around the reduction in warm bias in ship SST over recent years and the increase in amount of ship SST data ingested into ICOADS R3.0.2 by the additional ingestion of BUFR format data.

Helen Beggs: What caused the reduction in overall warm bias over the past few years, particularly since 2016, in the ship SST observations from the GTS?

Chunying Liu: Ship SSTs are now mostly measured by engine intake or hull sensors. These should be colder than the drifters as they are deeper, but historically these have been biased warm, but that has been decreasing over time as e.g. remote reading has allowed sensors to be installed near the inlet giving a measurement more representative of the ocean than conditions in the engine room.

Haifeng Zhang: I suppose part of the reason why iQuam ships don't display a clearer decreasing trend (compared with CMC) especially over the recent 4-5 years might be that in iQuam, ICOADS R3.0.1 is being ingested instead of R3.0.2 at the moment. On slide 16 in Chunying's presentation, this ship-buoy difference starts to really converge to zero after 2015, when the difference between 3.0.1 and 3.0.2 begins to show.

CL: Our ICOADS3.0.2 data set have not yet been published. We will have a BETA release in July or August. I will let you know when ICOADS3.0.2 released.

HZ: We will shift to 3.0.2 when it's available. Everything about data sources in iQuam can be found in this webpage https://www.star.nesdis.noaa.gov/socd/sst/iquam/about.html - click on the 'Link' tab.

HB: The Bureau of Meteorology is also working to convert all our ship SST observations (including those provided by the IMOS project) to BUFR format. Once they are uploaded in BUFR format to the GTS you should be able to ingest our high-quality and high-resolution (1 minute) IMOS ship SST data into ICOADS.

2.3. A geometrical approach for Level 3 (super) collated and Level 4 SST analysis (Marouan Bouali)

2.3.1. Summary

Marouan's presentation on his novel method for gradient-based (super) collation of AMSR2, GMI, MODIS, VIIRS and *in situ* SST stimulated great interest amongst the session 3 participants. He demonstrated that this method allows preservation of statistics and dynamics without introducing artefacts and removes the need for single sensor bias correction. The approach is highly efficient, with one to two Fast Fourier Transforms and is robust to instrument noise (Gaussian and striping) and undetected clouds.

2.3.2. Discussion

All participants considered the Marouan's approach very new and interesting, and the presentation stimulated a very active discussion around its potential for preserving gradients and improving accuracy of level 3 and level 4 SST products.

Jean-Francois Piollé: It would be really great if you could share a python notebook implementing an example of your gradient based compositing, which we can replicate easily at home or try with the sensor(s) of our choice. Would you be able to do that?

Marouan Bouali: One of the requirements behind the funding of this project is for all developed algorithms to be implemented and used by a Brazilian operational agency first (IOUSP is mainly a research institute and does not get funding for operations). So unfortunately, at the current stage, we are in no position to share any code (maybe next year?). Operationalization or/and publication of the method will be discussed in the near future with the funding agency to determine the next steps of the project. Will keep you posted accordingly.

Helen Beggs: In your Summary slide you state that using your method there will be "no need for single sensor bias correction". Why?

MB: Standard compositing using two SST datasets that have strong biases with respect to each other leads to very clear artefacts. Applying a cross-sensor (or single sensor with respect to *in situ*) bias correction may reduce the visual impact of such artefacts but will affect gradients to some extent. When we shift to the gradient domain, we are only dealing with pixel-to-pixel variations (while biases tend to have much larger spatial scales), so we do not have to worry about differences in SST values between datasets in the merging process.

Irina Gladkova: Is it possible to have a sample of your L3S/L3C? Would be nice to compare and evaluate.

MB: Next month or so, I will generate a 5km L3S in the Brazil-Malvinas confluence region and the California Upwelling system using GMI, AMSR2, SNPP/JPSS1 VIIRS, Terra/Aqua MODIS and possibly SLSTR 1A/1B. Will share the link to a subsample of the dataset with you and anyone else interested once it's done.

Chris Merchant: It will be very interesting to see how you progress on creating analyses driven by gradients of SST fields. It is certainly to be hoped that this approach would preserve the gradient structure more faithfully than minimising SST error. Did I understand correctly that your method assumes the SST gradients in the L2/L3 input data are error free? Or at least unbiased?

MB: Absolutely, with this approach, gradients in L3C/L3S/L4 can only be as accurate as those observed at L2/L3U. Sometime in the future, we will explore the possibility of using such a method for the retrieval of SST at Level 2.

CM: So, it is clear that the errors in AMSR2 gradients and (say) VIIRS gradients are very different, because AMSR2 has much lower resolution and sharp gradients will often be significantly underestimated. You mentioned combining MW and IR data was possible -- what happens when the gradient estimates are so different?

MB: I wouldn't say that AMSR2 underestimates gradients compared to VIIRS, it is just not designed to see gradients below a given spatial scale (think of the gradient over a given pixel as the contribution of gradients ranging from large scale/mesoscale to the native resolution of the sensor). If we down-sample VIIRS data to a 25 km grid (AMSR2 native resolution), estimates of SST gradients will likely be of the same order as those from AMSR2. In other words, high resolution features observed in IR data are simply not seen in MW (i.e., null gradient field) hence the advantage of the gradient-based approach where one could (among other options) keep the highest gradients available to generate a L4 SST field.

Yukio Kurihara: How do you generate the temperature field from the gradient field?

MB: To get an SST field from its gradient field, we tackle the problem using computer vision variational models and minimize a quadratic or L1-norm based energy functional that measures the difference between the input gradient field and that of the solution we are looking for. The advantage of using a quadratic formulation over L1-norm is that we can get an analytical solution from the Euler-Lagrange equation using a Fourier transform. Once we have a solution in the SST value domain, we can modify its 1st, 2nd or nth order statistics with respect to the input observations.

YK: I guess it's also possible to take uncertainties in the data into account in the minimization. Are you already doing this?

MB: We are not using uncertainties in the minimization process. In fact, the main reason for shifting to the gradient domain is to avoid any assumptions (unlike OI) on error statistics. Including SST uncertainties in the gradient-based variational model, if at all possible, would defeat the very purpose of the technique. Uncertainties can however be used to improve statistics once an SST field is obtained from the estimated gradient field.

Korak Saha: The gradient approach seems to be addressing a couple of very important issues we have when we collate a few datasets to generate the L3C and L3S data. I have couple of questions. 1) In the gradient based approach I understand SSTs are converted into gradients then the FFT is used to collate the gradient fields, however, how are you getting back the SST fields after collation and merging, especially the L4 SST created using the AMSR-2 and *in situ* data using this gradient technique. 2) Same for the AMSR-2 L3C product what step is used to get back the SSTs from the gradient fields? 3) Also in the validation slide for the gradient L3C and L3Cg SSTs are each point daily global mean values of gradients?

MB: 1) and 2): We do not apply FFT on gradients. Gradients are included in a variational model. The analytical solution to the minimization of the model can be done using many techniques, FFT being one of them (although not the best. 3) Yes, the time series are generated by averaging the magnitude of SST gradients over the entire domain for each day. Note that if the Gulf Stream front is excluded, differences between gradients in L3C/L3S and L3C*g/L3S*g get even higher.

2.4. Ingesting VIIRS SST into the Bureau of Meteorology's Operational SST Analyses (Helen Beggs)

2.4.1. Summary

The Bureau of Meteorology (BoM) recently updated its operational daily optimally interpolated regional and global SST analyses (9 km RAMSSA and 25 km GAMSSA) to ingest NOAA's ACSPO VIIRS L3U SSTs from Suomi-NPP and NOAA-20 satellites. Other significant changes made at this time included increasing the background correlation length scales (from 20 km to 50 km for RAMSSA and from 50 km to 80 km for GAMSSA), updating the estimated STD for each input data stream (OBSESD) and updating GAMSSA's background field to relax to the previous week's BoM Global Weekly 1 degree SST analysis rather than the Reynolds and Smith (1994) 1961 to 1990 SST climatology. The update to RAMSSA on 17th November 2019 appeared to have minimal impact, but the update to GAMSSA on 29th April 2020 resulted in ~0.08 K reduction in robust standard deviation (RSD) compared with the GHRSST Multi-Product Ensemble (GMPE) and a reduction of ~0.05 K in robust standard deviation compared with independent Argo SST. The RSD of 25 km

GAMSSA minus GMPE is now similar to that of 10 km CMC, 5 km OSTIA or 5 km Geo-Polar Blend minus GMPE.

2.4.2. Discussion

Sasha Ignatov: I believe that following the GAMSSA upgrade, the "degraded innovation" [from matchups with buoy SSTs] may not necessarily be a bad thing, if your independent data (Argo floats mostly, but also GMPE to a large degree) show improved consistency. As we scientists know, a "partial derivative" approach would have been preferable, you have changed 5 things at a time and tend to attribute all blame/fame to only one factor which is adding VIIRS). I am unsure what effect the updated correlation scale had on all your analyses and statistics. Understand, though, that you work under many operational constraints, and try to minimize the upgrades. Overall, I believe that the GAMSSA update on 29 April is an improvement.

Helen Beggs: We performed many earlier tests over several months to arrive at our final configuration. However, I chose to present the innovation statistics for the final GAMSSA and RAMSSA configurations, which were the ones implemented in operations. Unfortunately, I was not able to test the impact of changing the climatology alone (from Reynolds and Smith, 1994 (1961-1990) to previous week's BoM 1 degree weekly SST analysis), which may have been considerable, due to operational constraints.

Andy Harris: It seems pretty clear that adding in a smattering of VIIRS has made a substantial improvement to GAMSSA. Regarding the actual methodology, can you explain a bit more about the observation correlation length scales you have used, and the justification for the thinning of the VIIRS data? I can think of no physical reason why a much higher resolution sensor (VIIRS) should be thinned more aggressively than NAVO GAC 9-km AVHRR SSTs (unless I have misunderstood what is going on). I do understand why MW data need a long observation correlation length scale, because the footprint is larger than the analysis grid, but the concept for high-resolution IR sensors eludes me.

HB: We use constant observation and background correlation length scales in RAMSSA and GAMSSA (as shown in the table in my presentation). Please see my RAMSSA 2011 AMOJ paper at http://www.bom.gov.au/jshess/papers.php?year=2011 for further details about how we use these correlation length scales in the OI system. Briefly: In the Bureau's OI SST analysis systems, the background field correlation length scale effectively gives the radius of influence of an observation to changes in the background field. Any feature smaller than the observation correlation length scale in extent and within the observation correlation time scale in time is treated by the OI analysis as noise. Observations separated by less than the observation correlation length scale and the observation correlation time scale will not have independent errors. When we initially tried ingesting the ACSPO VIIRS L3U data into RAMSSA and GAMSSA (after first gridding onto the RAMSSA 9 km and GAMSSA 25 km grid) we experienced unacceptable increase in SST artefacts and noise. After trying several combinations of observation correlation length scales (OBCSL) and Background Correlation Length Scales (BGCLS) and even changing the d1 and d2 (temporal decorrelation constants at mid-latitudes and low latitudes) and changing the weights of the input data streams we were no closer to reducing this noise. The Brasnett and Surcel Colan (2016) paper on ingesting VIIRS SSTs into CMC states that analysis quality decreases if density of the observation dataset is too large and the error correlations are neglected. The satellite retrievals (particularly VIIRS) are thinned prior to assimilation into the CMC OI analysis so they do not receive undue weight in the analysis. We measured the observation correlation length scale of the VIIRS L3C data ingested into test RAMSSA and it was longer than either the AVHRR or AMSR2 datasets, so although it was OK for us to ingest AVHRR at 9 km resolution and AMSR2 at 25 km resolution into RAMSSA, ingesting VIIRS gridded to 9 km caused the OI analysis to produce spurious artefacts. I experimented with various degrees of thinning and landed on thinning VIIRS in RAMSSA to 1/3° x 1/3° and in GAMSSA to 1/2° x 1/2°, although would like to tune further.

Wen-Hao Li: Do the upgraded GAMSSA and RAMSSA apply to the whole of the data records or only to the forward data stream?

HB: There are no plans (or funding) to reprocess RAMSSA or GAMSSA L4 at this stage to ingest VIIRS data prior to the operational upgrades.

Yukio Kurihara: I have a question on OBSESD. Is this a STD of buoy data? I can't see the difference between Australian STD and OBSESD in the slide 6.

HB: The OBSESD is an estimate of the total expected error and is calculated as STD (with respect to buoys) + | bias (with respect to buoys) |. This is very crude but appears to work. In fact, as I demonstrate in the innovation statistics in Slide 7, updating the OBSESD values in RAMSSA (thereby the relative weights of the various satellite data streams) to more up-to-date and realistic values, has a significant effect on the RAMSSA innovation statistics, reducing the STD by 0.016 K. Other L4 systems (like OSTIA) use the sses_standard_deviation values in the L2P or L3U files to weight the various input SST values. However, I treat all SST data from the one satellite equally. As mentioned on slide 3 I subtract sses_bias from AVHRR and VIIRS data, but not AMSR2. However, AMSR2 has become more biased lately so I may decide to subtract sses_bias after all.

3. SUMMARY OF POSTERS AND FORUM DISCUSSIONS

3.1. Improvements of the Daily Optimum Sea Surface Temperature (DOISST) Version 2.1 (Boyin Huang)

3.1.1. Summary

Boyin's poster describes the newly released (March 2020) NOAA/NESDIS/NCEI Daily OISST v2.1 blended SST analysis (aka "Reynolds Daily SST"), which largely mitigates the recent cold bias issues exhibited since 2016 in the DOISSTv2.0 analyses. The cold biases in DOISST v2.0 have been effectively reduced from -0.14 °C to -0.04 °C by changing the ship SST bias-correction from -0.14 °C to -0.01 °C, using ICOADS R3.0.2 buoy and ship SST data derived from BUFR and TAC data (see Chunying Liu's Session 3 presentation), and including Argo SSTs above 5 m depth. The impact of using Metop-B instead of NOAA-19 GAC AVHRR SST data is trivial because both Metop-B and NOAA-19 SSTs are adjusted by the same *in situ* SST observations. The DOISSTv2.1 daily analyses are available in GHRSST GDS2 L4 format from 1 January 2016 to present from JPL PO.DAAC and NOAA/NCDC, and NOAA plans to reprocess back to 1981.

3.1.2. Discussion

Helen Beggs: Are the statistics in Table 1 relative to Argo SST or to GMPE?

Boyin Huang: Table is relative to Argo. RMSDs are slightly higher when compared against GMPE.

HB: Considering that Metop-A is now in a drifting orbit (and getting quite old) does NCEI plan to ingest new satellite SST data streams, such as from Metop-C GAC AVHRR, NPP and NOAA-20 VIIRS into DOISST?

BH: VIIRS will be added after we reprocess v2.1 back to 1981.

HB: Are you interested in the DOISSTv2.0 (1981-2015) and DOISSTv2.1 (2016-present) being included in the GHRSST IC Task Team's Task 1 (Inter-comparison of SST analyses for climate studies)?

BH: I saw our names listed in Chunxue Yang's video presentation, and we will participate in the inter-comparison.

Xu Li: I suppose that the lost buoys are included in all the tests you show.

BH: Yes. The lost buoys are included in using the ICOADS R3.0.2.

XL: What does it mean exactly, "replacing ships bias from 0.14 to 0.01"?

BH: The ship biases are reducing after 2006, but a constant of 0.14°C was applied in OISST v2.0. We reduced the constant to 0.01°C after 2016 based on the latest statistics.

XL: Are more data available after the switch from NCEP archive to ICOADS R3.0.2?

BH: Yes.

XL: You did show the impact of the lost buoys, correct? Based on our experience, it has a significant impact, including making the SST warmer in a few areas.

BH: Yes. The use of ICOADS R3.0.2 greatly reduced the cold biases of OISST in the tropical and southern hemisphere oceans, particularly in the Indian Ocean.

3.2. OSTIA: past and future developments (Simon Good)

3.2.1. Summary

Simon's poster summarised the current and future UK Met Office Operational Sea Surface Temperature and Ice Analysis (OSTIA) system that produces near real-time daily foundation SST analyses and hourly average skin SST analyses in GHRSST GDS2 L4 format (see http://ghrsst-pp.metoffice.gov.uk/ostia-website/index.html). The OSTIA L4 has recently been reprocessed for CMEMS to cover the period 1981 to 2018. In December 2019 the OSTIA L4 system started to ingest satellite SST observations from NOAA-20 VIIRS and Sentinel-3B SLSTR, adding to the other satellite SST data streams ingested (NPP VIIRS, Sentinel-3A SLSTR, NOAA-19 GAC AVHRR, Metop-B GAC AVHRR, GCOM-W AMSR2, GOES-13 MSG4 SEVIRI).

3.2.2. Discussion

Helen Beggs: Several of the L4 products that you monitor using Argo SST actually ingest Argo data, such as MUR, RTG and DOISSTv2.1. I am not sure if FNMOC, DMI or K10 ingest Argo. It would be helpful in the GMPE Argo monitoring web page (http://ghrsst-pp.metoffice.gov.uk/ostia-website/gmpe-argo-stats.html) to mention which SST analyses ingest Argo data, as the validation of these using Argo is less informative.

SG: That's useful to know about these analyses using Argo data. I had thought that most/all did not include them to keep them independent for validation purposes.

Igor Tomazic: when you introduce SLSTR dual view as a reference sensor, is it also foreseen that you will reprocess OSTIA for the period when SLSTR is available (from 04/2016)?

SG: We won't reprocess the near real time OSTIA. However, we do have a similar reprocessed foundation SST dataset available on CMEMS: https://resources.marine.copernicus.eu/?option=com_csw&task=results?option=com_csw&view=details&product_id=SST_GLO_SST_L4_REP_OBSERVATIONS_010_011. This is generated using the same techniques as the near real time data, although some of the input data are different and it is bias corrected to ESA CCI and C3S data.

Hao Zuo: Could you let us know at which stage you have frozen your OSTIA system for reanalysis production? And will this reprocessed OSTIA product be kept up-to-date? We would like to avoid any jumpiness when switching from REP OSTIA to NRT OSTIA due to system differences.

SG: The reprocessed OSTIA is generated using a system that is consistent with the current near real time production system (i.e. after the improvements introduced in March 2019). It currently reaches the end of 2018 but we plan to extend it in the future. The hope is to eventually reach approx. a month delay to real time. The reprocessed OSTIA is bias corrected to ESA CCI and C3S data, while the near real time data are bias corrected to VIIRS and (soon) SLSTR so there is a potential for a jump if you need to switch between the two.

Alexander Ignatov: Your Met Office report showed sensitivity studies performed so far, but adding SLTSR to VIIRS as a reference will be done in the next OSTIA upgrade, correct?

SG: That's correct about SLSTR. The operational implementation of using SLSTR in the reference datasets is expected to be late this year.

AI: In your "Relative to OSTIA" time series on the left, do you subtract OSTIA's SD in RMS-sense (i.e., delta = sqrt(abs(bias^2-OSTIA_bias^2))*sign(bias-bias_OSTIA)? Or in a simple "additive" sense, i.e. delta=bias-OSTIA_bias? For SDs, seems to make more sense to do in RMS sense, just wondering how you calculate it.

SG: The relative plot shows the difference between OSTIA-Argo SD and the other Analysis-Argo SDs.

3.3. The recent update of SST analysis in NCEP GFS and a few related fundamental issues (Xu Li)

3.3.1. Summary

Xu Li's poster described recent changes to the NCEP Global Forecasting System's (GFS) SST analysis (NSST): (i) the addition of two more AVHRR radiance data streams from NOAA-19 and Metop-B (to the existing NOAA-18 and Metop-A data streams), (ii) stricter constraints on the SST climatology, and (iii) modified background handling for situations of recently melted sea ice. Recent developments for further NSST improvement include a new background error correlation length, new correlation length dependent thinning scheme for AVHRR and VIIRS radiances with thinning box sizes reduced to 25 ~ 100 km, addition of NPP and NOAA-20 VIIRS radiances, and rejection of the partly cloudy AVHRR radiances.

3.3.2. Discussion

Helen Beggs: Not sure if you are aware that NOAA-18 and NOAA-19 satellites are in drifting orbits and the AVHRR L0 to L1 calibrations are compromised, due to the satellites having been in full sunlight for several months at a time. How do you correct in your NSST system for poor AVHRR L0 to L1 calibrations? Do you bias-correct the radiances (L1) or bias-correct the SSTs (L2)?

Xu Li: In the NSST, the input is L1 (radiance), and there is a bias correction in the GSI (the atmospheric data assimilation system in the NCEP GFS, and the NSST analysis is a part of GSI) applied to the radiances, therefore, we cannot see the issue related to the NOAA-19 orbital degradation. But a more detailed check is probably necessary.

HB: Does the NSST analysis use Argo SST in any of the processing system? That is, would Argo SST provide an independent validation source?

XL: Basically, no Argo data is assimilated in the NSST. Yes, we can try to do the verification against Argo.

HB: If it is not possible to provide the NSST L4 files to the GHRSST community then would you consider validating NSST against GMPE and Argo SST, as is done for most other operational global SST analyses?

XL: I will push to make the NSST as one of the GHRSST L4 products. Extensive comparisons have been done against OSTIA, CMC and others, and will be done in the future, even in further detailed comparisons.

HB: If you supply NSST as a GHRSST GDS2.0 L4 (or even just a simple netCDF file) then it can be included in other GHRSST L4 inter-comparison activities, such as the UK Met Office's GMPE or NOAA/STAR's SQUAM web sites.

XL: The inter-comparison is always one of our tasks, particularly, the NSST is relatively young, the experiences from other products are valuable, for example, we didn't use the SST climatology as a constraint to get a better background (which is important when the observation coverage is poor), since there is not a forward/prediction model for NSST analysis.

Ian Dragard: Where can we find more information about the NSST? Do you recommend a webpage, article, presentation, or other bibliographic sources to find this information?

XL: A paper or an NCEP technical report is in a draft only. Currently, you can find the info on the NSST at:

Derber, J., and X. Li, 2018: Assimilating SST with an atmospheric DA system. ECMWF Workshop on Sea Surface Temperature and Sea Ice Analysis and Forecast, Reading, United Kingdom, ECMWF, 27 pp., https://www.ecmwf.int/node/17984.

P.J., Minnett, A. Alvera-Azcarate, T.M. Chin, G.K. Corlett, C.L. Gentemann, I. Karagali, X. Li, A. Marsouin, S, Marullo, E. Maturi, R. Santoleri, S. Saux Picart, M. Steele, J. Vazquez-Cuervo (2019), Half a century of satellite remote sensing of sea-surface temperature. Remote Sensing of Environment, Volume 223. https://doi.org/10.1016/j.rse.2019.111366.

There is a web site to briefly describe it:
https://www.emc.ncep.noaa.gov/emc/pages/numerical_forecast_systems/sst.php

Chris Merchant: The linear diurnal warming "profile" is interesting. When you say it doesn't need a reset overnight, is that because the depth smoothly becomes a maximum or large value and the heat in the diurnal layer is distributed across that depth?

XL: Yes, your understanding is correct. There is a threshold or maximum of the diurnal warming layer depth in the model, which is 30 meters (In Fairall's model, COVERV3.0, it is 19 meters). Since the convective adjustment is introduced, the stronger mixing reduces the heat content relative to a mixed layer, the convective adjustment action leads to larger warm layer depth. A reset is done once the depth reaches 30 m. That is equivalent to distributing the heat across that depth, which can be understood as so-called entrainment at the bottom of the mixed layer in the ocean, I think. As we know, there are three stability criteria in PWP model, Static, Mixed layer and Shear flow. The DTM-1p (NCEP diurnal warming model) is derived with mixed layer stability only with the linear profile, considering the time dimension (a static stable profile can become static unstable at the next time step), the 2nd criterion in the PWP model is applied. I'd like to point out that the 3rd one, shear flow one is not in yet, which can lead to more mixing at the bottom of the warm layer.

3.4. Towards 2nd reanalysis of NOAA AVHRR GAC Data (RAN2): Evaluation (Victor Pryamitsyn)

3.4.1. Summary

Victor's poster described the initial "beta" version of the second phase of NOAA's AVHRR GAC Reanalysis (RAN) project, covering the period 1981 to present (NOAA-07/09/11/12/14/15/16/17/18/19) and using the NOAA enterprise Advanced Clear-Sky Processor for Ocean (ACSPO) SST system. Validation results were presented for the initial beta RAN2 SST dataset covering Sep 1981 to Dec 2003. Two SST products are produced by ACSPO and available in the L2P/L3U files:

(i) Global Regression (GR), aka "Sub-skin" SST (sensitive to "skin" SST) and trained using global iQuam matchups and de-biased with respect to "depth" SST;

(ii) Piecewise Regression (PWR), aka "Depth" SST (a better proxy of "depth" SST) and trained using subsets of the same matchups.

The poster compared the RAN2 beta night-time SST verification against drifting and tropical moored buoy SST with similar validations from Pathfinder (PF) v5.3 and Climate Change Initiative (CCI) L2P v2.1 SSTs, both derived from GAC AVHRR brightness temperatures. The presentation demonstrated that (i) RAN2 typically provides more clear-sky observations, (ii) in accuracy/precision of sub-skin SST with respect to *in situ* SST, RAN2 outperforms PF, and often CCI. The temporal stability of satellite minus *in situ* bias is stable in RAN, by design, and RAN2 depth SST validates against *in situ* SST better than the sub-skin SST. The sensitivity of the CCI SST is closer to the optimum of 1 and less variable than in RAN2 B01 SST.

3.4.2. Discussion

Most of the extensive discussion concentrated on the relative advantages/disadvantages of methods for deriving and validating AVHRR SST values in the 1980's when *in situ* data were sparse.

Stéphane Saux Picart: I understand the RAN2 "depth" SST is generated using a set of coefficients calculated daily by regression against *in situ* measurements. Are these *in situ* measurements independent from the ones you used for verification?

VP: Both 'skin' and depth SST's are retrieved with daily variable coefficients (lookup tables), calculated from the same matchups, but with different algorithms and time sliding windows. We are using the same set of clear-sky matchups for training and testing, but time windows for training and testing are different.

Chris Merchant: Getting zero apparent bias and minimum apparent variance on the same dataset used to train an algorithm is automatic. It means we can't conclude much about errors for parts of the ocean with little data, which is a problem in the early record (when the geographical sampling was very uneven).

VP: I agree, but with the data we have for 1980-1990 and the early AVHRR's instabilities it is the best we can do.

Boris Petrenko: If we separate matchups into two parts, we would degrade the approximation of matchups in the area where they are available, but still would not be able to say anything about the area where matchups are unavailable.

Alexander Ignatov: Chris, nothing is different from the 2016 Rem. Sens. paper www.mdpi.com/2072-4292/8/4/315. In CCI I believe you anchor AVHRR radiances to (A)ATSRs from 1991-on, and to *in situ* SST in prior years? Unsure how much different it is from what we do in RAN?

Owen Embury: Strictly we anchor NOAA-12 onwards to (A)ATSR, while NOAA-7, 9, and 11 are to *in situ*. This means:

- For NOAA-12 onwards the AVHRR data has not been tuned to *in situ*, so you can use any or all types of *in situ* for validation.
- For NOAA-7, 9, 11 we used ship observations from even days of the year to train the retrieval:
    - you can use drifters, tropical moorings etc. for validation
    - you can still use ship observations from odd days of the year (but be aware that each ship has contributed different obs. to training the retrieval).

AI: Owen, we also trained the three pre-N12 satellites against a combination of D+TM+S. (Drifters, Tropical Moorings, and Ships). The same consideration: number of match-ups with D+TM was too small to reliably calculate the regression coefficients. And ships were much more numerous. But validated against D+TM only (which were a handful, as you know, in early satellite era).

The fundamental difference between the CCI and RAN: you try to stay as independent of *in situ* as possible. For the early AVHRRs, this requires some other anchoring - to (A)ATSRs, or to *in situ*. We state this complexity upfront and try to reconcile the unstable satellite data with (also not so stable, and sparse in the 1980s) *in situ*, as much as possible. Many L4 users are after the foundation SST anyway, so "fusion" with *in situ* SST is not such a bad thing for them (even desirable). Our focus is on coverage and SDs. These are more objective metrics, and the ones our users are probably more concerned with, given sparse and unstable data in the early era.

CM: I would not make any claims about stability or uncertainty on the basis of applying data back to the data they are tuned to. Doing this is not validation, it is just showing the residuals of a regression fit. Stability assessments and uncertainty validation in CCI are based on independent data -- we often used GTMBA, for example, which is not used at all in any tuning step whatsoever. Same with Argo.

AI: The "dependent" and "independent" data sets should both be as globally representative as possible. That means that both be largely representing the same "general population". If that is the case, then both should be closely "correlated", anyway. But the stability of coefficients depends on the number of matchup datasets.

Gary Corlett: Victor, can you provide some more details on how you generate matchups (i.e. what spatial and temporal limits etc.?). Also, do you have any daytime results or have you looked at the dependence on zenith angle, TCWV etc. yet, or is it too early in the RAN2 development process? You note the temporal stability of RAN2 is better than both PF and CCI - what methodology did you use to assess this? There are other *in situ* datasets such as Argo, radiometers, XBTs, MBTs, CBTs, that can provide some independence to the validation. Do you have plans to use these?

VP: (i) The details for the matchup can be found in http://www.mdpi.com/2072-4292/8/4/315 . We have both night and daytime results, but in this poster show only nights due to the space constrains; we have all the dependencies you mentioned in our quality control system (SQUAM). I hope we will publish everything at the final release of RAN2. (ii) The temporal stability relative to *in situ* matchups is due to the fact we calculate the coefficients for the retrieval algorithm from fitting matchups in a sliding temporal window. (iii) RAN2B01 ends at 2004, the Argo data are available only after 2006 and we use it in our quality control system (SQUAM). Some of the datasets you mentioned are in the process of assimilation into SQUAM.

GC: I just wondered if you had estimated the stability or had developed a new method (Dave Berry from NOCS has been leading on this within CCI; see https://www.mdpi.com/2072-4292/10/1/126). Point taken on Argo but the plots go to about 2008, so I might have been confused. The 'other' data [radiometers, XBTs, MBTs, CBTs] seem to be useful going back to the '80s (I use them all as a single miscellaneous dataset) and seem to be close to the quality of drifters.

AI: "I just wondered if you had estimated the stability or had developed a new method" - no and we don't pretend to. We just reconciled the AVHRR record with available *in situ* data. The RAN is as stable (or unstable) as the *in situ* data. AVHRR is linked to *in situ*.

"Point taken on Argo but the plots go to about 2008, so I might have been confused." - We state it in both Boris's and Victor's presentations that the RAN2B01 dataset we are looking at covers from 1981-2003. It's work in progress so some new years are being added and looked at, and we should not have shown years outside of this range.

Of course, when the complete RAN2 is produced (from 1981 till how late we manage to extend it as the N18 and N19 are already very sub-optimal now, so might need to stop in 2018 or 2019), it will be completely evaluated similarly to RAN1 including against Argo floats. RAN1 was only compared to PF - RAN2 will be compared to CCI, too. Based on RAN1 analyses, Argo closely reproduces what we see against drifters, but much more noisy (because of 2 orders of magnitude fewer match ups, even in best of times).

Kay Kilpatrick: I am surprised by the consistent ~ -0.2K and greater cold bias in your figure for the PF time series. I suspect that there is a problem in your plot and that it is really a plot of the PF skin temperature minus buoy temperature. The monthly mean values in your figure are in line with annual PF skin - buoy found here https://www1.ncdc.noaa.gov/pub/data/sds/cdr/CDRs/Sea_Surface_Temperature_Pathfinder/AlgorithmDescription.pdf .

I would also agree with Chris Merchant's comments that you need to have some form of cross validation if you want to make a statement that RAN2 stability is better than the other products.

RAN2 looks good but it could easily be over fit to the training data. Particularly when coefficients were estimated on a daily basis with less than ideal *in situ* data. During the n7-n11 period the available *in situ* data does not capture the full complement of atmospheres even when you add ships. It is not how many you have but where they are located that matters.

Korak Saha: It is good to see the comparison between RAN2, PF and CCI products. However, I have some doubts with the global mean bias plot for Pathfinder SST. As PF is a "skin" SST (though referred to as "sub-skin" in your poster), I presume you might have added 0.17 K to the PF data before calculating the difference field. If that is the case then I expect to see N7, N9-11 sitting at the -0.2 K and N14 and N16 sitting very near to "0" line. Am I missing something here?

VP: It is mentioned in the poster: "0.17 K was added to PF and CCI skin SST to facilitate comparisons with RAN “Sub-Skin” SST". That addition makes average difference values for CCI to be almost zero, but PF has some cold biases of -0.2 - 0.3 K , even when 0.17 K is added.

KS: The cold bias reported is 0.2K - 0.4K in the poster, that's what I wanted to highlight. Also it is possible that there is a bug somewhere in code as we get this value in the range of -0.2K to -0.1 K for the year 1981-2002.

3.5. Towards a 2nd reanalysis of NOAA AVHRR GAC Data (RAN2): Methodology (Boris Petrenko)

3.5.1. Summary

Boris's poster describes the modifications to the ACSPO L2P processing algorithms made during the RAN2 B01 reanalysis to process all NOAA AVHRR GAC SST data from NOAA-07/09/11/12/14/15/16/17/18/19 from

1981 to present. It is a companion to Victor Pryamitsyn's poster (see Section 3.4). During creation of the “B01" version of the RAN2 AVHRR SST dataset covering 1981-2002, modifications have been made to the ACSPO SST retrieval, training and cloud masking algorithms. These include: a) compensation of the sensor/orbital/calibration trends with variable daily regression coefficients; b) stable estimation of daily regression coefficients for both SST products with predefined sensitivity; c) filtering night-time warm SST outliers caused by solar impingement on the band 3/3b sensor.

Future development of RAN2 algorithms will aim to mitigate cold regional biases in retrieved SST (including those caused by contaminations of the atmosphere with volcanic dust) and explore potential correction of AVHRR brightness temperatures based on calibration parameters, available in L1B data.

3.5.2. Discussion

Stéphane Saux Picart: In your box 3, why do you have 2 sets of coefficients for your "sub-skin" SST and multiple sets for the "depth" SST? Is there a reason for that? Also when you train your regression coefficients do you select the matchups carefully and how?

Boris Petrenko: The "skin" SST uses two set of coefficients, one for day and one for night, both used globally. The "depth" SST is produced with a piece-wise regression algorithm. This algorithm uses multiple sets of coefficients, each trained on a separate subset of match-ups and selected by the regressors' values. This allows more precise approximation of *in situ* SST, although at the expense of sensitivity to "skin" SST.

AI: Stéphane, do I understand your question correctly: why is the sub-skin derived with Global Regression (GR), whereas the "depth" is derived with the piece-wise regression (PWR)? If this is what you asked, then the simple answer is: due to historical reasons. We came up with the GR first, and then when working on SSES, Boris explored the PWR. Which turned out to fit the *in situ* SST much better (but with a significantly reduced sensitivity). The PWR serves as a proxy for "depth", whereas the GR SST has high sensitivity, but larger SD with respect to *in situ*, and is hence a proxy for "sub-skin" (mainly because of larger regional biases, which the PWR does minimize). Ideally, and in the future, different but consistent forms of the algorithms (both PWRs or both GRs) will likely be needed.

Jon Mittaz: Boris, can you give a bit more detail of your process to remove warm pixels? Is this done at the SST level?

BP: Yes, it is done at the SST level, considering warm SST as outliers. The several predictors are used for this, such as solar and satellite angles, latitude, the consistency of the pixel with the training data set of matchups etc.

CM: It is a neat thought that the offset coefficient, which is easier to train, can be updated more frequently than the slope coefficients. How have you separated the training (box 4) and testing (box 6) matches -- e.g., randomly assigning per match, or per buoy ID etc.?

You showed N14. With the much fewer matches in the 1980s, is regularly updating the coefficients as possible? Or do you need longer windows?

BP: We did not separate training and validation data sets. All available matchups were used both for training and validation. I believe the goal of reanalysis is to fit all available data in the best way. In the 80s, i.e., for NOAA-7, -9 and -11, we used for training data from drifters, tropical moorings and ships. In 80's, the ships' SST were much more numerous, although less accurate, and this way of training has been much more efficient than using drifters and tropical moorings only. However, the validation results presented in Victor's poster are obtained without using ship data.

CM: Yes, using all the data to train presumably gives the best possible answer, but it means that the "validation" process does not inform you about the true levels of uncertainty and bias: the validation results are optimistic/unrealistic.

One idea is to do a train/test strategy just for uncertainty assessment: create independent train and test sets as independently as possible, train on the train set, and then validate on the test set. This gives a fairer understanding of the uncertainties -- pessimistic/realistic one could say, rather than optimistic/unrealistic. You can still use all data, as you have, for the "best possible" solution provided to users.

BP: Yes, I am familiar with the methodology of separating matchups into training and validation data sets. This may be useful for the analysis of the effect of the matchups' variability on SST estimates. At this point, however, we are most concerned with mitigating regional biases caused by, e.g., calibration issues and contamination of the atmosphere with volcanic dust. These effects, which make the largest contributions to SST from the earlier satellites, are best noticeable in SST - L4 SST rather than in SST - *in situ*. We may address the stability of SST estimates to training data set of matchups after we have learned how to deal with other sources of errors.

Kay Kilpatrick: Do you use any observation weighting function to the coefficient day within the +/- 45 or 180 day estimation window, or are coefficients basically a 3 month daily moving average? Could you clarify how you adjust the offset coefficient with 100 matchups, and how do you select which 100 matchups to use? With regard to using ship data for NOAA-7, -9, 11 do you use any type of transfer function to attempt to unify the depth and type of measurements from the ships as the proportion of bucket, ship intake, and hull contact measurement types changes significantly over time? I would think this could potentially be problematic, particularly for your SST depth algorithm which partitions the data into much smaller regression groups....for the early sensors you could get really biased offsets if, say, most of the records are ship intakes in one group and hull contact sensors in another, and bucket temperatures in a third. As to validation for the subsurface algorithm maybe use K-fold cross-validation so you can still take advantage of all the data. I have no good idea on how to easily validate daily coefficients for the SST depth algorithm where it clusters first, sometimes with just a few records, and then does a regression on each cluster.

Mike Chin: Is the RAN2 b01 data set available for the public yet?

VP: The RAN2 b01 data are available only for the internal STAR users, RAN2 b02 is under development right now, and the final RAN2 is planned to be archived and publicly available.

AI: We are still sorting out funding for this project. Given this is taken care of, we plan to release RAN2 in 2021. Are you thinking of extending your excellent MUR data set back to 1981? I thought about that and it would be with degraded spatial resolution (obviously) but still neat!

3.6. Optimum Interpolation Analysis for Sea Surface Temperature using the Oriented Elliptic Correlation Scales (Zhihong Liao)

3.6.1. Summary

Zhihong Liao's poster described a new optimal interpolation method to produce 0.25º level 4 (L4) SST analyses from Fengyun-3C (FY-3C) Visible and Infrared Radiometer (VIRR) SST observations using elliptically oriented correlation length scales. The resulting L4 product is compared against the traditional rectangular correlation length scales with respect to *in situ* SST and NOAA/NCEI Daily 0.25º OISST analyses. Statistical results for 2015 indicates that the SST results by using the oriented elliptical correlation scales is more effective than those using the rectangular correlation scales, and reduces the RMSE from 0.4194 K to 0.3816 K, but is larger than the DOISSTv2.0 with RMSE of 0.2780 K.

3.6.2. Discussion

Helen Beggs: Dear Zhihong and colleagues, I am sorry I missed the cut-off date to post to the GHRSST-XXI forum page. Thank you for sharing your poster on your very interesting OI method. You compare both your CMA SST analyses and NCEI's DOISSTv2.0 analyses against iQuam "*in situ* SST" but do not specify what type of platforms were used (drifting buoys, tropical moorings, ships, Argo, etc.). Note that NCEI's DOISSTv2.0 analyses ingest drifting and moored buoy SSTs at a higher weight than the ingested ship SST or AVHRR SST. Therefore, validating DOISSTv2.0 SST analyses using buoy SSTs is not informative. DOISST v2.0 does not ingest Argo float SST so this may be a useful independent data source for you to use for verification. You say in your poster that you use *in situ* SST data from the NOAA iQuam system. If you did ingest all available Argo SST (as well as buoy SST) then an effective method to compare your L4 analysis with other similar L4 analyses may be to compare your selected analyses against the daily GHRSST Multi-Product Ensemble (GMPE). See http://ghrsst-pp.metoffice.gov.uk/ostia-website/gmpe-monitoring.html . The near real-time GMPE daily 0.25 degree L4 files can be downloaded from:

https://resources.marine.copernicus.eu/?option=com_csw&view=details&product_id=SST_GLO_SST_L4_NRT_OBSERVATIONS_010_005 .

4. CONCLUSION

The extensive technical discussion that this session generated has illustrated the value of SST analysis and reanalysis practitioners meeting together regularly to exchange valuable information and compare techniques for deriving the most accurate/useful gap-free SST products derived from satellite observations.

S3 - ORAL PRESENTATIONS - EXTENDED ABSTRACTS

S3-1: THE INTERCOMPARISON OF SEA SURFACE TEMPERATURE PRODUCTS IN THE FRAMEWORK OF THE COPERNICUS CLIMATE CHANGE SERVICE

Chunxue Yang[1], Vincenzo Artale[1,2], Helen Beggs[3], Toshio Michael Chin[4], Vincenzo de Toma[2,5], Garrett Graham[6], Francesca Leonelli[1,7], Chongyuan Mao[8], Salvatore Marullo[1,2], Eileen Maturi[9], Bruno Buongiorno Nardelli[10], Andrea Pisano[1], Rosalia Santoleri[1]

(1) Institute of Marine Sciences, National Research Council of Italy, Rome, Italy
(2) ENEA; Italy, Email: chunxue.yang@artov.ismar.cnr.it
(3) Bureau of Meteorology, Melbourne, Australia
(4) Jet Propulsion Laboratory, NASA, USA
(5) Department of Physics, University of Rome “Tor Vergata”, Rome, Italy
(6) North Carolina Institute for Climate Studies
(7) Department of Mathematics, University of Rome “La Sapienza”, Rome Italy
(8) UK MetOffice, UK
(9) NOAA, U.S.
(10) Institute of Marine Sciences, National Research Council of Italy, Naples, Italy

SHORT ABSTRACT

The Copernicus Climate Change Service (C3S), the climate service initiative funded by the European Commission, aims to provide essential climate information to society, including citizens, business and policymakers, to understand climate change phenomenon and adapt to climate change impacts. We (CNR) are coordinating the Quality Assessment of Essential Climate Variables (ECVs) Products (including ocean, atmosphere and land) in the framework of C3S. The main objective is to assess essential climate variables based on products available in the Climate Data Store (CDS) of C3S, including reanalyses and L3 and L4 satellite products, and establish relations of trust between climate information providers and various downstream users.

Sea surface temperature (SST) is a key parameter to assess the state of the global climate system and monitor its variations on interannual and (multi)decadal timescales. Inter-comparison of SST re-analyses is thus an important step to inform users about the characteristics of different products, helping them to select the one that suits their applications best. We will provide guidance for users to do climate studies and climate applications with scientific input based on our scientific expertise.

In collaboration with the GHRSST Inter-comparison Task Team, we created an ensemble of seven SST analyses for comparison, including products available on CDS-C3S and provided by GHRSST data providers, mapping to a common 1 degree grid and monthly averages. At the first stage we performed basic diagnostics including mean climatology, time series, and linear trends of each ensemble member, and differences of each ensemble with respect to the ensemble mean. The El Niño Southern Oscillation (ENSO) is selected as a specific case study to evaluate the representation of ENSO in the ensemble SST products, applying the Principle Component Analysis (PCA) method. Further analysis, such as SST gradients, will be performed in the next step to advance the SST inter-comparison activities.

Article submitted for publication

S3-2: DAILY ICOADS3.0.2 AND ITS IMPACT ON DOISST

Chunying Liu[1,2], **Boyin Huang**[1], **Eric Freeman**[1,2], **Huai-min Zhang**[1], **Elizabeth C. Kent**[3], David I. Berry[3], Steven J. Worley[4], Thomas Cram[4], Zaihua Ji[4], Mathieu Ouellet[5], Isabelle Gaboury[5], Angela R. Sallis[1,6]

(1) NOAA National Centers for Environmental Information, Email: chunying.liu@noaa.gov
(2) Riverside Technology, inc. Fort Collins, CO, USA
(3) National Oceanography Centre, Southampton, UK
(4) National Center for Atmospheric Research, Boulder, CO, USA
(5) Fisheries and Oceans Canada, Ontario, Canada
(6) General Dynamics Information Technology, Stennis Space Center, MS USA

1. INTRODUCTION

In 2003, the World Meteorological Organization (WMO) approved a policy that all observational data exchanged internationally on the WMO Global Telecommunication System (GTS) be migrated from the Traditional Alphanumeric Codes (TAC) to the Table Driven Code Forms (TDCF) such as the Binary Universal Form for the Representation (BUFR) of meteorological data format. To align with the WMO policy, many countries and programs have, in recent years, begun switching to BUFR or are currently in the process of switching over to BUFR. The number of marine *in situ* reports in the current operational International Comprehensive Ocean-Atmosphere Data Set (ICOADS) Release 3.0.1 has been decreasing since 2016 due to the switching of TAC to BUFR. The situation is especially severe for the drifting buoy reports. The coverage of buoy sea surface temperature (SST) has decreased from nearly 40% in 2016 to as low as 5% by 2019 based on monthly 2 degree grid box. To meet the needs of the marine *in situ* data users such as the SST community, a new version of ICOADS, Release 3.0.2, has been developed by blending both TAC and BUFR data from NOAA's National Weather Service Telecommunications Gateway (NWSTG).

2. EXTENDED ABSTRACT

In this paper, we describe how the daily ICOADS R3.0.2 was created. Then we compare the ICOADS R3.0.2 and ICOADS R3.0.1. The comparison results shows that the total marine reports number of ships, moored buoys, and drifting buoys of ICOADS R3.0.2 increased by about 30% and the data coverage of the above 3 platforms increased by about 33% based on monthly 2 degree grid box. Finally, we focus on the SST study from different platforms such as ships, drifting buoys, and moored buoys. We first explore the homogenization of the SSTs from different platforms, and then we assess the impact of the SSTs from each platform on daily Optimum Interpolation Sea Surface Temperature (OISST). Finally, by applying the daily ICOADS R3.0.2 to OISST, we show the improvement of OISST such as the cold bias reduction on the global and regional scales.

3. FIGURES AND TABLES

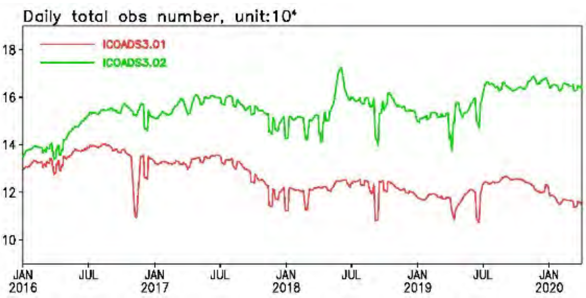

Figure 1: daily total number of reports

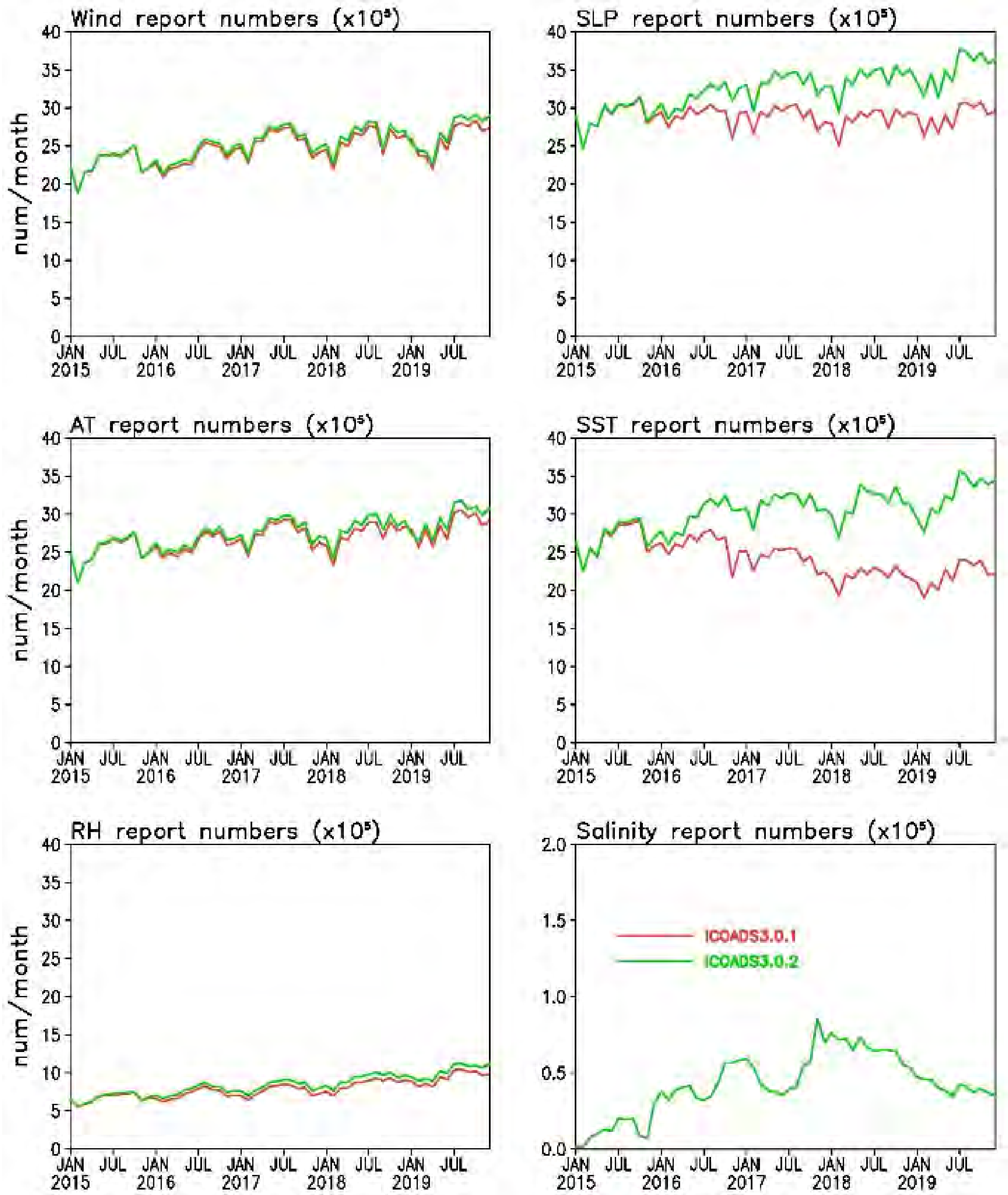

Figure 2: Report number of essential climate variables.

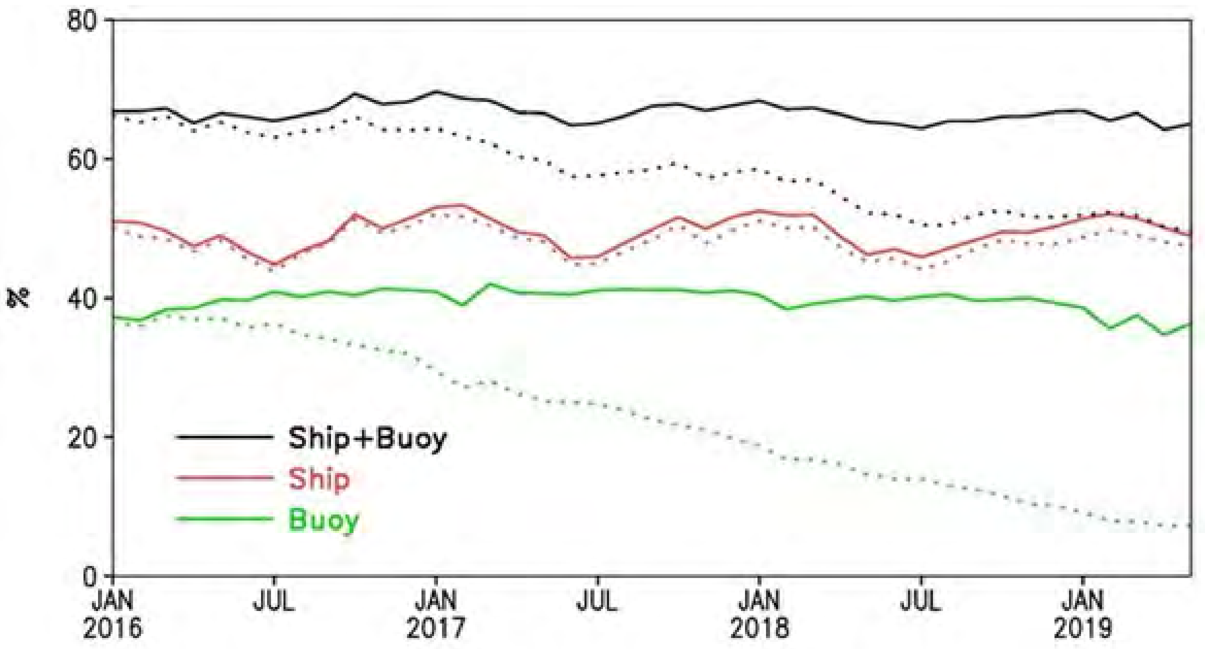

Figure 3: Global SST coverages on monthly 2°×2° grids. Solid lines represent ICOADS R3.0.2 and dotted lines represent R3.0.1.

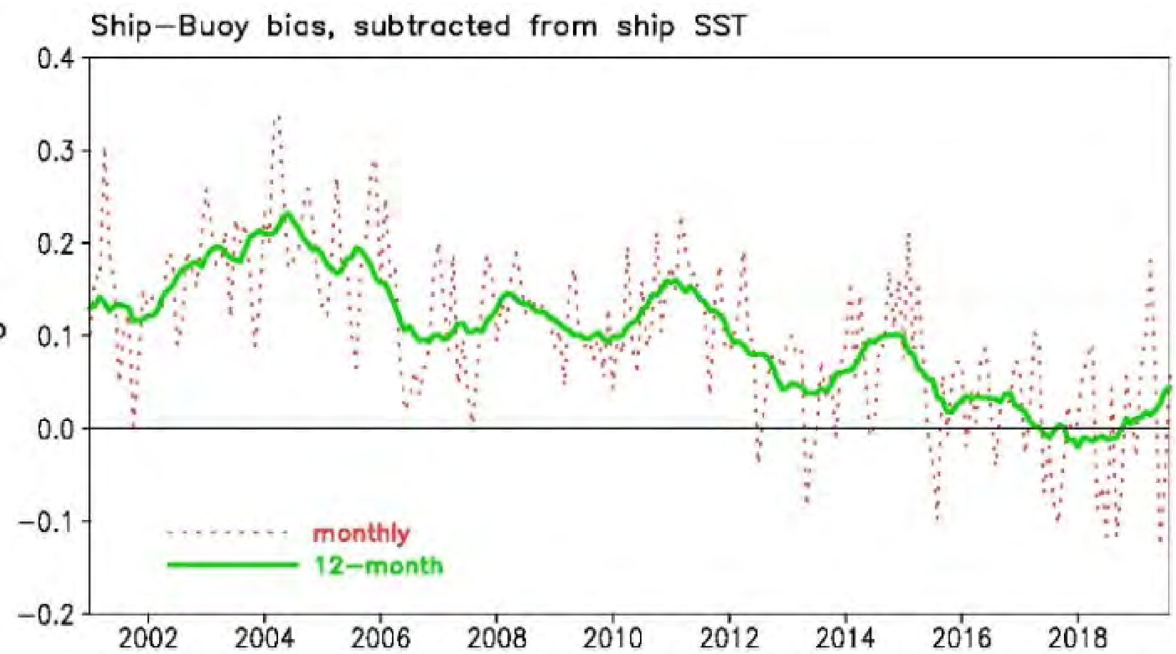

Figure 4: Monthly (dotted red) and 12-month running averaged (solid green) ship SST biases (°C) defined as the difference between ship and buoy SSTs.

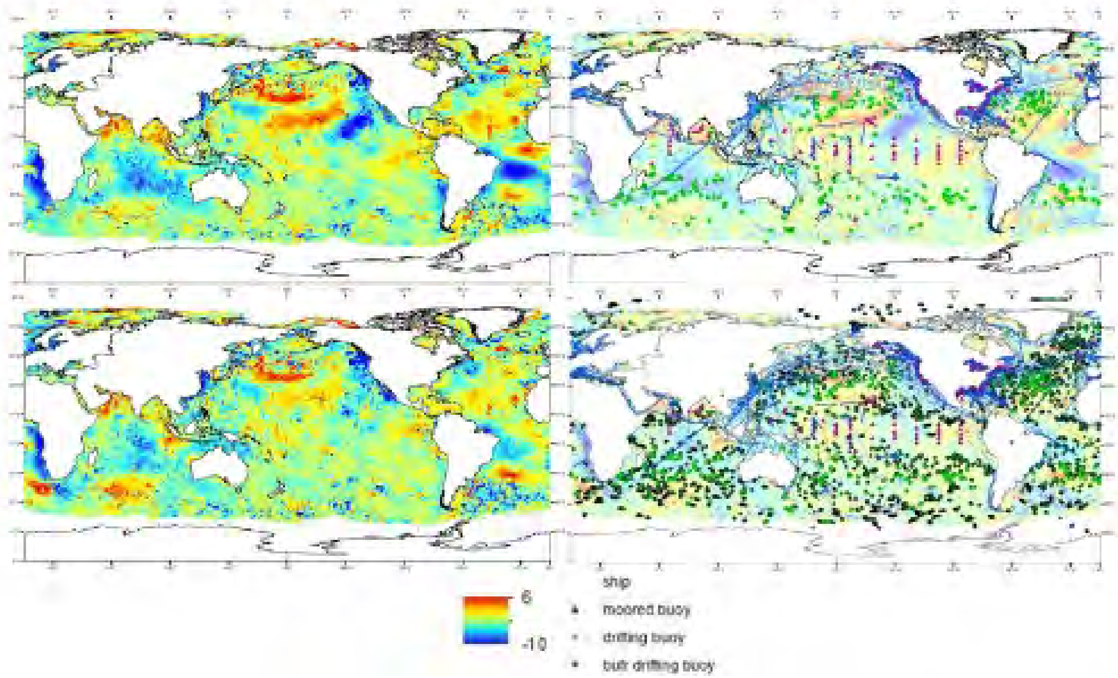

Figure 5: OISST anomaly relative to the GMPE and Drifting buoy, moored buoy, and ship observations overlaid on OISST. Top left: OISST using NCEP TAC anomaly relative to GMPE. Bottom left: OISST using R3.0.2 anomaly relative to GMPE. Top right: Drifting buoy, moored buoy, and ship of observations of NCEP TAC overlaid on OISST using NCEP TAC. Bottom right: Drifting buoy, moored buoy, and ship of observations of R3.0.2 overlaid on OISST using R3.0.2.

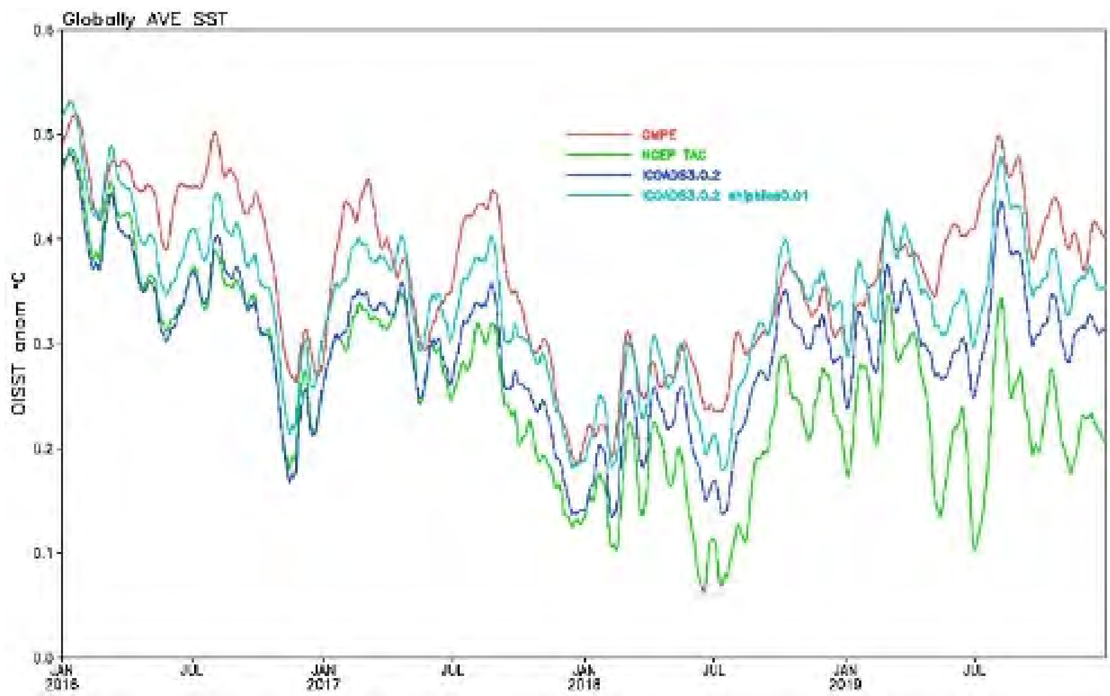

Figure 6: Globally average SST anomalies

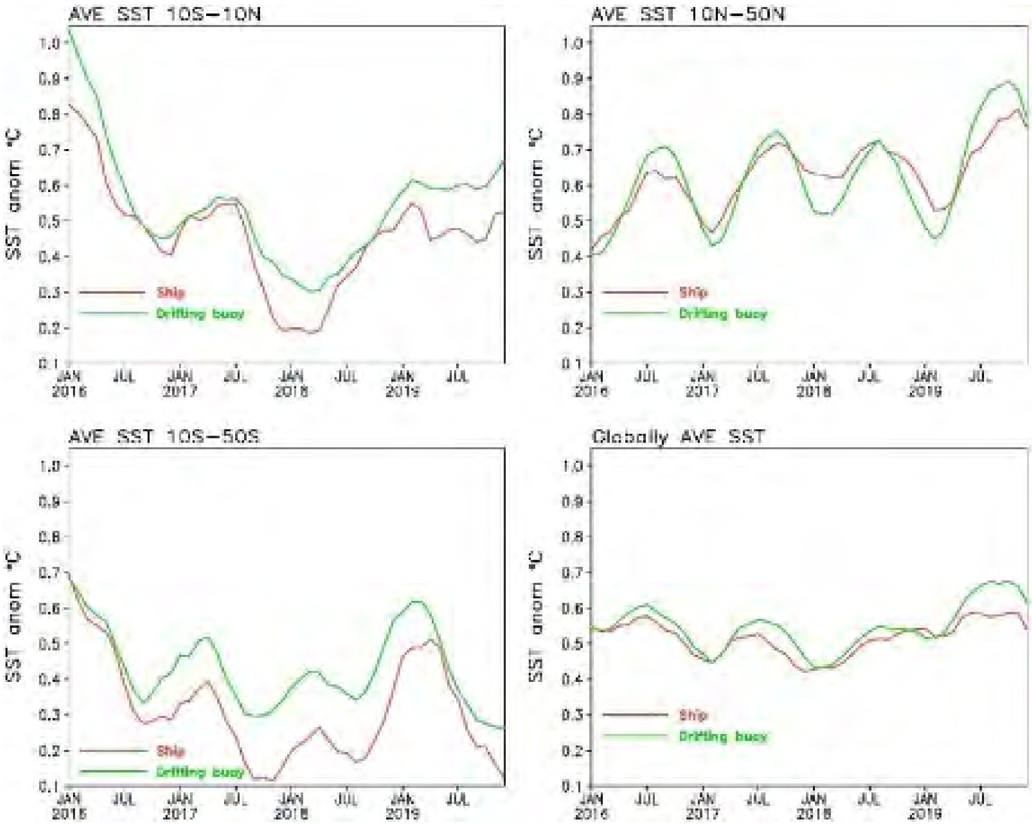

Figure 7: Monthly SST difference between ship and drifting buoy SST anomalies

4. RESULTS

4.1. Comparisons between ICOADS R3.0.2 and R3.0.1

ICOADS R3.0.1 has been updated to R3.0.2 by adding BUFR data ingested from NWS. The main part of BUFR + TAC merge is duplicate elimination. Ideally, duplicate reports can be identified by exact comparison (exact match) of location, time, and weather/marine fields. But due to the different data sources and transmission methods, slightly different conversion techniques and interpretations have made duplicates more difficult to identify. Reports that were once exactly the same now have random or systematic differences in one or more of their fields. For example, the latitude and longitude from some reports of TAC stream are in the tenths of a degree, but the same reports from BUFR stream are in the hundredths of a degree. The exact match comparison would separate them as unique reports. To eliminate potential duplicates due to changes in precisions, we allow 0.05 degree tolerance to define a duplicate.

Figure 1 shows the daily total number of reports. The red line is ICOADS R3.0.1 and the green line is ICOADS R3.0.2. Clearly there is an increase of reports since 2016 due to the BUFR data input. By April 2020, there are 5.0 million reports in R3.0.2, and only 3.5 million reports in R3.0.1.

Figure 2 displays that the numbers of essential climate variable (ECV) observations are generally higher in R3.0.2 than in R3.0.1. The numbers of wind speed and direction, air temperature (AT) and relative humidity (RH) observations are slightly higher in R3.0.2 than in R3.0.1. In 2019, the number of sea level pressure (SLP) observations is about 2.8 million in R3.0.1, but increased to 3.7 million in R3.0.2; from 2015 to 2019, the number of sea surface temperature (SST) observations decreased from about 2.7 million to 2.2 million in R3.0.1, but increased from about 2.7 million to 3.5 million in R3.0.2.

The increase in observation numbers also results in an increase of spatial coverage. For example, R3.0.2 SST coverage is about 65%, while R3.0.1 SST coverage is only 50% based on area-weighted 2° boxes (Figure 3).

4.2. ICOADS R3.0.2 impacts on OISST

The daily 0.25° optimum interpolation sea-surface temperature (OISST) analysis uses satellite and *in situ* SST estimates for a global SST analysis. Cold biases were found in OISST in recent years, which were suspected to be caused by the sparse buoy observations.

Three experimental runs were designed to investigate if the sparse buoy observations contribute to the cold bias. All the runs use the same satellite data METOP-A and METOP-B and the same NCEP ice. There are three scenarios for *in situ* SST. In scenario 1, observations from the NCEP TAC data were used. In scenario 2, observations from ICAODS R3.0.2 with ship bias of 0.14°C with respect to buoy were used. Ship SSTs are now mostly measured from engine intake or hull sensors. Remote reading has allowed sensors to be installed near the inlet so ship SST quality is getting better. As shown in Figure 4, the warm bias of ship SST has been smaller since 2016. Therefore, in scenario 3, the ICOADS R3.0.2 observations with ship bias of 0.01°C were used.

Figure 5 presents scenarios 1 and 2 OISST anomalies relative to the GHRSST Multi-Product Ensemble (GMPE) for 14 August 2018. As can be seen, the cold bias was obvious in scenario 1 when *in situ* SST data were from NCEP TAC only (top left panel), and it became much smaller in scenario 2 with data from ICOADS R3.0.2 (bottom left panel). The right panels display drifting buoy, moored buoy, and ship observations from NCEP TAC (top right panel) and ICOADS R3.0.2 (bottom right panel) overlaid on the OISST anomaly relative to the GMPE. Cold biases (in blue in the maps) tend to occur where drifting buoy observations are sparse.

The above result indicates that ICOADS R3.0.2 does improve the OISST, but we still see cold biases in some regions such as the Indian Ocean and East Pacific Ocean. This may be caused by the overcorrection of the ship warm bias. So in Scenario 3, ship bias is set as 0.01°C instead of 0.14°C. Figure 6 shows globally averaged SST anomalies for GMPE (red), and OISST from the three scenarios: scenario 1 with NCEP TAC feed (green), scenario 2 with ICOADS R3.0.2 and ship bias 0.14°C (blue), and scenario 3 with ICOADS R3.0.2 and ship bias 0.01°C (light blue). We can see the cold biases are further reduced in scenario 3 run due to the ship bias changed to 0.01°C.

To further remove the cold bias in OISST, we need to investigate the SST heterogeneity between different platforms. Figure 7 exhibits the monthly SST difference between ship and drifting buoy SSTs collocated to 2° box. We can see the SST difference between drifting buoys and ships vary among different zones and along the time. To further improve the OISST quality, we need to investigate spatial and temporal differences of the bias between different platforms.

5. CONCLUSION

ICOADS R3.0.2 is much improved from R3.0.1. It increases data volumes, ocean data coverages, and the number of observations of Essential Climate Variables (ECVs). ICOADS R3.0.2 greatly improves OISST. It has reduced known cold biases especially where drifting buoy observations are sparse. SSTs from different observing platforms in R3.0.2 are heterogeneous on global and regional scales, and the biases change with time. Future study is needed to show the SST differences between the different platforms and their variations with time. By taking a regional scale and dynamic bias correction, we may further improve the quality of OISST as well as other related SST products.

S3-3: A GEOMETRICAL APPROACH FOR LEVEL 3 (SUPER) COLLATED AND LEVEL 4 SST ANALYSIS

Marouan Bouali [(1)], Paulo Polito [(1)] and Olga Sato [(1)]

(1) Institute of Oceanography of the University of São Paulo, Brazil , Email: marouan.bouali@usp.br

1. INTRODUCTION

Many studies rely on the use of satellite-based SST to investigate the spatial distribution and temporal variability of ocean frontal activity. This is due to the important role played by ocean fronts and gradients on several fields such as fisheries, ecosystem management, ocean-atmosphere interaction and acoustic communication. Also, climatologies of SST gradients can serve the operational production of accurate SST datasets as they can be used as input in cloud masking algorithms to mitigate the misclassification of fronts as clouds.

Currently, the validation of satellite-based SST relies only on a statistical comparison with independent *in situ* measurements, which does not provide much insight into the accuracy of SST gradients. As such, proper selection of an SST product for the analysis of SST fronts/gradients remains unaddressed.

While L4 products offer major practicality from a user perspective (i.e., gap-free), the interpolation in space and time required to generate these products does not ensure that extracted gradients correspond to those observed at Level 2/Level3U.

The latest generation of GHRSST products, i.e., L3 “Collated” (L3C) and L3 “Super-Collated”, L3S, provide a new perspective for the community of physical oceanographers interested in ocean dynamics. However, this depends largely on the way they are produced. For example, a L3C SST combines data from the same instrument over a given period of time to increase coverage. When small differences exist between successive observations (due to diurnal warming, angular biases, missing values), the compositing tends to introduce artefacts that translate as artificial high gradients which do not correspond to true SST features. In passive microwave SST from AMSRE/AMSR2, these can be typically seen along the edge of swaths derived from the ascending and descending orbits.

In this study, we introduce preliminary results obtained with a new technique for compositing/merging SST datasets. By exploiting the fact that at the grid level, pixels can be seen as SST gradients instead of SST values the proposed approach allows to simultaneously preserve the statistics and geometry of Level 2/L3U observations when producing L3C, L3S and Level 4 SST.

2. DATA (L3C)

We focused on the Gulf Stream region as it is well known for strong mesoscale and submesoscale activity. Using one year (2018) of L3U AMSR2 SST produced by Remote Sensing Systems (RSS), we generated two separate products, i.e. one using standard compositing and one using the proposed gradient-domain merging. For statistical validation, we used drifting and coastal moored buoys obtained from NOAA/NESDIS iQuam v2.1. Figure 1 illustrates how the statistical characteristics of the two products, i.e., bias and standard deviation with respect to *in situ*, are almost identical. This consistency does not hold when analysing the magnitude of SST gradients as can be seen in Figure 2.

We note that gradients derived from the standard composite display higher magnitudes and temporal variability compared to the gradient-domain merged product ($L3C^{*G}$). These differences are only due to the introduction of artificial gradients when statistically compositing SST data, as is illustrated in Figure 3.

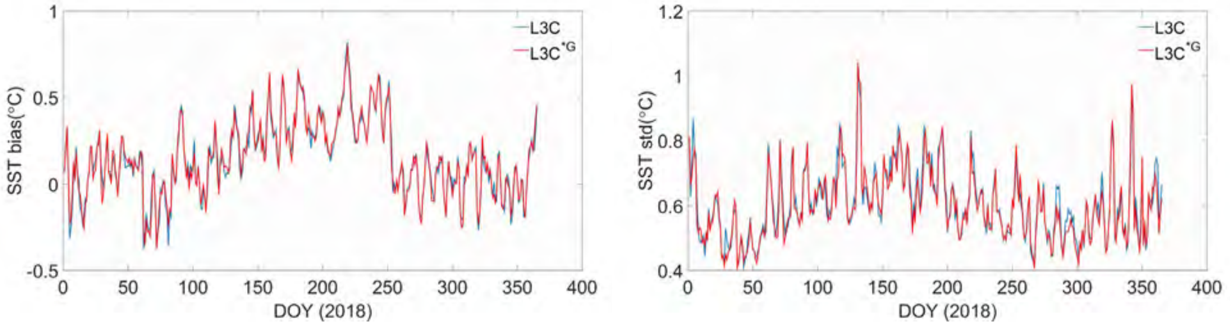

Figure1: Bias (left) and standard deviation (right) with respect to in situ measurements for standard compositing L3C and the gradient-domain approach L3C^{*G}

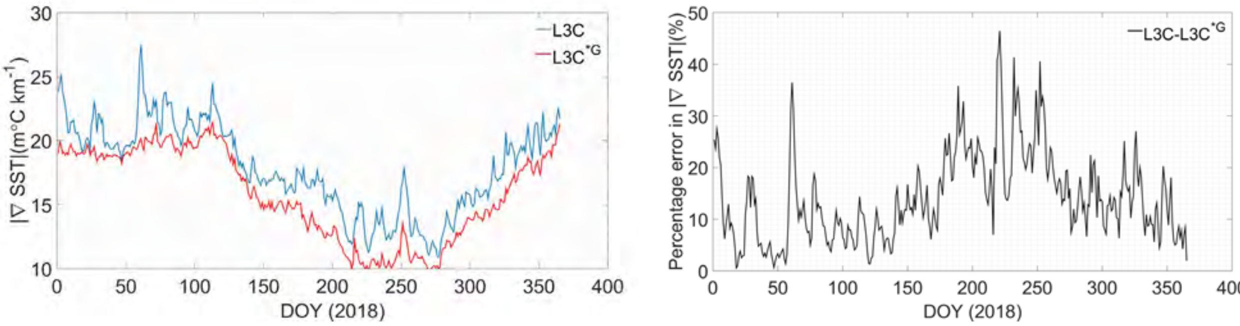

Figure 2: Time series of SST gradient magnitudes averaged over the entire Gulf Stream region for the year 2018, using standard compositing L3C and the gradient-domain approach L3C^{*G} (left) Percentage error in the magnitude of SST gradients (right)

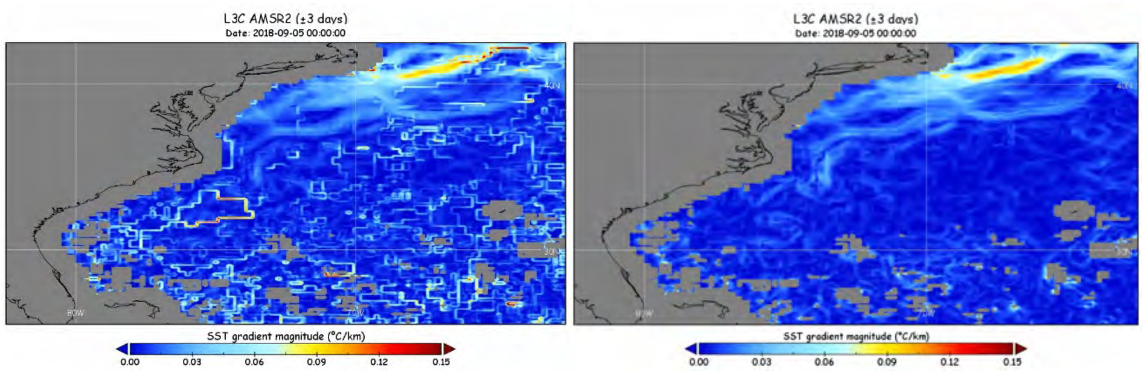

Figure 3: SST gradient magnitude for the period from Sep 2-8 2018 in the Gulf Stream region derived from standard compositing L3C (left) and the gradient-domain approach L3C^{*G} (right)

3. CONCLUSION AND FUTURE WORK

Standard compositing based on (weighted) averaging introduces strong artefacts that affect the spatial distribution, magnitude and temporal variability of SST gradients. Merging SST observations acquired over a time window and/or from multiple instruments using gradient-based computer vision algorithms can overcome these limitations. Further, the proposed methodology offers additional advantages as it 1) does not require single sensor bias correction 2) is computationally efficient (insensitive to the amount of L2 datasets ingested) 3) is robust to unmasked clouds and sensor noise 4) can ingest gradients captured by moving *in situ* sensors like drifting buoys, ships and Saildrone.

Future work will include testing and validation over several dynamic regions such as the Brazil-Malvinas confluence region and the California Current Upwelling System.

S3-4: INGESTING VIIRS SST INTO THE BUREAU OF METEOROLOGY'S OPERATIONAL SST ANALYSES

Helen Beggs[(1)], Lixin Qi[(2)], Pallavi Govekar[(3)] and Christopher Griffin[(4)]

(1) Bureau of Meteorology, Melbourne, Australia, Email: helen.beggs@bom.gov.au
(2) Bureau of Meteorology, Melbourne, Australia, Email: lixin.qi@bom.gov.au
(3) Bureau of Meteorology, Melbourne, Australia, Email: pallavi.govekar@bom.gov.au
(4) Bureau of Meteorology, Melbourne, Australia, Email: christopher.griffin@bom.gov.au

ABSTRACT

We describe the method used to ingest Visible Infrared Imaging Radiometer Suite sea surface temperature data into the Australian Bureau of Meteorology's operational daily temperature analyses and demonstrate the effect on accuracy and quality of these analyses.

1. INTRODUCTION

Since 2006, the Bureau of Meteorology (BoM) has produced daily optimally interpolated (OI) foundation sea surface temperature (SST) analyses over the Australian region and global domain. The Regional Australian Multi-Sensor SST Analysis (RAMSSA: Beggs et al., 2011) provides boundary conditions for the BoM's regional numerical weather prediction (NWP) models (ACCESS-R2 and ACCESS-C3), while the Global Australian Multi-Sensor SST Analysis (GAMSSA: Zhong and Beggs, 2008) provides boundary conditions for global NWP models (ACCESS-G3 and ACCESS-TC) and initial conditions for seasonal prediction models (POAMAv2 and ACCESS-S2). Both analyses provide SST products to forecasters and the general public (http://www.bom.gov.au/marine/sst.shtml, Figure 1). In addition, GAMSSA contributes to the GHRSST Multi-Product Ensemble (http://ghrsst-pp.metoffice.gov.uk/ostia-website/gmpe-monitoring.html).

The RAMSSA and GAMSSA GHRSST Data Specification v2.0 format level 4 (L4) files (GHRSST Science Team, 2012) from 2006 to present are publicly disseminated via NASA/JPL's PO.DAAC (https://podaac.jpl.nasa.gov) and the Australian Ocean Data Network (AODN: https://portal.aodn.org.au/). The GHRSST-format level 2 pre-processed (L2P) products, used as inputs, are derived from satellite infrared sensors, such as the Advanced Very High Resolution Radiometer (AVHRR), and microwave sensors, such as the Advanced Microwave Scanning Radiometer 2 (AMSR2).

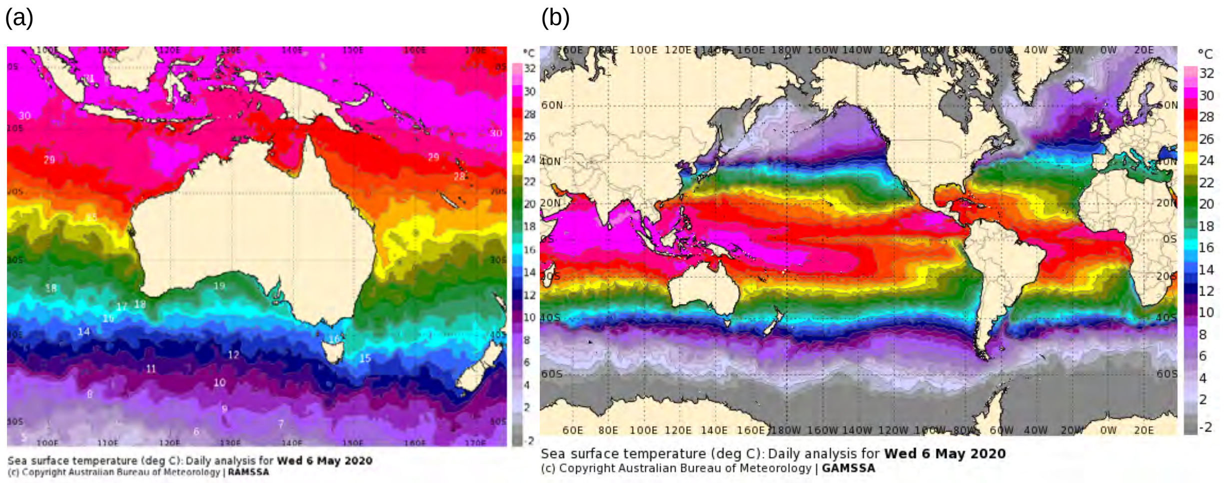

Figure 1: Example of foundation SST for 6th May 2020 from BoM Daily L4 analyses (a) RAMSSA and (b) GAMSSA, formed from NAVOCEANO GAC AVHRR L2P (Metop-A, Metop-B), JAXA AMSR-2 L2P, ACSPO VIIRS L3U (Suomi-NPP, NOAA-20) SST and in situ SST (ships, buoys).

From 2018 to early 2020, we experimented with ingesting NOAA's Advanced Clear Sky Processor for Ocean (ACSPO) 0.02º Suomi-NPP and NOAA-20 VIIRS L3U SST data (Petrenko et al., 2010; 2014) into near real-time 1/4º GAMSSA and 1/12º RAMSSA SST analyses. Operational RAMSSA ingested Suomi-NPP and NOAA-20 VIIRS data from 17th November 2019 and operational GAMSSA from 29th April 2020. The VIIRS data from these two afternoon-orbiting satellites complement the Global Area Coverage (GAC) AVHRR L2P SST data from the morning-orbiting Metop-A and Metop-B satellites, supplied by the US Naval Oceanographic Office (NAVO), and the AMSR-2 L2P SST data from the afternoon-orbiting GCOM-W satellite, provided by the Japan Aerospace Exploration Agency (JAXA).

2. RAMSSA/GAMSSA SYSTEM CONFIGURATION CHANGES

The BoM routinely downloads real-time ACSPO VIIRS L3U files from NOAA's Production Distribution and Access portal. Night-only VIIRS L3U (quality level 5, sses_bias subtracted) SST depth data are collated to daily 1/4º and 1/12º L3C SST_{fnd} composites for ingestion into the GAMSSA and RAMSSA analyses. Data are further thinned by striding to 1/2º (GAMSSA) and 1/3º (RAMSSA). Thinning the VIIRS data in this manner is necessary, as analysis quality decreases if the density of the observation dataset is too large and the error correlations are neglected (Brasnett and Surcel Colan, 2016). The satellite retrievals (particularly VIIRS) are thinned prior to assimilation into the Canadian Meteorological Centre (CMC) OI analysis so they do not receive undue weight in the analysis (Brasnett and Surcel Colan, 2016). The observation correlation length scale of the VIIRS L3C data ingested into test RAMSSA is longer than either the 9 km AVHRR or 25 km AMSR2 datasets, and it was found that ingesting VIIRS gridded to 9 km caused the RAMSSA OI analysis to produce spurious SST artefacts.

In order to reduce innovation standard deviation compared with drifting and tropical moored buoy SST_{fnd}, the background correlation length scales were increased from 20 km to 50 km for operational RAMSSA on 17th November 2019, and from 50 km to 80 km for operational GAMSSA on 29th April 2020 (see Table 1). The background field correlation length scale effectively gives the radius of influence of an observation to changes in the background field. Any feature smaller than the observation correlation length scale in extent and within the observation correlation time scale in time is treated by the OI analysis as noise. Observations separated by less than the observation correlation length scale and the observation correlation time scale do not have independent errors.

	Old GAMSSA	New GAMSSA	Old RAMSSA	New RAMSSA
Satellite SST Inputs	NAVO GAC AVHRR (MA, MB) JAXA AMSR-2	NAVO GAC AVHRR (MA, MB) JAXA AMSR-2 ACSPO VIIRS L3U (NPP, N20)	NAVO GAC AVHRR (MA, MB) JAXA AMSR-2 ACSPO VIIRS L3U (NPP, N20)	NAVO GAC AVHRR (MA, MB) JAXA AMSR-2 ACSPO VIIRS L3U (NPP, N20)
In situ SST Inputs	Buoys and Ships (from GTS)	Buoys and Ships (from GTS)	Buoys, ships, Argo, XBT, CTD (GTS)	Buoys, ships, Argo, XBT, CTD (GTS)
Sea-ice Inputs	NCEP 1/12º sea ice analysis (Grumbine, 1996)	NCEP 1/12º sea ice analysis (Grumbine, 1996)	NCEP 1/12º sea ice analysis (Grumbine, 1996)	NCEP 1/12º sea ice analysis (Grumbine, 1996)
10 m Wind speed Inputs	ACCESS-G2 3-hourly 2º	ACCESS-G3 3-hourly 2º	ACCESS-R2 hourly 1º	ACCESS-G3 hourly 1º
Obs. Correlation Length Scale (km)	20	20	12	12
BG Correlation Length Scale (km)	50	80	50	50
Obs Estimated STD (OBSESD)	Calculated from 1-31 Oct 2014 satellite SST vs Buoy statistics	Calculated from 1-31 Dec 2019 satellite SST vs Buoy statistics	Calculated from 16 Mar – 4 Apr 2017 satellite SST vs Buoy statistics	Calculated from 1-31 Dec 2019 satellite SST vs Buoy Statistics
Background Field	Previous day's GAMSSA plus Reynolds and Smith (1994) climatology	Previous day's GAMSSA plus BoM Global Weekly 1º SST (Smith et al., 1999)	Previous day's RAMSSA plus BoM Global Weekly 1º SST (Smith et al., 1999)	Previous day's RAMSSA plus BoM Global Weekly 1º SST (Smith et al., 1999)

Table 1: The configuration of the old and new RAMSSA and GAMSSA systems. Operational RAMSSA and GAMSSA were updated to the new configurations on 29th April 2020. Changes are highlighted in red.

Other significant changes made to both systems on 29th April 2020 included updating the observation estimated standard deviation (OBSESD) for each input data stream (shown in Table 2) and updating GAMSSA's background field to relax to the previous week's BoM Global Weekly 1 degree SST analysis (Smith et al., 1999) rather than the Reynolds and Smith (1994) 1961-1990 SST climatology. An additional change to experimental GAMSSA is that the background field is now formed from a weighted combination of the previous day's GAMSSA analysis and the BoM Global Weekly 1º SST_{blend} analysis.

Sensor	Matchups	Bias (K)	STD (K)	OBSESD (K)
AVHRR (Metop-A)	14315	0.079	0.457	0.54
AVHRR (Metop-B)	12774	0.052	0.496	0.55
AMSR2 (GCOM-W)	134141	0.162	0.536	0.70
VIIRS (Suomi-NPP)	4113	-0.037	0.363	0.40
VIIRS (NOAA-20)	4276	-0.019	0.362	0.38

Table 2: Matchup bias and standard deviation (STD) statistics for each satellite SST_{fnd} data stream ingested into RAMSSA compared with drifting and tropical moored buoy SST_{fnd} observations for 1st to 31st December 2019 over the RAMSSA domain (60° E to 190° E, 70° S to 20° N). Data are matched if within the same 1/12° latitude x 1/12° longitude RAMSSA grid cell and the same UTC date. The Observation Estimated Standard Deviation (OBSESD) is an estimate of the total expected error and is calculated as STD + | bias | (Beggs et al., 2011). It is used to give a relative weight to each input data stream. OBSESD for buoys is set to 0.4 K, and ships is set to 1.2 K.

3. IMPACT OF INGESTING VIIRS DATA INTO RAMSSA AND GAMSSA

The update to operational RAMSSA on 17th November 2019 to ingest VIIRS data had little positive impact on innovation statistics compared with collocated drifting buoys and moorings, with a reduction in innovation STD cf. buoys of 0.002 K in experimental RAMSSA between 17th October and 13th November 2019. However, updating the OBSESD values on 29th April 2020 with low values assigned to VIIRS data, giving them higher weight in the OI analysis (Table 2), reduced the RAMSSA innovation STD by a further 0.016 K (Table 3).

Analysis	Global Matchups	Global Bias (K)	Global STD (K)	Australian Matchups	Australian Bias (K)	Australian STD (K)
Operational RAMSSA (inc. NPP/N20 VIIRS and old OBSESDs)				85189	0.127	0.670
Experimental RAMSSA (inc. NPP/N20 VIIRS and new OBSESDs)				88782	0.112	0.654
Operational GAMSSA	214165	0.056	0.647			
Experimental GAMSSA (inc. NPP/N20 VIIRS)	214082	0.063	0.662			
CMC 0.1deg (inc. NPP VIIRS)	343463	0.037	0.627	74826	0.061	0.627

Table 3: Innovation statistics for each Analysis SST_{fnd} (Date) minus drifting and tropical moored buoy SST_{fnd} (Date + 1 day) observations for 13th February to 28th April 2020 over the global domain and RAMSSA domain (60° E to 190°E, 70° S to 20° N).The update to GAMSSA on 29th April 2020 resulted in a reduction of ~0.04 K in robust standard deviation (RSD) compared with independent Argo SST (Figure 2(a)) and ~0.08 K reduction in RSD compared with GMPE (Figure 2(b)). The RSD of 25 km GAMSSA minus GMPE is now comparable to that of 10 km CMC, 5 km UKMO OSTIA or 5 km NOAA Geo-Polar Blend minus GMPE.

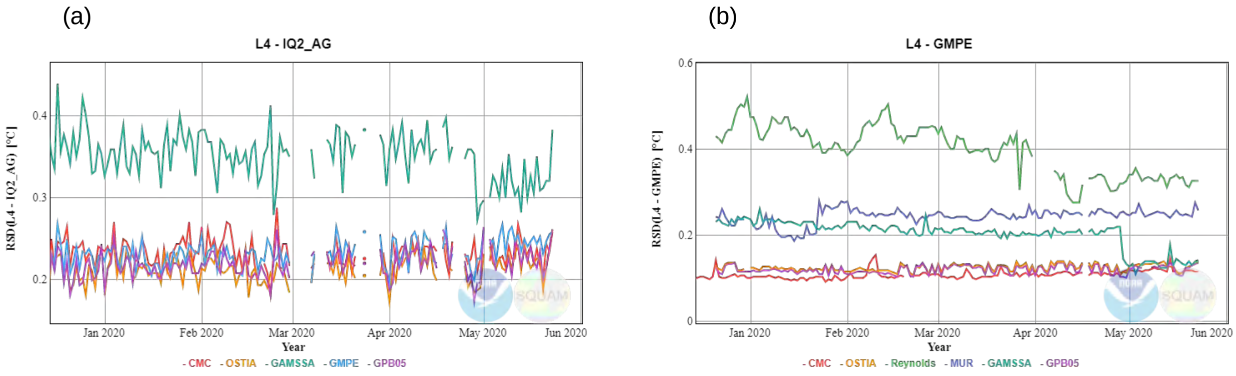

Figure 2: Robust Standard Deviation of various global SST analyses (L4) minus (a) Argo SST, and (b) 25 km GMPE (source https://www.star.nesdis.noaa.gov/socd/sst/squam/analysis/l4/, accessed 27th May 2020).

Examples of the old (operational) and new (experimental) RAMSSA and GAMSSA SST maps are shown in Figure 3(a)-(d). For comparison, the CMC's 0.1º daily foundation SST analysis (Brasnett and Surcel Colan, 2016) is also shown (Figure 3(e)).

(a) Operational RAMSSA

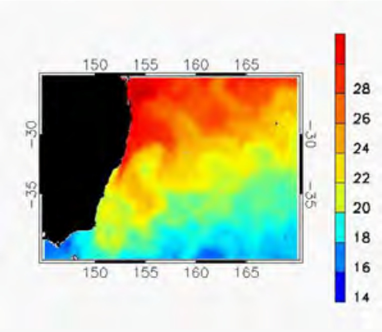

(b) Experimental RAMSSA

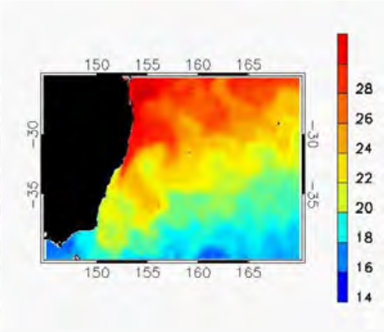

(c) Operational GAMSSA

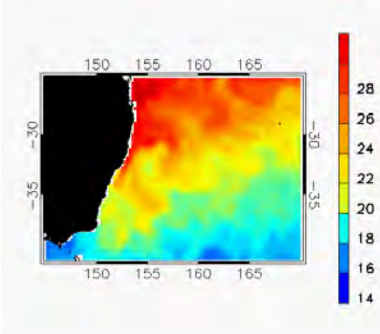

(d) Experimental GAMSSA

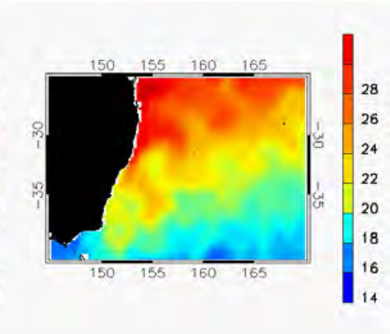

(e) CMC 0.1deg

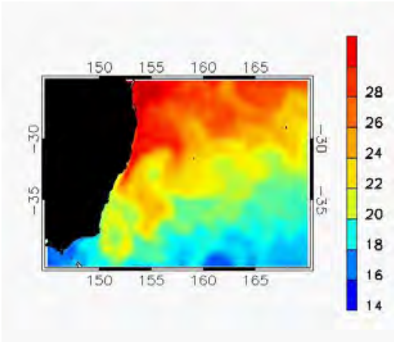

Figure 3: Example of foundation SST in the East Australian Current for 1st April 2020 from daily Multi-sensor L4 analyses (a) operational RAMSSA, (b) experimental RAMSSA (ingesting VIIRS L3U SST), (c) operational GAMSSA, (d) experimental GAMSSA (ingesting VIIRS L3U SST) and (e) CMC0.1deg (ingesting VIIRS L3U SST) (Brasnett and Surcel Colan, 2016).

4. FUTURE WORK

On 6th July 2020, 4 km resolution NAVO version 2 (v2) Metop-B GAC AVHRR L2P data replaced 9 km resolution NAVO v1 Metop-A GAC AVHRR L2P SST in operational RAMSSA and GAMSSA systems. The upgrade resulted in a further decrease in RSD of GAMSSA minus GMPE of around 0.01 K but no change in

RSD of GAMSSA minus Argo SST. We plan to ingest NAVO's v2 Metop-C GAC AVHRR L2P data by the end of 2020.

5. REFERENCES

Beggs H., A. Zhong, G. Warren, O. Alves, G. Brassington and T. Pugh (2011). RAMSSA – An Operational, High-Resolution, Multi-Sensor Sea Surface Temperature Analysis over the Australian Region, *Australian Meteorological and Oceanographic Journal*, **61**, 1-22, 2011 http://www.bom.gov.au/jshess/papers.php?year=2011

Brasnett, B. and Surcel Colan, D. (2016). Assimilating Retrievals of Sea Surface Temperature from VIIRS and AMSR2, *J. Atmospheric and Oceanic Tech*., https://doi.org/10.1175/JTECH-D-15-0093.1

GHRSST Science Team (2012). The Recommended GHRSST Data Specification (GDS) 2.0, document revision 5, available from the GHRSST International Project Office, 2012, pp 123. https://www.ghrsst.org/wp-content/uploads/2016/10/GDS20r5.pdf

Grumbine, R.W. (1996). Automated Passive Microwave Sea Ice Concentration Analysis at NCEP. *Tech. Note,* NOAA/NCEP, 13 pp.

Petrenko, B., A. Ignatov, Y. Kihai, and A. Heidinger (2010). Clear-Sky Mask for ACSPO. JTech, 27, 1609-1623.

Petrenko, B., A. Ignatov, Y. Kihai, J. Stroup, P. Dash (2014). Evaluation and Selection of SST Regression Algorithms for JPSS VIIRS. JGR, 119, 4580-4599, doi: 10.1002/2013JD020637

Reynolds, R. W., and T. H. Smith (1994). Improved global sea surface temperature analyses using optimum interpolation, *j. Climate*, **7**, 929-948.

Smith, N.S., Ebert, B. and Warren, G. (1999). The Bureau of Meteorology SST Analysis System. *An informal paper produced as background for the OOPC/AOPC Workshop on SST Analyses for Climate, International Research Institute, LDEO, Palisades NY USA, Nov 10–12, 1998.*

Zhong, A., and Beggs, H., (2008). Analysis and Prediction Operations Bulletin No. 77 - Operational Implementation of Global Australian Multi-Sensor Sea Surface Temperature Analysis *(web document)*, 2 October 2008. http://www.bom.gov.au/australia/charts/bulletins/apob77.pdf

S3 - POSTER PRESENTATIONS - SHORT ABSTRACTS

S3-P1: IMPROVEMENTS OF THE DAILY OPTIMUM SEA SURFACE TEMPERATURE (DOISST) VERSION 2.1

Boyin Huang[(1)], Chunying Liu[(2)], Viva Banzon[(1)], Eric Freeman[(2)], Garret Graham[3], Bill Hankins[(2)], Tom Smith[(4)], and Huai-Min Zhang[(1)]

(1) NOAA National Centers for Environmental Information, Asheville, North Carolina, Email: boyin.huang@noaa.gov

(2) Riverside Inc, Government Contractor at NOAA NCEI, Asheville, North Carolina

(3) Cooperative Institute for Climate and Satellites, North Carolina State University, Asheville, North Carolina

(4) NOAA/NESDIS/STAR, College Park, Maryland

SHORT ABSTRACT

NOAA/NESDIS/NCEI Daily Optimum Interpolation Sea Surface Temperature (SST) version 2.0 (DOISST v2.0) blended *in situ* ship and buoy SSTs with satellite SSTs derived from Advance Very High Resolution Radiometer (AVHRR). DOISST v2.0 exhibited a cold bias in the Indian Ocean, South Pacific, and South Atlantic due to a loss of drifting-buoy SSTs by a gradual switching from the Traditional Alphanumeric Codes (TAC) data to the Binary Universal Form for the Representation (BUFR) data. The cold bias is about -0.14°C on global average and -0.28°C in the Indian Ocean from January 2016 to August 2019.

The reasons for these cold biases are explored by six progressive experiments. These experiments show that those cold biases can effectively be reduced by adjusting ship SSTs with available buoy SSTs, using the latest available ICOADS R3.0.2 derived from BUFR and TAC, and including Argo observations above 5 m depth. However, the impact of using Metop-B instead of NOAA-19 is trivial, since their biases are adjusted by *in situ* SSTs. In addition, the warm bias in the Arctic can be improved by applying freezing-point instead of regressed ice-SST proxy.

S3-P2: OSTIA: PAST AND FUTURE DEVELOPMENTS

Simon Good, Chongyuan Mao, Toby Searle, Mark Worsfold

UK Met Office, FitzRoy Road, Exeter, Devon EX1 3PB, Email: simon.good@metoffice.gov.uk

SHORT ABSTRACT

The Operational Sea Surface Temperature and Ice Analysis (OSTIA) has been run operationally for over 10 years to produce daily, globally complete maps of foundation sea surface temperature (SST) in near real time. It has changed considerably over the years, both in terms of the satellite inputs and the software used to generate the analyses. For example, significant updates have included changes to the reference sensor used to bias correct other satellite data, switching to underpin the system with the NEMOVAR variational data assimilation scheme instead of an optimal interpolation-like scheme and improving the feature resolution of the analyses. These changes and their impacts will be reviewed and future planned developments discussed.

S3-P3: THE RECENT UPDATE OF SST ANALYSIS IN NCEP GFS AND A FEW RELATED FUNDAMENTAL ISSUES

Xu Li[(1)], Andrew Collard[(1)]

(1) IMSG at EMC/NCEP/NOAA, Email: Xu.Li@noaa.gov

SHORT ABSTRACT

The Sea Surface Temperature (SST) analysis within the NCEP GFS, referred to as NSST (Near-Surface Sea Temperature), became operational in July 2017 and has undergone several upgrades since then. The most recent updates include the use of more observations, stronger SST climatology constraints and the modified handling of the background for situations when the sea ice has just melted.

The definition of the foundation temperature, which is commonly used as the analysis variable in SST products, is revisited. The foundation temperature is defined as the temperature at a depth where the diurnal warming is negligible in GHRSST community. It is proposed that the temperature at the base of the diurnal warm layer defines the variable more physically. One of the major difference between these two definitions is that, for the current definition, the foundation temperature varies with the time on an hourly time scale. As shown from 6-hourly NSST foundation analysis, it does still have diurnal variability, which is usually smaller than 0.2 K, but can be up to 0.5 K over some local areas.

The impact of convective adjustment (free convection), which is usually missing in most of the diurnal warming models, is demonstrated based on experiments with the current NCEP GFS.

S3-P4: TOWARDS 2ND REANALYSIS OF NOAA AVHRR GAC DATA (RAN2): EVALUATION

Victor Pryamitsyn[1,2], Alexander Ignatov[1], Boris Petrenko[1,2], Olafur Jonasson[1,2], Yury Kihai[1,2]

(1) STAR, NOAA Center for Weather and Climate Prediction (NCWCP), 5830 University Research Ct, College Park, MD 20740, USA;

(2) Global Science and Technology, Inc., 7855 Walker Dr # 200, Greenbelt, MD 20770, USA

Email: victor.pryamitsin@noaa.gov

SHORT ABSTRACT

Since 1981, multiple NOAA satellites carried the AVHRR/2 and /3 instruments suitable for global SST retrievals with 4 km resolution at nadir, using spectral bands centred at 3.7, 10.8 and 12 µm. Several multiyear SST datasets have been created, to support long-term/climate studies and applications. NOAA is now working on the 2nd Reanalysis of AVHRR GAC data (RAN2) with the NOAA Advanced Clear-Sky Processor for Oceans (ACSPO) system. As a first step, the RAN2 Beta 1 (RAN2B01) dataset was produced using data of NOAA-07/09/11/12/14/15/16 data from 1981-2002. This presentation evaluates the performance of this initial data set, by comparing it with two other reprocessed AVHRR GAC datasets available for this period: the NOAA-NASA Pathfinder v.5.3 (PF) and the ESA Climate Change Initiative v2.1 (CCI). Time series of number of clear-sky ocean observations, global biases and standard deviations with respect to *in situ* SST, and sensitivity to "skin" SST, are systematically compared, and regional biases additionally analysed using Hovmöller diagrams. Since RAN is linked to *in situ* data (within a sliding window), its biases with respect to *in situ* SST are expected to be closer to zero, and stability in time improved, compared with PF/CCI, and this is indeed the case. Other than this observation, the RAN2B01 tends to show more retrievals (wider coverage) than in PF/CCI, and lower standard deviations with respect to *in situ* SST. This performance superiority is somewhat degraded during two several-months periods, following two large volcanic eruptions, of Mt. Pinatubo (June 1991) and Mt. Hudson (August 1991), respectively. Also, RAN2B01 sensitivities tend to be slightly smaller than 1, and more variable than in CCI. Improvements of the RAN2 performance are being explored and will be implemented before the final RAN2 release, pending another round of comprehensive comparisons against PF and CCI.

S3-P5: TOWARDS 2ND REANALYSIS OF NOAA AVHRR GAC DATA (RAN2): METHODOLOGY

Boris Petrenko[1,2], Victor Pryamitsyn[1,2], Alexander Ignatov[1], Yury Kihai[1,2]

(1) STAR, NOAA Center for Weather and Climate Prediction (NCWCP), 5830 University Research Ct, College Park, MD 20740, USA
(2) Global Science and Technology, Inc., 7855 Walker Dr # 200, Greenbelt, MD 20770, USA
Email address: boris.petrenko@noaa.gov

SHORT ABSTRACT

The objective of the 2nd AVHRR GAC SST Reanalysis (RAN2) is to consistently reprocess all available 4 km GAC L1b data from multiple NOAA satellites from 1981 to present. RAN1 undertaken in 2015 processed NOAA-16/17/18/19 and Metop-A AVHRR GAC data from 2002-on. The RAN2 Beta01 (B01) discussed in this presentation processed data of NOAA-7/9/11/12/14/15/16 data from 1981-2002, pending inclusion of RAN1 period from 2002 onwards before final release of RAN2.

The RAN1 and RAN2 ACSPO algorithms were optimized to effectively fit *in situ* SST. RAN2 ACSPO was additionally modified to mitigate specific issues intrinsic to the earlier AVHRR instruments. The ACSPO generates two SSTs: Global Regression (GR), highly sensitive to “skin” SST, and Piecewise Regression (PWR), more precise with respect to “depth” SST. In RAN2, the regression coefficients are recalculated daily, using matchups with *in situ* SSTs within 1±45 days window for the GR, and 1±180 days window for the PWR. This minimizes variability of global SST biases with respect to *in situ* SST, caused by the AVHRR instabilities. The RAN2 QC includes a set of sensor-specific filters, which screen out occasional failures of the 3.7 µm band typical for earlier AVHRRs. Other issues to be dealt with back to 1981, include sharp decrease of high-quality *in situ* SST data from drifters, and questionable quality of L4 SST analyses.

This presentation describes the RAN2 B01 algorithms and demonstrates their effects on retrieved SST. For cross-evaluation with other available SST data sets, see presentation by V. Pryamitsyn et al. The RAN2 B02 dataset is currently under development, with the emphasis on minimization of regional SST biases. Work is underway with the NOAA Geo-Polar Blended (GPB) L4 SST group, to produce GPB RAN2 B01 from the ACSPO RAN2 B01 L2P SST, and use it as the improved first guess in RAN2 B02 L2P.

S3-P6: OPTIMUM INTERPOLATION ANALYSIS FOR SEA SURFACE TEMPERATURE USING THE ORIENTED ELLIPTIC CORRELATION SCALES

Zhihong Liao[(1)], Bin Xu; Lei Zhang,

(1) National Meteorological Information Centre, China Meteorological Administration
Email: liaozh@cma.gov.cn

SHORT ABSTRACT

Abstract: Optimum Interpolation (OI) analysis is made for the Sea Surface Temperature (SST) product of Fengyun-3C (FY-3C) Visible and Infrared Radiometer (VIRR), and novel oriented elliptic correlation scales are used in the SST analysis and compared to the traditional rectangular correlation scales, then the results are evaluated against the measurements of *in situ* SST and OISST products. Statistical results for 2015 indicates that the SST results by using the oriented elliptic correlation scales is more effective than those using the rectangular correlation scales, which decrease the value of RMSE from 0.4194℃ to 0.3816℃, but it is much larger than the OISST products with the RMSE of 0.2780℃. It is demonstrated that there are still a lot of errors in the SSTs of FY-3C VIRR, which makes the poor quality of these SST analysis products, while the oriented elliptic correlation scales for SST has a better performance than the rectangular correlation scales in OI analysis.

SCIENCE SESSION 4: SERVICES AND PRODUCTS

S4 - SESSION REPORT

Misako Kachi[(1)], Edward M. Armstrong[(2)], Owen Embury[(3)]

(1) Japan Aerospace Exploration Agency, Japan, Email: kachi.misako@jaxa.jp
(2) NASA Jet Propulsion Laboratory, USA, Email: edward.m.armstrong@jpl.nasa.gov
(3) University of Reading, UK, Email: o.embury@reading.ac.uk

1. INTRODUCTION

Science Session 4 "Services and Products" was held on Wednesday, June 3rd, 2020. Misako Kachi chaired the session, and Edward Armstrong and Owen Embury served as co-chairs. The session consisted of four oral presentations and ten poster presentations. One poster was withdrawn.

2. ORAL PRESENTATIONS

2.1. Empowering Transformational Science by Chelle Gentemann

Chelle Gentemann presented an overview of new cloud-based analytics optimized data stores and tools, including Python, xarray and zarr. Cloud-based solutions can significantly reduce the time needed for data analysis as users no longer need to download, organise, and prepare data files. During discussions there were two main topics. Firstly, there was interest in having a GHRSST collection of Python tutorials or notebooks to help users. Secondly, data providers were interested to know what preferred cloud optimized formats and workflows are available to get SST datasets into the cloud catalogues.

2.2. Connecting Users and Applications with PO.DAAC hosted GHRSST data by Edward M. Armstrong

Edward M. Armstrong presented overview of existing PO.DAAC tools and services that can be used for SST and ocean analysis based on Python and NCO, and Cloud-based open sources, such as GitHub, Jupyter and Binder. Future PO.DAAC missions and datasets, such as ECCO II, Sentinel-6 and SWOT, will be 100% cloud-based, and many new tools and services have been developed or are in construction. During discussion, there were several questions regarding availability of the Ocean Phenology toolkit that will be on a public site soon. Another question was regarding the product format of future PO.DAAC missions and datasets since they will be cloud-based but many files are still in a traditional netCDF format; the PO.DAAC is continuing to develop optimization strategies for cloud storage and access.

2.3. A Lagrangian Global Dataset of Sea Surface Temperature by Shane Elipot

Shane Elipot presented a new Lagrangian SST dataset that has been developed to accompany the on-going hourly drifter product from the Global Drifter Program (GDP). Dataset of hourly estimated position and velocity has been released in Elipot et al. (2016) and the goal of the study is to add SST hourly estimates to this dataset. Methodology is that along-trajectory SST temporal evolution is modelled as a sum of a daily mean, a tendency term and a diurnal oscillation with 3 harmonics. This dataset will be new global tool for studying air-sea interactions and general circulation. There were active discussions about quality control of near-real-time drifter buoys, and possibility of applying the method to existing datasets, such as NOAA's iQuam, HRSST.

2.4. Ingesting SLSTR SST into IMOS Multi-sensor SST composites by Pallavi Govekar

Pallavi Govekar presented the addition of SLSTR L2P data on Sentinel-3A and Sentinel-3B provided by EUMETSAT to the Integrated Marine Observing System (IMOS) Multi-sensor L3S SST products that already include NOAA-18, Metop-B, Suomi-NPP and NOAA-20. Addition of SLSTR L2P SST data slightly improves spatial coverage of the highest quality and initial validation with buoy SST indicates marginally better statistical parameters than the existing operational one. In future work, more extensive validation will be performed, and experimentation with the addition of Himawari-8 SST to IMOS L3S in conjunction with development of a SSES model that could be applied to all sensors contributing to the L3S SST for uniform quality checking. There were some questions and comments about utilization of SSES information that is prepared by each data producer. SSES_bias adjustment was applied in compositing each sensor’s SST to IMOS L3S, but development of a more consistent SSES model for all sensors is necessary to enable the remapping of SST to a more uniform quality level.

3. POSTER PRESENTATIONS

The poster session of the Services and Products session included 10 posters (one withdrawn) covering a wide variety of technical descriptions, and progress of new and updated GHRSST data services and science processing systems. These posters drew significant interest from the meeting participants with an unknown number of poster views but over 100 discussion topics and replies between the authors and participants.

On the services side, there were several posters on tools and interfaces such as overview of the NOAA iQuam *in situ* data monitor, and the Oceanview image visualization services. Related to this were descriptions of discovery and subsetting services for the NASA PO.DAAC and an overview of the Copernicus training and user support. An underlying foundation of many of these services is their accessibility via well described APIs and their use as data recipes in Jupyter notebooks for user consumption.

Data processing and extraction services were also featured highly in the session. For example, a new data extraction/reduction service was described from the ESA Climate Change Initiative for its popular L4 dataset. In addition the NOAA, CMEMS, NAVOCEAN data processing chains or service chains were featured in a number of different posters that ran the gamut of describing ongoing and emerging dataset production for AVHRR Metop, SLSTR, VIIRS and merged L3S all of which are of high value to the research community.

S4 - ORAL PRESENTATIONS - EXTENDED ABSTRACTS

S4-1: A NEW ERA OF SCIENCE

Chelle Gentemann

Farallon Institute, California, USA, Email: cgentemann@faralloninstitute.org

SHORT ABSTRACT

How will science change in the next decade? During the past few years there has been an explosive growth in computational power, data availability, data volume and the open source software movement. In combination, these factors have resulted in the democratization of advanced computational tools and platforms for diverse commercial and scientific applications. There is now a rich ecosystem of easily-accessible, open source software that enables Earth system science at a scale and ease unimaginable only a few years ago. This transformation is not by accident, the Pangeo open science community has been funding development in this area with the goal of creating a community platform for Big Data geoscience. Practically, for scientists, the effect of these changes are to vastly shrink the amount of time spent data wrangling, freeing up more time for science. This shift in paradigm has lowered the threshold for entry, expanded the user pool, and increased opportunity for collaboration, while promoting scientific innovation, transparency, and reproducibility. The efficiency of open source software, new data analysis methods, and greater computational power enables new approaches for answering oceanographic research questions, conducting instrument calibration and algorithm validation, and streamlining data access, use, and availability. GHRSST has worked for over 20 years to harmonize sea surface temperature measurements from space by ensuring strict metadata standards and creating a collaborative community. How can we ensure GHRSST is poised to utilize these new resources and grow as a community?

S4-2: CONNECTING USERS AND APPLICATIONS WITH PO.DAAC HOSTED GHRSST DATA

Edward M. Armstrong[(1)], Wen-Hao Li[(2)], Yibo Jiang[(1)], Chelle Gentemann[(3)]

(1) Jet Propulsion Laboratory, California Institute of Technology, Pasadena, CA, 91109 USA, Email: edward.m.armstrong@jpl.nasa.gov
(2) Raytheon Corp., Pasadena, CA 91101, Email: wen-hao.li@jpl.nasa.gov
(3)Farallon Institute, Petaluma CA 94952, Email: cgentemann@faralloninstitute.org

1. INTRODUCTION

The 80+ GHRSST public datasets represent a rich resource for sea surface temperature research and applications given their time series length, resolution, spatial coverage, varying measurement types and processing levels, and availability in the full spectrum of PO.DAAC tools and services ecosystem. The PO.DAAC has created a publicly accessible recipe suite for the user community to perform straightforward yet powerful computations on GHRSST data using python recipes, Jupyter notebooks, R, Matlab, and the NCO programming language. These recipes include numerical computations for regional and global SST trends, anomaly derivations, EOF analysis, climate signal reproduction, and ocean phenology. For example, one recipe reproduces a famous SST based warming figure from the Fourth National Climate Assessment (USA) while another focuses on quantifying the regional changes in ocean SST phenology. Most are python-based while some contain hybrid calls and leverage the NCO programming interface too. All are available on the PO.DAAC user forum (https://podaac.jpl.nasa.gov/forum/) and/or via the open source NASA GitHub repository (https://github.com/nasa/podaac_tools_and_services). Several are available in the Jupyter notebook framework including podaacypy (https://github.com/nasa/podaacpy), a recipe for GHRSST granule metadata discovery and application, and more recently a Jupyter notebook developed to support data analysis and visualization of a cloud-based Zarr formatted Level 4 MUR dataset in the AWS Open Data Registry. Throughout the summer of 2020, the PO.DAAC intends to add and migrate more of its numerical recipes to the Jupyter notebook framework and publish them on its open source GitHub repository.

2. EXISTING SERVICES

The PO.DAAC maintains a broad array for web services and interfaces for accessing GHRSST data (https://podaac.jpl.nasa.gov/dataaccess). Besides the PO.DAAC Drive HTTPS interface and protocol (the recent replacement for public FTP), the PO.DAAC maintains services including OPeNDAP, THREDDS, Live Access Server, SOTO, HiTIDE, and is evaluating ERDDAP and improving SOTO with data analytics (Figure 1.)

Service Name	Access	Visualization	Analysis	Subset	X-Format	FAIR
Drive	Direct, WebDav API	NO	NO	NO	NO	A
Web Services	Direct, API Query	YES	via API	YES	via API	FAIR
OPeNDAP	Direct, API Query	NO	via API	via API	YES	AIR
THREDDS	Direct, API Query	YES	via API	via API	via API	AIR
Live Access Server	Direct, GUI Query	YES + Animation	YES	YES	YES	AIR
SOTO	API/GUI Query	YES + Animation	TBD	NO	NO	AR
HITIDE / L2SS	Direct, API/GUI Query	YES	via API	YES	YES	AR
JSON-LD Tagging	3rd Party Search	NO	NO	NO	NO	FA

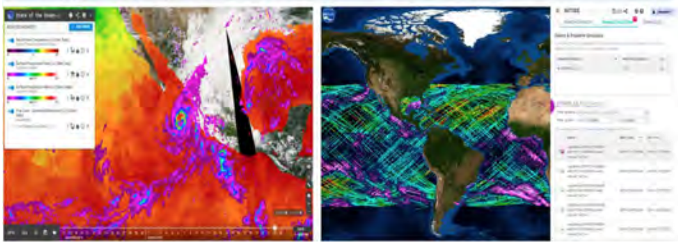

Figure 1: List of PO.DAAC services and tools for supporting GHRSST data access and visualization

3. DATA RECIPES AND PO.DAAC FORUM

The PO.DAAC also maintains a user forum with over 50 data recipes (https://podaac.jpl.nasa.gov/recipes), many of them using GHRSST data. These include recipes for Reading/Translation, Access/Services, Visualization, Numerical Analysis, and Tutorials. Among the recipes are SST trend analysis and visualization using the NCO toolkit, and recently a python based ocean phenology recipe to calculate phenology detection and characterization using primarily SST data such as AVHRR_OI, CMC, and MUR. An example of an output is shown in Figure 2.

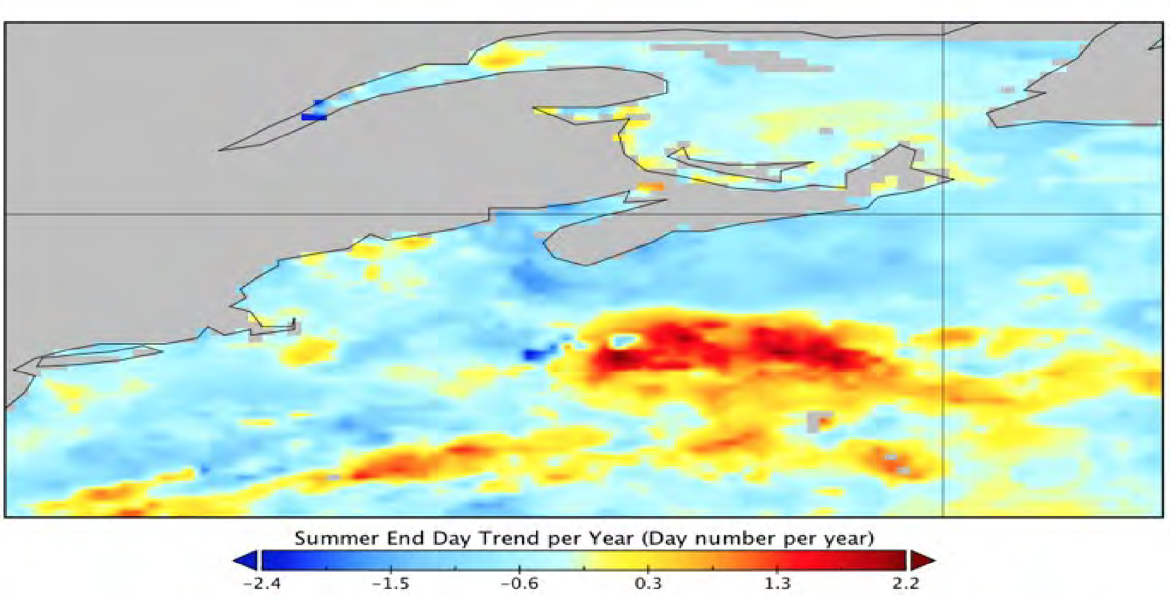

Figure 2: Trends in the ***Start Day of the summer season*** *in the New England coastal region based on the CMC0.2deg dataset (from 1992-2016). In this coastal region there is an overall trend to the summer season starting* ***earlier and earlier****. This combined with summer duration output can be used to assess the impact of regional warming and change.*

4. JUPYTER NOTEBOOK RECIPES

Jupyter Notebooks are popular interfaces and methods for sharing python based data recipes and capabilities. One recipe of note developed by the PO.DAAC is *podaacpy*, a python module for interacting with PO.DAAC web services for data/metadata discovery and access. An example of its use can be found here: https://github.com/nasa/podaacpy/tree/master/examples

These Jupyter recipes and others can be found on the PO.DAAC Github site for open source software (https://github.com/nasa/podaac_tools_and_services). This site will be the entry gateway for future notebooks including those for data subsetting, regridding and reprojection, and visualization that are currently under development.

```
In [ ]: from IPython.display import Image
        Image(filename='ASCAT_geometry.jpg')

In [ ]: #First lets import the libraries we require
        from pprint import pprint
        from podaac import podaac as podaac
        from podaac import podaac_utils as utils
        from podaac import drive as drive

In [ ]: #Then we can create instances of the classes we will use
        p = podaac.Podaac()
        u = utils.PodaacUtils()
        d = drive.Drive('podaac.ini', None, None)

In [ ]: # Let's discover PO.DAAC Wind data relating to Hurricane Florence, which
        #  was a very recent major hurricane to impact Southeastern US
        #    https://en.wikipedia.org/wiki/Hurricane_Florence
        # Using specific parameters to confine the discovery space, we opt for the full
        # metadata record in atom format
        ds_result = p.dataset_search(keyword='ASCAT',
                                     start_time='2018-09-12T00:00:01Z',
                                     end_time='2018-09-14T11:59:59Z',
                                     short_name='ASCATA-L2-Coastal',
                                     process_level='2',
                                     bbox='-81,28,-67,40',
                                     pretty='True',
                                     _format='atom',
                                     full='True')
        print(ds_result)

In [ ]: #Because we requested the Full response, we can actually extract the
        # PO.DAAC Drive URL for all granules contained within this dataset.
        search_str = 'https://podaac-tools.jpl.nasa.gov/drive/files/'
        drive_path = [ str(i) for i in ds_result.strip().split() if search_str in i ][0]
        print(drive_path[5:])

In [ ]: #Next, lets search for Granules of interest relating to the above discovery operation
        #Lets execute a search for specific granules from the following dataset
        # MetOp-A ASCAT Level 2 Ocean Surface Wind Vectors Optimized for Coastal Ocean
        # https://podaac.jpl.nasa.gov/dataset/ASCATA-L2-Coastal
        # ...based upon temporal (start and end) and spatial contraints.
        result = p.granule_search(dataset_id='PODAAC-ASOP2-12C01',
                                  start_time='2018-09-12T00:00:01Z',
                                  end_time='2018-09-14T11:59:59Z',
                                  bbox='-81,28,-67,40',
                                  sort_by='timeAsc',
                                  items_per_page='400',
                                  _format='atom')
        #print(result)
        searchStr = 'totalResults'
        numResultsStr = [ str(i) for i in result.strip().split() if searchStr in i ]
        print(numResultsStr)
```

Figure 3: The podaacpy Jupyter notebook

5. CLOUD BASED DATASETS AND EMERGING CAPABILITIES

The PO.DAAC is evolving to a location agnostic data services model where consumers will discover, interact, transform and extract data in cloud storage. Many tools and services (such as the aforementioned Jupyter notebooks) have been developed or are in construction in support of the emerging SWOT mission (launch 2021) datasets that will be entirely ingested, managed and distributed from the Amazon Web Service (AWS) cloud. In the shorter term, the PO.DAAC will make available the entire MODIS Terra L2P time series and other satellite products in an AWS cloud test bed repository to provide the opportunity for the community to familiarize themselves with satellite data and services in a cloud environment.

The PO.DAAC also recently collaborated with the Farallon Institute to make available the popular MUR dataset in a cloud optimized Zarr format as part of the AWS Open Data Registry (https://registry.opendata.aws/mur/). The MUR Zarr dataset is hosted in a Pangeo/Dask/Jupyter ecosystem allowing users to assign compute cycles and rapidly perform complex time series analysis on the entire MUR record from 2002-2020.

ACKNOWLEDGEMENTS

These activities were carried out at the Jet Propulsion Laboratory, California Institute of Technology, under a contract with the National Aeronautics and Space Administration (80NM0018F0848). Dedicated funding for PO.DAAC activities is through a grant from NASA's ESDIS Project.

S4-3: A LAGRANGIAN GLOBAL DATASET OF SEA SURFACE TEMPERATURE

Shane Elipot[(1)], Rick Lumpkin[(2)], Luca Centurioni[(3)]

(1) Rosenstiel School of Marine and Atmospheric Science, University of Miami, Miami, FL, USA, Email: selipot@rsmas.miami.edu
(2) NOAA Atlantic Oceanographic and Meteorological Laboratory, Miami, FL, USA, Email: rick.lumpkin@noaa.gov
(3) Scripps Institution of Oceanography, San Diego, CA, USA, Email: lcenturioni@ucsd.edu

Sea Surface Temperature (SST) is the primary quantity by which the ocean forces climate processes in the atmosphere. It is thus crucial to not only gather observations of SST but also understand the dynamical processes controlling their time and spatial evolutions. The predominant *in situ* observational system by which SST has been observed in the last decades is the global array of surface drifters from the Global Drifter Program (GDP, Lumpkin and Pazos, 2007). In addition to the historical uniform dataset at 6 hourly intervals of position and velocity, the GDP also distributes an hourly product (Elipot et al., 2016). This high resolution global dataset of oceanic near-surface velocity has become possible due to (i) the increasing number of satellites forming the Argos constellation originally used to track drifters, and (ii) the more than 97% transition to positioning drifters by GPS satellites and transmitting their data via the Iridium satellite constellation. Compared to the 6 hourly product, the hourly product is a dramatic improvement in the time resolution of the data, reducing data gaps and providing considerably better resolution of oceanic variability than was previously possible (Elipot et al., 2016).

To the high-frequency dataset of position and velocity, we are adding a Lagrangian companion dataset of hourly SST estimates with the goal of contributing to the understanding of the spatiotemporal variability of Lagrangian SST measurements. The sampling patterns and sampling frequencies of the raw drifter SST dataset are not uniform because of the different manufacturers and changes that occurred over time, hence the dataset is heterogeneous. The goal is to generate a uniform dataset that can be used to spatially and temporally analyse SST measured by drifters along their Lagrangian trajectories. We have devised a two-step procedure to estimate SST at the top of every hour. The first step consists of obtaining SST estimates at all original and irregular observations times, and the second step consists of interpolating or extrapolating these estimates to estimates at the top of each hour. The goal of the first step is to despike the original SST data, or reduce the noise in the data by fitting a local model of SST temporal variations. The goal of the second step is to homogenize the temporal distribution of the estimates, and align these with the existing dataset of position and velocity.

The local temporal model s_m for an observed SST value s_k around an observation time t_k is chosen as the sum of a polynomial s_P of order P to capture low frequencies variations, and a daily oscillation s_D with N harmonics of the diurnal frequency to capture the diurnal variability. As such, the linear model s_m contains P+1+2N parameters which are to be estimated at every observation time t_k. Practically, we chose P=1 and N=3 on the basis of the analysis of a subset of drifters. The actual method to estimate the parameters of the model is adapted from the locally weighted scatter plot smoothing (LOWESS) method introduced by Cleveland (1979). This locally-weighted least squares method is deemed robust because it is iterative, and it is found appropriate in our case because drifter SST time series are often spiky (Figure 1). In summary, at each original uneven sampling time t_k, we obtain 8 estimated parameters: a mean SST from low-frequency processes, a SST tendency term, and 3 diurnal parameters of amplitude and of phase. All of these parameters can be studied independently or jointly in terms of their spatial distribution, variance, etc.

The second step of the overall method is to estimate the model parameters and the SST at the top of each hour, at the same times as the times for position and velocity are estimated completely independently (Elipot et al. 2016). To do so, we apply two different interpolation methods, one for the background and polynomial model s_P and another one for the diurnal model s_D. For the background model, we take advantage that the values of P derivatives are estimated at all times t_k. We use a scheme which is a hybrid of interpolation and extrapolation where the estimated parameters of the model and its derivative up to order P are used in an intrapolation formula, a variant of Taylor expansion (Kraaipoel, 2003). For the diurnal SST component, the interpolation consists in extrapolating forward in time the diurnal component from the previous estimated time

t_k and extrapolate backward in time the diurnal component from the next estimated time t_{k+1}, and weighting linearly in time these two extrapolated values in order to not damp the diurnal oscillation as a linear interpolation would do. The total SST estimate at time *t* is the sum of the two interpolations. The interpolation also provides the variance of the hourly estimates by propagating the calculated variances from the uneven estimates. Ninety-five percent confidence intervals are calculated by multiplying the square root of the variance by 1.96 assuming normally distributed observations.

In the end, the new SST dataset to be released contains over 178,002,728 estimates set of 8 parameters of the model, and 146,323,140 interpolated set of diurnal and non-diurnal (low frequency) SST matching currently version 1.03 of the hourly velocity drifter dataset of Elipot et al. (2016). Preliminary analyses of the final dataset of hourly SST demonstrates that the density of the data is sufficient to finely map globally various SST seasonal characteristics such as SST anomalies, tendencies, diurnal harmonics amplitude and phase, total diurnal variance (Figure 2). We argue that this dataset constitutes a new global tool to study air-sea interactions and general ocean circulations.

FIGURES AND TABLES

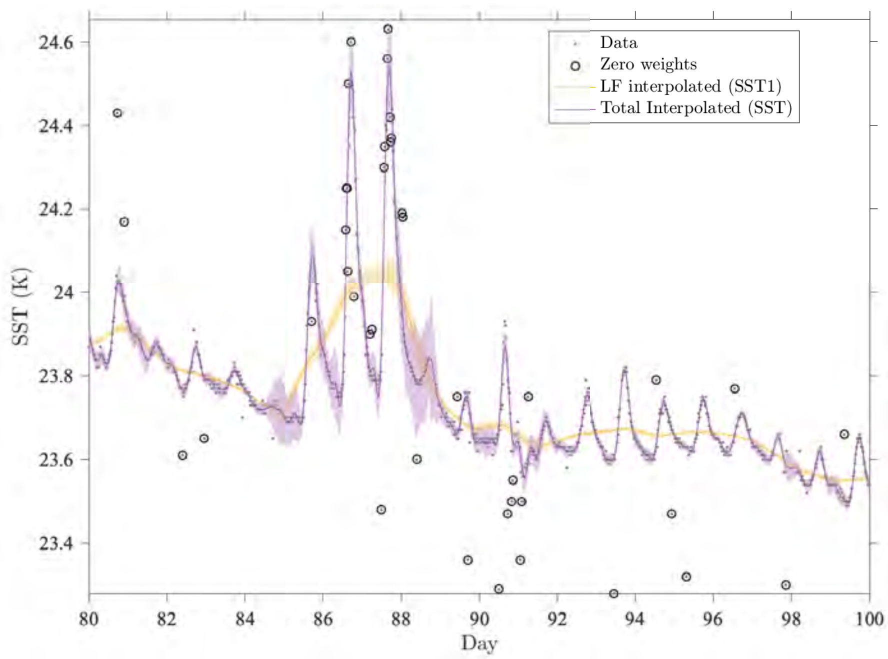

Figure 1: Example of derivation of the hourly drifter SST product. The raw data are uneven in time. The method weights the raw data and ``zero weighted" data are ultimately not used for final estimations. The result of the evenly hourly interpolated polynomial model s_P, as well as the evenly hourly interpolated total model including the diurnal model s_D, are shown as a continuous curves. Shading indicates 95% confidence intervals.

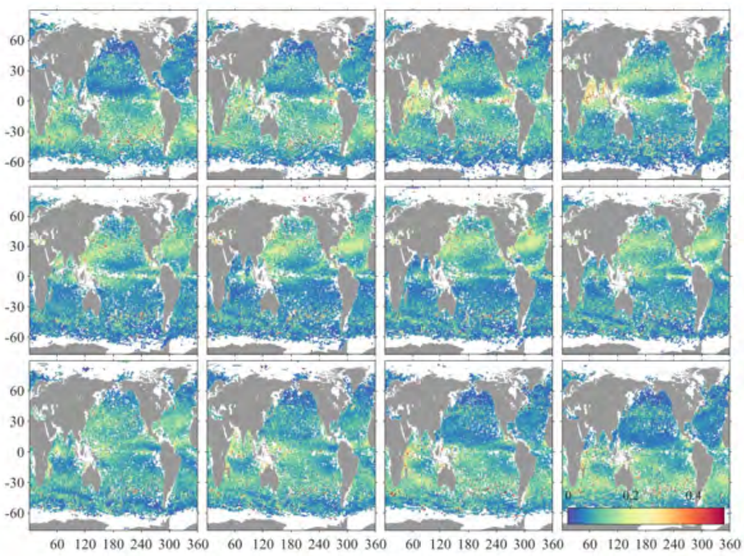

Figure 2: Monthly average diurnal cycle amplitude calculated from the drifter SST dataset (in Kelvin). Going from left to right and top to bottom, January is in the top left corner and December in the bottom right corner.

REFERENCES

Cleveland, W. S. (1979). Robust Locally Weighted Regression and Smoothing Scatterplots. *J. Am. Stat. Assoc. 74*, 829–836.

Elipot, S., R. Lumpkin, R. C. Perez, J. M. Lilly, J. J. Early, and A. M. Sykulski (2016). A global surface drifter data set at hourly resolution. *J. Geophys. Res. Ocean. 121*(5), 2937–2966.

Kraaipoel, D. A. (2003). Seismic ray fields and ray field maps : theory and algorithms. Ph. D. thesis.

Lumpkin, R. and M. Pazos (2007). Measuring surface currents with Surface Velocity Program drifters: the instrument, its data, and some recent results, in Lagrangian Analysis and Prediction of Coastal and Ocean Dynamics, pp. 1–23. Cambridge University Press.

S4-4: INGESTING SLSTR SST INTO IMOS MULTI-SENSOR SST COMPOSITES

Pallavi Govekar[(1)], Christopher Griffin[(2)] and Helen Beggs[(3)]

(1) Bureau of Meteorology, Melbourne, Australia, Email: pallavi.govekar@bom.gov.au
(2) Bureau of Meteorology, Melbourne, Australia, Email: christopher.griffin@bom.gov.au
(3) Bureau of Meteorology, Melbourne, Australia, Email: helen.beggs@bom.gov.au

ABSTRACT

The Australian Bureau of Meteorology (BoM) produces operational, real-time Multi-sensor SST level 3 products by compositing SST from Advanced Very High Resolution Radiometer (AVHRR) sensors on METOP-B and NOAA-18, along with SST from Visible Infrared Imaging Radiometer Suite (VIIRS) sensors on Suomi-NPP and NOAA-20 polar-orbiting satellites. In response to user requirements for gap-free, highest spatial resolution, best quality and highest accuracy SST data, the Bureau is experimenting with compositing SST data from the Sea and Land Surface Temperature Radiometer (SLSTR) with SST from VIIRS and AVHRR sensors to construct new "Multi-sensor L3S" products for the Australian Integrated Marine Observing System (IMOS) project. Here we discuss our method to combine data from different sensors and present validation of the Multi-sensor L3S SST against *in situ* SST data. The addition of SLSTR data slightly improves spatial coverage of the 0.02° x 0.02° Multi-sensor L3S SST than are available from composites of AVHRR and VIIRS only. The Multi-sensor L3S agrees well with SLSTR. Given the accuracy and better data coverage of SLSTR data compared to *in situ* data, Sentinel-3A and Sentinel-3B can be used as reference sensors for validation of most of the IMOS satellite SST products.

1. INTRODUCTION

Several satellites provide Sea Surface Temperature (SST) data. Spatial coverage may be improved by merging data from satellite sensors that have different equatorial crossing times (ECT). The Australian Bureau of Meteorology (BoM) produce operational Multi-sensor L3S SST products (Beggs et al., 2019; Griffin et al., 2017) in the GHRSST GDS2.0 format (GHRSST Science Team, 2012) using infrared data from Polar orbiters:

- NOAA-18 AVHRR (Equatorial Crossing Time (ECT) 9:15 am/pm)
- Metop-B (ECT 9:30 am/pm)
- Suomi-NPP VIIRS (ECT 1:30 pm/am)
- NOAA-20 VIIRS (ECT 1:30pm/am)

There is a huge demand for gap-free, highest special resolution SST products from our users such as IMOS OceanCurrent, and the BoM ReefTemp Next Generation coral bleaching nowcasting service. To meet this demand, the Bureau is experimenting with compositing SST data from new advanced satellite sensors with data from currently used satellite sensors.

The EUMETSAT Sentinel-3A and Sentinel-3B satellites were launched in 2016 and 2018, respectively. Both satellites carry SLSTR and have an ECT of 10 am/pm. EUMETSAT produces SLSTR L2P products for both Sentinel-3A and Sentinel-3B satellites. We investigated the effect of adding SLSTR to our current Multi-sensor L3S in terms of spatial coverage and overall accuracy.

2. DATA

BoM downloads SLSTR L2P files using the Copernicus Hub on NCI at http://dapds00.nci.org.au/thredds/fileServer/fj7/Copernicus/Sentinel-3/SLSTR/SL_2_WST/catalog.html. As recommended by EUMETSAT, only Dual view data with quality level 5 were used.

Other data ingested into the test Multi-sensor L3S products are:

- BoM High Resolution Picture Transmission (HRPT) AVHRR L2P from NOAA-18 (Griffin et al., 2017)

- OSI-SAF (Full Resolution Area Coverage) FRAC AVHRR L2P SST products for Metop-A and Metop-B (available from ftp://eftp1.ifremer.fr/cersat-rt/project/osisaf/data/sst/l2p/global/avhrr_metop_b/)
- NOAA/NESDIS/STAR "ACSPO" VIIRS_NPP and VIIRS_N20 0.02º single swath, composite "L3U" SST products (on IMOS grid) (available at https://coastwatch.noaa.gov/cw/satellite-data-products/sea-surface-temperature/acspo-viirs.html)

3. METHOD

3.1. Constructing IMOS L3U SST

As part of the Integrated Marine Observing System (IMOS: www.imos.org), BoM produces GDS2.0 L3U SST products on the IMOS 0.02º grid over two Australian and Southern Ocean domains for each above mentioned satellite sensor. Only the files that have data in the IMOS Australian domain (20° N-70° S, 60° E-190° E) are processed further. l2p_flags are redefined using ancillary fields (e.g. sea ice, winds, dt_analysis) that are used for standard IMOS L3U files.

In order to merge with IMOS AVHRR L3U SSTs, these L3U SSTs are modified such that the "remapped" quality_level is redefined as the minimum of the original quality_level and quality level, q_s, calculated using Sensor Specific Error Statistics (SSES), using sses_bias (μ_{sses}) and sses_standard_deviation (σ_{sses}) estimates, thus:

$$q_{\text{sses}} = \frac{1}{\sqrt{2}}\sqrt{\max\left(\left(\frac{\sigma_{\text{sses}}}{\sigma_0}\right)^2 + \left(\frac{\mu_{\text{sses}} - \mu_0}{\sigma_{\text{sses}}}\right)^2 - 1, 0\right)}$$

$$q_s = \lfloor 5 \exp^{\eta q_{\text{sses}}} \rceil$$

The half square brackets in the q_s equation represent the "nearest integer" function. Also, q_s is capped at 5 to be consistent with the GHRSST quality_level definition.

Different data sources can then be combined using q_s, provided that

$$\eta/\sigma_0 = \text{constant}$$

The quality scaling parameter, η, is chosen such that the degradation in quality determined by SSES measurements is similar to the observed degradation in quality_level over a period of time where the sensor is known to perform well. Note that during periods of degraded performance, the number of retrievals of high q_s will decrease, as it will during times of the day when performance may also be questionable due to uncertainties associated with the retrieval method. Therefore, during daytime the SSES quality level per multi-sensor L3S grid cell is generally less than the original quality levels originally provided by data producers, due to the daytime SSES bias and standard deviation values being higher than during night. The adjustment to the quality_level in this fashion is done for the following reasons:

(a) BoM compositing algorithms use sses_bias, sses_standard_deviation and degrees of freedom as parametric quality assessments, and quality_level as a non-parametric measure. Only highest non-parametric quality data are combined parametrically. Thus, we need a good way to compare in absolute terms the quality of data streams from a non-parametric standpoint.

(b) To be able to track degradation in quality over the platform life. Allows us to combine "old" platforms with "new" platforms with appropriate quality assessment.

(c) To reflect the greater uncertainty of measurement and degraded quality as the uncertainty and deviation from *in situ* measurement increases. Both of these lead to a greater uncertainty, so that the skin measurement follows the validation and the method degrades the quality accordingly.

(d) Allows supplier quality assessment based on other metrics to be included in the discussion. We do not increase quality_level, only degrade it. This will tend to push quality assessments down, but they remain closer to an absolute (over time) assessment.

3.2. Constructing IMOS L3C SST

Merged L3C SST over a given time period and location is defined as a weighted average of the best quality source L3U pixels on the IMOS 0.02-degree grid

$$T_{\text{satellite},C,j} = \frac{\sum_{i\in j} \frac{n_{U,i}}{\sigma^2_{U,i}} T_{\text{satellite},U,i}}{\sum_{i\in j} \frac{n_{U,i}}{\sigma^2_{U,i}}}$$

Where, η_U- degree of freedom and σ_U – estimate of the measurement error (Griffin et al., 2017).

Examples of the IMOS L3C remapped quality level from the various platforms are shown in Figure 1.

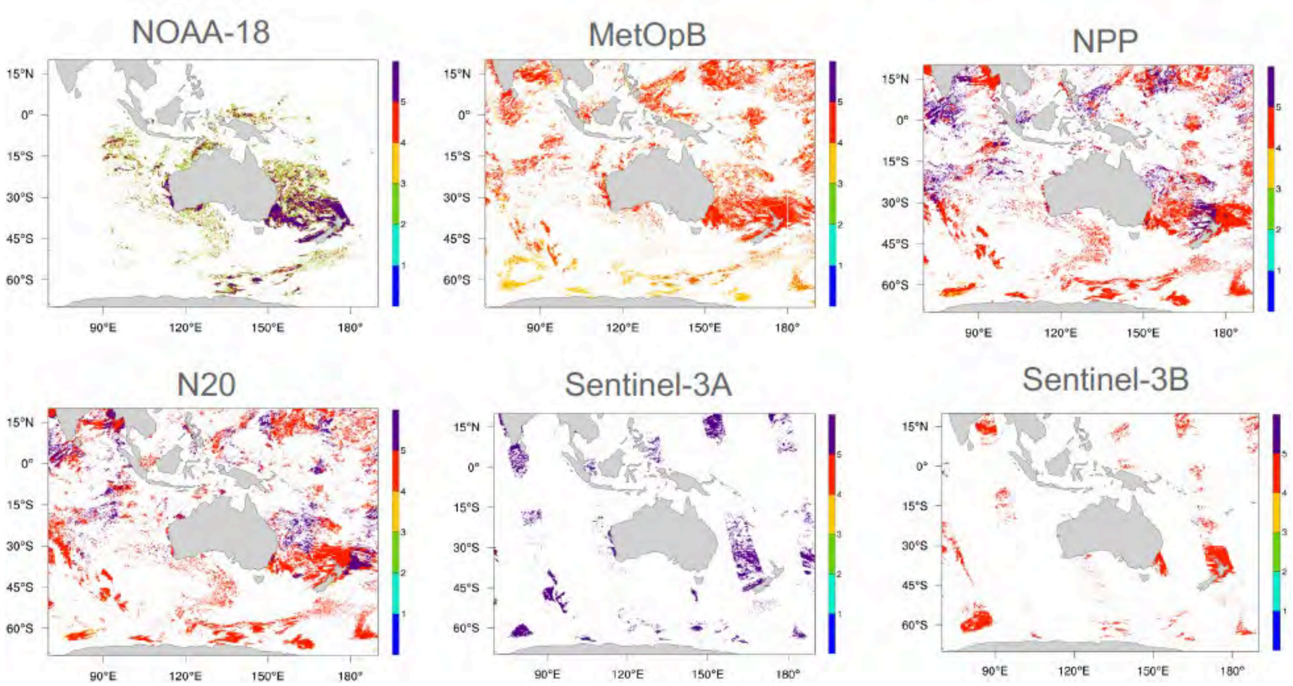

Figure 1: Remapped quality level for L3C-1day night file for 31 January 2020.

Compared to other satellite sensors, Sentinel-3A and Sentinel-3B have less data coverage owing to their narrower swaths in the L3C 1day SST product (see Figure 1). The validation of L3C 1day night files against drifting buoys and tropical moorings, shows that Sentinel-3A and Sentinel-3B have less bias than any other satellite sensor and similar standard deviation (SD) to the other satellite sensors (see Figure 2).

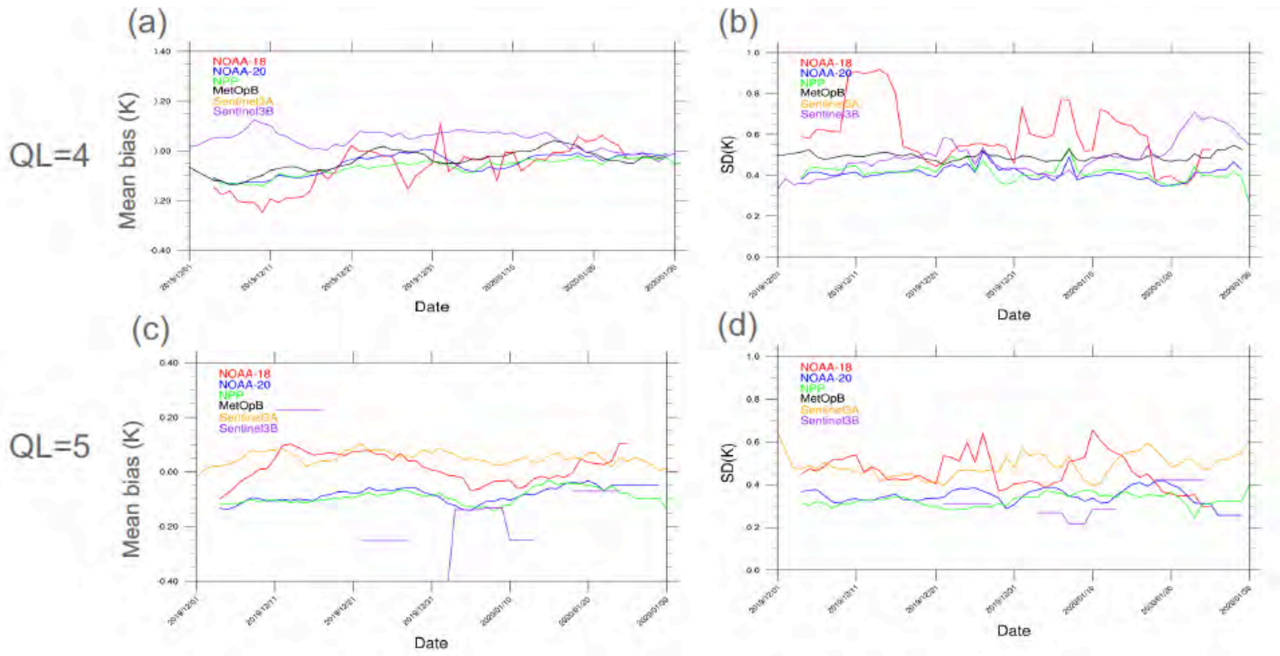

Figure 2: L3C-01day, night only, weekly statistics, 1 Dec 2019 - 31 Jan 2020, mean bias for (a) quality level 4 and (c) quality level 5, and standard deviation for (b) quality level 4 and (d) quality level 5, when compared with Drifting and tropical Moored buoy SST. Note: Mean bias = SST - in situ SST + 0.17 (in Kelvin), Matchups thresholds: < 10 km distance and < 6 hr time.

3.3. Constructing IMOS Multi-sensor L3S SST

The L3C data from the six sensors are composited to construct our new "Multi-sensor" L3S product. The quality level of all AVHRR, VIIRS and SLSTR data are remapped, and then used with an equal weighted averaging method to construct the Multi-sensor products. Before compositing data from all sensors together, the SSES bias was subtracted from the SST field for each sensor (Griffin et al., 2017).

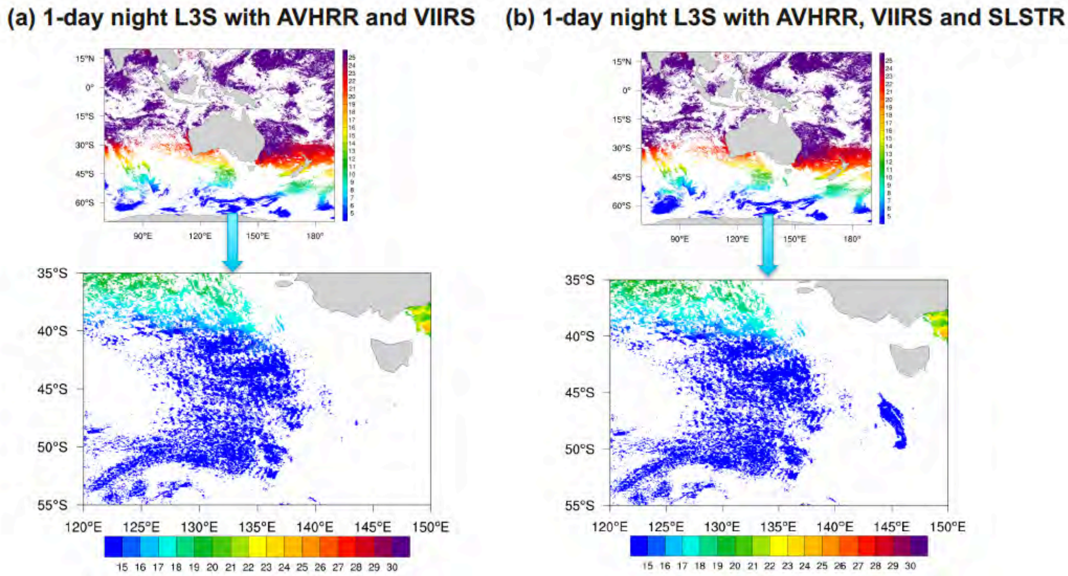

Figure 3: Sea surface temperatures with quality level 4 and 5 for L3S-1day night file from (a) NOAA-18, Metop-B, NPP and N20 and (b) NOAA-18, Metop-B, NPP, N20, Sentinel-3A and Sentinel-3B for 31 January 2020.

It was found that addition of SLSTR data slightly improves spatial coverage for Multi-sensor L3S SSTs (Figure 3). Ingesting SLSTR slightly improves the bias and makes little impact to standard deviation (Figure 4).

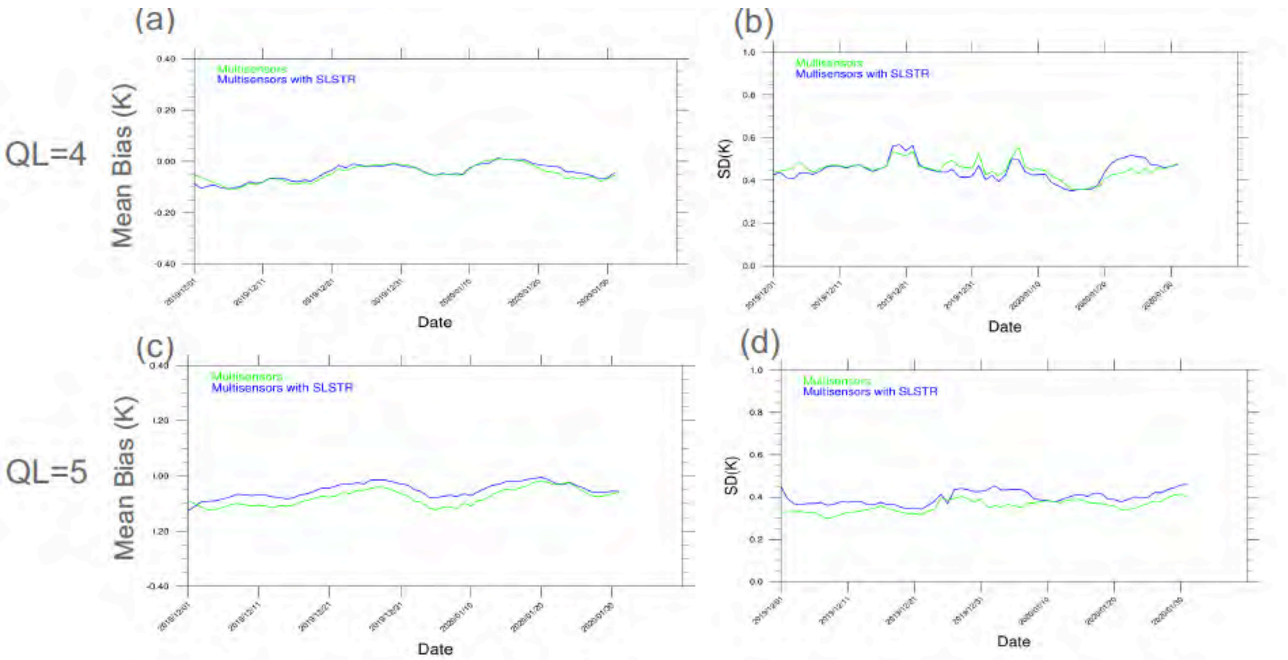

Figure 4: L3S-1day, night only, weekly statistics, 1 Dec 2019 - 31 Jan 2020, mean bias for (a) quality level 4 and (c) quality level 5, and standard deviation for (b) quality level 4 and (d) quality level 5, when compared with Drifting and tropical Moored buoys. Note: Mean bias = SST - in situ SST + 0.17 (in Kelvin), Matchups thresholds: < 10 km distance and < 6 hr time.

4. USING SLSTR L3C SST FOR VALIDATION

Operational Multi-sensor L3S-1day was also validated against SLSTR L3C-1day, night only, daily statistics, QL ≥ 4,1 Dec 2019 - 31Jan 2020, with the results shown in Figure 5. Multi-sensor L3S shows good agreement with SLSTR.

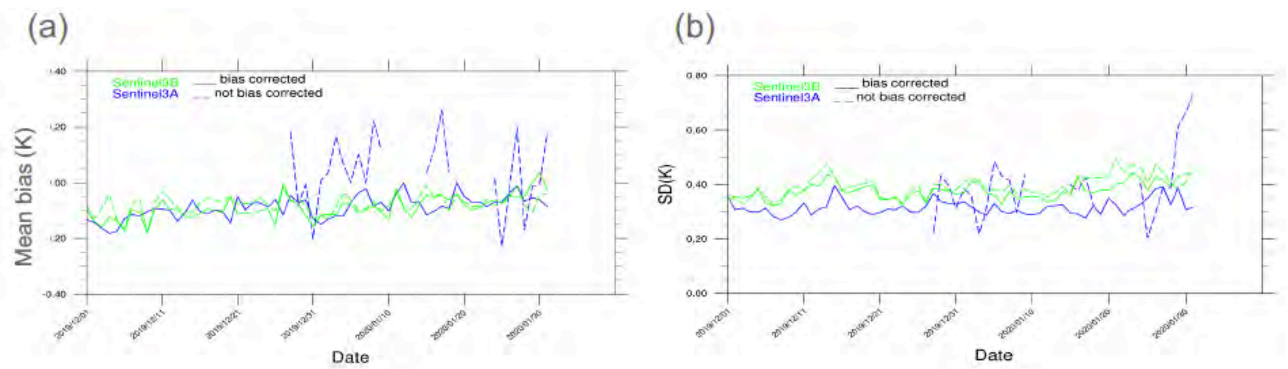

Figure 5: L3S-1day, night only, daily statistics, 1 Dec 2019 - 31 Jan 2020, QL ≥ 4, (a) Mean bias and (b) standard deviation when compared with SLSTR L3C SST. Note: Mean bias = SST – L3C SLSTR SST. Matchup thresholds: < 10 km distance and < 6 hr time.

Initial validation (1 Dec 2019 – 31 Jan 2020) indicates that additional ingestion of SLSTR data into the Multi-sensor L3S provides marginally better statistical parameters than operational Multi-sensor L3S, when compared with buoy SSTs. The narrower swath width of Sentinel-3A and Sentinel-3B limit their use to provide specialised products. However, given the accuracy and better data coverage of SLSTR data compared to *in situ* data, Sentinel-3A and Sentinel-3B can be used as reference sensors for validation of most of the other IMOS satellite SST products.

5. FUTURE WORK

Addition of SLSTR does not significantly improve spatial coverage of Multi-sensor L3S SST products. The users need for validated; accurate SST products can be facilitated with use of SLSTR data owing to its accuracy.

Over the coming year we intend to more extensively validate Sentinel L3C/L3S and experiment with adding Himawari-8 SST data to IMOS Multi-sensor L3S composites. We will investigate developing an SSES model that could be applied to all sensors contributing to the Multi-sensor L3S SSTs so that quality level can be remapped more uniformly. Rather than ingesting SLSTR SSTs into Multi-sensor L3S, we will experiment with using bias-corrected SLSTR SSTs to bias-correct Himawari-8 SST in real-time.

We will also investigate using bias-corrected SLSTR SST for validation of *in situ* corrected data sources (IMOS AVHRR and VIIRS), and *in situ* SST used for validation of SLSTR corrected sources (e.g. IMOS Himawari-8).

6. REFERENCES

Beggs, H., Griffin, C. and P. Govekar (2019). New IMOS multi-sensor sea surface temperature composites provide better coverage and accuracy, *IMOS web article, 21 February 2019,* http://imos.org.au/fileadmin/user_upload/shared/SRS/SST/Beggs_2019_IMOS_Multi-sensor_L3S_article_21Feb2018.pdf

GHRSST Science Team (2012). The Recommended GHRSST Data Specification (GDS) 2.0, document revision 5, available from the GHRSST International Project Office, 2012, pp 123. https://www.ghrsst.org/wp-content/uploads/2016/10/GDS20r5.pdf

Griffin, C., H. Beggs and L. Majewski (2017). GHRSST compliant AVHRR SST products over the Australian region – Version 1, *Technical Report, Bureau of Meteorology, Melbourne, Australia, 151 pp.* http://imos.org.au/fileadmin/user_upload/shared/SRS/SST/GHRSST-DOC-basic-v1.0r1.pdf

S4 - POSTER PRESENTATIONS - SHORT ABSTRACTS

S4-P1: TOWARDS GLOBAL L3S PRODUCTS AT NOAA

Olafur Jonasson[(1)], Irina Gladkova, Alexander Ignatov, Yury Kihai

(1) NOAA STAR, 5830 University Research Court, College Park, MD 20850,
Email: Olafur.Jonasson@noaa.gov

SHORT ABSTRACT

NOAA produces a wide range sea surface temperature (SST) products from both polar and geostationary sensors using its Advanced Clear Sky Processor for Oceans (ACSPO) enterprise system. Current operational polar products include from two VIIRSs onboard NPP/N20 and three AVHRR FRACs onboard Metop-A/B/C. In addition, two MODIS SST products from Terra and Aqua are also routinely generated on an experimental basis. All polar ACSPO products are produced in 10 minute granules on the original swath (L2P) as well as 0.02° gridded uncollated (L3U) projections. Despite a much lower data volume of L3U compared to L2P, users are still overwhelmed with the large number of files and the need to deal with regional and cross-sensor biases, and residual cloud in each individual product. Many users interested in high resolution SST have resorted to using level (L4) analysis products like JPL MUR despite somewhat degraded feature resolution. To meet users' needs for "one good high-resolution global SST" that preserves high feature resolution, mitigates residual cloud and biases, and greatly improves coverage while reducing data volume, the NOAA SST Team is developing a new line of global multi-sensor "super-collated" L3S products. The ACSPO L3Ss comprise an afternoon ("PM") product, which currently includes two VIIRSs aboard NPP/N20, and a mid-morning "AM" product, which currently includes three AVHRR FRACs aboard Metop-A/B/C. In the future, METimage onboard EPS-SG and MODIS Terra will be added to the AM line and J2/N21 and MODIS Aqua to the PM line, respectively. PM and AM products are split into night time and daytime files, resulting in 4 files per day. We describe the ACSPO collation algorithm and demonstrate improvements in accuracy and imagery compared to uncollated L3U data, and present current state of development and evaluation of the L3S products.

S4-P2: CMEMS SST-TAC: ACHIEVEMENTS DURING THE SECOND YEAR (2019) AND EVOLUTIONS PLANS IN 2020

Andrea Pisano(5), Chongyuan Mao(1), Simon Good(1), Jacob Hoeyer(2), Emma Saux Picart(3), Jean François Piollé(4), Cristina Tronconi(5), Rosalia Santoleri(5), Bruno Buongiorno Nardelli(6)

(1) Met Office, United Kingdom
(2) Danish Meteorological Institute (DMI), Denmark
(3) Metéo France, France
(4) Ifremer, France
(5) Institute of Marine Sciences (ISMAR), Italian National Research Council (CNR), Rome, Italy,
Email: andrea.pisano@cnr.it
(6) Institute of Marine Sciences (ISMAR), Italian National Research Council (CNR), Naples, Italy

SHORT ABSTRACT

The Sea Surface Temperature Thematic Assembly Centre (SST-TAC) is one of the Copernicus Marine Environment Monitoring Service (CMEMS) elements in charge of providing accurate operational near-real time (NRT) and reprocessed (REP) satellite-based SST products covering the Global Ocean and the European Seas.

One of the main objectives of the SST-TAC is to provide continuous evolutions aiming at the improvement of the global and regional SST products. Main evolutions include the increase of SST-TAC products portfolio, modifications of the algorithms, and ingestion of new available upstream satellite sensor and temporal extension of REP products to present. Our aim is to show the more recent and relevant evolutions carried out within the SST-TAC, and those planned in 2020.

In 2019, a huge effort has been dedicated to the assessment and integration of SLSTR-3A/3B L2P SST data in all the NRT SST products. The impact of Sentinel SLSTR showed different results depending on the specific algorithm and configurations adopted in each of the processing chains. Small to neutral improvements have been observed in the Global Ocean SST product, provided by OSTIA system, and in the Baltic Sea, North Atlantic Sea and European Sea SST products, where only the dual view is used. Slightly higher improvements are obtained for the Mediterranean SST product, where the dual view of S3A SLSTR is used as reference sensor and including the nadir view of both S3A/S3B data in the bias-correction processing step.

In 2019, the new level 4 climate data record provided by the ESA CCI and C3S initiatives was also made available through CMEMS. During 2020, all the existing SST-TAC REP products will be updated based on the ESACCI/C3S dataset. The updated REP products will be used to provide updated Ocean Monitoring Indicators (OMIs), i.e. indices based on SST used to track the ocean state under current global warming.

S4-P3: ADVANCING DATA DISCOVERY AND SERVICES IN SUPPORT OF THE GHRSST COMMUNITY

Wen-Hao Li[1], Edward Armstrong[2], Jorge Vazquez[2]

(1) Raytheon IIS, Pasadena, CA, Email: wen-hao.li@jpl.nasa.gov
(2) Jet Propulsion Laboratory, California Institute of Technology, Pasadena, CA

SHORT ABSTRACT

NASA's Physical Oceanography Distributed Active Archive Center (PO.DAAC) is a Global Data Assembly Center (GDAC) for the GHRSST project. PO.DAAC has been continuously advancing the data tools and services to increase the data discoverability, interoperability, usability, and sustainability of the GHRSST data products. In recent years, PO.DAAC has made significant improvements in supporting the GHRSST data archiving and distribution. Several key sea surface temperature (SST) products from regional data providers (ABoM, JPL, and OBPG) have been updated to newer versions providing improved science-quality and near-real-time SST. PO.DAAC has also made tremendous progress in improving data discovering tools and services to reduce the barriers of data search and usage, especially focused on visualization, analytics, subsetting, extraction, and data transformation through RESTful APIs, GUI-based tools/services, and data recipes. In addition, the data citation metrics which tracks the data usage in research publications have been added to the GHRSST dataset landing pages, which provides useful information on how and where the data is used. Currently, PO.DAAC is preparing to roll out a refreshed web portal interface to provide more intuitive user experience and efficient browsing functionality to help simplify the data discovery and access experience. PO.DAAC is also in the process of adding some GHRSST datasets into AWS cloud platform. In this presentation, we intend to inform the GHRSST community of these recent developments and future plans to continue advancing services at PO.DAAC.

S4-P4: EUMETSAT COPERNICUS MARINE TRAINING AND USER SUPPORT

Hayley Evers-King[1], **Sally Wannop**[1], **Christine Traeger-Chatterjee**[1], **Lauren Biermann**[2]

(1) EUMETSAT, Eumetsat Allee 1, Darmstadt, 64295, Germany
(2) Plymouth Marine Laboratory
Email: Hayley.EversKing@eumetsat.int

SHORT ABSTRACT

EUMETSAT provides user support and training for all users of the Copernicus Marine Data Stream (CMDS). The CMDS refers to all the level 1 and level 2 marine data from sensors on the Sentinel-3 and Jason-3 satellites, including ocean colour, sea surface temperature, and surface topography data. Details on the products and processing methodologies are available through handbooks, product notices, and a number of services including a help desk, and online forum. The training service aims to support all users wishing to explore potential applications of the CMDS. The service is primarily based around the delivery of two week, blended courses with both an online and classroom component. The online component is hosted on a Moodle platform and uses a variety of prepared resources including short articles, videos, software installation, and basic software tutorials; supported by discussion forums, to prepare participants for the classroom phase. The classroom phase is focused on practical work, with no lectures given. Participants are led through examples of workflows using SNAP and Jupyter Notebooks/Python, and are then given one-on-one/small group trainer support to work for three days on personal projects that they defined during the online phase. These projects yield a diverse range of synergistic use cases of ocean remote sensing data for societally relevant applications. The training service has also run a variety of collaborative courses with community led initiatives, and proposes to develop online courses and resources in response to community needs. Feedback and requests from the GHRSST community are welcomed.

S4-P5: A COMPARISON BETWEEN IQUAM AND "EXTERNAL" *IN SITU* SST QUALITY CONTROLS

Haifeng Zhang[1,2], Alexander Ignatov[1], Dean Hinshaw[1,3]

(1) NOAA/STAR, College Park, MD 20740, USA;
(2) CIRA, Colorado State University, Fort Collins, CO, USA;
(3) GST, Inc., MD, USA
Emails: haifeng.zhang@noaa.go v; alex.ignatov@noaa.gov ; dean.hinshaw@noaa.gov

SHORT ABSTRACT

In situ sea surface temperature (SST) measurements play a key role in satellite SST calibration/validation (Cal/Val) and data assimilation. Although *in situ* SSTs are generally considered more accurate than satellite retrievals and treated as "ground truth", their quality, nonetheless, varies across different types of platforms and sensors, or may even change in time/space for a specific instrument. Proper quality control (QC) is needed before *in situ* measurements can be used with confidence. Currently, the *In Situ* Quality Monitoring system (iQuam) developed by NOAA in 2009 (https://www.star.nesdis.noaa.gov/sod/sst/iquam/; Xu and Ignatov, 2014) is widely used in the GHRSST community. The iQuam gathers *in situ* SSTs from many available data sources and applies a uniform QC to different datasets, to generate QC'ed data with iQuam quality flags (QFs) appended. At the same time, many providers of the data ingested as input in iQuam, e.g. ICOADS (International Comprehensive Ocean-Atmosphere Data Set) and IMOS (Integrated Marine Observing System), perform their own QCs and append their QFs to their products. These "external" QFs are also reported in iQuam files, side-by-side with the iQuam QFs. Based on limited (and undocumented) analyses, NOAA recommends using uniform QFs produced by iQuam, rather than "external" QFs. This study aims to perform more systematic analyses of the relative performance of iQuam QFs versus data–providers' supplied QFs. A "confusion matrix" analysis is employed for each data source, to quantify the commonalities and differences. Ultimate objectives of this study are to better understand various QC algorithms, document their relative performance and merits, better inform iQuam users, and potentially improve iQuam QC in the future releases of this NOAA product.

S4-P6: THE OCEANVIEW (OV): TOWARDS A WEB-APPLICATION FOR INTEGRATED VISUALIZATION OF SATELLITE, IN SITU, AND MODEL DATA & OCEAN EVENTS – THE CONCEPT AND THE PLAN

Prasanjit Dash[(1,2)], **Paul DiGiacomo**[(1)]

(1) NOAA STAR SOCD
(2) Colorado State University, CIRA
E-Mail: Prasanjit.Dash@noaa.gov

SHORT ABSTRACT

The satellite oceanography community generates a large amount of remotely-sensed products along with a sizeable amount of *in situ* measurements. The data available are aimed at characterizing the state of the ocean and the overlying atmosphere, e.g. Sea Surface Temperature (SST), Ocean Colour (OC), Sea Surface Height (SSH), Sea Surface Salinity (SSS), Sea Surface Wind (SSW), Geostrophic Currents, and True Colour images. Along with satellite and *in situ* measurements, various model data are also available, e.g. Global Forecast Model (GFS) 10 m wind speed. Some of these thematic fields are more data-rich than others, e.g. SST and OC, but generally speaking, a large amount of information about the oceans is readily available. These datasets combined have helped us to incrementally improve upon our past understanding of the ocean. However, an integrated visualization of these datasets from an oceanographer's perspective is still non-trivial. One of the major support tools in this pursuit is improved visualization of the information available to us through scientific and technical breakthroughs. The OceanView (OV) is a step towards comprehensive visualization of multiple ocean products available from the Satellite Oceanography and Climate Division (SOCD) of NOAA STAR, model data from NCEP GFS, and ocean events from various federal agencies.

The OV is being conceptualized to enable simultaneous displaying of raster data (e.g. SST maps), vector information (points, lines, and polygons) and special vectors (velocity information). It will also offer various map-interactions and map-controls and choice of coordinate-reference-system (Geographic, Arctic, Antarctic). The raster maps provide a context and the annotated vector information provides further insight. A major focus is also on search and visualization of events, e.g. hurricanes. The OV will be publicly released in 2021 and presented in detail. This preliminary presentation aims at sharing our vision, interactively soliciting feedback from the community, and gauging further features of interest.

S4-P7: STATUS OF VIIRS SST PRODUCTS AT NOAA

Olafur Jonasson[(1)], Alexander Ignatov[(1)]

(1) NOAA STAR, 5830 University Research Court, College Park, MD 20850,
Email: Olafur.Jonasson@noaa.gov

SHORT ABSTRACT

Visible Infrared Imager Radiometer Suite (VIIRS) is the newest generation of earth observing sensors, currently flown onboard NPP (launched in 2011), N20/J1 (launched in 2017) and will be aboard N21/J2 (planned for launch in 2022). NOAA produces operational VIIRS SST products from NPP/N20 in GDS2 compliant L2P (swath) and L3U (0.02º; gridded) formats using its Advanced Clear Sky Processor for Oceans (ACSPO) enterprise system. The current version is ACSPO V2.61, which went operational in April 2019. Earlier dates back to the beginning of both missions have been reprocessed at NOAA STAR, providing a uniform-quality “VIIRS Reanalysis 2” (RAN2) SST dataset. The RAN2 superseded the RAN1, performed in 2015 using ACSPO v2.40 and covering a period from March 2012 to December 2015 (NPP only). In addition to including N20, RAN2 improved quality and uniformity of SST time series, by starting from L0 data and working with the NOAA calibration team to minimize the effects of VIIRS warmup cool-down (WUCD) on SST (RAN1 suffered from quarterly ~ 0.25 K warm biases in daytime SST during WUCD calibration exercises). ACSPO 2.61 also introduced resampled imagery (to fill bow-tie deletion zones), more accurate clear-sky mask and inclusion of the 8.6 micron band in SST retrieval. Unlike RAN1 which was never archived, the RAN2 data are publicly available via NASA PO.DAAC, NOAA NCEI and NOAA CoastWatch, with dates after April 2019 to present supplemented with data processed in near real-time. This poster presents results of RAN2 SSTs validation in SQUAM, using match-ups with *in situ* data from NOAA iQuam. In late 2020, ACSPO will be upgraded to V2.80. Improvements include reduced over-screening of cold fronts in dynamic regions, removal of cloud tests based on radiative transfer simulations (replaced with non-RTM based alternatives), and adding two data layers with thermal fronts. The possibility of generating RAN3 with ACSPO 2.80 is now being considered.

S4-P8: STATUS OF METOP SST PRODUCTS AT NOAA

Victor Pryamitsyn[1,2], Alexander Ignatov[1], Boris Petrenko[1,2], Olafur Jonasson[1,2], Yury Kihai[1,2]

(1) NOAA STAR, Center for Weather and Climate Prediction (NCWCP), 5830 University Research Ct, College Park, MD 20740, USA;

(2) Global Science and Technology, Inc., 7855 Walker Dr # 200, Greenbelt, MD 20770, USA

Email: victor.pryamitsin@noaa.gov

SHORT ABSTRACT

Metop-A, Metop-B, and Metop-C (launched on 19 October 2006, 17 September 2012, and 7 November 2018, respectively) all fly sun-synchronous “mid-morning” stable orbits @9:30am/pm, and carry Advanced Very-High-Resolution Radiometer (AVHRR) with a capability to store onboard and transmit to the ground high-resolution (~1km at nadir; ~6km at swath edge, 2,800 km swath) Full-Resolution Area Coverage (FRAC) data. NOAA produces operational AVHRR FRAC SST products from Metop-A/B/C in GDS2 L2P and 0.02º gridded L3U formats using its Advanced Clear Sky Processor for Oceans (ACSPO) enterprise system. The current ACSPO v2.70 went operational in May 2019. Currently, the Metop data are not archived and only available at CoastWatch website as a 2 weeks rotating buffer. AVHRR FRAC SST Reanalysis 1 (“FRAC RAN1”) is underway from 2006 onwards to create a uniform long-term data set, to supplement the “GAC RAN2” and be used as input into “AM-L3S” fused, and geo-polar blended L4.

In this presentation we discuss FRAC RAN1 Beta01 and its validation against *in situ* data from NOAA iQuam. FRAC RAN produces two SSTs: Global Regression (GR) (with high sensitivity to “skin” SST) and the Piecewise Regression (PWR) (a better proxy of "depth" SST). The regression coefficients for both are recalculated daily, to minimize variability of global biases with respect to *in situ* SST caused by the variable AVHRR calibration and seasonal matchup distributions. We demonstrate the effect of using variable coefficients by comparing with SST biases calculated with fixed coefficients.

The Metop First Generation will be succeeded with Metop Second Generation (Metop-SG), with the first Metop-SG-A satellite expected to be launched in 2022. NOAA plans to process Metop-SG data. ACSPO is being tweaked to be able to process METimage L1b data, and generate SST product for the use as input in two NOAA fused/blended products: Level 3 Super-collated (L3S) and Level 4 Geo-Polar analysis.

S4-P9: DATA REDUCTION SERVICE FOR THE V2.1 SEA SURFACE TEMPERATURE ANALYSIS FROM THE ESA CLIMATE CHANGE INITIATIVE

Chris Merchant, Owen Embury, Niall McCarroll and Charles Roberts

Department of Meteorology, University of Reading, Reading, UK
Email: c.j.merchant@reading.ac.uk

SHORT ABSTRACT

The v2.1 climate data record (CDR) for sea surface temperature (SST) includes an analysis product that combines the SSTs from all lower-level observations at 0.05°, daily resolution. Per-datum uncertainty and consistent sea ice concentration (from other sources) are also provided. Despite the data reduction achieved by the analysis process, the dataset volume is ~440 GB, since the record is now ~38 years long.

Some users wish to undertake climate analyses at coarser spatio-temporal resolution, but may be daunted by the regridding task and be unclear about how to estimate the regridded uncertainty. Pre-calculating all such users' requirements is not possible, since surveys have shown there is a wide variety of potential spatio-temporal combinations required. For this reason, a regridding service has been established that regrids to user-requested space-time resolution on the fly, and alerts the user when the resulting data are available for download. Options are limited to selected multiples of the underlying analysis resolution, but it is hoped that many users' requirements will be well served. How the calculation of cell-mean SST is treated in sea-ice covered areas (where no SST observations were present) can be specified by the user, as can the error correlation length-scale assumptions used for uncertainty propagation to the target grid. The user can select absolute or anomaly SST output data, the latter being relative to the climatology of 1982 - 2010.

S4-P10: NAVOCEANO SST PROCESSING

Danielle Carpenter[1], Dan Olszewski, Valinda Kirkland, Michelle Little

(1) Naval Oceanographic Office, Stennis Space Center, MS 39522 US
Email address: danielle.carpenter@navy.mil

SHORT ABSTRACT

The Naval Oceanographic Office (NAVOCEANO) Data Collection Division is responsible for providing near-real-time sea surface temperature (SST) measurements to the US Navy and national/international partners. The Naval Research Lab (NRL) at Stennis Space Center provides the research and development of the SST processing for numerous satellite data sets that are operationally processed at NAVOCEANO. This SST data is assimilated in the Navy's Global Ocean Forecast System (GOFS) and Global Environmental Model (NAVGEM) and soon in the Navy Global Earth System Prediction Capability (ESPC). NAVOCEANO is a member of the Group for High Resolution SST (GHRSST) science group operationally providing and acquiring GHRSST datasets.

SCIENCE SESSION 5: APPLICATIONS

S5 - SESSION REPORT

Chair: Jorge Vazquez[(1)]
Co-chairs: Sujuan J Wang[(2)], Salvatore Marullo[(3)]

(1) Jet Propulsion Laboratory/California Institute of Technology, Email: jorge.vazquez@jpl.nasa.gov
(2) National Satellite Meteorological Center, Met Administration, China
(3) Agenzia Nazionale per le Nuove Tecnologie, l'Energia e lo Sviluppo Economico Sostenibile, Frascati, Italy

INTRODUCTION

In our section we had four oral presentations and three posters.

1. ORAL PRESENTATIONS

1.1. Comparison of multiple SST products using the Marine Heatwave Tracker – R.W. Schlegel (S5-1)

The first talk by Robert Schlegel presented an interesting application for heatwave detection and analysis. This could be a promising and alternative way to monitor global ocean warming rather than the classical view of mean, variance and trends which was, by the way, very nicely presented by Pastor in his poster. Comparisons were made using several GHRSST data sets.

Very interesting on how results were separated based on the strength of the Heat Wave. The results are very useful to SST users.

1.1.1. Discussion

There was a lot of discussion. Some of the key points included how the ice mask extent and flagging could affect results in the Polar Regions. Suggestions were raised about how to address some of these issues, inclusive of not using any pixels that are possibly affected by ice in the Marine Heatwave derivation. Other issues raised that could possibly affect the differences seen in the multiple data sets included the gridding algorithms used as well as cloud masking. For application in coastal areas, gridding resolution was a key issue. Also, there were discussions on the addition of other data sets to the tracker, including JMA and CSIRO products. Also discussed was using OISST V2.1. Issues were raised about limitations of using products due to data gaps. There was complete agreement that this was a very important application of GHRSST data to a real use case, the detection of marine heatwaves. Several questions were raised also on the possibility of the application of the Marine Heatwave Tracker in Real Time? The current lag is the best that can be done, but possible improvements may happen in the future.

1.2. Integrating regionally optimised sea surface temperature and ocean colour earth observation products to detect and monitor harmful algal blooms in support of small scale fishers and the abalone aquaculture industry in the Southern Benguela Upwelling System – C. Whittle, M. Smith, S. Bernard, R. Molapo, L. Vhengani (S5-2)

Christo Whittle presented the South Africa effort for the monitoring of the marine environment in a context of sustainable use of marine resources in the presence of recurrent harmful algal blooms. Christo did a very interesting comparison between the ocean colour data and GHRSST SST data, using them as markers for the harmful algal blooms. Specific examples were given with respect to the Benguela upwelling region.

1.2.1. Discussion

Very positive comments about the application of both SST and Ocean Colour to detecting harmful algal blooms. One question raised was the application of the MODIS reprocessed product which has potential for improvements in cloud masking. This could potentially have significant impacts, especially in coastal regions. A major point brought out by Cristo was the relationship between the harmful algal blooms and reduced productivity. New improved reprocessing efforts, specifically MODIS with improved cloud masking, could significantly impact the predictability and understanding of impacts.

1.3. Multi-Decadal Examination Of Thermal Habitat Suitability For The Endangered Delta Smelt In The San Francisco Estuary Using Landsat 5, 7, And 8 - G. Halverson, C. Lee, G. Hulley, E. Hestir, K. Cawse-nicholson, B. Bergamaschi, B. Palmieri, A. Osti, S. Acuña, N. Tuffilaro, R. Radocinski, G. Rivera, C. Ade, T. Sommer (S5-3)

On the other hand, the presentation of Gregory Halverson opens a window on internal water applications using unusual (for the GHRSST group) satellite methods based on Landsat data and demonstrating the usefulness of the methodology for very practical environmental applications.

1.3.1. No discussion questions.

1.4. On the use of sea surface temperature (SST) for improving the altimeter derived surface currents: a sensitivity study to SST products – D. Ciani, M-H Rio, B. Buongiorno Nardelli, S. Marullo, H. Etienne and R. Santoleri (S5-4)

The presentation of Daniele Ciani represents an ideal methodological effort to synergistically use different satellite products. I am sure that the inclusion of the future CIMR SST and Salinity data will contribute to enhance the potentiality of this already promising method. A major conclusion and very relevant for the future was the inhomogeneity of the SST gradients. A primary reason was the issue of cloud cover and smoothness that occurs.

1.4.1. Discussion

Discussions arose as to the use of L4 GHRSST products for gradient calculations. Issues were raised specifically as to feature detection and interpolation and smoothing of the data. The interpolation and smoothing inherent in L4 products can degrade the capability to accurately isolate oceanic features. Example was given of the MUR SST product which, under cloud free pixels has the advantage of the higher resolution, but this can be lost under cloudy conditions where features can be missed or identified improperly. The issue was raised about the application of the methodology to L3 products and potentially L2 products to better isolate oceanic features.

2. POSTER PRESENTATIONS

2.1. NOAA’s Ocean Heat Content Suite for the Indian Ocean – E. Maturi, D. Donahue (S5-P1)

The poster of Eileen Maturi and co-authors presented the NOAA’s Indian Ocean Heat Content Product and represent a very useful product for climate studied. Additionally, a global OHC product would be very helpful for Hurricane season.

2.2. Address Tropical Climate Variability with Neural Network Models _ D. Leonelli, C. Yang, S. Marullo, A. Pisano, C. Cammarota (S5-P2)

The poster by Leonelli and co-authors shows part of her Mathematics PhD program focused on time series analysis and dynamical systems in a statistical mechanics framework.

In our opinion this represents a first effort of bridging the theoretical world of the mathematicians with the geophysical world. So many times, we have seen beautiful theorems and models without applications and geophysical or environmental problems that suffered from the lack of adequate interpretative models. In our opinion this poster could be promising starting point towards an effective collaboration between the two worlds.

2.3. Mediterranean, almost 40 years of continued warming – F Pastor, J.A. Valiente, S. Khodayar (S5-P3)

S5 - ORAL PRESENTATIONS - EXTENDED ABSTRACTS

S5-1: COMPARISON OF MULTIPLE SST PRODUCTS USING THE MARINE HEATWAVE TRACKER

Robert W Schlegel

WHOI, Woods Hole, MA, USA, Email: rschlegel@whoi.edu

1. ABSTRACT

In a warming world it is increasingly important that the accuracy of SST products be maintained to the highest standard possible. This is important not just for detecting a secular trend in the data, but for the accurate detection of extreme values, based on a reliable climatological mean. There are however many issues that may negatively affect the accuracy of an SST product. For example, when the amount and quality of *in situ* collected SST used for interpolation in remotely sensed products waxes and wanes, large warm or cold biases may be introduced. The cold biases of up to 2° C in the last few years of the NOAA OISST v2.0 product being one such example. It is therefore important that the difference in ocean temperature extremes, known as marine heatwaves (MHWs), be publicly documented so that end users may make informed decisions as to their choice of product. The difference between MHWs detected in three SST products is highlighted here using an operational SST analysis platform: the Marine Heatwave Tracker (http://www.marineheatwaves.org/tracker.html). This interactive web application was designed to track the occurrence of MHWs globally in near real time and has been running since late 2018, with historic records dating back to 1982. By integrating multiple SST products into the Tracker in near-real-time it is possible to compare their accuracy for the detection of MHWs operationally on a global scale. The products used in this comparison were the NOAA Optimum Interpolation (OI) SST v2.0 + v2.1 (Reynolds et al., 2007; Banzon et al., 2016; Banzon et al., 2020), Climate Change Initiative (CCI) SST v2.1 + v2.0 (Merchant et al., 2019), and the Canadian Meteorological Center (CMC) SST v2.0 + v3.0 (Brasnett 2008; Brasnett 2012; Brasnett and Colan, 2016). All three products were regridded to the 1/4° daily NOAA grid. It was found that the CCI and CMC products tended to report higher rates of category three and four MHWs, while NOAA reported more category two events. The MHWs detected in all three products became less similar the further back into the historic record one looked, with CMC becoming the most dissimilar. Likewise, the MHWs detected in all three products converged in similarity towards the present, with NOAA converging the least. The most important finding of the comparison of the three products was how dissimilar they were more than ~70 degrees from the equator (Figure 1). This is likely attributed to the different ice cover algorithms employed by the products and to how well each product ingests/interpolates high latitude data.

2. FIGURE

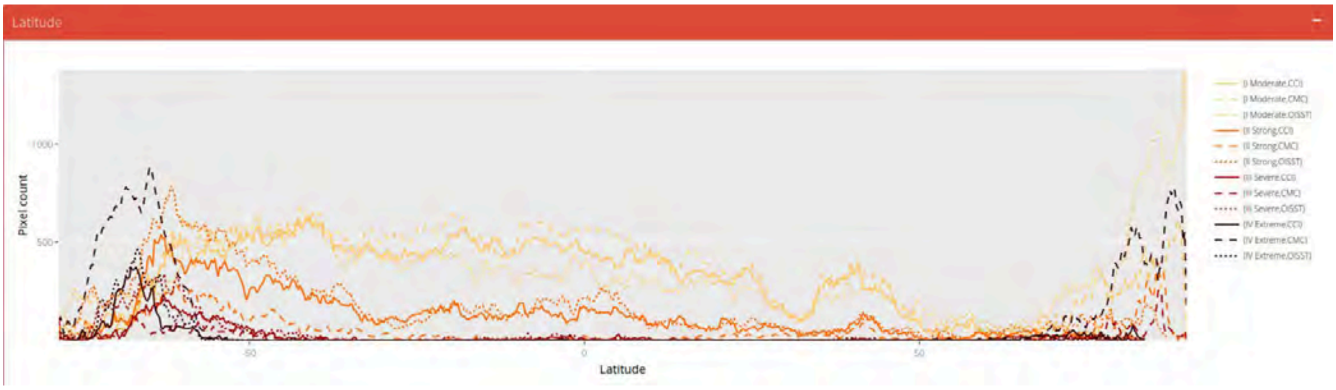

Figure 1: Line plot showing the (dis)similarity of recorded MHW categories for three different SST products at different latitudes during 1992. The count of MHW categories by pixel are shown on the y-axis and latitude on the x-axis. The

different products are shown with different line types and the different MHW categories are shown with different colours. Larger peaks in the lines denote a higher count of MHWs at the corresponding latitude on the x-axis. Please go to the Marine Heatwave Tracker (http://www.marineheatwaves.org/tracker.html) and click on the 'Comparison' tab for interactive access to the results.

3. CONCLUSION

The most important finding of the comparison of the three products was how dissimilar they were more than ~70 degrees from the equator (Figure 1). This is likely attributed to the different ice cover algorithms employed by the products and to how well each product ingests/interpolates high latitude data.

4. REFERENCES

Banzon, V., Smith, T. M., Chin, T. M., Liu, C. Y., & Hankins, W. (2016). A long-term record of blended satellite and *in situ* sea-surface temperature for climate monitoring, modeling and environmental studies.

Banzon, V., Smith, T. M., Steele, M., Huang, B., & Zhang, H. M. (2020). Improved Estimation of Proxy Sea Surface Temperature in the Arctic. *Journal of Atmospheric and Oceanic Technology*, *37*(2), 341-349.

Brasnett, B. (2008). The impact of satellite retrievals in a global sea-surface-temperature analysis. *Quarterly Journal of the Royal Meteorological Society*, *134*(636), 1745-1760.

Brasnett, B. (2012). A 20-year Reanalysis of Sea Surface Temperature. In *Report CMC*.

Brasnett, B., & Colan, D. S. (2016). Assimilating retrievals of sea surface temperature from VIIRS and AMSR2. *Journal of Atmospheric and Oceanic Technology*, *33*(2), 361-375.

Merchant, C. J., Embury, O., Bulgin, C. E., Block, T., Corlett, G. K., Fiedler, E., ... & Eastwood, S. (2019). Satellite-based time-series of sea-surface temperature since 1981 for climate applications. *Scientific data*, *6*(1), 1-18.

Reynolds, R. W., Smith, T. M., Liu, C., Chelton, D. B., Casey, K. S., & Schlax, M. G. (2007). Daily high-resolution-blended analyses for sea surface temperature. *Journal of Climate*, *20*(22), 5473-5496.

S5-2: INTEGRATING REGIONALLY OPTIMISED SEA SURFACE TEMPERATURE AND OCEAN COLOUR EARTH OBSERVATION PRODUCTS TO DETECT AND MONITOR HARMFUL ALGAL BLOOMS IN SUPPORT OF SMALL SCALE FISHERS AND THE ABALONE AQUACULTURE INDUSTRY IN THE SOUTHERN BENGUELA UPWELLING SYSTEM

Christo Whittle[(1)], Marie Smith[(1)], Stewart Bernard[(1)], R. Molapo[(2)], L. Vhengani[(2)]

(1) Marine Earth Observation, Smart Places, CSIR,Cape Town, South Africa
(2) NextGen Enterprises and Institutions, CSIR, Pretoria, South Africa
Email: cwhittle@csir.co.za

ABSTRACT

The Southern Benguela Upwelling System (SBUS) is seasonally afflicted by the occurrence of harmful algal blooms (HAB), often referred to as red tides. A range of algal species, responsible for toxic blooms or adverse low oxygen concentrations within the nearshore water column, are commonly found in SBUS embayments where they sometimes proliferate rapidly under ideal conditions during the latter part of the upwelling season. Harmful impacts of HAB occurrence include the mortality of fish and other animals, thereby posing a significant threat to the livelihood of small scale fishers and the successful operation of aquaculture farms. A global increase in HAB episodes demands that resource managers and health officials be provided with state-of-the-art scientific services that will promote decisive action to mitigate against the severity of HAB impacts. Earth observation products such as sea surface temperature (SST) and ocean colour (OC) are invaluable tools in recognising physical factors that promote HAB initiation, retention and advection. However, these products often provide inadequate spatial or temporal coverage when examining scenes derived from individual sensors. The CSIR Marine Earth Observation Group has developed regionally optimised SST and OC products from the MODIS, SLSTR and OLCI sensors to include in an environmental risk assessment and early warning service in support of small scale fishers and aquaculture farms operating in the SBUS. This paper provides a description of earth observation service development, and its application during a recent bloom event, illustrating the coordinated, applied industrial and research use of EO data in synergy with the CEOS Ocean Variables Enabling Research and Applications for GEO (COVERAGE) model.

1. INTRODUCTION: THE NEED FOR AN OCEANS AND COASTAL INFORMATION MANAGEMENT SYSTEM

South Africa has an expansive (~1,553,000 km^{2}), but underexploited, marine exclusive economic zone that exceeds the size of her terrestrial territory, and manages a coastline of 3,924 km (van Wyk 2015). Economic actors within South Africa's coastal and near-coastal zone include small-scale fishers and a burgeoning aquaculture farming industry. Many coastal communities around the world that traditionally earned a livelihood from the sea have faced unemployment and extreme poverty, due to the mismanagement and overexploitation of marine living resources. In July 2014 the South African Government launched Operation Phakisa, an initiative aimed at fast-tracking the delivery of some of the priorities outlined in the National Development Plan (Vision 2030). The National Development Plan is the country's socio-economic development blueprint which enjoins citizens to create a better life for all citizens in an inclusive society. Phakisa means "hurry up" in Sesotho (one of South Africa's indigenous languages). Operation Phakisa provides a mechanism to stimulate South Africa's "Blue Economy" and harness some of the socio-economic benefits for the upliftment of poverty-stricken coastal communities.

To facilitate the management and growth of a Blue Economy under Phakisa, the South African Government initiated the development of the National Oceans and Coastal Information Management System (OCIMS). In a collaborative partnership led by the Department of Environmental Affairs, the Council for Scientific and Industrial Research manages the OCIMS system design and implementation. The implementation of OCIMS incorporates infrastructure and system design that allows for the integration of information from satellite, *in situ*, model and lab-based sources into user co-developed decision support tools that address early warning support, operations support, compliance and enforcement, as well as planning and assessment within South

Africa's coastal and marine exclusive economic zone. OCIMS draws on regional earth observation expertise and knowledge of South African coastal systems to produce relevant information that will have a measurable impact on the South African socio-economic landscape by identifying, interpreting and monitoring environmental factors that affect the sustainable exploitation of living and other marine resources. In this document we describe the development and successful implementation of an OCIMS "Decision Support Tool" (DeST): The Fisheries and Aquaculture DeST.

2. BACKGROUND: IMPACTS OF HABS ON SMALL SCALE FISHERS AND ABALONE AQUACULTURE

West Coast rock lobster, also known as crayfish, is an important resource to small scale fishers on the west coast of South Africa. Here coastal communities rely on seasonal catches to earn a livelihood. During February and March 2015 large marine mortalities resulted in the removal of 415 tons of rock lobster, 21 tons of mussels and various fish species from the beaches within the St Helena Bay area (Ndhlovu et al 2017). This huge loss of valuable marine resources was due to the presence of large harmful algal blooms (HABs), also known as red tides. Although red tide organisms are known for the toxins that they produce (Pitcher & Calder 2000), most of the ecological harm results from the high biomass that they are able to achieve. After the collapse of high biomass blooms due to the exhaustion of available nutrients, the subsequent decay of bloom organisms sometimes leads to hypoxic events (Pitcher & Probyn 2016) that result in dramatic fatalities of marine organisms.

Aquaculture farming offers significant potential for rural development and economic advancement, especially in marginalised coastal communities. The advent of Operation Phakisa has provided significant stimulus for growing and transforming the aquaculture sector in South Africa. Implementing Operation Phakisa initiatives within the aquaculture sector has proved to be quite successful, providing employment to rural communities and increasing the overall South African aquaculture production, thereby generating considerably more revenue within the national economy. Currently aquaculture farming includes finfish, mussels, oysters, as well as the land-based farming of abalone. Globally South Africa was the third largest producer of farmed abalone in 2016 (Antoni, 2018). This sector of South African aquaculture farming presents the greatest potential for growth in the medium term because of the product's high market value, while also generating approximately one job for every ton of abalone produced (Kilian, 2016). Although there are 12 abalone farms along the coastline between Hondeklipbaai on the west coast and East London on the east coast, the heart of South Africa's abalone farming industry is found in Walker Bay. Land-based abalone farms circulate 1.2-1.5 million litres of seawater per hour and one of the biggest threats to production is posed by harmful algal blooms in the adjacent marine environment. In January 2017 Walker Bay was inundated by a large red tide that impacted 3 land-based abalone farms, causing the death of several million abalone and financial losses in excess of R50 million (Pitcher et al 2018). All the aquaculture industries are to some extent susceptible to the negative impact of red tides, whether directly through the assimilation of toxins, mechanical damage, or indirectly through the anoxia from bloom-collapse.

Seasonal occurrence of red tides is a common theme within the SBUS and their effects are felt from St Helena Bay on the west coast to Algoa Bay in the south-east. Red tides are most common during the latter part of the upwelling season, when the contribution of dinoflagellates to the phytoplankton community is greatest, due to the increased prevalence of prolonged periods of marine surface boundary layer stratification under low wind conditions (Pitcher et al 2010). Intermittent episodes of active coastal upwelling, followed by wind relaxation, result in distinctive SST patterns readily observed on satellite data. Alternating periods of surface layer instability and stratification not only determine patterns of phytoplankton succession, but also the subsequent translation and concentration of large blooms. Satellite-derived chlorophyll-a concentration (Chl-a) is a convenient proxy for near surface phytoplankton biomass. The Fisheries and Aquaculture DeST was specifically developed to provide information on useful indicators such as Chl-a and SST, at a high spatial resolution and low latency, to facilitate the early detection and subsequent monitoring of red tides, thereby informing decisive actions that diminish the harmful impacts associated with their occurrence. One of the fundamental strengths of the DeST is its use of regional algorithms developed by the CSIR to overcome the limitations inherent in SST declouding and Chl-a algorithms that were developed for global applications.

2.1. Data and methods

2.1.1. Benguela optimized MODIS SST

Daily nighttime and daytime Moderate Resolution Imaging Spectroradiometer (MODIS) Aqua and Terra level 2 SST data (R2014.0) covering the period 2003 to 2014 were acquired from NASA Goddard Space Flight Centre's Ocean Biology Processing Group (OBPG) website (https://oceancolor.gsfc.nasa.gov). Standard cloud flagging options for MODIS SST either removes too many valid ocean pixels (Figure 1b) or retains the pixels representing cloud edges (Figure 1c) (Du Fois et al 2012; Liu & Minnett 2016). The CSIR Earth Observation Group developed an SST cloud flagging procedure that reduces the impact of cloud edge pixels on single overpasses (Figure 1d). To improve the retrieval of valid SST data, each pixel was tested for validity by confirming that the absolute value of the difference between the measured SST value and a 5-day average of all available MODIS SST pixels at that location was within 1.5 times its climatology monthly standard deviation. Cloud presence is further reduced by generating daily averages of declouded single overpass scenes from both MODIS sensors using daytime and nighttime data (Figure 1e). The final product retains more SST pixels and accurately represents the physical phenomena in the Southern Benguela, while retaining the strong gradients associated with the edge of upwelling plumes and the Good Hope Jet Current (Figure 1f). This Benguela optimized SST was validated against the GHRSST Multi-scale Ultra-High Resolution SST product and *in situ* data. SLSTR data will be added to the Benguela SST product to maintain the time-series continuity.

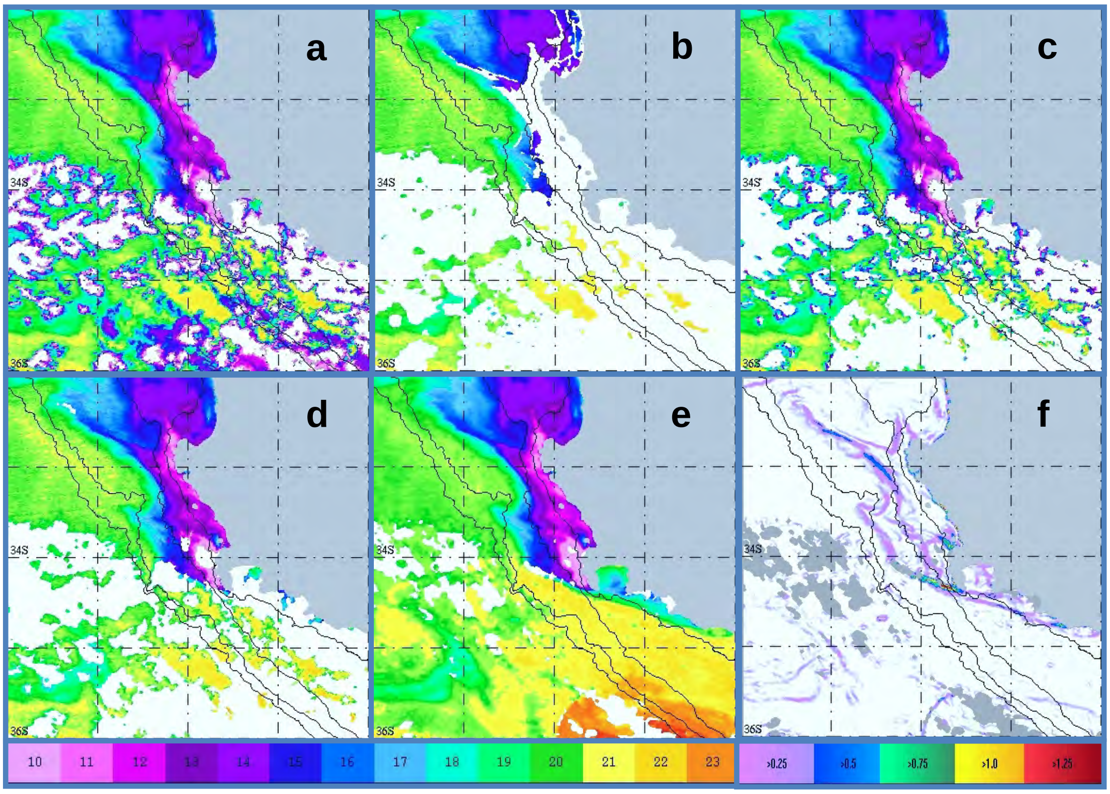

Figure 1: MODIS Aqua daytime SST images (a, b, c, d) of the SBUS (32°-36° S; 16°-20° E) for 28 January 2003 illustrating how different flagging procedures affect SST data retrieval. The daily average SST composite (e) and SST gradients (f) for the same region are also shown. The colour bar on the left represents SST from 10 °C to 23 °C and the colour bar on the right indicates gradient strength from 0.25 °C to 1.25 °C per kilometre.

2.1.2. Benguela optimized MODIS Chl-a

Level 2 MODIS Chl-a and normalized fluorescence line height (nFLH) products (R2014.0) for both Aqua and Terra covering the period 2003 to 2014 were acquired from the OBPG website. Under most conditions, any water leaving radiance contribution in the near infrared is considered as radiance contributed by aerosols and subsequently removed from the empirical blue-green MODIS Chl-a product (Siegel et al 2000). The removed Chl-a values are shown as flagged in Figure 2a. This assumption holds except in coastal environments with large reflectance contributions from surface sediments, or very high biomass biological blooms (Shanmugam & Tholkapiyan, 2013). Since the empirical Chl-a algorithm fails to produce an accurate result under high biomass conditions, it is necessary to switch to an alternate Chl-a retrieval algorithm when encountering these pixels. Satellite-derived FLH is mainly correlated with Chl-a through first-order linear functions at low Chl-a values, or power functions at higher Chl-a values (Huot et al 2005). The CSIR EO Group derived Chl-a from the MODIS nFLH product using a power function and used the result to develop a switching algorithm for MODIS to accurately track high biomass values associated with HABs (Figure 2b). Chl-a values for the switching algorithm were determined by retaining the MODIS OC3 algorithm for values ≤10mgm^{-3}, using the nFLH-derived Chl-a algorithm where OC3 values ≥30mgm^{-3} and a gradual blend from OC3 to nFLH-derived Chl-a from >10 mg·m^{-3} to <30 mg·m^{-3}. The Benguela Optimized MODIS Chl-a product showed increased pixel retrieval, reduced overestimation of Chl-a >10mg·m^{-3} and an improved correlation with higher biomass values when validated against *in situ* data.

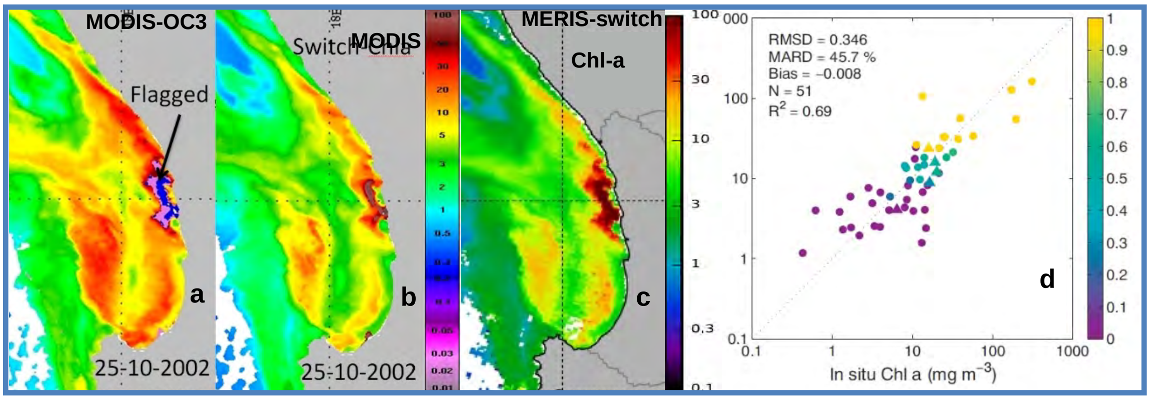

Figure 2: MODIS OC3 Chl-a (a), MODIS switch Chl-a (b) and MERIS switch Chl-a for 25 October 2002 in the SBUS (31°-34° S; 17°-19° E). The colour bars adjacent to the maps represent Chl-a in mg·m^{-3}. Scatterplot showing the relationship between in situ Chl-a and satellite-derived reflectance from MERIS (circles) and OLCI (triangles) (Smith et al. 2018). The colour bar indicates the weighting of the G2B algorithm.

2.1.3. Benguela optimized OLCI Chl-a

Reduced resolution level 2 ocean colour products for the Ocean and Land Colour Instrument (OLCI) instrument aboard the Sentinel-3A and Sentinel-3B satellites were obtained from the EUMETSAT Copernicus Online Data Access website (https://coda.eumetsat.int/). Medium Resolution Imaging Spectrometer (MERIS) reduced resolution level 2 ocean colour products were obtained from the MERIS Catalogue and Inventory website (https://merisrr-merci-ds.eo.esa.int/merci/welcome.do). The Empirical blue-green algorithms used to retrieve Chl-a for the MERIS and OLCI sensors present similar accuracy issues when high biomass pixels are encountered. The CSIR EO Group developed a novel technique to apply and blend two different Chl-a algorithms, an empirical blue-green algorithm for low to moderate biomass and a red-NIR band-ratio algorithm for moderate to high biomass. This blending method is based on the 708/665 nm reflectance wavelength ratio, where the blue-green algorithm is applied when the ratio is <0.75, the red-NIR algorithm is applied at values >1.15, whilst the two are blended between these values (Smith et al. 2018). Figure 2c illustrates that the MERIS switching algorithm is well-correlated with the MODIS switching algorithm. Perceived disparities in the images (Figure 2b and Figure 2c) are due to the slight differences in colour maps used in the visualization. The Benguela optimized MERIS/OLCI switching algorithm showed superior performance in the southern Benguela compared to any single algorithm when compared to *in situ* data (Figure 2d).

3. DISCUSSION

Although OCIMS supports the general socio-economic potential and ecological conservation of South Africa's oceans and coasts, the HAB DeST specifically provides information to the small scale fishers, aquaculture industry and environmental managers, allowing the timely implementation of appropriate mitigation steps. Risk assessment and monitoring are based on quantified understanding of bloom dynamics, hypoxic impacts and earth observation capabilities. The OCIMS tool is making a significant impact in several spheres of South Africa's Blue Economy management. In 2019 a large HAB in Walker Bay resulted in no mortalities due to improved farm mitigation measures, and information from the aquaculture and fisheries tool, on bloom location and operational planning.

4. GHRSST FEEDBACK

Jorge Vazquez noted that the work presented in this document illustrates the critical importance of reprocessing efforts of MODIS, VIIRS, etc. with improved cloud masking. He also agreed that appropriate SST and Chl-a products are critical for applications to coastal economic activities impacted by HABs. Ed Armstrong pointed out that the reprocessed V2019 MODIS SST data should show a significant improvement in cloud identification and that the MODIS Ocean Color parameters are scheduled for reprocessing in late 2020. He also suggested some more SST products to add to the daily average composite potential fisheries management applications that are being exploited by US research teams.

5. REFERENCES

Antoni, M-L., (2018). In South Africa, abalone farming goes for gold, *Global Aquaculture Advocate*, https://www.aquaculturealliance.org/advocate/south-africa-abalone-farming-goes-gold/

Dufois, F., Penven, P., Whittle, C.P., & Veitch, J., (2012). On the warm nearshore bias in Pathfinder monthly SST products over Eastern Boundary Upwelling Systems. *Ocean Modelling, 47,* 113-118.

Huot, Y., Brown, C.A., & Cullen, J.J., (2005). New algorithms for MODIS sun-induced chlorophyll fluorescence and a comparison with present data products. *Limnology and Oceanography: Methods, 3,* 108-130.

Kilian, A., (2016). Abalone Spearheading SA's Aquaculture Sector, *Engineering News*, https://www.engineeringnews.co.za/article/abalone-spearheading-sas-aquaculture-sector-2016-03-09

Liu, Y., & Minnett, P.J., (2016). Sampling errors in satellite-derived infrared sea surface temperatures. Part I: Global and regional MODIS fields. *Remote Sensing of Environment, 177,* 48-64.

Ndhlovu, A., Dhar, N., Garg, N., Xuma, T., Pitcher, G.C., Sym, S.D., & Durand, P.M., (2017). A red tide forming dinoflagellate *Prorocentrum triestinum*: identification, phylogeny and impacts on St Helena Bay, South Africa, *Phycologia*, *56:6,* 649-665, DOI: 10.2216/16-114.1

Pitcher, G.C., & Calder, D., (2000). Harmful algal blooms of the southern Benguela Current: a review and appraisal of monitoring from 1989 to 1997. *South African Journal of Marine Science, 22,* 255-271.

Pitcher, G.C., & Probyn, T.A., (2016). Suffocating Phytoplankton, Suffocating Waters - Red Tides and Anoxia. *Frontiers in Marine Science, 3:186*, DOI: 10.3389/fmars.2016.00186

Pitcher, G.C., Figueiras, F.G., Hickey, B.M., & Moita, M.T., (2010). The physical oceanography of upwelling systems and the development of harmful algal blooms. *Progress in Oceanography, 85*, 5-32, DOI: 10.1016/j.pocean.2010.02.002

Pitcher, G.C., Foord, C.J., Macey, B.M., Mansfield, L., Mouton, A., Smith, M., Osmond, S.J., & van der Molen, L., (2018). Devastating farmed abalone mortalities attributed to yessotoxin-producing dinoflagellates. *Harmful Algae, 81*, 30-41, DOI: 10.1016/j.hal.2018.11.006

Shanmugam, P., (2012). CAAS: an atmospheric correction algorithm for the remote sensing of complex waters. *Annales Geophysicae, 30,* 203-220; doi: 10.5194/angeo-30-203-2012.

Siegel, D.A., Wang, G.M., Maritorena, S., & Robinson, W., (2000). Atmospheric correction of satellite ocean colour imagery: the black pixel assumption. *Applied Optics, 39,* 3582-3591.

Smith, M.E., Robertson Lain, L., & Bernard, S., (2018). An optimized chlorphyll a switching algorithm for MERIS and OLCI in phytoplankton-dominated waters. *Remote Sensing of Environment, 215,* 217-227, DOI: 10.1016/j.rse.2018.06.002

Van Wyk, J-A., (2015). Defining the blue economy as a South African strategic priority: toward a sustainable 10th province?. *Journal of the Indian Ocean Region, 11:2,* 153-169, DOI: 10.1080/19480881.2015.1066555

S5-3: MULTI-DECADAL EXAMINATION OF THERMAL HABITAT SUITABILITY FOR THE ENDANGERED DELTA SMELT IN THE SAN FRANCISCO ESTUARY USING LANDSAT 5, 7, AND 8

Gregory Halverson(1), **Christine Lee**(1), **Glynn Hulley**(1), **Erin Hestir**(3), **Kerry-Anne Cawse-Nicholson**(1), **Brian Bergamaschi**(5), **Brenden Palmieri**(2), **Amye Osti**(2), **Shawn Acuña**(4), **Nick Tufillaro**(6), **Robert Radocinski**(1), **Gerardo Rivera**(1), **Christiana Ade**(3), **Ted Sommer**(7)

(1) NASA Jet Propulsion Laboratory, California Institute of Technology
Email: gregory.h.halverson@jpl.nasa.gov
(2) 34 North, Metropolitan Water District of Southern California
(3) University of California, Merced
(4) Metropolitan Water District of Southern California,
(5) United States Geological Survey,
(6) Oregon State University,
(7) California Department of Water Resources

SHORT ABSTRACT

This study uses Landsat 5, 7, and 8 to examine trends in water surface temperature spanning 1984-2018, relative to the thermal tolerance of the endangered Delta Smelt (*Hypomesus transpacificus*) and two non-native fish, the Largemouth Bass (*Micropterus salmoides*) and Mississippi Silverside (*Menidia beryllina*). The accuracy of the Landsat water surface temperature (WST) products were validated using two *in situ* stations instrumented with thermal radiometers on Lake Tahoe and the Salton Sea (ρ = 0.98, R^2 = 0.96, p < 1%, n = 1849) with a bias of -0.03 from 1999-2018. Thermally unsuitable habitat, defined as WST pixels exceeding critical thermal maximum for each species, were assessed for each Landsat acquisition, compared inter-annually by maximum. This study found that the changes in area deemed thermally unsuitable for the Delta Smelt increased at the fastest rate (2.2 $km^2 \cdot yr^{-1}$) in comparison to the Largemouth Bass (0.48 $km^2 \cdot yr^{-1}$) and Mississippi Silverside (0.3 $km^2 \cdot yr^{-1}$), underscoring that these non-native species are currently advantaged in habitat conditions that are getting warmer. This study also observes a statistically significant (p < 1%) inverse relationship between increases in thermal maximum surface area and decreases in the smelt abundance index derived from the CA Department of Water Resources Fall Midwater Trawl (ρ = -0.75, R^2 = 0.55, p < 1%, n = 33). These findings provide a potential metric for leveraging remote sensing information as a first order proxy for thermal habitat suitability in support of management and restoration actions.

Article submitted for publication

S5-4: ON THE USE OF SEA SURFACE TEMPERATURE (SST) FOR IMPROVING THE ALTIMETER DERIVED SURFACE CURRENTS: A SENSITIVITY STUDY TO SST PRODUCTS

Daniele Ciani[(1)], Marie-Hélène Rio[(2)], Bruno Buongiorno Nardelli[(3)], Salvatore Marullo[(4)], Hélène Etienne[(5)] and Rosalia Santoleri[(1)]

(1) Consiglio Nazionale delle Ricerche, Istituto di Scienze Marine, Rome, Italy
Email: D.Ciani daniele.ciani@cnr.it, R. Santoleri: rosalia.santoleri@cnr.it
(2) European Space Agency, European Space Research Institute, Frascati, Italy
Email: Marie-Helene.Rio@esa.int
(3) Consiglio Nazionale delle Ricerche, Istituto di Scienze Marine, Naples, Italy
Email: bruno.buongiornonardelli@cnr.it
(4) Agenzia Nazionale per le Nuove Tecnologie, l'Energia e lo Sviluppo Economico Sostenibile, Frascati, Italy
Email: salvatore.marullo@enea.it
(5) Collecte Localisation Satellites, Ramonville St-Agne, France. Email: hetienne@groupcls.com

1. INTRODUCTION

Oceanic currents are a key factor in modulating both the short-term and climatological dynamics of the ocean-atmosphere system. At large scale, their monitoring is needed to evaluate the meridional transport of heat and salt and better predict ocean thermohaline circulation variability and changes. At the oceanic meso- to sub-mesoscales, the characterization of the marine currents is also crucial. Mesoscale eddies are non-stationary and energetic recirculation features with horizontal scales of 10 to 100 km and can persist on timescales of weeks to months. They can migrate for several miles carrying heat, salt and nutrients, and their perturbations can drive intense vertical exchanges. Submesoscale features like eddies, fronts and filaments are characterized by spatial-temporal scales of 0.1 to 10 km and hours to days. Such small-scale, short-lived features can also generate significant heterogeneities in both horizontal and vertical velocities, affecting the local 3D transport properties. At the sea surface, the ocean current monitoring also serves several societal and environmental applications, including ship routing, safety and rescue activities and the monitoring of floating pollutants like oil slicks and plastic debris. All these applications necessitate an accurate, high spatial-temporal resolution monitoring of the upper layer oceanic currents. Since the early 1990s, radar altimeters onboard satellites have been providing indirect measures of the marine surface circulation at global scale (*Cazenave et al. 2018*). This is achieved by measuring the Sea Surface Height (SSH) relative to an equipotential surface (the so called geoid) and inferring the surface motion via the geostrophic approximation (*Vallis 2006*). This system has intrinsic limitations related to the sampling of SSH and to the approximation considered in the retrieval. Indeed, only larger mesoscale geostrophic processes can be described with this approach. Recently, *Rio and Santoleri 2018* (RS18 hereinafter) implemented an optimal combination of altimeter-derived geostrophic currents and higher resolution gap-free (Level 4, L4 hereinafter) SST data. The RS18 method, based on the theoretical and numerical studies of *Piterbarg 2009*, accounts for the source/sink terms of the SST evolution equation, related to the large scale interactions with the atmospheric boundary layer. RS18 showed that the dynamical information contained in SST data can be transferred into the geostrophic current field and enhance its effective spatial-temporal resolution. This was achieved by combining the global geostrophic currents distributed by the Copernicus Marine Environment Monitoring Service (CMEMS) with the global L4 SST data provided by REmote Sensing Systems (REMSS). The authors noted an improvement in most of the ocean, with the exception of the Southern Ocean, where the optimal combination of SST and geostrophic currents actually made ocean current retrievals worse.

With the aim of further investigating the optimal combination proposed by RS18, we tested the impact of using different SST data to reconstruct the global surface currents. RS18 relied on REMSS SST data (1/10° resolution), uniquely based on Infrared and Microwave Satellite observations. In the present study, we tested both the CMEMS OSTIA (1/20° resolution), and the Multiscale Ultra-High resolution SST (1/100° resolution), both relying on the interpolation of several satellite and *in situ* SST observations. We focused on the period ranging from 2014 to 2016, which yielded more accurate surface current reconstructions in RS18.

2. DATA AND METHODS

The following datasets were used in our study, all covering the period ranging from 2014 to 2016:

- The altimeter-derived sea surface currents computed at Collecte Localisation Satellites in the framework of the DUACS project and distributed by the CMEMS Sea Level Thematic Assembly Center: two different products were used, referred to as "2SAT" and "4SAT". Both products are gridded data provided on a regular 1/4° grid. The 2SAT product is calculated merging observations from two altimeters: Jason-2 and AltiKa, with Jason 3 only from March 2016. The 4SAT product is obtained using a four altimeters constellation: Jason-2(3), Cryosat, Altika and HY-2A. The 4SAT dataset can be seen as the best altimeter-derived surface current estimate in the 2014-2016 period. On the other hand, the 2SAT version is less accurate, being based on observations from only two altimeters like for the altimeter-derived currents of the early altimetry era (the early 1990s).

- The SST daily observations from the REMSS processing centre: we used the high resolution product based on the combination of microwave (from TMI, AMSR-E, AMSR2, WindSat and GMI) and infrared (Terra MODIS, Aqua MODIS, VIIRS) data. These SST observations are corrected using a diurnal model and represent a foundation SST (≃10 m depth). These data are calculated using an Optimal Interpolation scheme with 100 km and 4 days correlation scales and are provided on a ≃1/10° regular grid (http://www.remss.com);

- The SST daily observations from the Operational Sea Surface Temperature and Sea Ice Analysis (OSTIA) system: OSTIA uses satellite data including AMSR-E, AVHRR (GAC+LAC), IASI, SEVIRI, TMI, GOES, SSMIS, SSM/I sensors together with *in situ* observations to determine the sea surface temperature. The analysis is produced daily and is provided on a 1/20° regular grid;

- The Multiscale Ultra-high Resolution global SST analyses (MUR): such SST dataset relies on high and low resolution satellite observations in the microwave and infrared bands (e.g. from AMSR-E, AMSR-2, WindSat, AVHRR, MODIS). The satellite data are also merged with *in situ* SST estimates via a Multiresolution Variational Analysis Method (Chin et al. 2012). The analysis is produced daily and is provided on a 1/100° regular grid;

- The *in situ* derived sea surface currents (at 15 m depth) measured by SVP-type drogued drifting buoys: Such quality-controlled, six-hourly data are available from the NOAA AOML Surface Drifter Data Assembly Center (https://www.aoml.noaa.gov/phod/gdp/).

We reconstruct the oceanic surface currents relying on an optimized blending of coarse-resolution geostrophic currents from altimetry measurements and higher resolution multi-sensor SST products. These currents will be hereinafter referred to as optimal currents (OPC). The method rationale and theoretical background is described in *Piterbarg 2009* and its application to satellite derived data is thoroughly described in *Rio et al. 2016*, *Rio and Santoleri 20*18 and *Ciani et al. 2019* on both on global and regional scales. The sea surface currents are inferred from the SST dynamical evolution equation:

$$\frac{\partial SST}{\partial t} + u\frac{\partial SST}{\partial x} + v\frac{\partial SST}{\partial y} = F \quad (1)$$

In Equation (1), u and v are respectively the zonal and meridional components of the ocean surface flow, x and y are the zonal and the meridional directions and F is the forcing term, representing the source and sink terms for the SST dynamical evolution equation (that we approximate as a low-pass filtered SST temporal gradient). *Piterbarg 2009* derived the expressions of an optimized flow field accounting for the merged contribution of a large-scale, background flow with the dynamical information contained in high-resolution tracers.

If the background flow is given by the geostrophic currents and the high-resolution tracer by SST, the optimized zonal and meridional flows can be expressed by Equation (2):

$$\begin{aligned} u_{OPC} &= u_{GEO} - \frac{A(Au_{GEO} + Bv_{GEO} + E)}{A^2 + B^2} = u_{GEO} + u_{CORR} \\ v_{OPC} &= v_{GEO} - \frac{B(Au_{GEO} + Bv_{GEO} + E)}{A^2 + B^2} = v_{GEO} + v_{CORR} \end{aligned} \quad (2)$$

where the subscript (GEO/OPC) stand for (geostrophic/optimal current), A=∂xSST, B=∂ySST, E=∂tSST- F. Equation (2) expresses the *Piterbarg 2009* method rationale: the geostrophic currents are corrected by means of a factor (Ucorr, Vcorr) depending on the spatio-temporal derivatives of the high-resolution tracer observations and on the forcing term (F) regulating the tracer dynamical evolution.

3. RESULTS AND CONCLUSIONS

Based on three years (2014-2016) of daily global-scale OPC, we evaluate their improvements with respect to the altimeter-derived geostrophic (GEO) currents via the percentage of improvement (PI) index, expressed by (3).

$$PI_{U,V} = 100\left[1 - \left(\frac{RMSE_{U,V}^{OPC}}{RMSE_{U,V}^{GEO}}\right)^2\right] \quad (3)$$

In Equation (3) the subscripts U, V stand for zonal and meridional PI, respectively. The Root Mean Square Error (RMSE)OPC/GEO computation relies on the knowledge of a reference surface current, provided by the SVP drifters estimates detailed in Section 2. The PI regional variability (computed in 20° x 20° boxes) is depicted in Figure 1a-c.

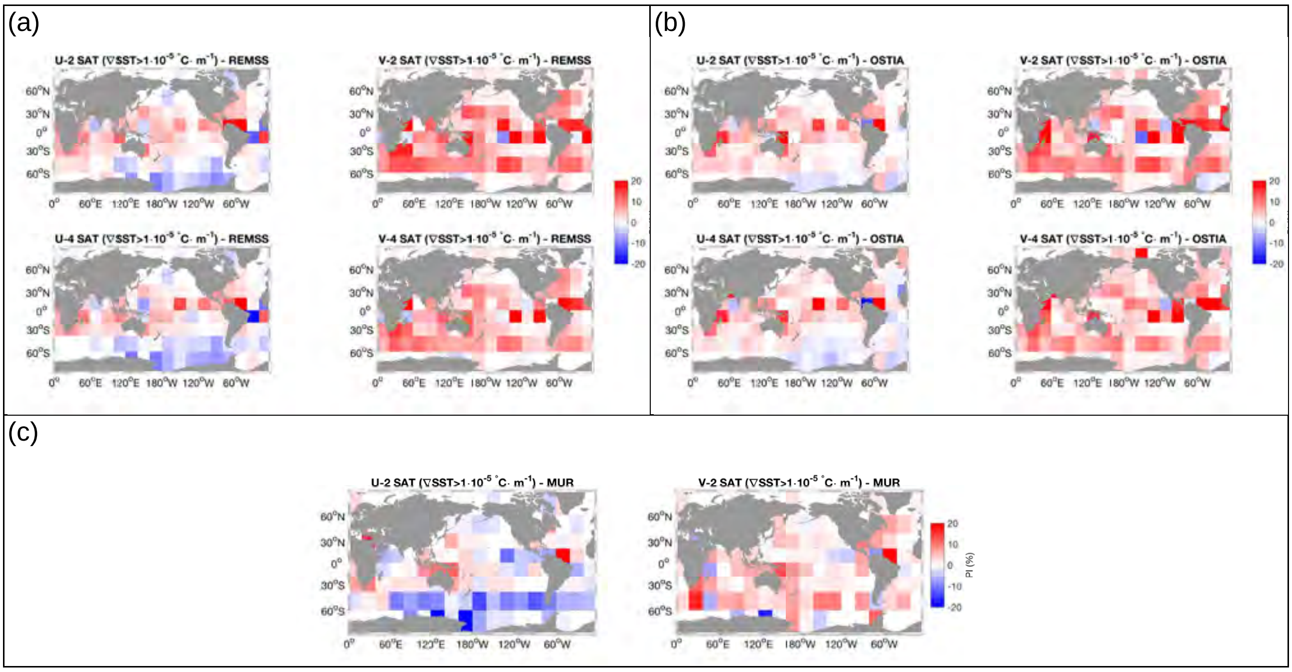

Figure 1: PI (binned in 20° × 20° boxes) of the OPC with respect to the geostrophic estimates (over 2014-2016). (a) OPC based on the DUACS "2SAT/4SAT" currents. Bottom row: Optimal currents based on the DUACS "4SAT" currents. The input SST is provided by REMSS. U and V stand for zonal and meridional currents, respectively. (b) Same as (a) but with the OSTIA SST. (c) Same as (a) but with the MUR SST (only the 2SAT case is presented).

The **OPC computed using the REMSS data** exhibit a PI exceeding 20% (up to 24% locally), with better performances for the meridional component of the motion and in the equatorial band. The results indicate that our method is more efficient when applied to low-quality altimetry products, as for the 2SAT case (see also *Pascual et al. 2006*). However, still in agreement with RS18,

Figure 1Figure 1 shows that even the 4SAT geostrophic currents do benefit from the optimal combination with SST. Indeed, local maximum improvements range from 10 to 20% in the equatorial band for both the zonal and the meridional currents. Therefore, combining the altimeter-derived currents with SST data is advantageous for both altimetry products based on information from two altimeters (like in the early altimetry era) and more recent versions combining observations from several altimeters. However, as previously emphasized by RS18, the optimal reconstruction of zonal ocean currents exhibits poor performance in high latitudes, as indicated by negative PIs that can reach -10%.

*The overall performances of the **OSTIA OPC** are consistent with the reconstructions obtained with the REMSS SST, shown in Figure*

Figure 11b. The regional variability of the PI is analogous, indicating that the optimal reconstruction brings larger benefits for the 2SAT case, particularly for the meridional component of the currents and in the equatorial band. The maximum improvements are smaller than for the REMSS OPC (mostly due to the smoother L4 SST analysis yielding smoother SST gradients than in the REMSS case). However, the degradation of the OSTIA zonal OPC in the Southern Ocean is reduced. We hypothesised this is due to the higher OSTIA SST (and SST gradients) quality at high-latitudes compared to the REMSS SST products. The OSTIA product relies on a larger number of input satellite SST estimates in the optimal interpolation algorithm, also including *in situ* SST observations, enabling higher quality SST retrievals in high-latitude areas (characterised by high cloud cover).

The **OPC derived from the MUR SSTs** are here presented for the 2SAT case (the 4SAT case is analogous). The MUR OPC showed reduced performances than in the REMSS and OSTIA cases. This is evident from Figure 1c. The zonal degradation area found at high latitudes is even more evident than in the REMSS-based optimal reconstruction. The zonal OPC are degraded compared to the Altimeter currents below 45°S as well as in the equatorial Pacific and Indian Oceans. This unexpected behaviour was caused by some inhomogeneities in the MUR L4 SST spatial gradients. Indeed, the MUR SSTs rely on the Multiresolution Variational Analysis algorithm (Chin et al. 2012), allowing to capture very fine resolution SSTs when high-resolution satellite infrared measurements are permitted (in clear sky conditions). Otherwise, only lower resolution SST estimates are used (e.g. microwave SSTs). As a result, the MUR L4 SSTs exhibited unequal effective spatial resolutions in adjacent areas of the ocean. This issue affected the computation of the correction factors for the geostrophic currents appearing in Equation 2. However, the MUR SSTs provided the best OPC estimates when the high SST resolution was achieved over extended time-periods (for example this was found in the Agulhas current retroflection area).

Concluding, the optimal combination of altimeter-derived currents and SST is a promising technique to improve the space-based retrieval of the marine surface currents at global scale, also providing an indirect validation framework to test the dynamical content of the L4 SST operational products. Our investigation revealed that the homogeneity of the input SST effective spatial resolution is the crucial requirement for an accurate surface currents reconstruction. In our analyses, this condition was best satisfied by the lower resolution L4 SST products (REMSS and OSTIA). Future satellite missions, like the ESA-Copernicus Imaging Microwave Radiometer will bring large benefits for the global SST observations and will certainly improve the quality of the L4 SST analyses, further enhancing the homogeneity of their spatial resolutions.

4. REFERENCES

Ballarotta, M.; Ubelmann, C.; Pujol, M.I.; Taburet, G.; Fournier, F.; Legeais, J.F.; Faugère, Y.; Delepoulle, A.; Chelton, D.; Dibarboure, G.; others. On the resolutions of ocean altimetry maps. *Ocean Science* 2019, *15*, 1091–1109

Cazenave, A.; Palanisamy, H.; Ablain, M. Contemporary sea level changes from satellite altimetry: What have we learned? What are the new challenges? Advances in Space Research 2018, 62, 1639–1653

Chin, T.M.; Vazquez-Cuervo, J.; Armstrong, E.M. A multi-scale high-resolution analysis of global sea surface temperature. Remote Sensing of Environment 2017, 200, 154–169.

Ciani, D.; Rio, M.H.; Menna, M.; Santoleri, R. A Synergetic Approach for the Space-Based Sea Surface Currents Retrieval in the Mediterranean Sea. *Remote Sensing* 2019, *11*, 1285.

Ciani, D.; Rio, M.-H.; Nardelli, B.B.; Etienne, H.; Santoleri, R. Improving the Altimeter-Derived Surface Currents Using Sea Surface Temperature (SST) Data: A Sensitivity Study to SST Products. Remote Sens. 2020, 12, 1601.

Pascual, A.; Faugère, Y.; Larnicol, G.; Le Traon, P.Y. Improved description of the ocean mesoscale variability by combining four satellite altimeters. Geophysical Research Letters 2006, 33.

Rio, M.H.; Santoleri, R.; Bourdalle-Badie, R.; Griffa, A.; Piterbarg, L.; Taburet, G. Improving the Altimeter-Derived Surface Currents Using High-Resolution Sea Surface Temperature Data: A Feasability Study Based on Model Outputs. Journal of Atmospheric and Oceanic Technology 2016, 33, 2769–2784.

Rio, M.H.; Santoleri, R. Improved global surface currents from the merging of altimetry and Sea Surface Temperature data. Remote Sensing of Environment 2018.

Vallis, G.K. Atmospheric and Oceanic Fluid Dynamics; Cambridge University Press: Cambridge, U.K., 2006; p. 745.

S5 - POSTER PRESENTATIONS - SHORT ABSTRACTS

S5-P1: NOAA'S OCEAN HEAT CONTENT SUITE FOR THE INDIAN OCEAN

Eileen Maturi[(1)], David Donahue[(1)]

(1) NOAA/NESDIS/STAR, NCWCP, COLLEGE Park, Maryland, 20740, USA
Email: Eileen.Maturi@noaa.gov

SHORT ABSTRACT

Very strong tropical cyclones (TC) occur in the Indian Ocean and an Ocean Heat Content (OHC) product has been proven essential for improving TC intensity forecasts and predicting coral bleaching events.

The OHC is a measure of the amount of heat energy (in units of $kJ \cdot cm^{-2}$) available to a tropical cyclone. This heat energy can be transferred to the lower atmosphere through sensible and latent heat fluxes. As moist air rises in a tropical cyclone, the condensation process that generates clouds and precipitation releases a tremendous amount of latent heat within the storm.

Two ingredients that are necessary for the development and maintenance of tropical cyclones are favourable wind conditions aloft and sufficiently warm water (27 ºC) which is captured by the 5 km Geo-Polar Blended SST Analysis a primary input to the generation of this product..

The OHC product is evaluated and valid for the entire year so we can understand the relationship between weather phenomena and the upper ocean OHC, such as the Madden-Julian oscillation and the Indian Ocean Dipole. There are important teleconnections between all ocean basins that will help us understand the weather patterns between the various basins.

S5-P2: ADDRESS TROPICAL CLIMATE VARIABILITY WITH NEURAL NETWORK MODELS

Francesca Elisa Leonelli[1,3], **Chunxue Yang**[1], **Salvatore Marullo**[2,1], **Andrea Pisano**[1], **Camillo Cammarota**[3],

(1) Istituto delle Scienze Marine- Consiglio Nazionale delle Ricerche (ISMAR-CNR)
(2) Agenzia nazionale per le nuove tecnologie, l'energia e lo sviluppo economico sostenibile (ENEA)
(3) Department of Mathematics, University of Rome "La Sapienza", Rome Italy
Email: francesca.leonelli@artov.ismar.cnr.it

SHORT ABSTRACT

Non-Linear Principal Component Analysis (NLPCA), as one type of Neural Network model, is an autoencoder equipped with a bottleneck layer and its role is to achieve dimension reduction to identify dominant processes. This method enriches classical PCA technique with the ability to extract nonlinear structures of processes in the data. NLPCA has been used in climate science, for example to analyse the most dominant interannual climate variability, the El Niño Southern Oscillation (ENSO) which is a non-linear atmosphere-ocean coupled processes.

Our objective is to evaluate the method capabilities by applying NLPCA to investigate the tropical climate variability patterns including ENSO, Indian Ocean Dipole (IOD) and Atlantic Modes (Atlantic Niño). The advantage of NLPCA will be investigated by comparing the representation of climate variabilities analysed with traditional PCA method. The data we use is an ensemble of five different Sea Surface Temperature (SST) satellite based products covering the period from 1982-2017.

Preliminary results show that the first leading mode of the linear PCA is in phase with ENSO in all SST products and the asymmetry characteristics of El Niño and La Niña events are well presented. Additionally, the comparison between PCA and NLPCA shows that the first leading mode, representing ENSO in NLPCA, explains larger variance than that in PCA, illustrating the nonlinearity of ENSO processes. As the most prominent and influential climate variability, ENSO has been well studied, however, the climate variability in other tropical oceans (Indian and Atlantic Oceans) plays an important role in global climate as well. The next step will be to apply both PCA and NLPCA methods in tropical Indian and Atlantic Oceans to investigate the nonlinearity of Indian Ocean Dipole and Atlantic mode. The final results covering the whole tropical regions, especially the advantage of NLPCA, will be presented during the meeting.

S5-P3: THE MEDITERRANEAN, ALMOST 40 YEARS OF CONTINUED WARMING

Francisco Pastor[(1)], J.A. Valiente[(1)], S. Khodayar[(1)]

(1) Fundación CAM, Paterna, Valencia, Spain
Email address: paco@ceam.es

SHORT ABSTRACT

The Mediterranean, especially its western basin, presents geographic and atmospheric characteristics making up a unique climatic and meteorological regime; having been classified as a hot spot for climate change. In this singular setting, the Mediterranean Sea plays a fundamental regulatory role in the climatology and meteorology of the area. Therefore, it is of great interest to study sea surface temperature, as well as its historical trend to analyse future climate scenarios. To this end, the largest available time series (1982-2019) of satellite data, with full coverage of the Mediterranean, has been studied to build an SST monthly climatology and trend analysis.

From the satellite data for 4248 regularly distributed points over the Mediterranean basin, daily temperature series have been constructed and its seasonally adjusted component has been evaluated. After this deseasonalization, a consistent warming trend of the sea surface temperature has been obtained during the analysis period. The way in which this heating has occurred has also been analysed finding that, for the global Mediterranean averaged temperature series, not only higher maximum temperature values have been recorded in recent years but, especially, that a higher frequency of high or relatively high daily values has been recorded. This reinforces the consistency of the temperature increase since it is not only based on the presence of more extreme values but on a homogeneous increase of high sea temperature records. In addition, there has also been an increase in the range of sea temperature values due to a greater relative growth of the maximum summer values compared to that recorded for winter minimums.

TASK TEAMS SESSION REPORTS

TASK TEAMS SESSION 1

Chair: Charlie Barron[(1)]

Co-Chairs: Misako Kachi[(2)], Craig Donlon[(3)]

(1) U.S. Naval Research Laboratory, USA Email: charlie.barron@nrlssc.navy.mil
(2) Japan Aerospace Exploration Agency, Japan Email: zpghrtts@ml.jaxa.jp
(3) European Space Agency, Noordwijk, Netherlands Email: craig.donlon@esa.int

ABSTRACT

The session featured five reports from GHRSST Task Teams

Summary of Presenters and Topics

1. TTS1-1 – Cloud Masking – Chris Merchant
2. TTS1-2 – Regional and Global Task Sharing– Jean-François Piollé
3. TTS1-3 – Single Sensor Error Statistics and L4 – Andy Harris
4. TTS1-4 – Pixel to Pixel Uncertainty – Peter Cornillion
5. TTS1-5 – Coral Heat Stress – User Needs – William Skirving

1. SUMMARY OF PRESENTATIONS

The highlights for each presentation and discussion are given below.

1.1. TTS1-1 Cloud Masking – *Chris Merchant*

Summary of activity from the Cloud Masking Task Team:
Chair: Chris Merchant

Aims for GHRSST XXI

- Establish membership
- Initiate two themes for collaborative action over next 12-18 months
- Collect proposals for other themes to pursue

Theme 1: Cloud masking in and near coastal boundaries (proposed: Chris Merchant)

- Issues associated SST within a few km of land
- Increased spatial variability of SST
- In some cases warmer than ambient SST of neighbourhood slightly farther offshore
- In some cases has elevated clear-sky reflectance due to shallows or suspended matter
- Uncertainty associated with pixels that partially impinge on land
- Consequence is that cloud mask within few km of land tends to be overly conservative
- Many SST users have a particular interest nearest the shore and are don't like excessive flagging of observations
- If valid SST near land are overly masked and SST nearest land are warm relative to offshore, the resulting sampling bias leads to a cold bias in the area average SST

- Invite participation of anyone who is active in this area of research

Theme 2: Cloud mask validation (proposed: Yukio Kurihara)

- How can we validate whether changes in cloud masking bring improvement?
- Various evaluation methods have different levels of objectivity and effort required
- SST validation statistics (outliers, asymmetry, etc.)
- Cross-comparison between cloud masks
- Comparison to expert-screened masks
- Comparison to cloud-mission data (A train)
- Comparison to ground-based cloud information
- Invite participation of anyone who is active in this area of research to work together, share ideas to make cloud masking easier and more informative

Confirm interest in participating in this task team by email: c.j.merchant@reading.ac.uk

Invitation for self-nomination by any interesting in co-chairing cloud masking task team (same address)

1.2. TTS1-2 Regional and Global Task Sharing– *Jean-François Piollé*

Summary of activity from the Regional and Global Task Sharing Task Team:
Co-chairs Jean-François Piollé, Ed Armstrong

Team has refined the system for data discovery, search, and access using a centralized catalogue with search relayed to subservices hosted by each DAC

Team activity

- Regular teleconferences
- Pilot project demonstrating central catalogue, federated query based on OpenSearch
- Released system architecture document
- Conducted survey of DACs and Producers

Conducted survey of DACs and Producers

- Assess readiness to implement task sharing system
- PO.DAAC, NOAA/NODC, NOAA/STAR, Eumetsat, JAXA, Ifremer, CNR, NAVO, ABoM, DMI, CMEMS (include point of contact)

Level of readiness – central catalogue

- Agree to maintain metadata description in central catalogue
- 5 of 7 provide OGC compliant catalogue or metadata
- No major implantation or operation issues

Level of readiness – data access for DACs

- HTTP(S) is mandatory
    - 5 of 7 provide already
    - One can implement at some point
    - One cannot implement, does provide FTP
- FTP strongly recommended

    - 3 provide
- HTTP(S) and/or FTP available for all DACs already
- OPeNDAP or THREDDS recommended
    - Provided by 3 DACs
    - Especially useful for L3/L4 products

Level of readiness – granule search (OpenSearch)
- 3 DACs provide
- 2 plan implementation in next 2 years
- This is the most complex service element to provide
- None of the existing services follow the same API; federated search at central level makes sense under these conditions, translating query to be compatible with different API

Items for discussion
- Review discussion
- Roadmap for implementation
- Issues with implementation
    - OpenSearch
        - Work-around solutions
        - Available software

1.3. TTS1-3 Single Sensor Error Statistics and L4 – *Andy Harris*

Summary of activity from the Single Sensor Error Statistics and L4 Task Team:
Co-chairs: Andy Harris, Simon Good

Raison d'être
- SSES and LF have been under consideration by the GHRSST Science Team for several years
    - in various forms
    - sporadic progress
- SSES represent the primary scientific "value-added" component of the GHRSST L2P products
    - Appropriate use in L4 products should lead to improved SST analyses
- Consideration in a task team framework can refocus efforts
    - Start with list of initial goals and questions

Main goals and questions
- Establish utility of current SSES (bias, SD)
    - Are they useful?
        - What metrics establish utility?
    - Which ones are most useful?
        - Evaluate differences in methods employed by various data providers, sensors
    - Make recommendations to data providers regarding methods
        - Which schemes work well, which don't
- How best to use current SSES?
    - Variations is usefulness under different analysis schemes
    - Why SSES have different impacts in different schemes
    - Recommendations to L4 producers as how to best employ SSES

- Forum on future evolution of SSES
    - How L2 providers might calculate correlated errors
    - How L4 producers might use correlated errors
    - How to remove dependence on drifting buoys and obtain properly representative uncertainties that are appropriate for assimilation into L4

Proposed experiments
- Time periods: Dec 2016 - Feb 2017 and June 2017 – Aug 2017
    - Spin-up as deemed appropriate by individual L4 producers
- Baseline experiments (subject to inputs used by the L4 producers)
    - Control using standard provider setup
    - No SSES provided (bias 0, fixed SD per sensor)
    - With bias (fixed SD)
    - With SD (0 bias)
    - With SD and bias
    - Example of OSTIA experimental results (Simon Good)
- Further experiments
    - Only use SSES for some sensors (the reference sensor)
    - Run with doubled and halved SSES SD
- Request that L2/3 providers provide information on how SSES are calculated

Next steps
- Agree on datasets
    - Perhaps not all providers use all datasets or use L3U vs L2P
    - Report improvements relative to individual baseline configurations
- Agree on metrics
    - Comparison with (e.g., Argo)
    - Question of independence
- Agree on timeline
    - Obtaining data, running experiments
- Intercommunication
    - Email exchanges, telcons/WebEx, workshop
        - Discuss results and refine experiments
        - Report findings next GHRSST meeting
    - COVID-19 remote working practices may facilitate virtual collaboration
    - Use EUMETSAT Moodle pages to facilitate collaboration

Participants
- L4 Providers
- L2/L3 providers

1.4. TTS1-4 Pixel to Pixel Uncertainty – *Peter Cornillon*

Summary of activity from the Pixel to Pixel Uncertainty Task Team:
Chair: Peter Cornillon

Task Team Members

Objective: address issues relating to the uncertainty of satellite-derived SST fields as it relates to the study of oceanographic features

Oceanographic features
- Currents, fronts, eddies, gradients, …
- Mesoscale and smaller, <O(100 km)
- Defined by **differences** in SST over spatial values of interest

The uncertainty in the **differences** in SST values over spatial scales is critical to these studies
- Absolute uncertainty of SST values is of lesser importance
- To date the SST community has been more focused on the latter uncertainty
- This task team focuses on the former uncertainty

Tasks
- Classifying of the types of problems contributing to these uncertainties
- Identifying of the ‘effects’ giving rise to these problems
- Outlining approaches to quantify the uncertainties of interest
    - Error propagation, a metrological approach propagating errors through the processing steps
    - Uncertainty determined from the variance of the SST fields themselves

1.5. TTS1-5 Coral Heat Stress – *William Skirving*

Summary of activity from the Coral Heat Stress Task Team:
Co Chairs William Skirving, Jonathan Mittaz, Craig Steinberg

Task Team members

Importance of coral reefs
- Coral reefs are more biodiverse than tropical rainforests
    - Coral reefs cover <1% of the world’s oceans
    - Coral reefs contain >25% of the ocean’s total species
- Coral reefs are the number one source of new medicines
    - Surpassed tropical rainforests over a decade ago
    - Key for possible cures for cancer, arthritis, bacterial infections, viruses, other diseases
- Coral reefs provide services vital to societies and industry
    - Globally, 0.5-1. billion people depend on healthy reefs for food, coastal protection, livelihoods
    - The value of these services is estimated to be US$10 trillion

Heat stress causes coral bleaching
- Mass coral bleaching as a result of climate change is main threat to global reefs
- Corals live in an symbiotic relationship with algae
    - Corals rely on algae for energy derived from photosynthesis
    - When temperatures reach 1°C above expected summer maximum, this symbiotic relationship becomes stressed

- Once enough heat stress is accumulated, the relationship breaks down and the algae are ejected from the coral host (called coral bleaching)
- If a coral remains bleached for long enough, it will eventually die
- Examples
  - American Samoa, 2014-2015
  - Jarvis Island, 2015-2016, 98% dead

GHRSST Coral Heat Stress Task Team Objectives

- Provide expert advice and recommendations to the GHRSST community on the satellite SST requirements for quantifying and monitoring the effects of heat stress on coral health

Coral Heat Stress SST recommendations regarding satellite SST data

- Stability through time
  - All coral heat stress products are anomaly based
  - Climatologies need to be set as far back as possible (early 1980s)
  - Need temporal stability of SST bias in SST time series
    - drift no worse than 0.05°C per decade
- Accuracy of geo-location
  - Many coral reefs close to coasts
  - SST over reef is typically cooler than nearby deep water during heat stress event
  - Need accurate geolocation, footprint shape of heat stress event
  - Avoid over-zealous land masking; users can apply own mask
  - Example Great Barrier Reef 2020
- Level 3 vs level 4 SST products
  - Heat stress is cumulative
  - Need SST to be temporally and spatially continuous
  - Level 4 SST is product of choice
- Daily average vs diurnal variability
  - Currently no ability to account for diurnal variability in heat stress calculations
  - Presently need single daily average SST
    - Based on night-time only SST or include diurnally corrected daytime SST
- Radiometric accuracy and spatial/temporal resolution
  - Accuracy of 0.2°C per pixel per retrieval
  - Accuracy is more important where SST > 25°C
  - Spatial resolution of 0.05° acceptable at present
  - Once capability to include diurnal variation is developed, temporal resolution would need to increase above daily
- Level 4 data density
  - As high as possible with global coverage
  - A measure of data density (actual retrievals per pixel) would be useful
- Use of in situ data in the derivation of SST
  - If in situ data are used (e.g. OSTIA), validate SSTs over reefs to ensure that in situ data are not biasing the reef SSTs
  - Note that the coral community have a significant amount of historical, on-going in situ data
- Modern SST retrievals vs historic retrievals
  - Improvements in near-real-time SST retrievals must ensure consistent bias with historic data

    - If bias of standard NRT product is not consistent with historical, consider running a second NRT product that maintains consistency with historical bias
    - Improvements in spatial, temporal, radiometric accuracy are helpful if bias remains consistent
    - Please recognize that reprocessed products are an integral part of operational anomaly products due to the need for historic data for the calculation of climatologies
- Importance of temperatures above 25°C
    - Corals stressed when temperatures exceed the expected summer time maximum
    - Accuracy and consistency of temperatures above 25°C are far more important than those below 25°C
- Regional analyses
    - Validation should be carried out regionally to avoid obscuring regional inaccuracies or biases within a global validation
    - These could be carried out in consultation with a coral reef specialist using the vast array of in situ data available on reefs worldwide

TASK TEAMS SESSION 2

Chair: Christopher Merchant[1]

Co-chairs: Lei Guan[2], Peter Minnett[3]

(1) University of Reading, UK, Email: c.j.merchant@reading.ac.uk
(2) Ocean University of China, Email: liumingkun@ouc.edu.cn
(3) Rosenstiel School of Marine and Atmospheric Science, University of Miami, U.S., Email: pminnett@rsmas.miami.edu

TTS2-1 - SHIPBORNE RADIOMETRY

Werenfrid Wimmer (University of Southampton) presented the TT progress and planning for future activities:

- Network is setup, more members always welcome
- Data format: L2R
- Protocols and procedures on webpage
- Archive: FTP server at IFREMER
- Next inter-comparison planning

The TT report also presented the archive data plots and archive issue log. During the TT reporting session, the optional/recommended variable in the L2R specification and the update of MDB with new radiometer datasets were discussed. Haifeng Zhang (NOAA) joined the TT.

TTS2-2 - GHRSST MATCH-UP DATASET

Igor Tomazic (EUMETSAT) presented the TT membership so far and proposed the following tasks:

- Compare match-up dataset (MD) tools
- Identify metrics and protocols
- A round-robin comparison of MDs
- A white paper

This task team hopes to use the TT forum between meetings.

TTS-3 - INTER-COMPARISON AND L4

Helen Beggs (ABoM) presented the TT report. This team has been active during the past year on Task 1 (Inter-comparison of SST analyses for climate studies) and Task 2. Task 3 is now starting.

At the 20th GHRSST Science Team Meeting (Frascati, June 2019) it was decided that the Climatology Task Team activities should expand to cover the inter-comparison of gap-free, level 4 (L4) SST analyses, as well as SST climatology datasets.

Currently, several near real-time GHRSST L4 products are compared and validated using the GMPE at NOAA/NESDIS/STAR SQUAM and UK Met Office GMPE web pages. However, these online tools do not cover all the more than 30 available SST analyses and reanalyses, or all those used for climate monitoring, and do not compare the ability of the products to accurately capture mesoscale features, such as fronts, particularly in coastal zones.

The following tasks are addressed:

Task 1: Inter-comparison of SST analyses for climate studies (led by Chunxue Yang, CNR/ISMAR)

Task 2: Understand differences among SST analyses and find ways to improve these products (led by Xu Li, NOAA/NCEP)

Task 3: Feature inter-comparison of SST analyses (led by Jorge Vazquez, NASA/JPL)

A report on Task 1 has been prepared for the Copernicus Climate Change Service and was reported by the lead author at this GHRSST meeting – see the report on the presentation of Chunxue Yang (Analyses and Reanalyses, Topic 5) for details. Beggs highlighted the finding that global mean warming trends in the analyses considered are consistent with previous published values for the period 1980 to 2005 in IPCC.

Task 2 address understanding differences between operational analysis products, and is led by Xu Li. An early activity is to compare analyses for 1 – 10 May 2020 in terms of number of buoy observations used by different analysis systems.

Task 3 will look at feature inter-comparison of SST analyses, led by Jorge Vazquez. Significantly, this will exploit saildrone capabilities and consider validation of gradients. For details see presentation in of Jorge Vazquez in Science Session 1. Prasanjit Dash has demonstrated a tool identifying fronts in the MUR analysis.

Future work will extend the Task 1 intercomparisons and compare with median ensemble SST. The forum suggested prioritising comparisons back during the 1980s, where there is probably more to be learned. The team will complete the drifting buoy counting exercise under Task 2 and will under Task 3 continue to look at gradient validation.

The importance of collaborating with the Climate Data Assessment Framework task team was emphasised, since protocols for long-term data assessment are already established within that TT and should be adopted where relevant.

TTS2-4 - HIGH LATITUDE SST

The High Latitude TT did not submit a report as the Team Leader, Chelle Gentemann, stepped down at the last GHRSST Science Team Meeting, and none of the other members volunteered for this post. An email exchange with the team members indicated that there is interest amongst most embers that the TT should continue as there are a number of pressing issues with retrieving accurate SSTs at High Latitudes. Mike Steele at the Applied Physics Laboratory has volunteered to take on the leadership role.

There has been much progress in the past year:

The MISST-3 Arctic Saildrone deployment was successfully completed in the summer of 2019, with two vehicles spending ~150 days at sea. The sampling was coordinated with those from NOAA PMEL in the same area – the Bering, Chukchi and Beaufort Seas, producing a very rich data set. The data from the MISST-3 Saildrones are available at the JPL PO.DAAC. The anticipated Saildrone deployment in the summer of 2020 was cancelled because of restrictions resulting from the Covid pandemic.

Research at RSMAS by Chong Jia for his MS degree has resulted in improved atmospheric correction algorithms for MODIS SSTskin retrievals at high northern latitudes, and these improvements are part of the R2019 reprocessing of the entire MODIS missions on Terra and Aqua. The reprocessed fields are available in L2p format from the PO.DAAC.

Researchers at the U.S. Naval Research Laboratory diagnosed anomalously cold SST retrievals using new Metop-C AVHRR software in beta tests for the U.S. Naval Oceanographic Office. Undetected cloud contamination occurred at high latitudes under twilight or low sun elevation conditions; application of a 4 μm brightness temperature night-time test resolved the issue.

An improved version of the NOAA OISST, v2.1, has been generated for the period 2016 to the present; Arctic SSTs are now more accurate.

At the Ocean University of China, estimates of SST retrieval accuracy from radiometers on the FY and HY satellites have indicated higher errors at high latitudes than elsewhere, and improving these will be the subjects of future research.

TTS2-5 - CLIMATE DATA ASSESSMENT FRAMEWORK

Jon Mittaz (Reading) presented the CDAF TT status. The CDAF framework is intended to support users of SST climate data records (CDRs) to understand the relative properties of such records. The concepts of the CDAF have previously been reported at length and were summarised again.

The TT in the next period will set up the baseline CDAF as a tool, and there are concepts for further tools and analysis thereafter, which could involve shared approaches via iPython Notebooks. Progress beyond the baseline is dependent on engagement of CDR producers with the baseline CDAF, so a key point is the degree to which the GHRSST community will adopt the CDAF tool once it is available.

The importance of the L4 Intercomparison Task Team using the CDAF within their work was also emphasised in the discussion accompanying the report.

SECTION 3: APPENDICES

APPENDIX 1 – LIST OF PARTICIPANTS

GHRSST XXI SCIENCE TEAM MEETING,
ON-LINE, 1-4 JUNE 2020

First name	Surname	Email address
Aida	Alvera Azcarate	a.alvera@ulg.ac.be
Ed	Armstrong	edward.m.armstrong@jpl.nasa.gov
Vincenzo	Artale	vincenzo.artale@enea.it
Charlie	Barron	charlie.barron@nrlssc.navy.mil
Carla	Barroso	carla.barroso@ipma.pt
Helen	Beggs	helen.beggs@bom.gov.au
Piero	Bernardo	piero.bernardo@usp.br
Paban	Bhuyan	pkb10@iitbbs.ac.in
Marouan	Bouali	marouanbouali@gmail.com
Hakim	Boulaassal	h.boulaassal@uae.ac.ma
Silvia	Bragaglia-Pike	sbp9@leicester.ac.uk
Claire	Bulgin	c.e.bulgin@reading.ac.uk
Bruno	Buongiorno Nardelli	bruno.buongiornonardelli@cnr.it
Madeleine	Cahill	madeleine.cahill@csiro.au
Danielle	Carpenter	danielle.carpenter@navy.mil
Kenneth	Casey	kenneth.casey@noaa.gov
Sandra	Castro	sandrac@colorado.edu
Jean-François	Cayula	jf_cayula@yahoo.com
Luca	Centurioni	lcenturioni@ucsd.edu
Emma	Chalençon	emma.chalencon@orange.fr
Yan	Chen	yan@ouc.edu.cn
Yoon Ling	Cheong	gylcheong@gmail.com
T. Mike	Chin	mike.chin@jpl.nasa.gov
Daniele	Ciani	daniele.ciani@cnr.it
Carol-Anne	Clayson	cclayson@whoi.edu
Gary	Corlett	gary.corlett@eumetsat.int
Peter	Cornillon	pcornillon@me.com
Erik	Crosman	etcrosman@wtamu.edu
Peng	Cui	cuipeng@cma.gov.cn
Rita	Cunha	rita.cunha@colabatlantic.com
Ian	Dragaud	iandragaud@lamma.ufrj.br
Prasanjit	Dash	prasanjit.dash@noaa.gov
Prasanth	Divakaran	prasanth.divakaran@bom.gov.au

First name	Surname	Email address
Craig	Donlon	craig.donlon@esa.int
Jacqueline	Dumas	jacqueline.dumas@dfo-mpo.gc.ca
Mark	Eakin	mark.eakin@noaa.gov
Steinar	Eastwood	s.eastwood@met.no
Shane	Elipot	selipot@rsmas.miami.edu
Owen	Embury	o.embury@reading.ac.uk
Luis	Escudero	lescudero@imarpe.gob.pe
Agnieszka	Faulkner	agnieszka.walenkiewicz@pgr.reading.ac.uk
Eric	Freeman	eric.freeman@noaa.gov
Rishi Kumar	Gangwar	rgphybhu@gmail.com
Lucile	Gaultier	lucile.gaultier@oceandatalab.com
Chelle	Gentemann	cgentemann@gmail.com
Denis	Gilbert	denis.gilbert@outlook.com
Irina	Gladkova	irina.gladkova@gmail.com
Cristina	Gonzalez-Haro	cgharo@icm.csic.es
Simon	Good	simon.good@metoffice.gov.uk
Pallavi	Govekar	pallavi.govekar@bom.gov.au
Chris	Griffin	christopher.griffin@bom.gov.au
Lei	Guan	leiguan@ouc.edu.cn
Andy	Harris	Andy.Harris@noaa.gov
Jacob	Hoeyer	jlh@dmi.dk
Verena	Hormann	vhormann@ucsd.edu
Boyin	Huang	boyin.huang@noaa.gov
Xinmei	Huang	xinmei.huang@bom.gov.au
Zhi	Huang	Zhi.Huang@ga.gov.au
Lars	Hunger	lars.hunger@noaa.gov
Alexander	Ignatov	alex.ignatov@noaa.gov
Jordi	Isern-Fontanet	jisern@icm.csic.es
Andrew	Jin	agj2109@columbia.edu
Olafur	Jonasson	olafur.jonasson@noaa.gov
Misako	Kachi	kachi.misako@jaxa.jp
Alexey	Kaplan	alexeyk@ldeo.columbia.edu
Hugh	Kelliher	hugh.kelliher@spaceconnexions.com
Kay	Kilpatrick	kkilpatrick@miami.edu
Hee-Young	Kim	heeyoungkim@snu.ac.kr
JaeGwan	KIM	kimjgwan@korea.kr
Kamran	Koohi	kamrankoohestani@gmail.com
Balasaheb	Kulkarni	balasahebk@yahoo.com

First name	Surname	Email address
Yukio	Kurihara	ykuri.kiyo@gmail.com
Martin	Lange	martin.lange@dwd.de
Arrow	Lee	arrow.lee@stfc.ac.uk
Eun-Young	Lee	eunyounglee@snu.ac.kr
Francesca Elisa	Leonelli	francesca.leonelli@artov.ismar.cnr.it
Ninghui	Li	925966258@qq.com
Wen-Hao	Li	wenhaoli@jpl.nasa.gov
Xu	Li	xu.li@noaa.gov
Zhuomin	Li	lizhuomin@stu.ouc.edu.cn
Zhihong	Liao	liaozh@cma.gov.cn
Michelle	Little	michelle.c.little1@navy.mil
Bailu	Liu	bailu_0126@163.com
Chunying	Liu	chunying.liu@noaa.gov
Mingkun	Liu	liumingkun@ouc.edu.cn
David	Lloyd	david.lloyd@um.edu.mt
Rick	Lumpkin	Rick.Lumpkin@noaa.gov
Bingkun	Luo	lbk@rsmas.miami.edu
Hermann	Luyt	harry.luyt@gmail.com
Chongyuan	Mao	chongyuan.mao@metoffice.gov.uk
Salvatore	Marullo	salvatore.marullo@enea.it
Eileen	Maturi	eileen.maturi@noaa.gov
Jackie	May	jackie.may@nrlssc.navy.mil
Niall	McCarroll	n.f.mccarroll@reading.ac.uk
Bruce	McKenzie	bruce.mckenzie@navy.mil
David	Meldrum	dunfraoch@gmail.com
Christopher	Merchant	c.j.merchant@reading.ac.uk
Peter	Minnett	pminnett@rsmas.miami.edu
Jonathan	Mittaz	j.mittaz@reading.ac.uk
Nicole	Morgan	nicole.morgan@csiro.au
Tim	Nightingale	tim.nightingale@stfc.ac.uk
Anne	O'Carroll	anne.ocarroll@eumetsat.int
Keiichi	Ohara	ohara.keiichi@jaxa.jp
Ana	Oliveira	ana.oliveira@colabatlantic.com
Gang	Pan	gpan@scsio.ac.cn
Kyung-Ae	Park	kapark@snu.ac.kr
Francisco	Pastor	paco@ceam.es
Bruno	Pereira	bruno.science@usp.br
Boris	Petrenko	boris.petrenko@noaa.gov

First name	Surname	Email address
Kirstin	Petzer	kirzypetzer@gmail.com
Jean-François	Piollé	jfpiolle@ifremer.fr
Andrea	Pisano	andrea.pisano@cnr.it
J. Xavier	Prochaska	jxp@ucsc.edu
Victor	Pryamitsyn	victor.pryamitsyn@noaa.gov
K	Pugazenthi	pugazenthi002@gmail.com
Greg	Reed	gregreed98@gmail.com
Charles	Roberts	c.j.roberts@reading.ac.uk
Korak	Saha	korak.saha@noaa.gov
Toshiyuki	Sakurai	tsakurai@met.kishou.go.jp
Michela	Sammartino	michela.sammartino@artov.ismar.cnr.it
Rosalia	Santoleri	rosalia.santoleri@cnr.it
Olga	Sato	olga.sato@usp.br
Stéphane	Saux Picart	stephane.sauxpicart@meteo.fr
Rory	Scarrott	r.scarrott@ucc.ie
Robert	Schlegel	robert.schlegel@dal.ca
Toby	Searle	toby.searle@metoffice.gov.uk
Alexander V	Semenov	alexvladsemenov@gmail.com
Lijian	Shi	shilj@mail.nsoas.org.cn
Janice	Sisson	janice.sisson@bom.gov.au
William	Skirving	william.skirving@noaa.gov
Grant	Smith	grant.smith@bom.gov.au
Marie	Smith	ocean.chiq@gmail.com
Robert	Smith	robert.smith@otago.ac.nz
Mauricio	Soares da Silva	soares@lamma.ufrj.br
Michael	Steele	mas@apl.washington.edu
Craig	Steinberg	c.steinberg@aims.gov.au
Susan	Sun	susan.sun@metoffice.gov.uk
Swathy	Sunder	swathy.na007@gmail.com
Dorina	Surcel Colan	dorina.surcel-colan@canada.ca
Goshka	Szczodrak	gszczodrak@miami.edu
Pradeep	Thapliyal	pkthapliyal@gmail.com
Igor	Tomazic	igor.tomazic@gmail.com
Cristina	Tronconi	cristina.tronconi@artov.ismar.cnr.it
Jorge	Vazquez	jorge.vazquez@jpl.nasa.gov
Karen	Veal	klv3@le.ac.uk
Sujuan	Wang	wangsj@cma.gov.cn
Brian	Ward	bward@nuigalway.ie

First name	Surname	Email address
Li	Wei	VE1207@outlook.com
Christo Peter	Whittle	cwhittle@csir.co.za
Gary	Wick	gary.a.wick@noaa.gov
Ruth	Wilson	ruth.wilson@spaceconnexions.com
Werenfrid	Wimmer	w.wimmer@soton.ac.uk
Hye-Jin	Woo	hyejinwoo@snu.ac.kr
Mark	Worsfold	mark.worsfold@metoffice.gov.uk
Chunxue	Yang	chunxue.yang@cnr.it
Minglun	Yang	minglunyang@sdu.edu.cn
Haifeng	Zhang	haifeng.zhang@noaa.gov
Huaimin	Zhang	huai-min.zhang@noaa.gov
Lei	Zhang	zhanglei3505962@126.com
Yongsheng	Zhang	yongsheng.zhang@noaa.gov
Xuepeng	Zhao	Xuepeng.Zhao@noaa.gov
Hao	Zuo	hao.zuo@ecmwf.int

APPENDIX 2 – GXXI - PARTICIPANTS PHOTO

As the GHRSST meeting this year was online, we were unable to gather participants for the traditional group photo as in previous years. However, a group photo Padlet was set up for participants to add their photos.

The link to view the Padlet is: https://padlet.com/TrainingEUMETSAT/1eq0d1zfvvjeie64.

If you participated in the meeting and did not yet add your photo, you can still do so by accessing the Padlet and clicking on the pink blob (with a plus sign) at the bottom of the screen on the right (see below).

Please note: if you are likely to want to log back in to edit your post, please log in to the Padlet using a Google/Microsoft/Apple/Padlet account before making your post. You can set up a Padlet account for free.

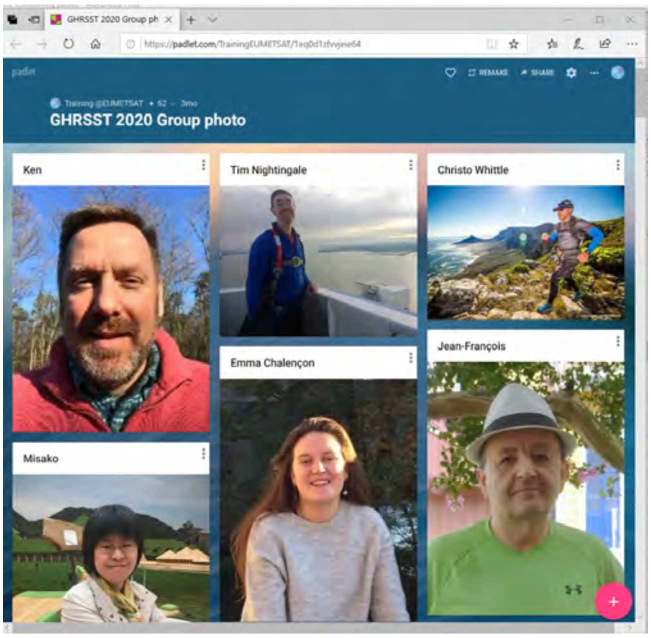

APPENDIX 3 – SCIENCE TEAM MEMBERS 2019-20

Anne O'Carroll (Chair)	EUMETSAT, Darmstadt, Germany
Ed Armstrong	NASA JPL PO.DAAC, USA
Viva Banzon	NOAA/NCDC, USA
Charlie Barron	US Naval Research Laboratory, USA
Helen Beggs	Bureau of Meteorology, Melbourne, Australia
Maouan Bouali	Institute of Oceanography of the University of Sao Paulo, Brazil
Kenneth S Casey	NOAA/NESDIS NODC, USA
Sandra Castro	University of Colorado, Boulder, USA
Jean-François Cayula	Vencore, Inc, Stennis Space Center, Mississippi, USA
Mike Chin	NASA JPL, USA
Carol Anne Clayson	WHOI, USA
Peter Cornillon	University of Rhode Island, USA
Prasanjit Dash	NOAA, USA
Craig J Donlon	European Space Agency, The Netherlands
Steinar Eastwood	Met.no, Norway
Owen Embury	University of Reading, UK
Chelle Gentemann	Earth and Space Research, USA
Simon Good	MetOffice, UK
Lei Guan	Ocean University of China, China
Andrew Harris	NOAA/NESDIS ORA, USA
Jacob Høyer	Danish Meteorological Institute, Denmark
Alexander Ignatov	NOAA/NESDIS/STAR, USA
Misako Kachi	Japan Aerospace Exploration Agency (JAXA), Japan
Alexey Kaplan	Columbia University, USA
Ioanna Karagali	Technical University of Denmark, Denmark
Prabhat Koner	ESSIC, University of Maryland, USA
Yukio Kurihara	Japan Aerospace Exploration Agency (JAXA), Japan
W Timothy Liu	NASA JPL, USA
Yang Liu	RSMAS, University of Miami, USA
Salvatore Marullo	ENEA, Italy
Eileen Maturi	NOAA/NESDIS/STAR/SOCD/MECB, USA
Christopher Merchant	University of Reading, UK

Peter Minnett	RSMAS, University of Miami, USA
Jonathan Mittaz	University of Reading, UK
Tim Nightingale	Rutherford Appleton Laboratory, UK
Kyung-Ae Park	Seoul National University, Korea
Jean–François Piollé	IFREMER, France
Toshiyuki Sakurai	Japan Meteorological Agency (JMA), Japan
Rosalia Santoleri	ARTOV.ISAC.CNR, Italy
Stéphane Saux Picart	Météo-France, France
Dorina Surcel Colan	CMC - Environment Canada
Igor Tomazic	EUMESTAT, Darmstadt, Germany
Jorge Vazquez	NASA JPL PO.DAAC, USA
Sujuan Wang	National Satellite Meteorological Center, Met Administration, China
Christo Whittle	CISR, South Africa
Gary Wick	NOAA ETL, USA
Werenfrid Wimmer	University of Southampton, UK

LAST PAGE